

**Development of an Expert System Interface for the
Automated Analysis of the Sheet drawing Metal
Forming Process using Finite Element Analysis
Techniques.**

James Conerney

This dissertation is submitted in satisfaction of the requirements for the
degree of Masters in Engineering
in
Mechanical Engineering
at the
Galway Mayo Institute of Technology



Supervisor : Mr Gerard O Donnell

Submitted to the National Council for Educational Awards
September 1999

Abstract

The objective of the work presented in this thesis was to develop an expert system for sheet metal forming. In doing so an examination, of implicit and explicit Finite Element Analysis (F.E.A) codes and methodologies was conducted. Guidelines as to how best to carry out simulations of sheet drawing, were developed. Work was conducted into deep drawing and shallow drawing of non complex shapes, because of the many analytical, and empirical studies conducted on cup and box drawn shapes. The process parameters effecting drawing of complex parts are present in drawing of non complex parts such as cup and box shapes. A valuable insight into drawing of complex parts can be attained economically, with the proposed study of drawing of non complex parts, such as cup and box shapes. Modelling and solution variables present in implicit and explicit F.E.A. codes are explored by the modelling of non complex parts such as cup and box shapes.

Deep drawing is a common process used in the manufacture of auto body components; cans, cups, bathtubs, sinks, and other similar items by drawing rolled sheets into there final geometric form. Configuration of a new deep drawing process is highly empirical with many parameters determined by trial and error. Large deformation numerical Finite Element Analysis of the deep drawing process can be applied to shorten the process reconfiguration time and remove the expense of trial production runs of parts. In the research work reported in this thesis parametric studies are performed on critical deep drawing parameters. The findings are presented and are incorporated into the Expert System for Metal forming.

Material non linearity is introduced by a description of drawing blank material plasticity. The discussion on plasticity introduces rate independent material behaviour models, typically used to model the behaviour of Steel and Aluminium Blanks. The Taguchi method of experiment design and results analysis is applied to develop strategies for the design of best practice finite element simulation of cup drawing. The expert system for cup drawing contain domain knowledge in the form of analytical model and dedicated automatic development of Finite Element Analysis simulations which is developed in ANSYS command script files. The control aspects of the expert system utilises goal and data driven reasoning within the control algorithm. A blackboard architecture to the expert system is promoted with the ANSYS Advanced Parametric Design Language (APDL) macro programming language.

CONTENTS

Section	Topic	Page No.
---------	-------	----------

Chapter 1 : Sheet Metal Forming

1.1	Chapter Introduction.	1
1.2	Sheet Metal Forming.	1
1.3	Deep Drawing of a Cup.	2
1.4	Historical review of Finite Element Analysis in Metal Forming.	3
1.5	Introduction to Finite Element Analysis.	5
1.6	Chapter Conclusion.	5

Chapter 2 : Analytical Studies in Metal Forming

2.1	Chapter Introduction.	7
2.2	Theoretical approach to solutions in Metal Forming.	7
2.3	Slip line field theory.	7
2.4	Upper Bound theory.	8
2.5	Slab Analysis.	8
2.6	Chapter Conclusion.	11

Chapter 3 : Finite Element Analysis Metal Forming Theory

3.1	Chapter Introduction.	12
3.2	Finite Element Analysis of Metal Forming.	12
3.3	Finite Element Analysis an Introduction.	13
3.4	Introduction to Non-Linear Finite Element analysis.	17
3.5	Solution Schemes of Non Linear Finite Element Analysis.	20
3.6	Convergence criteria.	21
3.7	Chapter Conclusion.	23

Section	Topic	Page No.
---------	-------	----------

Chapter 4 : Plasticity Theory.

4.1	Chapter Introduction.	24
4.2	Plasticity a historical Outline.	24
4.3	Plasticity material non-linearities.	26
4.4	Plasticity Theory.	28
4.5	Stress and Strain indicators for Metal Forming.	34
4.6	Introduction to Predictor Corrector Scheme	35
4.7	Anisotropy.	38
4.8	Chapter Conclusion.	39

Chapter 5 : Sheet Metal Forming

5.1	Chapter Introduction.	40
5.2	Formulation of small and large strain methods.	40
5.3	Small / Infinite strain.	40
5.4	Large / Finite strain.	41
5.5	Explanation of Implicit and Explicit time integration schemes.	43
5.6	Contact considerations of Finite Element Analysis Codes.	50
5.7	Tool Blank friction.	56
5.8	An Investigation into possible hour glass modes in deep drawn process modelling .	57
5.9	Kinetic Energy Consideration.	60
5.10	Solution convergence enhancement of Implicit code with observations drawn from ANSYS 5.3 Implicit code.	62
5.11	Solution convergence problems and enhancement of Explicit code with observations drawn from Ls DYNA Explicit code.	64

Section	Topic	Page No.
5.1	Considerations for Dynamic simulations.	65
5.2	Chapter Conclusion.	65

Chapter 6 : Finite Element Analysis Modelling.

6.1	Chapter Introduction.	66
6.2	Finite Element Analysis mathematical systems.	66
6.3	Finite Element Analysis Simulation of the drawing process.	68
6.4	Deep drawing simulation.	69
6.5	Finite Element Analysis model types.	70
6.6	The need for explicit and implicit Finite Element Analysis.	75
6.7	Discretisation of a circular blank.	77
6.8	Mesh sensitivity study.	79
6.9	Box Drawing.	81
6.10	Formability in Sheet Drawing.	85
6.11	Chapter Conclusion.	90

***Chapter 7 : Expert System Rule development by Taguchi
experimental design and results analysis.***

7.1	Chapter Introduction.	91
7.2	The Taguchi method of experiment design and analysis of results.	91
7.3	Signal to Noise ratio as a measure of variability.	96
7.4	Two step optimisation by analysis of variance.	97

Section	Topic	Page No.
7.5	Sensitivity study of punch and die Tooling radius to Cup formability.	99
7.6	Punch force in Drawing.	106
7.7	Paramaterisation of explicit finite element metal forming simulation variables by Taguchi methods.	110
7.8	Redraw process system appraisal conducted in Finite Element Analysis.	115
7.9	Chapter Conclusion.	117

Chapter 8 : Expert System Architecture.

8.1	Chapter Introduction.	118
8.2	What is an Expert System.	119
8.3	How the Cup draw expert system works.	121
8.4	Modelling within an expert system framework.	122
8.5	Blackboard Architecture.	123
8.6	Control Domain	125
8.7	Domain Knowledge.	129
8.8	Search strategies for expert systems.	130
8.9	Knowledge based expert system versus Rule base expert system.	132
8.10	Uncertainty in rule based knowledge base.	135
8.11	Fuzzy set theory.	138
8.12	Software Choice.	138
8.13	Expert system user interface.	139
8.14	Chapter Conclusion.	147

Section	Topic	Page No.
9	Thesis Summary	148

APPENDICES

APPENDIX A		
	<i>Lagrangian Multipliers.</i>	A - 1
APPENDIX B		
	<i>Expert System Software Code Architecture.</i>	B - 1
APPENDIX C		
	<i>Finite Element Analysis ANSYS Pre-processor Simulation Command Code.</i>	C - 1
APPENDIX D		
	<i>User Interface Software Code.</i>	D - 1
APPENDIX E		
	<i>Expert System Rule Base.</i>	E - 1
APPENDIX F		
	<i>Main File Control File A.P.D.L Coding.</i>	F - 1
APPENDIX G		
	<i>Post Processing A.P.D.L Command Log Scripts.</i>	G - 1
APPENDIX H		
	<i>A user friendly Expert System for Deep Drawing of Cylindrical Cans.</i>	H - 1
APPENDIX I		
	<i>A sample description of the Finite Element Analysis results Plates.</i>	I - 1

Organisation of dissertation

Chapter 1 : Sheet Metal Forming

Introduces the Deep Drawing process, presents a history of Finite Element Analysis applications to Metal Forming and introduces the basics of the Finite Element Analysis method.

Chapter 2 : Analytical studies in metal forming

This chapter gives an account of the current analytical methods that are applied to validate the sheet drawing process. A study of the work to date in analysing the sheet drawing process from leading exponents is documented.

Chapter 3 : Finite Element Analysis Metal Forming Theory

Introduces the concept and system equations that describe the Finite Element Method (F.E.A). The specialised non linearities that are present in metal forming such as, material, geometry and tool contact are introduced. Methods employed to simulate such phenomena are introduced and developed.

Chapter 4 : Plasticity Theory

This chapter explains the phenomenon of plasticity in metallic materials. The theory behind rate independent plasticity is developed. The anisotropic effect of sheet metal blanks is introduced and a model to account for this is presented.

Chapter 5 : Large Strain Large Deformation Finite Element Analysis Solution Convergence

The convergence difficulties experienced by large strain and large deformation process of metal forming are documented. Strategies are presented that promote a converged solution. The following analysis types are introduced; Implicit static, Implicit dynamic, Explicit dynamic.

Chapter 7 : Expert System Rule Development by Taguchi Experimental Design and results Analysis of Finite Element Analysis

This chapter is dedicated to developing rules for the Expert System. The developed rules take the form of suggested process parameters to meet the required cup specifications. The Taguchi method of experiment design and results analysis is used to develop the F.E.A models and analysis the results of the simulation.

Chapter 8 : Expert System Architecture

This chapter introduces the concept of an expert system. A detailed description of knowledge based and rule based expert systems is described. Control and domain aspects are discussed with respect to the expert system for cup drawing. Backward and forward chaining search algorithms are explained and implemented in the cup drawing expert system. The Graphical user interface is presented outlining its form and application.

List of Figures

Figure	Description
6.1	Wall Thickness distribution
6.1.1	Contour plot of equivalent plastic strain
6.1.2	Deformation stages in Deep drawing
6.1.3	Meshing schemes analysed for quadrant of blank sheet.
6.1.4	Un-smoothed stress distribution over Elements
6.1.5	Mesh Sensitivity Study
6.1.6	Box drawing Tool geometry
6.1.7	Finite Element representation of tooling
6.1.8	Thickness distribution along profile o-a
6.1.9	Thickness distribution contour plot
6.2.1	Radial displacement contour plot
6.2.2	Geometry of the OSU Formability Test
6.2.3	OSU model
6.2.4	Contour plot of thickness distribution for OSU test specimen
6.2.5	Contour plot of 1 st principle
6.2.6	Contour plot of 2 nd Principle strain
6.2.7	Forming Limit Diagram
7.1	Taguchi Method for design of Experimentation
7.2	ANOVA Mean and Signal to noise plots
7.3	Effect of Die Profile on Formability
7.4	Deep drawing geometry
7.5	Cup Wall Thickness
7.6	F.E.A resulting thickness distribution
7.7	ANOVA mean and signal to noise plots
7.8	Punch load versus punch travel
7.9	Punch force verses Punch displacement for analysis A
7.10	Punch force verses Punch displacement for analysis B
7.1.1	Punch force verses Punch displacement for analysis C
7.1.2	Element characteristic length
7.1.3	ANOVA mean and signal plots
7.1.4	Redraw Tooling
7.1.5	Reverse Redrawing Tool Geometry
7.1.6	Redraw analysis Punch Force versus Punch stroke.
8.1	The components of a basic system
8.2	Blackboard Architecture
8.3	Control domain architecture of Expert System
8.4	Domain aspects of the Expert System
8.5	Search tree topology
8.6	Solution chaining strategy
8.7	Control Knowledge domain development
8.8	Dept first search strategy

Figure	Description
6.1	Wall Thickness distribution
6.1.1	Contour plot of equivalent plastic strain
6.1.2	Deformation stages in Deep drawing
6.1.3	Meshing schemes analysed for quadrant of blank sheet.
6.1.4	Un-smoothed stress distribution over Elements
6.1.5	Mesh Sensitivity Study
6.1.6	Box drawing Tool geometry
6.1.7	Finite Element representation of tooling
6.1.8	Thickness distribution along profile o-a
6.1.9	Thickness distribution contour plot
6.2.1	Radial displacement contour plot
6.2.2	Geometry of the OSU Formability Test
6.2.3	OSU model
6.2.4	Contour plot of thickness distribution for OSU test specimen
6.2.5	Contour plot of 1 st principle
6.2.6	Contour plot of 2 nd Principle strain
6.2.7	Forming Limit Diagram
7.1	Taguchi Method for design of Experimentation
7.2	ANOVA Mean and Signal to noise plots
7.3	Effect of Die Profile on Formability
7.4	Deep drawing geometry
7.5	Cup Wall Thickness
7.6	F.E.A resulting thickness distribution
7.7	ANOVA mean and signal to noise plots
7.8	Punch load versus punch travel
7.9	Punch force verses Punch displacement for analysis A
7.10	Punch force verses Punch displacement for analysis B
7.1.1	Punch force verses Punch displacement for analysis C
7.1.2	Element characteristic length
7.1.3	ANOVA mean and signal plots
7.1.4	Redraw Tooling
7.1.5	Reverse Redrawing Tool Geometry
7.1.6	Redraw analysis Punch Force versus Punch stroke.
8.1	The components of a basic system
8.2	Blackboard Architecture
8.3	Control domain architecture of Expert System
8.4	Domain aspects of the Expert System
8.5	Search tree topology
8.6	Solution chaining strategy
8.7	Control Knowledge domain development
8.8	Dept first search strategy
9	Cup drawing Expert System Topology

Nomenclature

The following is True unless explicitly directed otherwise.

k	<i>stiffness matrix / stiffness</i>
f	<i>Externally applied force</i>
u	<i>Nodal displacement</i>
α	<i>Yield surface translation</i>
r	<i>Residual force</i>
B	<i>Shape function derivative matrix</i>
M^T	<i>Matrix transpose</i>
σ	<i>Direct stress</i>
τ	<i>Shear stress</i>
E	<i>Young's modulus</i>
ν	<i>Possion's Ratio</i>
L	<i>Derivatives Matrix</i>
N	<i>Shape Function</i>
ε	<i>Direct Strain</i>
μ	<i>Friction Co-efficient</i>
ξ	<i>Damping ratio</i>
ω	<i>Frequency</i>
m	<i>Mass</i>
c	<i>Damping ratio / Courant time step</i>
λ	<i>Lagrangian operator</i>
g	<i>node element gap</i>
ρ	<i>Density</i>

Acknowledgements

I wish to express my gratitude to my research supervisor Mr Gerard O Donnell, for his continued guidance through the course of my research and in reviewing this manuscript with many constructive suggestion as to its form.

I thank Dr. Patrick Dellassus for helping me to achieve a knowledge of large strain and large deformation mechanics.

I thank the Mechanical/Industrial Engineering department at The Galway Mayo Institute of Technology for enabling me to partake in this study.

I tank my fellow research students for their inspiration and help notably John Doyle for shearing his knowledge of metal forming and Richard Maxwell for introducing me to the Taguchi method.

Chapter 1 : Sheet Metal Forming

1 Introduction

This Chapter introduces the Deep Drawing process, presents a history of Finite Element Analysis applications to Metal Forming and introduces the basics of the Finite Element Analysis method.

1.2 Sheet Metal Forming

The process of sheet drawing has three distinct modes of deformation, bending, drawing and stretching Eshel.G [1.1]. The proportions of each mode that a region within the blank is exposed to depends on the geometry of the drawn part and the metal flow, which is dependent on the material strain hardening path.

The Bending and stretching mode occurs as the blank is bent over the tool radius, the deformation is driven by developing bending stress as the material does not slip perfectly over the tool radius. The blank is stretched due to the resistance built up by blank tool friction.

The drawing mode is signified when the blank is subjected to a combination of a compressive and tensile axial stress state Eshel.G [1.1]. This occurs at the flange region and in the developing wall sections. For (bending and stretching) and (drawing) modes the friction force does not constrain the flow of the blank into the die cavity Eshel.G. [1.1].

During the stretching mode excessive friction or draw beads, restricts fully the flow of material, thereby promoting stretching. Stretching is characterised by a bi-axial tensile stress state. Unlike drawing, stretching inevitably results in thinning Eshel.G. [1.1]. For the drawing mode to prevail, the effective stress induced by the punch should exceed the instantaneous flow stress throughout the free flange of the blank ensuring that flow continues (i.e. flow over the die rim). Flow in the outermost region of the flange may be delayed or completely halted as a result of high resisting frictional stresses, or high flow stress, due to work hardening as outlined by Eshel.G. [1.1]. Flange thickening towards the rim amplifies both cases. Thus in later stages of a draw a combination of stretching and drawing is more apparent, with varying contributions from each mode. The instant that the flow of the blank edge has halted, stretching becomes the dominant mode of deformation. Otherwise the dominant mode of deformation is drawing.

1.3 Deep Drawing of a Cup

In a quest to develop a better understanding of the deep drawing process the cup drawing process will be examined, as presented in Figure 1.1. The punch presses the central part of the disk through a circular die to form the bottom of the cup. The gap between the punch and the die is termed the clearance, without the clearance the process becomes a combined operation of deep drawing and ironing of the cup wall. The pressure applied by the punch to the bottom of the cup is transmitted as a tensile force, to the flange, through the thin walls of the cup. As a result, the flange is pulled inward through the die, to form the wall of the cup. The effect of the continuously decreasing radius in this flange zone, is to induce a compressive hoop stress, resulting in an increase in material thickness, due to Poisson's strains. The task of the blank holder is to ensure the flange remains flat, its tendency to wrinkle is removed by the force applied by the blank holder. As the material forms the wall of the cup it is thinned by plastic bending while under a tensile radial stress as it passes over the die radius. The material that forms the bottom of the cup, which was in contact with the bottom of the punch, is thinned to a lesser extent, as it is subjected to stretching and sliding over the punch head. The sliding is resisted to some degree by the friction between punch and blank.

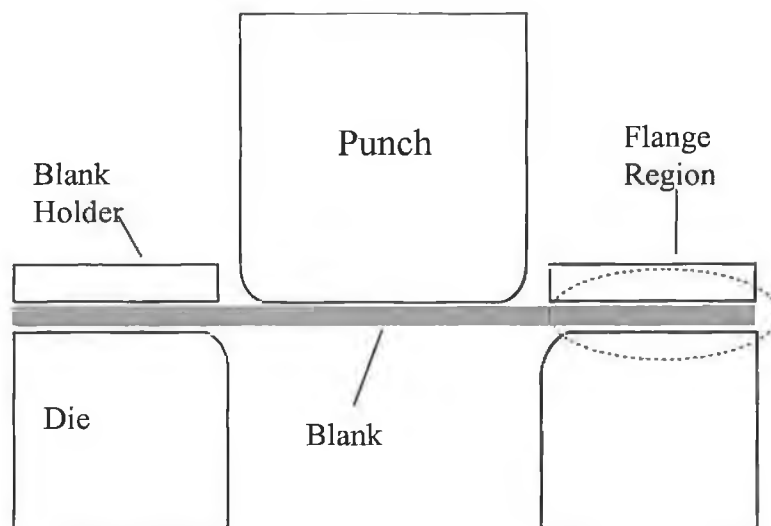


Figure 1.1 : Deep Drawing Operation

1.4 Historical Review of FEA in Metal Forming

The development of non linear finite element methods have enabled the analysis of many complex problems. The use of the finite element method for problems of large strain plasticity has gradually increased over the last 20 years, but widespread industrial recognition of the technique's value has been lacking until recently. Hartery,P Pillinger,J Sturgress,C [1.2].

Thus the view of metal forming industries world wide in the late 1970's and early 1980's is considerably different than the current view in the areas of analytical applications to their technology. The decade of the 1980's resulted in a revolutionary implementation of new technologies in these areas. Some of the most dramatic advances came in the form of the design and analysis tools for metal forming engineers and metallurgist. The use of finite element methods in the design and manufacturing cycle has expanded from large aerospace forgers to a wide range of companies in cold, warm and hot forming, of materials for medical, aerospace, defence, automotive and other diverse industries.

The history of metal working is based on a highly empirical, nearly artisan form of technology prior to 1980's, the trial and error method was frequently used to design and optimise the metal forming process. This is in large part due to the fact that complex forming problems were not easily solved using the analytical tools available. Computers were slow, expensive and cumbersome. A major advancement in metal working simulation technology occurred when in the early 1980's the Finite Element Method (FEM) program ALPID (Analysis of Large Plastic Incremental Deformation) ALPID [1.3], was developed at Battle as a part of a U.S. Air Force contract. Over the next few years the features developed in ALPID were implemented in many commercial FEM codes. Industrial acceptance of this technology grew rapidly when forging design engineers presented success stories at conferences and in technical journals. The growth of this technology is further due to the dramatic reduction of price, increase of performance in computers and competitive pressures in metal forming industries.

The current standard for metalforming simulations, includes a robust and thoroughly validated process model with the capability to deal with real forming variables. These include the ability to intelligently remesh based on criteria that are defined prior to the start of the simulation with the assurance of a mesh that will not lose, mask or dilute information that is key to the simulation such as the state variables. In most forming processes, rigid dies are a reasonable

approximation of the actual process. In some processes, though it is imperative that the interaction between the form and non negligible die deformations are accounted for, as die deflections can influence material behaviour or flow.

A knowledge of residual stresses is important when determining the appropriate process plan which is dependent on heat treatment operations. To meet these important requirements, a large deformation, large rotation elastoplastic material model has been incorporated in the algorithms of current FEM codes. While currently the vast majority of work is completed using 2-D approximations, 3-D codes are emerging that mirror real world problems more accurately. One major issue with 3-D simulation is that of mesh generation and regeneration. To automate this procedure, both structured and non structured mesh generation and regeneration techniques have been developed Wu,w,t. Lig,j .Tang,j,p and Tszeng,t,c [1.4]. Martins p,a,f. Marmelo,j,m,cp Rodrigues,j,m,c and Barata,m,j,m[1.5]. Other issues currently being addressed include the improvement of computational procedure, representation of object geometry interface to and from CAD systems, and visualisation of simulation results.

Past and present FEM research work on metal forming is documented in the proceedings of two major international conferences, that of Numiform [1.6] and the international conference on metal forming [1.7].

1.5 Introduction to Finite Element Analysis

The finite element method is a computer based numerical technique used by engineers to solve complex problems in stress analysis, vibrations, heat transfer, fluid flow, acoustics and magnetic fields. In conventional problem solving engineers and scientists tend to solve large complex problems by sub-dividing them into smaller more manageable units, which is analogous to finite element method “elements”. Having obtained a solution for one section, or “element” of the problem, the solution procedure is applied to the remaining sections in turn, often using the partial solution obtained earlier in the analysis process. The overall solution is based on a summation or an FEM process called “assembly” of all of the partial solutions, from the intermediate stages of the problem. The Finite Element Method technique gets its name from the procedure of assuming the area / volume / region under investigation, can be modelled as a series of small individual units or elements of finite size hence the name “Finite Elements”. The complete model of the problem is obtained by assembling the individual elements to produce the overall model geometry. The finite element method relies on the manipulation of several defined matrices to establish a solution for an engineering problem. These matrices are developed from the input associated with a given problem. The basic steps of the finite element method are presented in Figure 1.2.

1.6 Conclusion

In summary the F.E.A method has been applied to the metal forming process since the early 80's with ever increasing success. The theory of the F.E.A. method introduced in this chapter is further expanded upon in chapter 3.

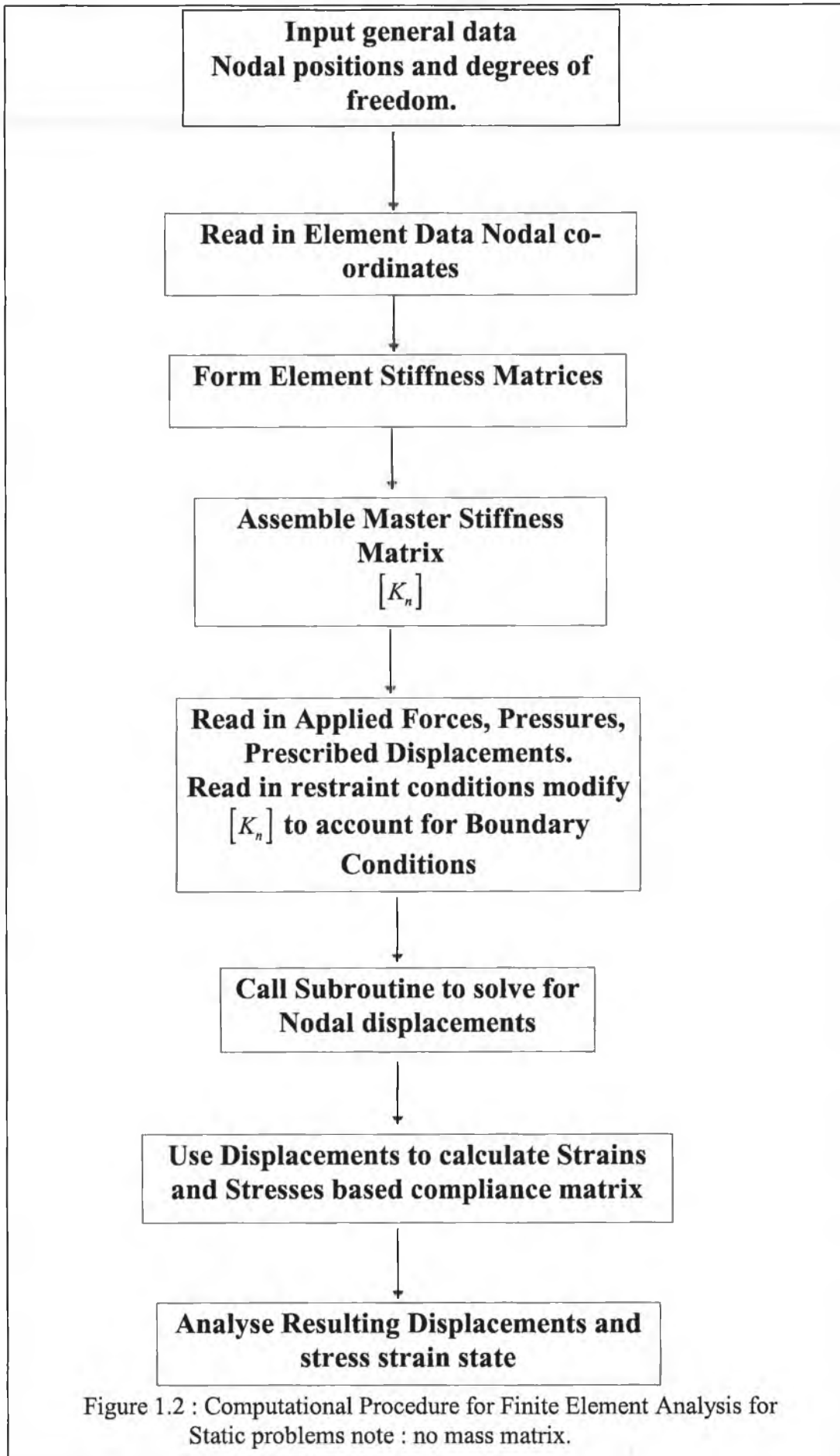


Figure 1.2 : Computational Procedure for Finite Element Analysis for Static problems note : no mass matrix.

Chapter 2 : Analytical studies in metal forming

2.1 Introduction

This chapter gives an account of the current analytical methods that are applied to validate the sheet drawing process. A study of the work to date in analysing the sheet drawing process from leading exponents is documented.

2.2 Theoretical Approach to Solutions in Metal Forming

The main objectives of metal forming theory is to predict metal deformation and the forces required to produce it. Knowledge of local stress and strain can help in predicting causes of failure in the final product. These factors govern the type of process chosen and the size of equipment required. Prior to the advent and subsequent proliferation of the finite element analysis method the major tools employed in metal forming were the highly approximate methods. The slip line analysis, slab analysis and upper bound solution were the main theoretical methods applied to metal forming. Slip line analysis is only applicable in a two dimensional case where the subject is undergoing plane strain [2.1]. Upper bound solution and slab analysis is applicable in two dimensional plane stress, plane strain and axi symmetric conditions [2.2].

Working loads and the energy consumed will also be greatly influenced by appropriate selection of the process parameters, including the pass schedules(intermediate drawing operation to attain the desired drawn shape), lubrication, temperature, speed and tool profile. This work will focus primarily on pass schedules and tool profile.

2.3 Slip Line Field Theory

Slip line theory simplifies complex three dimensional metal forming problems into an analogous plane strain problem. Since plastic material tends to deform in all directions, to develop a plane strain condition it is necessary to constrain flow in one direction. This constraint is produced where only part of the material is deformed and the rigid elastic material outside the plastic region prevents the spread of deformation. Slip line field theory is based on the fact that any general state of stress in plane strain consist of pure shear plus a hydrostatic pressure. The slip line field theory for plane strain allows the determination of stresses in a plastically deformed body, when the deformation is not uniform throughout the body. In addition to requiring plane

strain conditions, the theory assumes an isotropic, homogeneous, rigid ideal plastic material. For such a non strain hardening material the shear strength k is constant.

2.4 Upper Bound Theory

Slip line field theory is very accurate if the assumed conditions are satisfied. It is however time consuming and it is often satisfactory to use a simple quick, and approximate bounding technique. The upper bound [2.3] metal forming theory divides the plastically deforming body into simple zones, usually triangular which remain rigid but are separated from adjacent triangles by lines of tangential velocity discontinuity. The implied pattern of velocities must be compatible

with the externally imposed conditions, as verified by drawing a hodograph (metal deformation velocity diagram). The applied load is assumed to advance with some fixed velocity, which may be taken as unity, thereby performing work at a fixed rate. If there are no other losses this is exactly balanced by the rate of performing work by shearing on all the discontinuities. If the length of a discontinuity is S , the shearing force F acting over it will be for unit width in plane strain, $Fu = kS$. Since the shear yield stress k is the same everywhere. If the magnitude of the velocity discontinuity is u , the rate of performing work by the force F will be $Fu = kuS$. The total rate of performing work internally is thus $\frac{dW}{dt} = \sum kuS$. The rate of performance of work externally by an applied pressure P acting on a area $l \times a$ at velocity l is simply Pa . Equating these $Pa = \sum kuS$.

There will be many possible velocity fields, but the one most likely to operate will be the one requiring the least load [u]. Once the metal starts to deform, there is no way in which the load, can rise to the level needed to operate some more resistive mode. This method is conservative in its calculation of deformation loads. The resulting force will be at least sufficient to perform the operation hence as the name implies the predicted load will be an upper bound solution.

2.5 Slab Analysis

Slab Analysis involves the division of the sheet blank geometry into zones which are exposed to similar forms of deformation. When applied to deep drawing the zones are the flange region, the

deformation zone at the tool radii and the wall deformation zone. These deformation zones are solved by conditions of equilibrium, to arrive at the local state of stress.

Slab Analysis

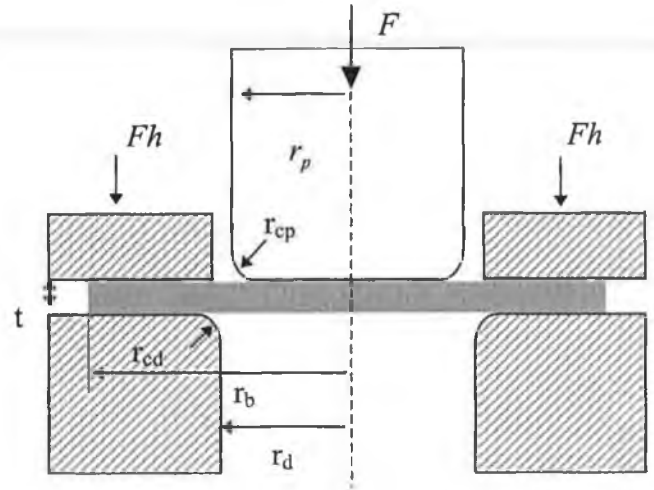


Figure 2.1 : Deep Drawing Geometry

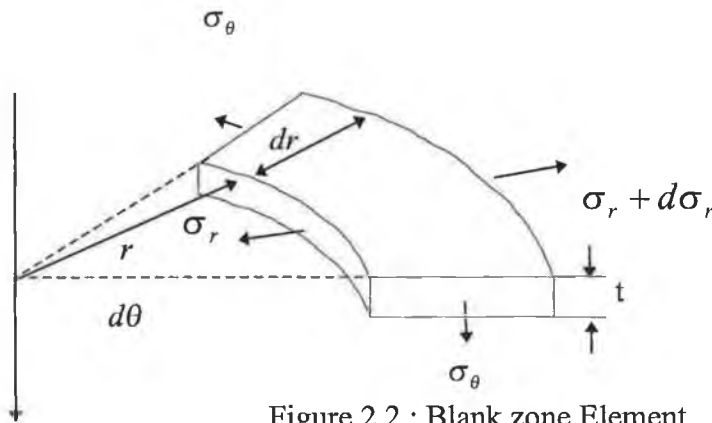


Figure 2.2 : Blank zone Element

Fh is the blankholder force

$$\text{Radial Stress due to } Fh = \sigma_r = \frac{2\mu Fh}{2\pi r_h t} \quad (1.1)$$

Consider the element in Figure 1.4 for equilibrium we have

$$r + d\sigma_r + \sigma_r dr - \sigma_\theta dr = 0 \quad (1.2)$$

Assuming σ_r and σ_θ to be principal stresses and using The Tresca yield criterion gives

$$(\sigma_r - \sigma_\theta) = 2k \quad (1.3)$$

Substituting from equation 1.3 for σ_θ into equation 1.2 Gives

$$\frac{dr}{r} + \frac{d\sigma_r}{2k} = 0 \quad (1.4)$$

Integrating equation 1.4 gives :

$$\frac{\sigma_r}{2k} = C - \ln r \quad (1.5)$$

The boundary conditions can be used to obtain an expression for the constant of integration C.

At $r=r_b$, The outer radius of the blank $\sigma_r = \frac{2\mu Fh}{2\pi r_b t}$ from equation 1.

$$\text{Therefore } C = \frac{\mu Fh}{2\pi k r_b t} + \ln r_b$$

Substituting from C into equation 1.5 Gives the general Expression

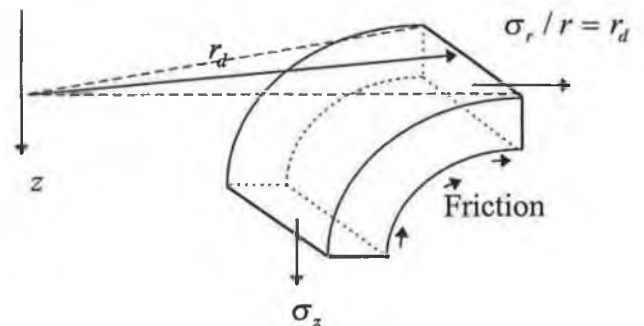
$$\frac{\sigma_r}{2k} = \frac{\mu Fh}{2\pi k r_b t} + \ln \frac{r_b}{r} \quad (1.6)$$

The radial stress at the beginning of the die corner, at $r = r_d = (r_p + t)$ is given by

$$\frac{\sigma_{rd}}{2k_{at r=rd}} = \frac{\mu Fh}{2\pi k r_b t} + \ln \frac{r_b}{r_d} \quad (1.7)$$

As the work piece is drawn over the die corner the radial stress, given by equation 1.7 is increased to σ_z . Due to the effects of frictional forces on the corner.

Effect of friction at corners



$$\frac{\sigma_z}{\sigma_{rd}} = e^{\mu \frac{\pi}{2}} \quad (1.8)$$

Figure 2.3 : Tool Radius deformation Zone

The blank holder force can be found from $Fh = \beta\pi r_b^2 k$ (1.9)

Where β lies between (0.02 – 0.08)

An estimate of the required drawing force can be obtained using equation 1.8

$$F = \sigma_z 2\pi r_p t \quad (1.1.1)$$

2.6 Conclusion

The aforementioned method of slip line field theory, upper bound theory and slab analysis do not sufficiently account for plasticity, and don't take into account the change in thickness of the blank over the drawing process. Hence they are only applicable as approximate indicators of deformation loads, (i.e. Punch forces).

Chapter 3 : Finite Element Analysis Metal Forming Theory

3.1 Introduction

This chapter introduces the concept and system equations that describe the Finite Element Method. The specialised non linearities that are present in metal forming such as, material, geometry and tool contact are introduced. Methods employed to simulate such phenomena are introduced and developed.

3.2 Finite Element Analysis of Metal Forming.

The following discussion rationalises the use of Finite Element Analysis for analysing Metal Forming processes, by comparing it with existing theory and knowledge. The main objective of metal working theory, are to predict metal deformation and the forces required to produce it. In addition a knowledge of local stress and strain can help in predicting causes of failure in the final product. These factors govern the type of process chosen and the size of equipment required. The working loads and the energy consumed will also be greatly influenced by appropriate selection of the process parameters, including the pass schedules, lubrication temperature, speed and Tool profile. This research is primarily concerned with the following process parameters, pass schedules, and Tool profiles. Many practical metal forming process are too complex for a theoretical treatment and existing empirical knowledge rules and formulas are incomplete resulting in the only effective solution being delivered by Finite Element Analysis.

Finite Element Analysis answers the above questions along with delivering solutions by establishing the kinematic relationship of shape, velocities, strains and strain rates between the deformed and un deformed part , that is to say predicting metal flow. Establishing the limits of formability or product viability that is to say determining whether it is possible to form the part without defects.

Predicting the forces and stresses necessary to execute the forming operation so that tooling and equipment can be designed or selected. Allows the study of finite element analysis on effects process variables on product quality and process economics by a simulation conducted in the virtual world of Finite Element Analysis.

3.3 Finite Element Analysis an Introduction

The finite element method is a numerical method of solving field problems in solid mechanics. The objective of approximate numerical structural analysis is to find displacement fields that minimise the potential energy for kinematically admissible fields [3.1]. The finite element method involves calculating the potential energy, as the sum of the energies of all the elements of the structure. In each element the unknown fields are represented by a linear combination of functions of spatial co-ordinates. The coefficients of this combination depend on the displacements of the nodes which belong to the element. These latter quantities constitute the unknowns of the problem (nodal unknowns or degrees of freedom). After imposing equality of nodal displacements at common nodes of elements, minimisation of the potential energy with respect to these displacements leads to a system of linear algebraic equations. Thus a problem of solving linear partial differential equations is replaced by that of solving a set of linear algebraic equations. After solving the system equations the displacement, strains and stresses at a point within the element are found.

To demonstrate the system equations are generalised by the use of a two dimension plane strain triangular element.

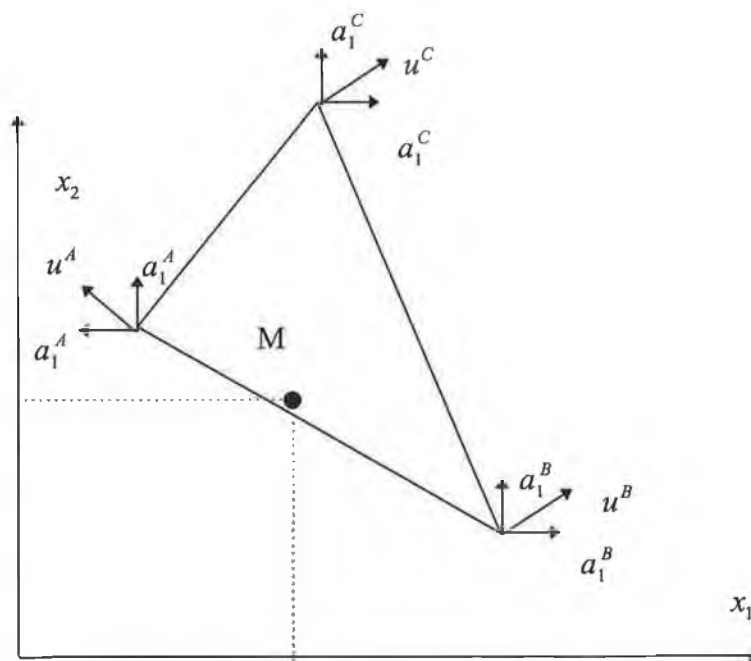


Figure 3.1 : Linear Triangular Element.

The displacement of a point M identified in Figure 3.1 by x_1, x_2 are written in the form of a column vector

$$U = \begin{bmatrix} U_1(x_1, x_2) \\ U_2(x_1, x_2) \end{bmatrix} \quad 3.1$$

The degrees of freedom of the element are the six displacement components belonging to nodes A,B,C,

$$\bar{q} = \begin{bmatrix} q_1^A \\ q_2^A \\ q_1^B \\ q_2^B \\ q_1^C \\ q_2^C \end{bmatrix} \quad 3.2$$

The unknown displacements u , can be represented by a combination of linear functions.

$$u = \begin{Bmatrix} u_1 \\ u_2 \end{Bmatrix} = \begin{Bmatrix} C_1 + C_2x_1 + C_3x_2 \\ C_4 + C_5x_1 + C_6x_2 \end{Bmatrix} \quad 3.3$$

Since at a node the displacement function u must assume values identical to the nodal displacements q , the six coefficients C_1, \dots, C_6 can be determined as linear functions of the six nodal displacements. The displacement function can then be expressed as :

$$u = \begin{Bmatrix} u_1 \\ u_2 \end{Bmatrix} = \begin{Bmatrix} N^{BC}(x_1, x_2)q_1^A + N^{CA}(x_1, x_2)q_1^B + N^{AB}(x_1, x_2)q_1^C \\ N^{BC}(x_1, x_2)q_2^A + N^{CA}(x_1, x_2)q_2^B + N^{AB}(x_1, x_2)q_2^C \end{Bmatrix} \quad 3.4$$

In the present case, the functions $N(x_1, x_2)$, called shape functions, are linear. In abridged notation, these relations may be expressed as :

$$u = Na \quad 3.5$$

The strain components, expressed as a column vector, are : in Newtonian indicial notation

$$\varepsilon = \begin{Bmatrix} \varepsilon_{11} \\ \varepsilon_{22} \\ 2\varepsilon_{12} \end{Bmatrix} = \begin{Bmatrix} u_{1,1} \\ u_{2,2} \\ u_{1,2} + u_{2,1} \end{Bmatrix} = Bq \quad 3.6$$

where B is a 3x6 matrix derived from N by differentiation. The factor 2 in the component $2\varepsilon_{12}$ is used in order to write the strain energy simply as $\sigma^T \varepsilon$ where in the case of isotropic elasticity and a state of plane stress the stress components are represented by the column vector.

$$\sigma = \begin{Bmatrix} \sigma_{11} \\ \sigma_{22} \\ \sigma_{12} \end{Bmatrix} = \frac{E}{1-\nu^2} \begin{bmatrix} 1 & \nu & 0 \\ \nu & 1 & 0 \\ 0 & 0 & \frac{1-\nu}{2} \end{bmatrix} \begin{Bmatrix} \varepsilon_{11} \\ \varepsilon_{22} \\ 2\varepsilon_{12} \end{Bmatrix} = a\varepsilon \quad 3.7$$

The equilibrium of an element is expressed by invoking the principle of virtual work with respect to an arbitrary kinematically admissible displacement field $u'(M)$ and the associated strain field $\varepsilon'(M)$. For any virtual displacement δq the sum of the internal and external work for the whole region is :

$$-\delta q^T r = \int_V \delta u^T b dV + \int_A \delta u^T t dA - \int_V \delta \varepsilon^T \sigma dV \quad 3.8$$

Where r is the applied loading vector, b is the body force, u is the nodal displacement.

In the above equations $\delta q, \delta u$, and $\delta \varepsilon$ can be completely arbitrary, providing they stem from a continuous displacement assumption. Thus the following system of algebraic equations hold

$$Ka + f = r \quad 3.9$$

$$K = \int_V B^T D B dV \quad 3.1.1$$

$$f = - \int_V N^T b dV - \int_A N^T t dA - \int_V B^T D \epsilon_0 dV + \int_V B^T \sigma_0 dV \quad 3.1.2$$

The formulation of the above equations, into the system equations, is by a variational solution of the above differential equations. The determination of the approximate solution uses a variational method, such as the Ritz method, or the Galerkin method. For linear problems, the weak formulation is equivalent to the minimisation of a quadratic functional $I(u)$ called the total potential energy in solid mechanics problems.

Finite element analysis theory and its application as computer software was born out of many advances in mathematics. These advances date back to the eighteenth century, in which pioneers in mathematics such as Lagrange Gauss Newton and Raphson contributed work that was employed in finite element analysis software. In essence their work in the earlier part of the 19th century, enables complex second order derivative equations such as stress functions to be approximated by linear quadratic lagrangian polynomials. These lagrangian polynomials in the finite element sense are refereed to as shape functions. These shape functions map the variations of a quantity, (which within the realm of our interest solid mechanics is stress) through out a discrete elemental space. The use of natural co ordinates to describe a domain and the use of variational calculus in formulating system equations, leads to a speedy implementation of finite element analysis solution on a digital computer.

The basis of the finite element analysis scheme is broken down as follows; the phenomenon to be analysed is represented over it physical space by many elements, this phase of modelling is refereed to as discretisation. The governing equations for the element are found by application of variational calculus. This general governing equation is provided by the shape functions of the element, which combine with the compliance matrix to give a elemental matrix referred to as the stiffness matrix. The next stage of solution is the formulation of the global stiffness matrix. This simply takes the form of assigning nodal points, represented as co efficient within the stiffens matrix. Put more simply the calculations of the equations for each occurrence of that element in the body, is simply, a task of substituting the nodal co-ordinates, of each element into the

general format. This stage is referred to as assemblage. Boundary conditions and loading are applied to these assembled equations to develop the system equations as outline above.

3.4 Introduction to Non Linear Finite Element Analysis.

As seen from section 3.2 linear finite elements establish the equilibrium equations as a relation between the applied loads f , stiffness matrix k , nodal displacements a and q the internal force.

$$Ka + f = 0 \quad 3.1.3$$

$$Ka = q \quad 3.1.4$$

$$K = \int_V B^T DB dV \quad 3.1.5$$

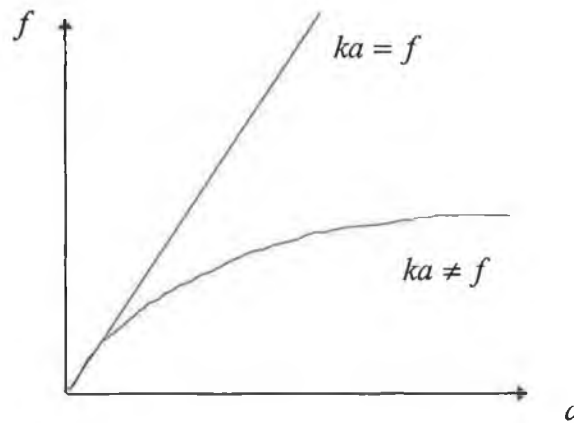


Figure 3.2 : Linear and non-linear element problem

If the displacement is known the external load follows directly from Equation 3.1.2, if the external load is prescribed the inverse relation must be determined. For linear problems the unknown displacement can be found explicitly by solving a system of linear equation of similar type to Equation 3.1.3.

For non-linear systems the internal force q is no longer a linear relationship. Thus it is necessary to solve the problem over a number of load steps $\Delta f_1, \Delta f_2$, where the corresponding displacement increments, $\Delta a_1, \Delta a_2$, are determined. Solution of non-linear finite element equations is based on a predictor-corrector strategy, that consist of three actions within a load step. The stages are prediction of the first displacement increment, a test of whether equilibrium

has been obtained and a strategy for correcting the first increment. When the applied forces and reactions are in equilibrium an additional load increment, Δf , is applied. A first estimate on the displacement, Δa_1 , is found by solving a linear tangent stiffness relation, of the form $K_t \Delta a_1 = \Delta f$. The tangent stiffness matrix, K_t , can be dependent on the current displacement, a , the current stress, σ and the preceding load history expressed by the state variable, α . Therefore the tangent stiffness matrix, K_t , is dependent on material displacement, stress state, and the state variable. i.e. $K_t = K_t(a, \sigma, \alpha)$. It is, however, often possible to distinguish between two types of non-linearity, geometrically non linear problems it is the generalised displacement gradient $a \bar{\nabla}$, that is non linear. The tangent stiffness thus becomes

$$K_t(a) = \int_V B^T(a) D B(a) dV \quad 3.1.6$$

In material non-linear problems it is the relation between the strain and stress that introduces the non-linearity. The material model is described by the constitutive matrix, C , giving the following tangent stiffness.

$$K_t(a, \sigma, \alpha) = \int_V B^T C(a, \sigma, \alpha) B dV \quad 3.1.7$$

The next step in the solution procedure is to verify whether the estimate corresponds to an equilibrium state, for this purpose the internal force has to be evaluated on the basis of the current displacement estimate. The computation of the internal force can be divided in two types of problem. In the first type of problem the internal force q , can be evaluated explicitly from the estimated displacement, a . This type of problem includes non linear, path independent material models, such as non-linear elasticity. The strain ε , is found from the displacement estimate, $\varepsilon = B a$, thus the internal force can be evaluated explicitly, as $\sigma = C(\varepsilon) \varepsilon$.

Path dependent material models, such as the elastic-plasticity, constitute the other class of non-linear problems. For such materials the stress in a point is dependent on the strain and stress history and therefore it is not possible to express the constitutive behaviour in terms of the total strain and stress. Instead an incremental formulation must be used. For rate independent materials the relation between the strain increment, $d\varepsilon$, and the stress increment, $d\sigma$, is given by a tangent stiffness relation. $d\sigma = C(\sigma, \varepsilon, \alpha) d\varepsilon$. The incremental tangent stiffness C , depends on

the current stress and strain, and on the stress history expressed in terms of some state variable, α . These are also path dependent and the evolution of the state variables must be formulated on an incremental form. The internal force, q , is found by integration of the total stress, σ , over the element. Because the constitutive behaviour is path dependent the stress at a point is found by integrating the incremental relation, and the state variable, α , over the complete load history. In practice this means that the load must be applied in a number of increments, each followed by equilibrium iterations. Within an iteration the finite stress increment, $\Delta\sigma$, and the increment in the state variables, $\Delta\alpha$, are evaluated from the estimated strain increment, $\Delta\varepsilon$. Having obtained convergence the total stress and state variables are updated by their increments.

Solution of non-linear problems with path dependent material models thus consists of two iteration levels; namely the global equilibrium iterations that determines the displacement, a , and iterations on point level within each element to integrate the stress, σ , and state variable, α for the estimated strain increment.

If the estimate does not represent equilibrium there must be a strategy for correcting it. The residual, which is the unbalance between the internal force and the external load, is usually the main component in the strategy. The residual may be regarded as that part of the load that has not yet produced any displacement. Its contribution to the displacement increment is found by solving another linear stiffness relation. Additional provisions such as restrictions on the magnitude of displacement increment and modifications of the external load can be employed to make the solution algorithm more robust. Evaluation of the residual and computation of corrector is termed equilibrium iterations. These are continued until the residual is smaller than a prescribed tolerance limit.

3.5 Solution Schemes of Non linear Finite Element Analysis

3.5.1 Newton Raphson

The solution of non-linear finite element problems usually consists of a series of load steps, each involving iterations to establish equilibrium at the new load level. Each converged load step marks a point on the equilibrium path of Figure 3.3.

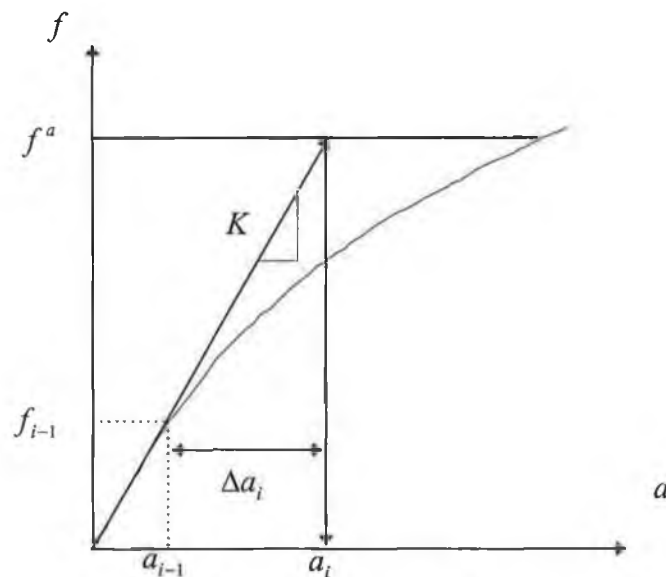


Figure 3.3 : Newton Raphson Scheme

Assuming that an equilibrium point (a_{n-1}, f_{n-1}) , has been established, a new load increment, Δf_1 , is applied. A first estimate on the increment, Δa_1 , is obtained by solving a system of linear equations.

$$K\Delta a_1 = \Delta f_1 \quad 3.1.8$$

Where K is a representative incremental stiffness matrix. Because the relation 3.1.3 is non-linear the first increment does not represent an equilibrium state and iterations must be performed in

order to determine the next point on the equilibrium path. The iterations may involve changes in both the displacement and the load increments. For iteration I the increment, Δa_i and Δf_i are modified by the sub increments, δa_i and δf_i as :

$$\begin{aligned}\Delta a_i &= \Delta a_{i-1} + \delta a_i \\ \Delta f_i &= \Delta f_{i-1} + \delta f_i\end{aligned}\quad 3.1.9$$

If the estimate, $(a_{n-1} + \Delta a_i)$, does not satisfy the equilibrium equation, there exists an unbalance between the internal force and the external load. This unbalance is termed the residual , r , and is defined as :

$$r_i = f_{n-1} + \Delta f_i - q(a_{n-1} + \Delta a_i) \quad 3.2.1$$

The residual, r_i , is usually the main component in the correction of the displacement increment in the following iteration. The residual, r_{i-1} , thus gives the sub increment, δa_i that can be found by solving an incremental stiffness relationship.

$$K\delta a_i = r_{i-1} \quad 3.2.2$$

Where K is a representative stiffens matrix. The residual scales the sub increment δa , and the stiffness matrix determines the direction of the correction.



3.6 Convergence Criteria

The iteration process described in the previous section continues until convergence is achieved. Convergence is assumed when the following condition is satisfied.

$$\|r\| < e_r r_{ref} \quad (\text{Out of Balance Force Convergence}) \quad 3.2.3$$

$$\begin{aligned}r &= f - q \quad (\text{Out of Balance Force}) \\ \| \Delta a_i \| &< e_a a_{ref} \quad (\text{Displacement increment Convergence})\end{aligned}\quad 3.2.4$$

Where e_r and e_a are “Tolerances” usually specified by the user of the FEA program. $\| \|$ is a vector norm, a scalar measure of the magnitude of the vector. Convergence is obtained when the size of the residual (amount of out of balance) is less than the “Tolerance” times a reference

value and/or when the displacement increment is less than a reference value. In the ANSYS FEA program the default is to use “out of balance” convergence checking only. For metal forming simulation where large displacements are inherently present, it is strongly recommended to activate both force and displacement convergence checking to ensure simulation accuracy. Typically the default tolerance value is about 0.1% for both e_r and e_u . For metal forming applications this work has found that a force convergence tolerance of 5%, lead to more acceptable solution times, with respect to convergence. While still maintaining process simulation validity.

3.6.1 Adaptive Descent

Adaptive Descent is a convergence enhancement method for non linear problems.

Adaptive Descent is a technique which switches to a “stiffer” matrix if convergence difficulties are encountered, and then switches back to the full tangent matrix as the solution converges. This approach tends to promote a rapid convergence rate. The stiff matrix is termed the secant matrix. The methods stiffness matrix is composed of the secant matrix and the full tangent matrix as outlined below.

$$[K_i^T] = \xi[K^S] + (1 - \xi)[K^T] \quad 3.2.5$$

Where : $[K^S]$ = The Secant Matrix

$[K^T]$ = The Tangent Matrix

ξ = The Descent Parameter $0 \leq \xi \leq 1$

The adaptive descent procedure is that the algorithm adaptively adjusts the descent parameter, ξ , during the equilibrium iterations as follows. At the start of each sub step the tangent matrix is used as, ξ , is set at zero. The residual is monitored over the equilibrium iterations. If the residual increases this indicates a divergence in solution, ξ , is set to 1 and the iteration is redone using the secant matrix. If the residual has decreased for a number of iterations in a row, ξ , is further reduced until its value is set at zero. At which time only the tangent matrix is used. If a negative main diagonal indicating an ill conditioned matrix is encountered the descent parameter, ξ , is again set to 1, the equilibrium iteration is redone using the secant matrix. The non linearities

which make use of adaptive decent include : Plasticity, Contact, large strains of which there is abundance in the field of metal forming simulation.

3.6.2 Line Search

Line Search is a convergence enhancement method for non linear problems. The Line Search method is used to improve on the Newton Raphson solution $\{\Delta u_i\}$ by scaling the solution vector by a scalar value termed the line search parameter. The line search parameter is obtained by minimising the energy of the system, which reduces to finding the zero of the non linear equation :

$$g_s = \{\Delta u_i\}^T \left(\{f\} - \{r(s\{\Delta u_i\})\} \right) \quad 3.2.6$$

where : s is the line search parameter

Iterations are continued until either g_s is less than $0.5 g_o$; g_s is not changing significantly between iterations. or Six iterations have been performed.

If $g_o > 0$, no iterations are performed and S is set to 1. S cannot fall below 0.05. The scaled solution $\{s\Delta u_i\}$ is used to update the current degree of freedom values $\{a_{i+1}\}$ and the next equilibrium iteration is performed.

3.7 Conclusion

This chapter has developed an understanding of the finite element method. Introduced and comprehensively explained the theory and methods applied by the F.E.A. software to simulate the metal forming process. A discussion of the above method when applied to metal forming within the F.E.A simulations conducted for this thesis is presented in section 5.10 F.E.A solution Convergence Enhancement.

Chapter 4 : Plasticity Theory

4.1 Introduction.

This Chapter explains the phenomenon of plasticity in metallic materials. The theory behind rate independent plasticity is developed. The anisotropic effect of sheet metal blanks is introduced and a model to account for this is presented.

4.2 Plasticity a Historical Outline [4.1]

Plasticity is the term given to the mathematical study of stress and strain in plastically deformed solids. The scientific study of plasticity of metals began in 1864 when Tresca published a preliminary account of experiments on punching and extruding of Metal. Which lead to his proclamation that a metal loaded plastically, when the maximum shear stress attained a critical value. Earlier work on plastic solids had been conducted by coulomb in 1773 Poncelet 1840 and Rankin in 1853 but it was restricted to the calculation of earth pressure on retaining walls. Tresca's yield criterion was applied by saint-Venant to determine the stresses in a plastic cylinder subject to torsion or bending in 1870 and in a completely plastic tube expanded by internal pressure in 1872 . Saint- Venant developed a system of equations governing the stresses and strains in two dimensional flow, stated that the relationship between stress and total plastic strain is non linear, he postulated that the direction of maximum shear strain rate coincided with the direction of maximum shear stress.

In 1871 Levy adopting saint Venants conception of an ideal plastic material, proposed three dimensional relations between stress and rate of plastic strain. At the dawn of the 20th century further experimental work lead to different conclusion and various yield criteria were suggested to deal with this, the most satisfactory was that of von Mises in 1913. Hencky applied von Mises work and stated that yielding occurred when the elastic shear strain energy reached a critical value. In 1920-1921 Prandtl showed that the two dimensional plastic problem is a hyperbolic from Hencky 1923 discovered simple geometrical properties of the field of slip-lines in a state of plane plastic strain. Work accounting for the variation of velocity across slip-line was developed by Geiringer in 1930. The effective application of plastic theory to technological processes began in 1925 when von Karman analysed, by an elementary method, the state of stress in rolling. In the following year Siebel put forward similar theories for wire drawing . It was not

until 1926 , when Lobe measured the deformation of tubes of various metals under combined tension and internal pressure, that the Levy Mises stress strain relations were shown to be valid . The theory was now generalised in two important directions first by Reuss in 1930 who made allowance for the elastic component of strain , following a earlier suggestion by Prandtl and secondly by Schmidt 1932 and Odquist 1933 who showed in slightly different ways, how work hardening could be brought within the frame work of the Levy-Mises equations.

Historically it has been proven by Reuss that during plastic deformation the strain increment $d\varepsilon$, produced at any instant in the process is directly related to the deviatoric stress σ' . Reuss assumed a direct proportionality between the deviatoric stress and the plastic strain increment as follows

$$d\varepsilon_p \propto \sigma' \quad : \quad d\varepsilon_x = \sigma'_x d\lambda \quad 4.1$$

Using the Ruess assumption, we can write, for plastic deformation

$$\left(d\varepsilon_{ij}\right)_p = \sigma'_{ij} d\lambda \quad 4.2$$

This equation is known as the Levy-Mises equation or flow rule.

When the elastic and plastic components of deformation are combined, while retaining the separation of the change in size and the change in shape then the following Prandtl-Reuss equations are developed.

$$\text{Shape Change } d\varepsilon'_{ij} = \left(d\varepsilon_{ij}\right)_p + \left(d\varepsilon_{ij}\right)_E = \sigma'_{ij} d\lambda + \frac{d\sigma'_{ij}}{2G} \quad 4.3$$

$$\text{Volume Change } d\varepsilon_{ii} = \left(d\varepsilon_{ii}\right)_p + \left(d\varepsilon_{ii}\right)_E = 0 + \frac{(1-2\nu)}{E} d\sigma_{ii} \quad 4.4$$

These are the Prandtl-Reuss equations and they can be used to define the transition between fully elastic and elastic/plastic behaviour of a material.

4.3 Plasticity Material Non-linearities

Material non linearities are due to the non-linear relationship between stress and strain, that is, the stress is a non linear function of strain. The relationship can be path dependent, so that the stress depends on the strain history as well as the magnitude of the strain itself. The materials that are analysed in this thesis are rate independent plasticity.

4.3.1 Rate independent plasticity

Rate independent plasticity is characterised by the irreversible straining that occurs in a material once a certain level of stress is reached. The plastic strains are assumed to develop instantaneously, that is, independent of time. There are a number of ways to characterise different types of material behaviour, such as :

- Bilinear Kinematic Hardening.
- Multilinear Kinematic Hardening.
- Bilinear Isotropic Hardening.
- Multilinear Isotropic Hardening.
- Power Law Plasticity
- Anisotropy.

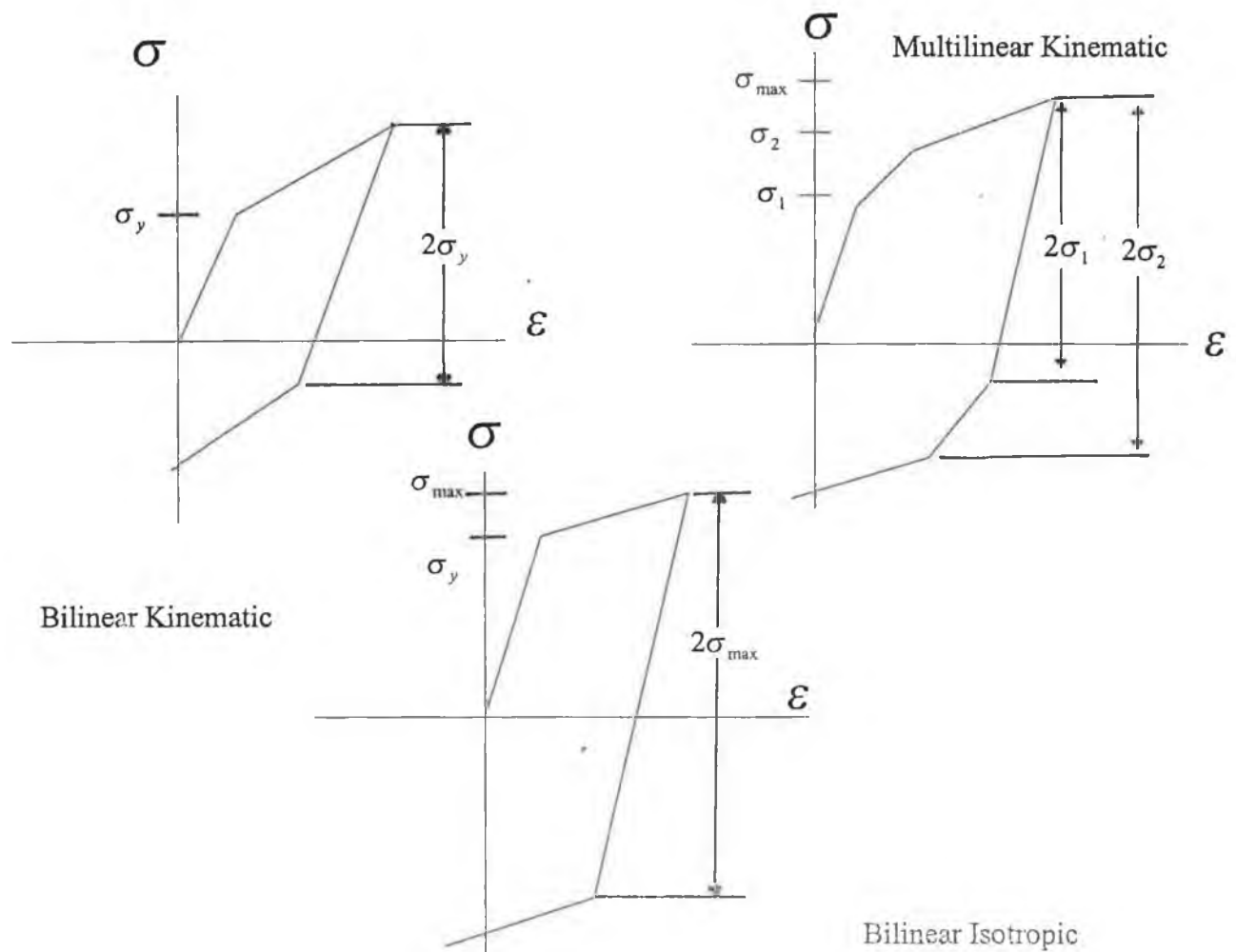


Figure 4.1: Stress-Strain Behaviour of each of the Plasticity Options

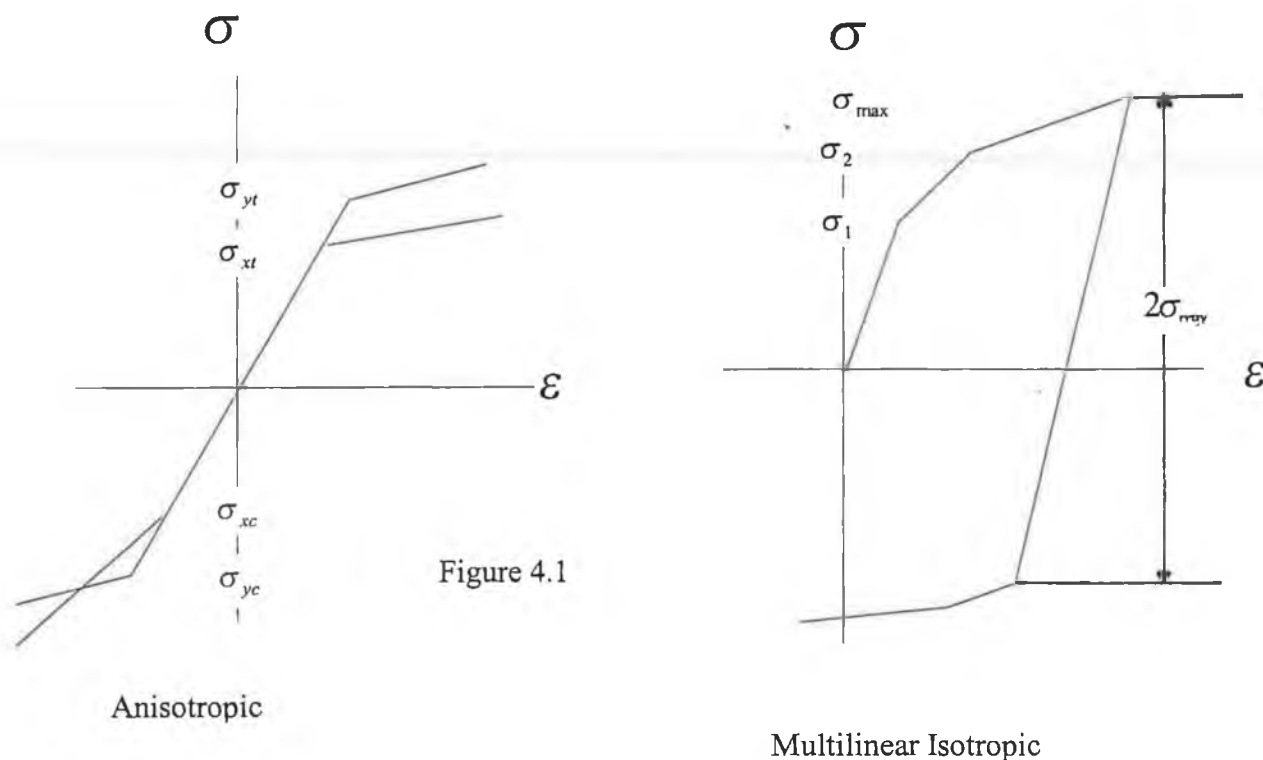


Figure 4.1

4.3.1.1 Bilinear/ Multilinear Isotropic Hardening.

The stress strain relationship is described by two straight lines for the Bilinear option and many straight lines for the Multilinear option as can be seen from figure 4.1. The strain hardening level sets the current yield stress level on the stress strain curve. For the isotropic cases the strain hardening level is computed from the evolution of the yield surface which expands about the deviatoric stress axis.

4.3.1.2 Bilinear/ Multilinear Kinematic Hardening.

The stress strain relationship is described by two straight lines for the Bilinear option and many straight lines for the Multilinear option as can be seen from figure 4.1. The strain hardening level sets the current yield stress level on the stress strain curve. For the kinematic cases the strain hardening level is computed from the evolution of the yield surface which is translated about the deviatoric stress axis.

4.3.1.3 Power Law Plasticity

The stress strain relationship is described by a straight line up to the yield stress, the plastic segment of the stress strain curve is described by an exponential relationship.

4.3.1.4 Anisotropy.

Due to the fact that tensile properties of sheet material may vary with direction, anisotropy models use information from tests conducted in different directions to formulate the yield stress.

In sheet metal forming applications the material models that more closely map the actual Metal behaviour are the power law plasticity options. However bilinear/ multilinear kinematic and bilinear/ multilinear isotropic hardening can be used as an approximate for some sheet metal models.

4.4 Plasticity Theory

Plasticity Theory provides a mathematical relationship that characterises the elasto-plastic, response of materials. There are three main features of rate-independent plasticity theory.

1. The Yield Criterion.
2. The Material Flow Rule.
3. The Material Hardening Rule.

4.4.1 Yield Criterion

The Yield Criterion determines the stress levels at which yielding occurs and when plastic deformation is initiated. In the case of a material simultaneously subjected to a number of stresses as in the metal forming process. The overall stress state of the material can be expressed as a function of the individual stress component $f\{\sigma\}$ generally referred to as the “Equivalent Stress”, “Effective Stress”, or “Generalised Stress”, σ_e . In terms of principal stresses the equivalent stress can be written as :

$$\sigma_e = f\{\sigma\} = \sqrt{\frac{1}{2}\{(\sigma_1 - \sigma_2)^2 + (\sigma_2 - \sigma_3)^2 + (\sigma_3 - \sigma_1)^2\}} \quad 4.5$$

When the equivalent stress is numerically equal to the material yield stress, σ_y , the material will yield and develop plastic strains.

$$\text{Plastic deformation occurs when } \sigma_e = f\{\sigma\} = \sigma_y \quad 4.6$$

If σ_e is less than σ_y , the material is elastic and the stresses will develop according to the elastic stress strain relationship. The equivalent stress can never exceed the yield stress of the material, because, plastic strains develop instantaneously, thereby reducing the stress state to the yield stress of the material.

4.4.2 Yield Surface

The Yield equation expressed in Equation 4.6 can be plotted in stress space to represent different types of material behaviour. These surfaces are known as yield surfaces, and any stress state inside a surface is elastic, and this stress state will not produce plastic strain. Any combination

of stresses which sits on the yield surface will produce yielding and plastic strains will then be generated.

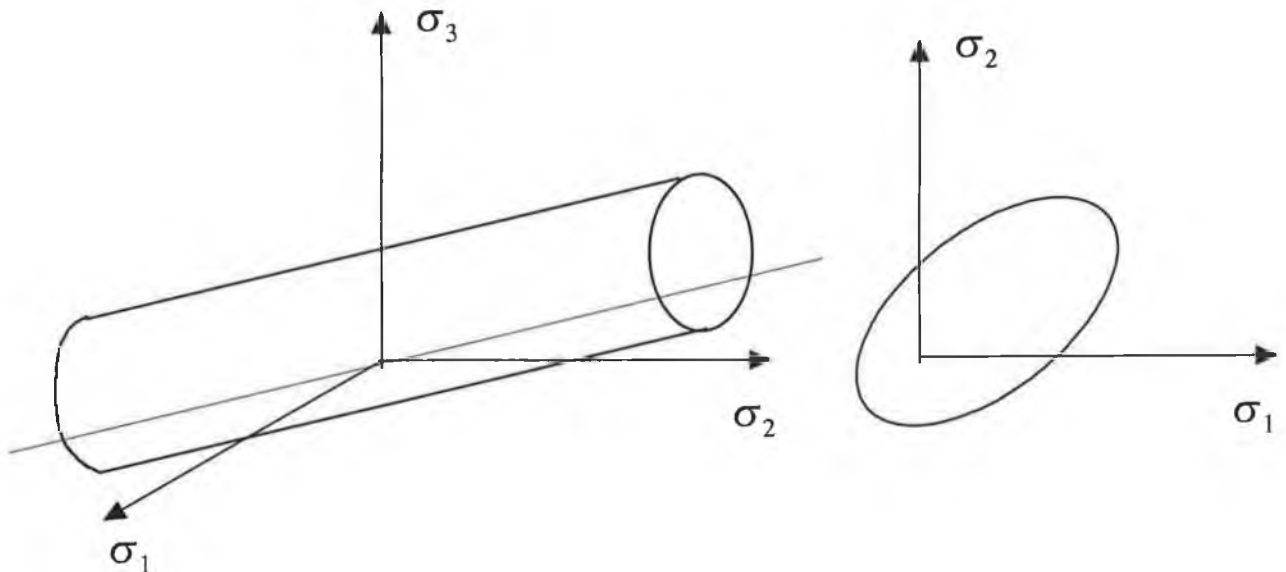


Figure 4.2: Yield Surface for Kinematic Hardening

4.4.3 Flow Rule

The Flow Rule determines the direction of plastic straining and is given by the expression :

$$\{d\epsilon^p\} = \lambda \left\{ \frac{\partial Q}{\partial \sigma} \right\} \quad 4.7$$

Where : λ = A plastic multiplier, this determines the amount of plastic straining.

$\{d\epsilon^p\}$ = The incremental plastic strain.

$\left\{ \frac{\partial Q}{\partial \sigma} \right\}$ = determines the direction of plastic straining.

Q = A function of the stress known as the plastic potential.

If $Q = F$, Since the yield function is generally assumed to be so. The flow rule is termed associative, and the plastic strains occur in the direction normal to the yield surface. When this

relationship is not satisfied the plasticity is termed non associative. This work is consider only with associative plasticity.

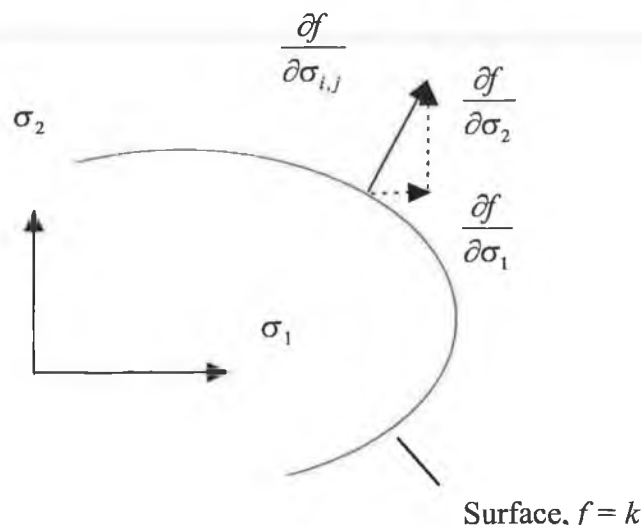


Figure 4.3 : Geometric representation of the normality rule of associated plasticity

4.4.4 Hardening Rule

The Hardening Rule describes the change in the yield surface with progressive yielding, so that the stress state for subsequent yielding can be established. Hardening rules are divided into isotropic and kinematic hardening.

In Isotropic hardening the yield surface remains centred about its initial centre line and expands in size as the plastic strains develop.

Kinematic hardening assumes that the size of the yield surface remains constant but translates in stress space with progressive yielding, as shown in Figure 4.4.

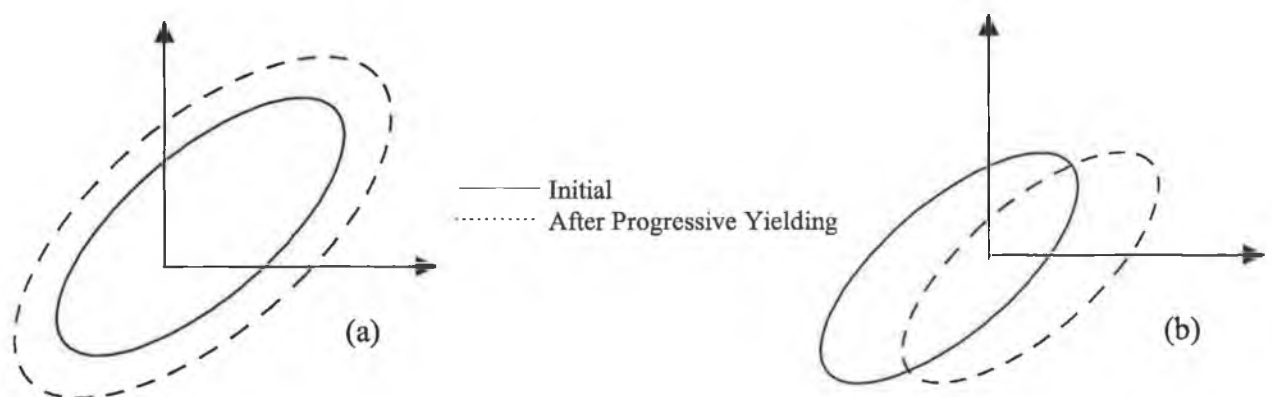


Figure 4.4 : Hardening rules (a) Isotropic work hardening ,(b) Kinematic hardening

4.4.5 Plastic Strain Increment

If the equivalent stress, σ_e , which is computed using the elastic properties, exceeds the material yield stress, σ_y , then plastic straining must occur. Plastic strains reduce the stress state, so that it satisfies the yield criterion, Equation 4.8.

$$f\{\sigma\} = \sigma_y \quad 4.8$$

The hardening rule states that the yield criterion changes with work hardening. If these dependencies are accounted for then Equation 4.8 represents the yield criterion. Alternatively the yield function is modified and written in the form :

$$F = (\{\sigma\}, \chi, \{\alpha\}) = 0 \quad 4.9$$

where : $\chi = \text{plastic work}$
 $\{\alpha\} = \text{The Translation of the yield surface}$

The terms χ and $\{\alpha\}$ are referred to as internal or state variables. The plastic work χ represents the sum of the plastic work performed over the history of the loading.

$$\chi = \int \{\sigma\}^T \{d\varepsilon^p\} \quad 4.1.1$$

The translation of the yield surface due to plastic deformation is also history dependent and is given as :

$$\{\alpha\} = \int C \{d\varepsilon^p\} \quad 4.1.2$$

Where C is a material parameter. $\{\alpha\}$ represents the location of the centre of the yield surfaces, and moves in the direction of plastic straining.

The yield function F, modified to take account of both plastic work and yield surface translation as given by equation 4.9 can be differentiated to give a minimum energy state :

$$dF = \left\{ \frac{\delta F}{\delta \sigma} \right\}^T \{d\sigma\} + \left\{ \frac{\delta F}{\delta \chi} \right\} d\chi + \left\{ \frac{\delta F}{\delta \alpha} \right\}^T \{d\alpha\} = 0 \quad 4.1.3$$

Equation 4.1.3 is called the plastic consistency condition.

From Equation 4.1.1 $d\chi = \{\sigma\}^T \{d\varepsilon^p\}$, and from equation 4.1.2 $\{d\alpha\} = C \{d\varepsilon^p\}$

Substituting these expressions into Equation 4.1.3 gives

$$\left\{ \frac{\delta F}{\delta \sigma} \right\}^T \{d\sigma\} + \frac{\delta F}{\delta \chi} \{\sigma\}^T \{d\varepsilon^p\} + \left\{ \frac{\delta F}{\delta \alpha} \right\}^T C \{d\varepsilon^p\} = 0 \quad 4.1.4$$

The stress increment $\{d\sigma\}$, can be computed from the elastic stress - strain relationships.

$$\{d\sigma\} = [D]\{d\varepsilon^e\} \quad 4.1.5$$

$$\text{but : } \{d\varepsilon^e\} = \{d\varepsilon\} - \{d\varepsilon^p\} \quad 4.1.5$$

Since the total strain increment $\{d\varepsilon\}$ can be divided into elastic and a plastic part.

Substituting Equation 4.9 into Equation 4.1.4 and 4.1.5 and combining Equation 4.1.4, 4.1.5 yields.

$$\lambda = \frac{\left\{ \frac{\delta F}{\delta \sigma} \right\}^T [D]\{d\varepsilon\}}{-\frac{\delta F}{\delta \chi} \{\sigma\}^T \left\{ \frac{\delta Q}{\delta \alpha} \right\} - C \left\{ \frac{\delta F}{\delta \alpha} \right\}^T \left\{ \frac{\delta Q}{\delta \sigma} \right\} + \left\{ \frac{\delta F}{\delta \sigma} \right\}^T [D] \left\{ \frac{\delta Q}{\delta \sigma} \right\}} \quad 4.1.6$$

The size of the plastic strain increment is therefore related to the total strain, $\{d\varepsilon\}$, the current stress state, $\{d\sigma\}$, and the specific terms of the yield and potential surfaces, χ , α , and C .

The plastic strains increment can now be obtained from the expression

$$\{d\varepsilon^p\} = \lambda \left\{ \frac{\delta Q}{\delta \sigma} \right\} \quad 4.1.7$$

$$[D^p] = [D^e] - \sigma'_{II} \quad 4.2.1$$

Where G is the shear modulus, $\sigma'_x, \sigma'_y, \sigma'_z$ are Deviatoric stresses and $\tau_{xy}, \tau_{xz}, \tau_{yz}$ are shear stresses S_e is from

$$S_e = \frac{2\sigma^2}{3} \left[\frac{H'}{3G} + 1 \right] \quad 4.2.2$$

4.5 Stress and Strain indicators for Metal forming.

A value of stress that is not variant in a changing co ordinate system, is provided by “General stress”, “Equivalent Stress” or “Effective Stress.

$$\sigma_e = \bar{\sigma} = \sqrt{\frac{1}{2} \left\{ (\sigma_1 - \sigma_2)^2 + (\sigma_2 - \sigma_3)^2 + (\sigma_3 - \sigma_1)^2 \right\}} \quad 4.2.3$$

In Equation 4.2.3 the general stress is expressed as a function of the principle stress, as is used for the von Mises yield criterion of Equation 4.5. The expression for the general stress in Equation 4.2.3 is based on the deviatoric stress state. In the same manner expressions for generalised strain can be developed. Of interest to metal forming is the “Equivalent Plastic Stress” and “Equivalent Plastic Strain”. High levels of equivalent plastic strain indicate areas of draw failure, due to rupture as a result of localised necking of material.

4.6 Introduction to Predictor Corrector Scheme

The explicit and implicit schemes evaluate a stress that does not lie on the yield surface. The predictor corrector scheme acts to correct this via a return mapping algorithm. The return mapping algorithm utilises iterations to ensure that the final stress fulfils the yield condition. The return mapping algorithm determines the stress increment $\Delta\sigma$. Initially an elastic predictor $\sigma_0 + \Delta\sigma^e$, is evaluated. The plastic correction $\Delta\sigma^p$, is then calculated in the updated point. This returns the stress along the gradient radically towards the yield surface, see Figure 4.5. As the yield surfaces in the two points are concentric circles the gradient is the same in the two points, the direction of the plastic correction is thus constant and only the magnitude, $\Delta\lambda$, which depends on the hardening modulus, H , remains to be determined.

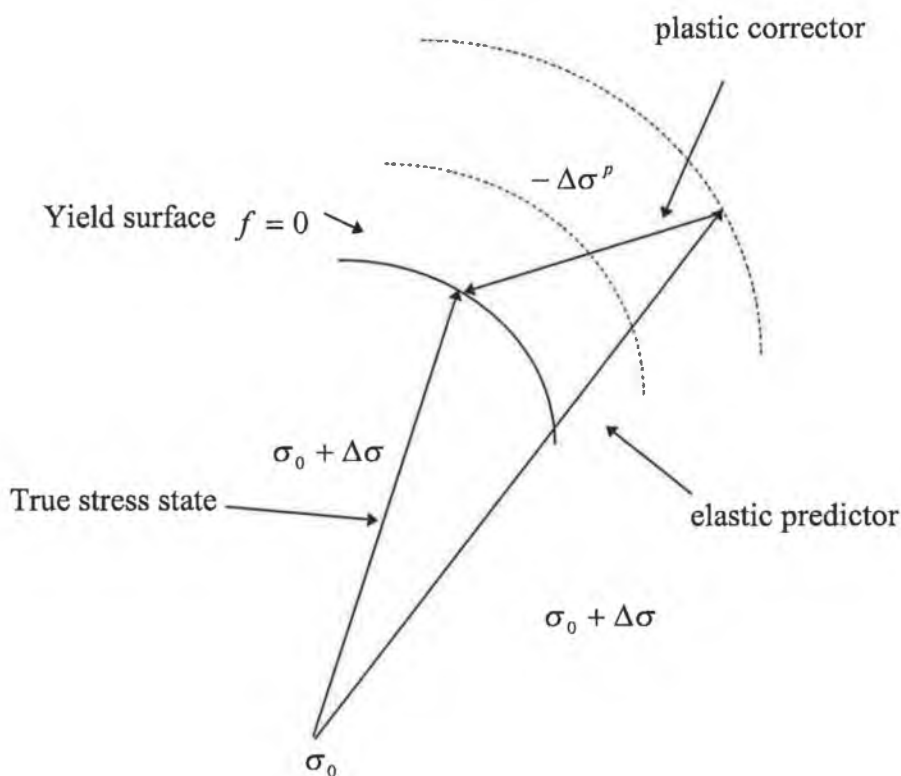


Figure 4.5: Backward Euler scheme: Return mapping

4.6.1 Implementation of the plastic consistency condition via a predictor corrector algorithm

An Euler backward scheme is used to enforce the plastic consistency condition as presented by equation 4.1.3. This ensures that the updated stress, strains and internal state variables are on the yield surface. The algorithm is as follows :

1. The material yield stress σ_y , given by Equation 4.8, is determined for this time step i.e. the yield stress for the current load step.
2. The stresses are computed based on a trial Strain $\{\varepsilon^{tr}\}$, which is the total strain minus the plastic strain from the previous increment or time point.

$$\{\varepsilon_n^{tr}\} = \{\varepsilon_n\} - \{\varepsilon_{n-1}^p\} \quad 4.2.4$$

n is the current time step, $n-1$ is the previous time step.

The trial stress can be calculated using Equation (4.2.5).

$$\{\sigma^{tr}\} = [D]\{\varepsilon^{tr}\} \quad 4.2.5$$

3. The Equivalent Stress σ_e , is evaluated at this stress level using equation 4.2.4. If σ_e is less than σ_y the material is elastic and no plastic strain increments are computed.
4. If σ_e exceeds the material yield stress, the plastic multiplier λ , is determined from equation 4.1.6 using a local Newton- Raphson iteration procedure.
5. The plastic strain increment $\{d\varepsilon^p\}$ is calculated from Equation 4.1.7.
6. The current plastic strain is updated using the expression

$$\{\varepsilon_n^p\} = \{\varepsilon_{n-1}^p\} + \{d\varepsilon^p\} \quad 4.2.6$$

and the elastic strain is obtained from the expression

$$\{\varepsilon^e\} = \{\varepsilon^{tr}\} - \{d\varepsilon^p\} \quad 4.2.7$$

7. The increment in the plastic work $\Delta\chi$, and the centre of the yield surface $\Delta\alpha$ are computed from the differentials of equation 4.1.1 and 4.1.2.

$$\Delta\chi = \{\sigma\}^T \{d\varepsilon^p\} \quad 4.2.8$$

$$\{\Delta\alpha\} = C\{d\varepsilon^p\} \quad 4.2.9$$

8. The current values for the plastic work and the centre of the yield surface are updated using the expressions:

$$\chi_n = \chi_{n-1} + \Delta\chi \quad 4.3.1$$

and

$$\{\alpha_n\} = \{\alpha_{n-1}\} + \{\Delta\alpha\} \quad 4.3.2$$

9. For output purposes, the equivalent plastic strain ε^p , the equivalent plastic strain increment $\Delta\varepsilon^p$, the equivalent stress σ_e , and the stress ratio N, are computed.

The stress ratio is expressed as $N = \frac{\sigma_e}{\sigma_y}$ 4.3.3

Where σ_e is evaluated using the trial stress $\{\sigma^r\}$. Therefore N is equal to or greater than one when plastic yielding is occurring and less than one when the stress is elastic.

The equivalent plastic strain increment is given as :

$$\Delta\varepsilon^p = \left(\frac{2}{3} \{\Delta\varepsilon^p\}^T \{\Delta\varepsilon^p\} \right) \quad 4.3.4$$

The equivalent plastic stress and strain parameters are used in various analysis option provided in the ANSYS elasto-plastic algorithm and many elasto-plastic finite element packages.

4.7 Anisotropy

The tensile properties of sheet material are not the same in all directions. This dependence of properties on orientation is called anisotropy. The type of anisotropy attributed to sheet metal is termed crystallographic anisotropy [4.3], which results from the preferred orientation of the grains which is produced by severe plastic deformation during manufacture. Since the strength of a single crystal is highly anisotropic, a severe deformation which produces a strong preferred orientation will cause a polycrystalline specimen to approach the anisotropy of a single crystal. The yield strength and to a lesser extent the tensile strength, are the properties most affected. The yield strength in the direction perpendicular to the main direction of working may be greater or less than the yield strength in the longitudinal direction, depending on the type of preferred orientation which exists. This type of anisotropy is most frequently found in non ferrous metals, especially when they have been severely worked into sheet. Practical manifestations of crystallographic anisotropy is the formation of ears or non uniform deformation in deep draw cups, or elliptical deformation of a tensile specimen.

4.7.1 Anisotropy in yielding

The yield criteria considered so far assume that the material is isotropic. While this may be the case at the start of plastic deformation, it certainly is no longer a valid assumption after the metal has undergone appreciable plastic deformation. The von Mises criterion as formulated in section 4.4.1 would not be valid for a highly orientated cold rolled sheet.

Hill [4.4] has formulated the von Mises yield criterion for an anisotropic material having orthotropic symmetry.

$$F(\sigma_y - \sigma_z)^2 + G(\sigma_z - \sigma_x)^2 + H(\sigma_x - \sigma_y)^2 + 2L\tau_{yz}^2 + 2M = 0 \quad 4.3.5$$

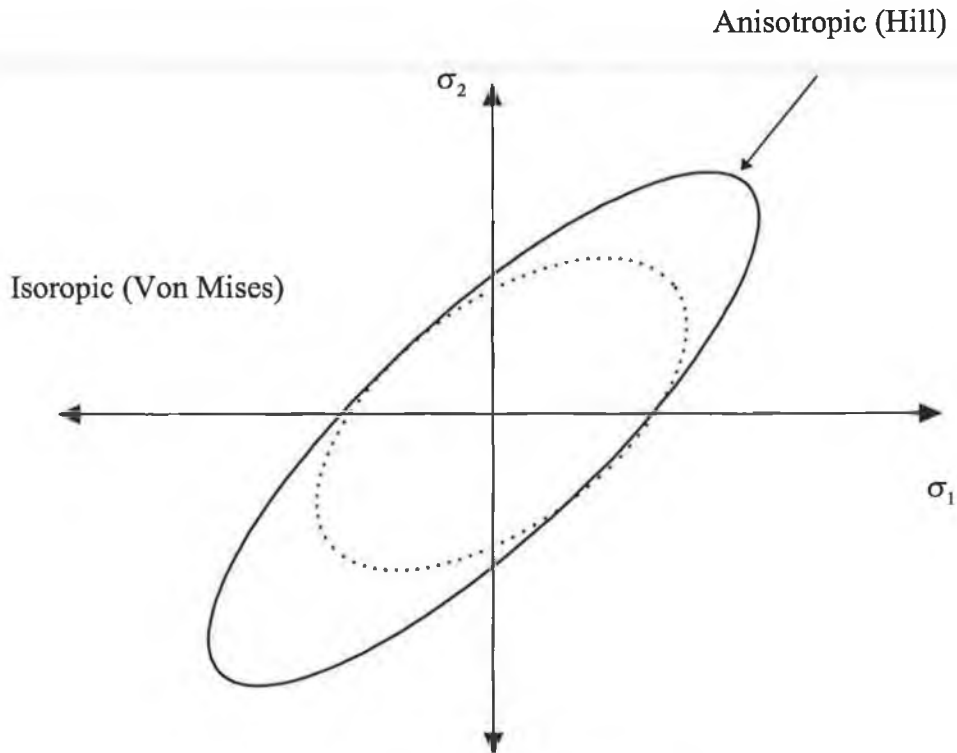


Figure 4.5 : Anisotropic Yield surface

4.8 Conclusion

This Chapter has outlined the historical development in the understanding of plasticity in metallic materials. Rate independent plasticity was introduced, the plasticity models utilised in the work conducted for this thesis are explained. The approaches and algorithms that model the phenomenon of plasticity are introduced and explained. Anisotropy effects of sheet metal blanks is explained and Hills criterion for anisotropic yielding is presented. These plastic models are applied to practical sheet metal process modelling in work documented in Chapter 6 Finite Element Analysis Modelling.

Chapter 5 : Finite Element Analysis Solution Convergence Enhancement

5.1 Introduction.

In this chapter the convergence difficulties experienced by the large strain and large deformation process of metal forming is documented. Strategies are presented that promote a converged solution. The following analysis types are introduced; Implicit static, Implicit dynamic, Explicit dynamic. The discussion is developed for convergence enhancement of the aforementioned analysis types.

This work is to examine the inherent difficulties that are experienced, when using explicit and implicit finite element code to simulate metal forming, namely ANSYS and Ls DYNA 3D. Convergence enhancement and simulation “tricks” that ensure these packages and similar packages actually give valid results are presented. It is important to have a deep understanding of the theory and coding of algorithms behind such packages, in order to be in a position, to comprehend program error out put, and develop corrective strategies, to ensure a valid solution. It is hoped that the succeeding sections develops this under standing in a clear manner for what is really a complex topic.

5.2 Formulation of small and large strain methods.

Strain within a deforming body can be successfully developed by small strain formulation as long as the strain experienced by the body is small. Metal forming deformation cannot be considered as a small strain condition, thus when small strain formulation is applied to metal forming processes substantial errors are developed.

5.3 Small/Infinite Strain [5.1]

Considering the linear static case of equation 3.9 the stiffness matrix is a function of the shape function and the elastic compliance matrix $\{D\}$ see section 4.4.6. The non linear case leads to the formulation of $\{k\}$ depending on the displacements of the nodal points, the strain rate of the elements, for small strain formulation.

When considering infinite strain formulation, the assumption is made that the plastic and elastic components of incremental strain can be separated.

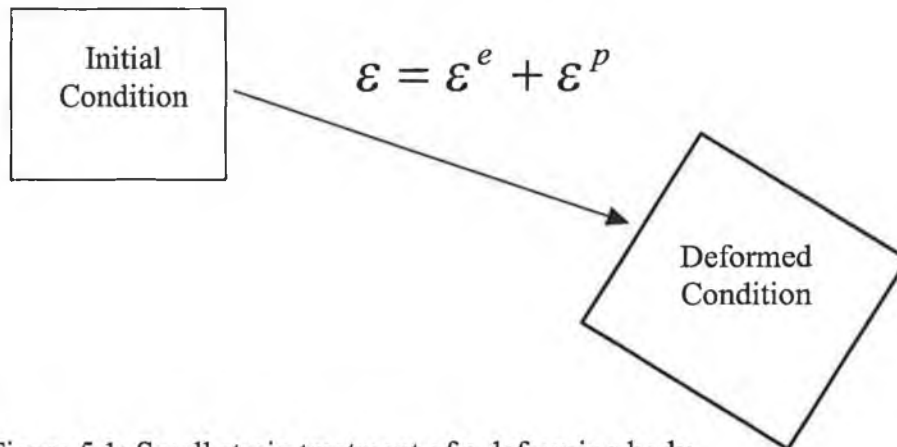


Figure 5.1: Small strain treatment of a deforming body.

Figure 5.1 represents the partition of strain into elastic and plastic strain. The formulation of the strain tensor ε is defined from the deformation rate tensor which is the symmetric part of the gradient of the displacement tensor as represented in equation 5.1.

$$\varepsilon = \frac{1}{2} \left[\text{grad } u + (\text{grad } u)^T \right] \quad 5.1$$

5.4 Large/Finite Strain [5.1]

The co-rotational formulation used by the updated lagrangian algorithm employed by ANSYS maintains incremental stability so long as the plastic strain increment is kept to within five percent. This limit on the plastic strain per equilibrium iteration has the effect of extending the solution time. Due to these non linearities leading to an iterative solution procedure a successful solution requires the satisfaction of convergence criterion at each incremental step. The convergence speed is problem dependent and failure to converge results in premature termination of the analysis. Plasticity considerations are merely a matter of ensuring that the load step increment does not develop plastic strain increments that are above the prescribed limit of 5%

for the implicit code mentioned. To this end the load step imposed displacement can be reduced to ensure such.

For sheet drawing simulation an overriding consideration is that of contact due to the large and geometrically complex area over which contact is taking place. Thus it is contact considerations that is more than likely to dominate convergence or non convergence.

For large strain the correct treatment for lagrangian formulation is based on the green lagrange tensor.

$$\Delta = \frac{1}{2}(F^T \cdot F - 1) \quad 5.2$$

Where a dot denotes the contracted product of the tensors on one index, and 1 is the unit second order tensor. Considering large deformation the constitutive laws for elastoplastic behaviour, is dependent on the separation of total strain into elastic and plastic strains. The steps for partition used for small strain is $\varepsilon = \varepsilon^e + \varepsilon^p$. This can only be generalised for large deformation through the introduction of a relaxed intermediate configuration. Figure 5.2 represents the decomposition of F into an inelastic deformation P between the initial and intermediate configuration, and an elastic deformation E between the intermediate configuration and the current one.

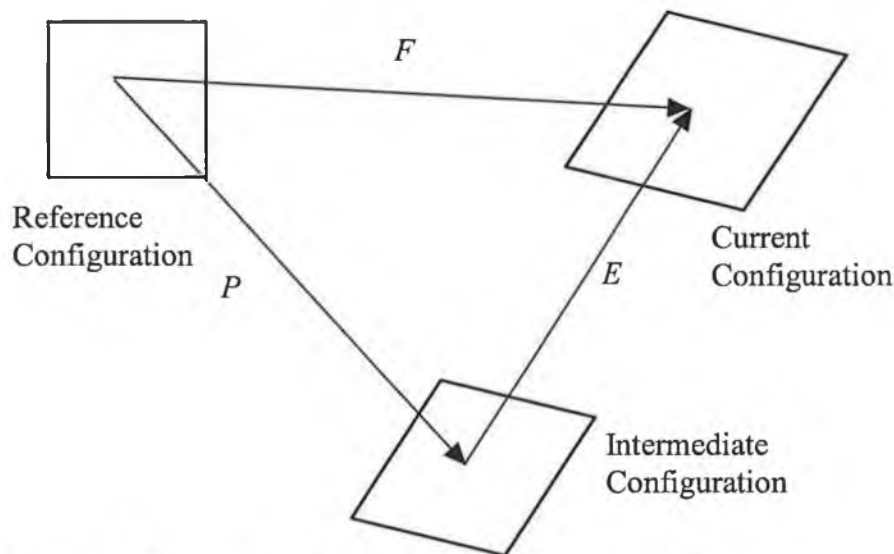


Figure 5.2: Large strain treatment of a deforming body.

In contrast with the small strain formulation, the total strain tensor, Δ , cannot be simply decomposed as the sum of the elastic strain tensor and inelastic strain tensor. The elastic strain tensor defined with respect to the intermediate configuration is $\Delta^e = \frac{1}{2}(E^T \cdot E - 1)$

The inelastic strain tensor defined with respect to the initial configuration is $\Delta^p = \frac{1}{2}(P^T \cdot P - 1)$.

Thus the nodal motion is decomposed into elastic decomposition and plastic decomposition as $F=E.P$. If this was implemented in ANSYS it would truly be a solution tool for metal forming as the current limit of plastic strain increment of 5% is prohibitive.

5.5 Explanation of implicit and explicit time integration schemes

Due to the high degree of non linearities in metal forming the solution has to be computed over a number of steps and equilibrium conditions satisfied for each increment of load. The time marching scheme that the increments are applied in can be implicit or explicit. The expert system models built in ANSYS utilise an implicit time scheme, those built in LS DYNA use a explicit scheme. Each scheme possesses distinct advantages and disadvantages which will be contrasted in the following sections.

5.5.1 Implicit Finite Element analysis

Implicit methods solve for equilibrium at the current time $t + \delta t$

$$k^T(U_{t-1})\delta U_t = F - R(U_{t-1}) \quad 5.3$$

$$\Delta U_t = \Delta U_{t-1} + \delta U_t \quad 5.4$$

Where $k^T(U_{t-1})$ is the tangent stiffness matrix of deformation system ΔU , F and R are the incremental displacement, applied external load and the internal load vectors, respectively. Due to the non linear nature of sheet forming an iterative procedure is used, with the load vector being applied incrementally to enable solution of these non linear equations. Use is made of the iterative solution process provided by the Newton Raphson scheme.

The non linearities present in sheet forming are plasticity of the drawn sheet and contact between the tooling and the sheet. Within the iterative solution procedure a successful solution requires the satisfaction of convergence criterion at each incremental step. The convergence speed is problem dependent and failure to converge results in a premature termination of the analysis. The implicit time step is unconditionally stable so real time analysis on rate sensitive materials can be conducted.

5.5.2 Explicit Finite Element analysis

Explicit methods solves for equilibrium at time step t by direct time integration using the central difference method .

$$a^t = (V^{t+\Delta t/2} - V^{t-\Delta t/2}) / \Delta t \quad 5.5$$

$$V^t = (U^{t+\Delta t} - U^{t-\Delta t/2}) / \Delta t \quad 5.6$$

$$M\Delta U^{t+\Delta t} / \Delta t^2 = F^t - R^t + M\Delta U^t / \Delta t^2 - CV^t \quad 5.7$$

$$\Delta U^t = U^t - U^{t-\Delta t} \quad 5.8$$

$$\Delta t \leq 2 \left[(1 + \xi^2)^{0.5} - \xi \right] / \varpi_{\max} \quad 5.9$$

where a is the acceleration, and V the velocity vectors. M and C are the diagonal mass and damping matrices, respectively. Δt is the time step for the time integration, ϖ_{\max} is the maximum eigen frequency of the system. ξ is the damping ratio of the highest mode. This explicit integration procedure is conditionally stable, where the time step Δt is subjected to a limitation via Equation 5.9. Since longer calculation time is necessary for the problems where the natural time is quit large, one has to reduce the natural time of a process, for example by artificially increasing the punch speed. Artificially increasing the mass density allows one to use

larger time step which makes it possible to complete the finite element analysis of sheet forming problem in fewer incremental steps. However such attempts at improving the analysis efficiency, result in an increase in the inertia effects which affect the accuracy of the solution. The detrimental effects of increasing inertia can be policed by reviewing the values for kinetic and internal energy over the solution time frame. Once the kinetic energy is less than ten percent of the internal energy an accurate solution is assured.

5.5.3 Dynamic Transient Analysis

The static force equilibrium equation of $\{F\} = \{k\}\{u\}$ is not applicable to the case when the body is in motion, then the effects of inertia must be included. This introduces time into the solution. So the force equilibrium equation for a dynamic case is :

$$\{F_{(t)}\} = [k]\{u\} + [C]\{\dot{u}\} + [M]\{\ddot{u}\} \quad 5.1.1$$

Further more when a body moves energy is dissipated proportional to the velocity which is termed viscous effects. This viscous effect is included via a structural damping matrix $[C]$.

In dynamic analysis the form of $[C]$ is not readily definable so it is developed via a pre transient modal analysis. Damping is difficult to measure, one possibility is to define it as a function of mass and stiffness, as in $[C] = \alpha[k] + \beta[M]$ called Rayleigh damping.

Within the ANSYS data base Alpha damping and Beta damping are used to define Rayleigh damping constants α and β .

Modal decomposition cannot be applied to non-linear problem such as metal forming hence a transient analysis of a metal forming process calls for the use of the “ Full Transient Method”. For a transient analysis some preliminary work is necessary to understand the dynamics of the problem. By doing a modal analysis, which calculates the natural frequencies values for alpha and beta and the correct solution time step can be arrived at. The values of α and β are not generally known directly, but are calculated from modal damping ratios, ξ .

ξ is the ratio of actual damping to critical damping for a particular mode of vibration. Where ω is the natural circular frequency of the mode, α and β satisfy the relation $\xi = \alpha/2\omega + \beta\omega/2$.

To specify both α and β for a given damping ratio ξ , it is commonly assumed that the sum of the α and β terms is nearly constant over a range of frequencies. Therefore two simultaneous equations are solved for α and β .

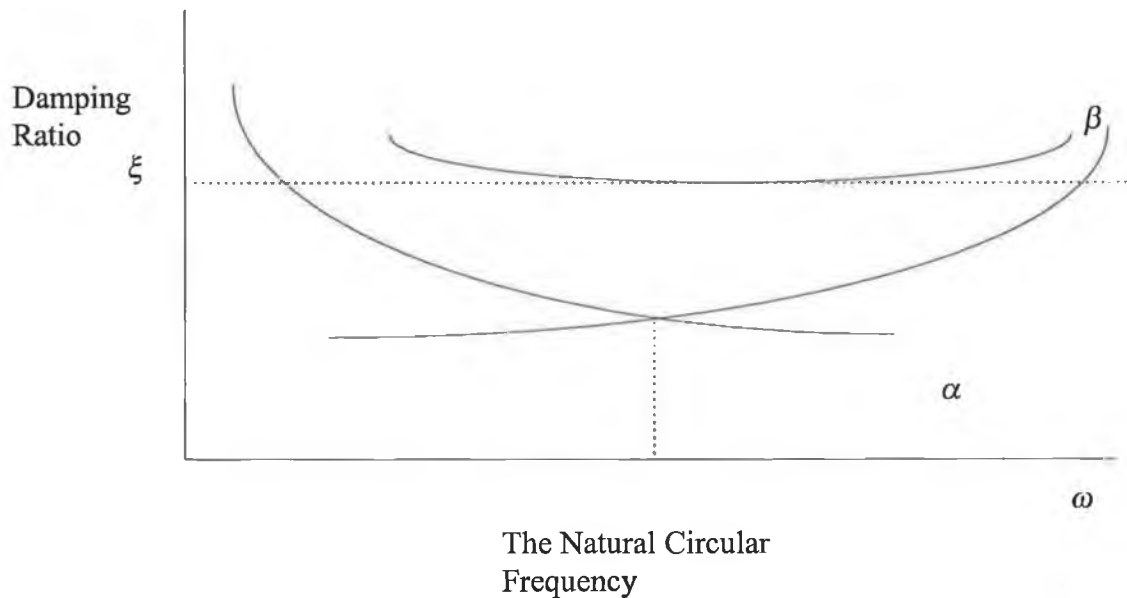


Figure 5.3 Damping Ratio Versus Frequency.

5.5.4 Dynamic Integration time step.

The accuracy of a transient dynamic solution depends on the integration time step the smaller the time step, the higher the accuracy. A time step that is too large will introduce error that affects the response of the higher modes and hence the overall response. A time step that is too small will waste computer resources. The integration time step should be small enough to resolve the motion response of the structure. Since the dynamic response of a structure can be thought of as a combination of modes, the time step should be able to resolve the highest mode that contributes to the response. For the Newmark integration scheme employed by ANSYS, it has been found that using approximately twenty points per cycle of the highest frequency results in a reasonably accurate solution. Therefore considering the above the Integration Time Step (ITS) = $1/20f$.

In dynamic problems involving contact, the time step should be small enough to capture the momentum transfer between the two contacting surfaces. Otherwise, an apparent energy loss will

occur and the impact will not be perfectly elastic. The integration time step is determined from the contact frequency (f_c) as : (I T S) = $1/Nf_c$

$$f_c = \left(\frac{1}{2\pi}\right)\sqrt{(k/m)} \quad 5.1.2$$

Where k is the gap stiffness, m is the effective mass acting at the gap, N is the number of points per cycle. To minimise the energy loss at least thirty points per cycle are needed. A modal analysis log file has been developed to compute the integration time step, α and β damping constants for the subsequent full transient analysis. The dynamic response of the blank will differ when the binder wrap phase has completed. Thus a pre stressed modal analysis was conducted to develop the time integration and arrive at suitable values for α and β damping. The ANSYS analysis command log file is documented as follows.

```
! prestressed modal analysis
/solu
antype,2           Transient modal analysis
upcoord,1,on      Current displacement given to nodes
modopt,subsp,1    Modal analysis subspace iteration extract one mode
nsel,s,loc,x,d/2  Select Nodes
d,all,all         Restrain Nodes
alls              Select all
mxpand,1          Expand one mode
psolve,triang     Partial solution with triangularised matrices

psolve,eigfull    Calculate the eigenvalues and eigenvectors using the full subspace

finish           Exit from processor

/solu            Enter the solution processor

psolve,eigexp     Expand the eigenvector solution
```

5.5.5 Transient Analysis set-up in ANSYS.

A transient analysis by definition involves loads that are functions of time. To specify such loads the load versus time curve is divided into suitable steps each corner on the load-time curve is one load step, as shown in figure 5.4.

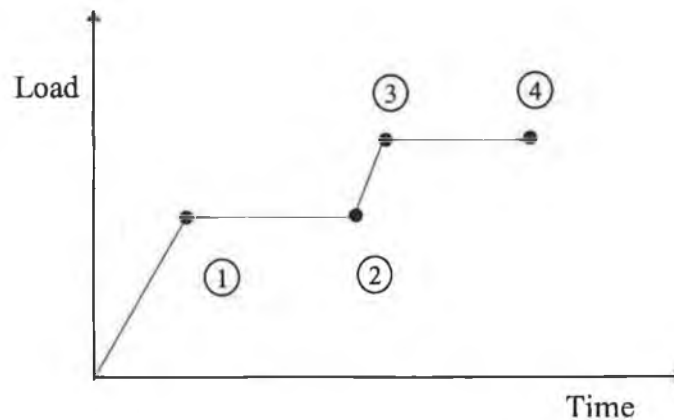


Figure 5.4 : Dynamic load versus time curves.

The first load step is to establish initial conditions. For each load step, a load and time value needs to be defined for metal forming simulations. The load step is ramped as shown in figure 5.4. Options such as automatic time stepping, adaptive decent and line searching were analysed. Then each load step is written to a load step file and solved. The following ANSYS command log file, documents the above procedure. The solution algorithm most suitable for transient metal forming analysis is the pre condition conjugate gradient and is employed in the following ANSYS transient log file.

/solu	
outres,all,all	<i>Solution writing to data base</i>
antype,4	<i>Perform a transient analysis</i>
nlgeom,on	<i>Include large deformation effects</i>
timint,on,all	<i>Transient effects on</i>
eqslv,pcg,10e-5,2	<i>Equation solver set to pre condition conjugate gradient type</i>
time,0.5	<i>Solution time = 0.5</i>
trnopt,full	<i>Transient analysis option full matrix method</i>
nsubst,5,200,5,off	<i>Number of subsets time step carry over off</i>

kbc,0	<i>Ramped load step</i>
autots,off	<i>Automatic time stepping off</i>
pred,on,,on	<i>Predictor activated in non linear analysis</i>
lnsrch,on	<i>Line search to be used with Newton Raphson</i>
nropt,1,,off	<i>Full newton raphson method</i>
neqit,50	<i>Maximum number of equilibrium iterations</i>
cnvtol,f,,0.05	<i>Force convergence values</i>
<i>!load step definition binder wrap</i>	
alls	
lswrite,1	<i>Write load step one "Binder Wrap"</i>
<i>!punch displacemant</i>	
nsubst,1,1,1,off	
cmsel,s,punch	<i>Select nodes in punch</i>
D,ALL,UX,0	<i>Displace punch elements</i>
D,ALL,UY,-5	
alls	
cnvtol,f,,0.05	
time,2	<i>Solution time = 2</i>
lswrite,2	<i>Write load step two</i>

5.6 Contact consideration of implicit FAE codes

The treatment of contact within the implicit ANSYS code is divided into penalty function only and combined penalty function and lagrangian multiplier. For the “penalty function only” the deformation mapping of the sheet blank under tool movement is driven by a simplex penalty formulation. The penetration distance of the contact node within the target surface is multiplied by a user specified contact stiffness with units of (N/M), to arrive at the contact force. The contact force is applied to the sheet blank contact element thus moving it to a position which it is hoped reflects the actual position.

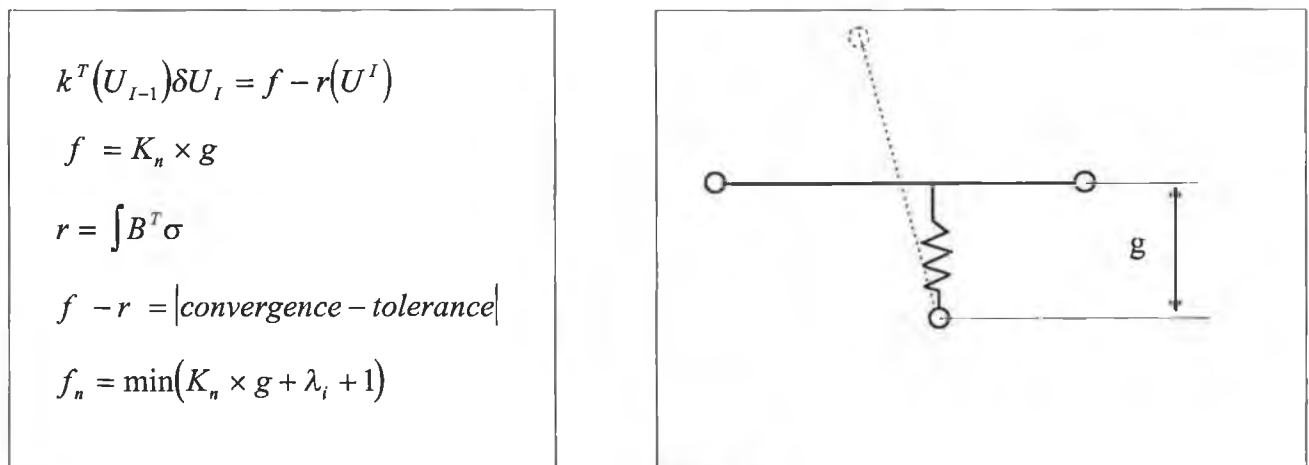


Figure 5.5 : Implicit contact

The combined penalty function and lagrangian multiplier method develops the restoring force between contacting bodies based on a condition of the penalty stiffness k_n and the force that is sufficient to push the two contacting surfaces back together or to within a acceptable tolerance zone that is user specified. Due to the system of equation formulation employed by the Lagrange multiplier method singular matrices can be developed, leading to termination of solution due to a unstable formulation of system equations, as explained in appendix A. [zienkiwicz]

The convergence is based on force, and if at the beginning of the analysis the contact elements describing the tools are not in initial contact, the calculated contact force f is zero. Hence contact force f is zero for the initial sub step, and subsequent sub-steps until contact has been initiated. As a consequence the force convergence uses a default minimum value to base the out of balance force convergence calculation on. This is prohibitively small and acts to reduce further subsequent target convergence criteria. Which leads to an aborted analysis due to non

convergence. The solution process is prematurely aborted due to the fact that the initial convergence tolerance was too small. To overcome this the contact elements representing the tooling should be developed with initial penetration. This ensures that the convergence tolerance is based on a more realistic value, ie. one which is based on the amount of initial penetration. The element resultant force r is developed as outlined by Figure 5.6, the resultant of the integration of the transposed shape function derivatives and the elemental stress.

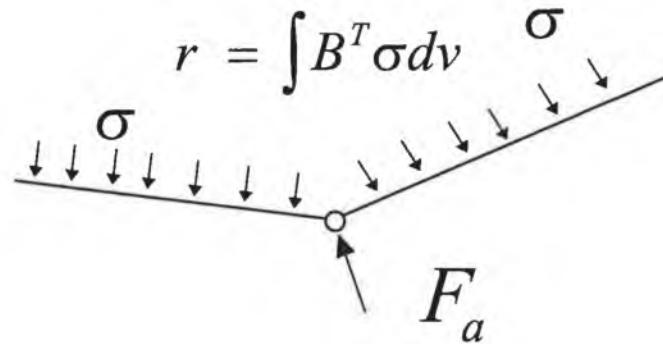


Figure 5.6 : Element resultant force r .

5.6.1 Contact considerations for Explicit code.

The contact algorithm used in sheet metal forming is sliding with closure and separation because the sheet blank can close on the tooling in one step of the forming process and separate in succeeding steps. This contact algorithm is a penalty method based on slave node penetration of master surfaces, developing an interface force which is applied. Between the slave node and its contact point.

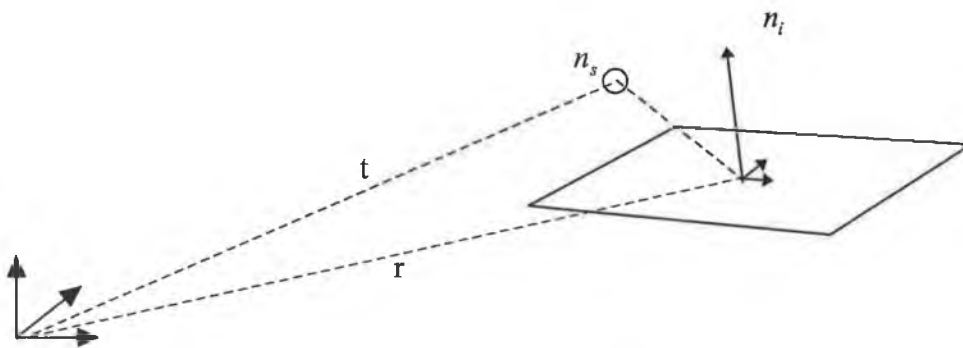


Figure 5.7 : Explicit Contact

Penetration of the slave node n_s through the master segment which contains its contact point is indicated if $l = n_i \cdot [t - r(\xi_c, \eta_c)] < 0$.

If the slave node has penetrated through the master segment, a interface force , f_s , vector the magnitude of which is proportional to the amount of penetration, is applied to the four nodes that comprise the master segment.

$$f_s = -lk_i n_i \quad 5.1.3$$

$$k_i = \frac{f_{si} k a_i^2}{v_i} \quad 5.1.4$$

The stiffness factor k_i for the master segment is given in terms of the bulk modulus k , the volume v_i , and the face area a_i of the element that contains the master surface. f_{si} is a scale factor for the interface stiffness and is normally defaulted to 0.1. Larger values may cause instabilities unless the time step size is scaled back in the time step calculation.

The contact time step is calculated from equation

$$\Delta t \leq \frac{2}{\varpi_{\max}} = \frac{2}{\sqrt{\frac{k_n}{m_n}}} = 2 \sqrt{\frac{m_n}{k_n}} \quad 5.1.5$$

If the courant critical time step as set by equation 5.1.6 is more than twice the contact time step of equation then solution instabilities will be encountered.

$$\Delta t = 0.9 \frac{l}{c} \quad 5.1.6$$

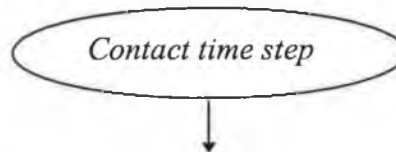
$$c = \sqrt{\frac{E}{\rho(1-\nu^2)}} \quad 5.1.7$$

Information on the contact time step and the courant critical time step can be found by accessing the d3hsp file that is created by LS-DYNA. An example of which follows.

*****lsdyna d3hsp file content*****

```

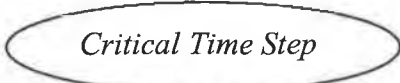
slave surface of interface # 1 type = 3
  surface time step = .103E-02 current minimum = .103E-02
master surface of interface # 1 type = 3
  surface time step = .378E-03 current minimum = .378E-03
slave surface of interface # 2 type = 3
  surface time step = .103E-02 current minimum = .378E-03
master surface of interface # 2 type = 3
  surface time step = .372E-03 current minimum = .372E-03
slave surface of interface # 3 type = 3
  surface time step = .103E-02 current minimum = .372E-03
master surface of interface # 3 type = 3
  surface time step = .569E-03 current minimum = .372E-03
    
```



The LS-DYNA3D time step size should not exceed .372E-03 to avoid contact instabilities. If the step size is bigger then scale the penalty of the offending surface.

100 smallest time steps

element	time step
shell 1106	.87541E-02



The contact time step can be altered by changing the stiffness of the rigid bodies representing the tooling. This can be achieved by simply changing the value of E Young's modulus for the rigid body. Alternatively the contact interface scale factor f_{st} can be altered in doing so, the contact time step for all the contact surfaces will be altered. Reffer to Equations 5.1.4 and 5.1.5. The first method delivers better flexibility in that independent surface contact time steps can be altered, note that changing young's modulus of a rigid body will not effect the models courant critical time step as it is dependent on elements contained on flexible bodies only.

5.6.2 Contact Damping Of The Explicit Method.

Due to the small critical time steps in explicit time integration, punch velocities are considerably increased, compared to reality to keep the solution time to within a practical level. As a result of this artificially fast dynamic behaviour oscillations may occur, which have to be damped out to achieve correct results. This requires that a damping value, is defined in the contact surface which is a percentage of critical damping, ξ , This damping value, ξ , depends on the interface frequency ω .

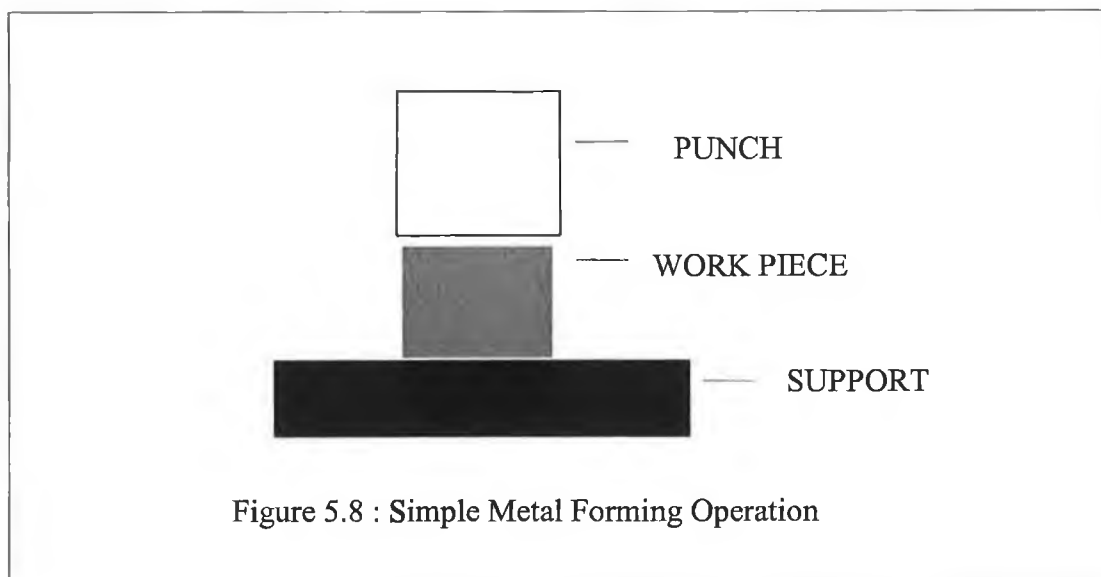
$$\text{as : } \xi = 2m\omega \qquad m = \min(m_{slave}, m_{master}) \qquad 5.1.8$$

Where ;

$$\omega = \sqrt{\frac{k(m_{slave} \cdot m_{master})}{m_{slave} + m_{master}}} \qquad k = \text{interface stiffness}$$

This frequency is estimated for the mass of the master node m_{master} and interpolation using the shape function of the target contact segment.

5.6.3 Mesh density at contact interface



Mesh density is a prime concern in FEA simulation of metal forming, in that adequate discretisation has to be ensured in order to develop sufficient contact restoring forces. These

contact restoring forces result from elemental stress which is highly dependent on element discretization. As can be seen from Figure 5.9 (a) with a low element density, describing the blank, at the blank rigid contact surface (i.e. Punch) interface. The required applied force f to ensure that the movement of the blank mirrors that of the punch is not developed. As in Figure 5.9 (b) this leads to non convergence of displacement for the penalty function only and the combined penalty function and lagrangian multiplier method. Simply by providing sufficient elements at the interface the blank is capable of following the punch motion and contact displacement convergence is assured. Secondly a low density mesh of the blank leads to an under valued r , which leads to contact non convergence due to a force imbalance between f and r . Again adequately high mesh densities ensure contact force convergence. Hence if contact convergence difficulties are present increasing the mesh density, will help to overcome contact convergence difficulties as represented by Figure 5.9 (b).

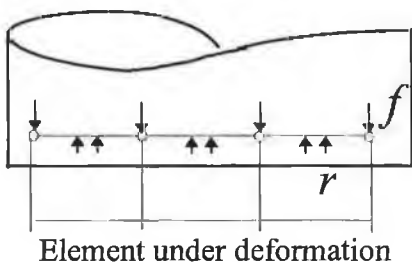


Figure 5.9 (a)

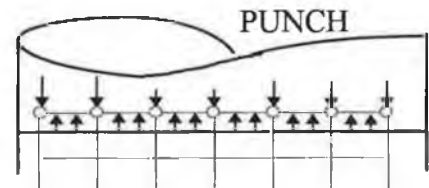


Figure 5.9 (b)

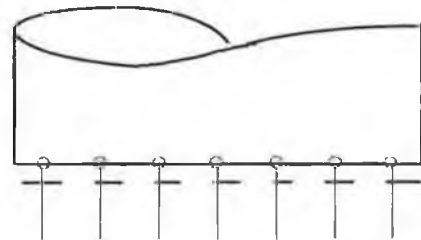
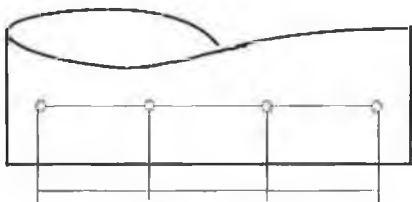


Figure 5.9 : Punch force Contact Interface Resultant Force

where : $f =$ Applied nodal forces from contact algorithm.
 $r =$ Element resultant force.

5.7 Tool Blank Friction

Assigning friction models to contact surfaces in sheet metal forming is difficult, since large variations in friction can be found over the contact surfaces. These variations depend on local conditions and local procedures in the manufacturing process. Friction in metal forming is accounted for by the shear friction model, or the coulomb friction model. The shear friction model is applicable to bulk forming processes such as forging. Friction effects in sheet metal forming is accounted for by the coulomb friction model. The implicit and explicit handling of friction differ as is outlined below.

Implicit codes such as ANSYS model friction as a rigid coulomb or a elastic coulomb model. The frictional force f_r in the rigid coulomb model is the coulomb factor μ multiplied by the normal pressure f_n .

$$f_r = \mu \cdot f_n \quad 5.1.9$$

The elastic coulomb model is a hybrid of the rigid coulomb model, it allows for a slip condition. Where the friction force is overcome and replaced with a tangential force dependent on node slippage multiplied by a user defined constant.

Explicit codes such as LS DYNA apply a linear coulomb friction model with a stick slip condition analogous to elasto-plasticity as described in [5.2] Schweizerhof, Hallquist. The coulomb model is close to values generally observed in experiments, as long as the interface pressure is not too large. If the tooling blank interface pressure is large, the resulting friction force is physically incorrect as a “fully stuck situation”. This must be avoided by limiting the friction force, which can be done by limiting the interface shear stress.

$$f_{tan\ g} = \min(f_{coulomb}, F_{limit} = k \cdot A_{master}) \quad 5.2.1$$

A_{master} area of master segment

k viscous friction factor

The viscous friction value as well as the coulomb friction value can be chosen to vary for each contact segment, providing a very variable tool for lubrication simulation.

5.8 An Investigation into possible hourglass modes of zero energy deformation in deep dawn process modelling.

Ls dyna utilises the one point quadrature of the Belytschko-Tsay element to reduce computational time. For the deep drawing simulations conducted, hour glassing was found to have an effect on the prediction of flange deformation. The zero energy modes develop deformation patterns that are similar to wrinkling prediction. Care must be taken not to mistake spurious hour glass modes with process conditions that may cause hour glassing. To demonstrate this a vertical cup drawing simulation was conducted with two different

levels of hour glass control. This hour glass control is set within the LS DYNA program for each material with the EDMP,HGLS command. The control is typically set from 0.01 to 0.05 effecting the element stiffens values. The simulated deformed shape presented in figure 5.1.1 was conducted with a hourglass control of 0.01. It is clear that the flange region is demonstrating what would normally be construed as wrinkling. However reference to the deformed shape of figure 5.1.2 resulting from a simulation conducted with the hour glass control set at 0.05 demonstrates that the flange region presents no sign of wrinkling. Thus the danger of a hour glass mode being misconstrued as a wrinkling process error of form is apparent. Hence it is suggested that deep drawing analysis be simulated with runs of increasing hour glass control to remove the problem.

This leads to another word of caution as the analysis should be monitored for the degree of hour glass energy, as a value of hour glass energy in excess of 10 % of the internal energy can invalidate results. The hour glass energy is monitored within Ls dydna with the following command setting

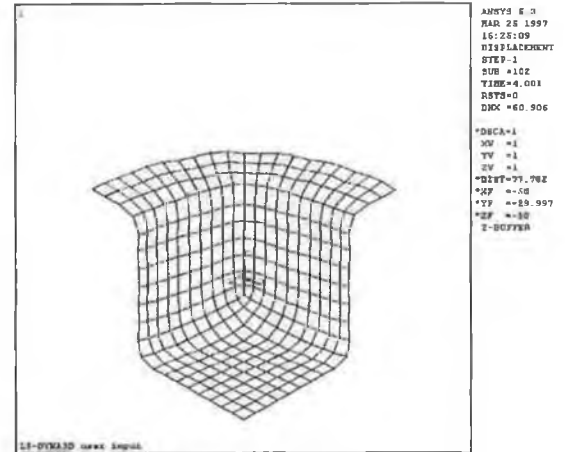


Figure 5.1.1 : Hour glass Control of 0.01

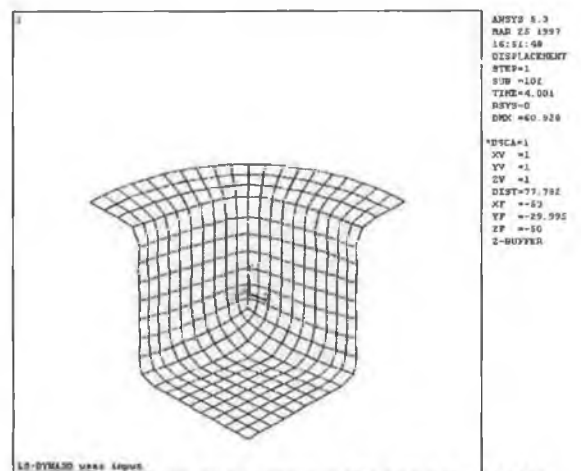


Figure 5.1.2 : Hour glass Control of 0.05

EDENERGY,1,0,1,0. Thus a plot of the internal and hour glass energy from the LS DYNA ascii output file MATSUM will enable the simulation to be monitored and assessed for a valid output. If the contribution of hour glass energy is excessive then the recommendation is to replace the element formulation to one of full integration which does not suffer from, zero energy deformation modes, but at an added COMPUTATIONAL cost. The computation cost can be in the order of eighth to ten times that for reduced integration.

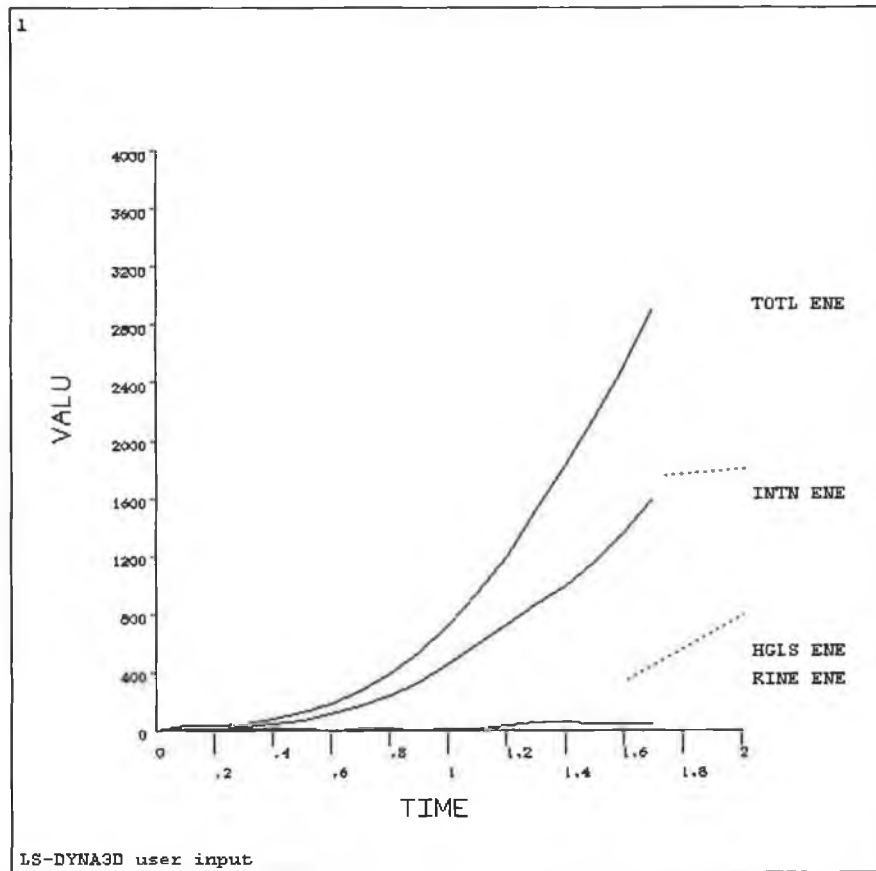


Figure 5.1.3 : Energy balance for cupping simulation

5.8.1 Hour Glassing Modes

The computational efficiency of the Belytschko-Tsay element is partially due to the under integration in the form of one point quadrature in the plane of the element. This results in spurious zero energy deformation for the one point integrated shell element. The hourglass shape vector τ_I is defined as :

$$\tau_I \text{ is defined as : } \tau_I = h_I - (h_j \hat{x}_{aj}) B_{aI}$$

$$\text{Where : } h = \begin{bmatrix} +1 \\ -1 \\ +1 \\ -1 \end{bmatrix} \quad 5.2.2$$

This represents the basis vector that generates the deformation mode that is neglected by one point quadrature.

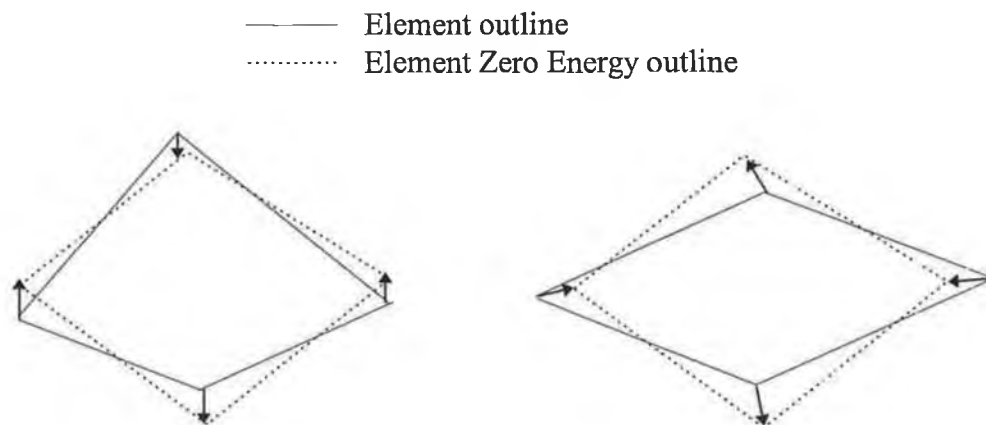


Figure 5.1.4 : Hourglass deformation modes for Belytschko Tsay

The hourglass shape vector operates on the generalised displacements, to produce the generalised hourglass strain rates, which deforms the elements as in figure 5.1.4 a process termed hourglass deformation.

5.9 Kinetic Energy Considerations

Kinetic energy considerations for sheet metal forming is dependent on the body forces that are developed by the blank. In order to ensure the integrity of a quasi-static simulation these body forces and thus the system kinetic energy has to be kept to a minimum. The recommendation is that the kinetic energy should be less than 10 % of the internal energy for a valid quasi-static metal forming simulation as suggested by the [5.3] Hallquist. The energy balance for a solution can be accessed from the ls dyna ascii output file MATSUM as in figures 5.1.5, 5.1.6, 5.1.7

Figure 5.1.5 demonstrates the energy balance for a valid quasi-static simulation where the above requirement is maintained. In situations where the kinetic energy is greater than 10% of the internal energy. The simulation is dominated by body forces of the blank, then the simulation is judged to be invalid. As is clearly the case with figure 5.1.6 which depicts a invalid solution.

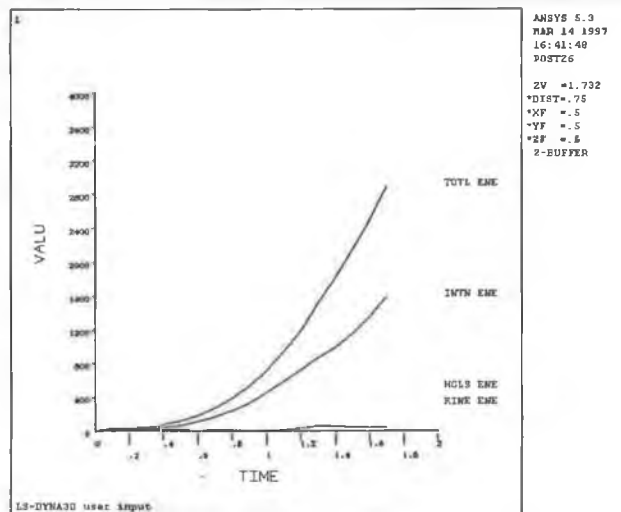


Figure 5.1.5 Energy Balance

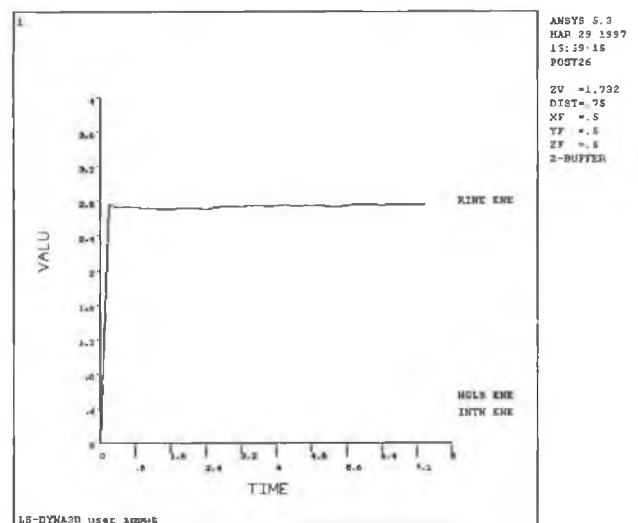


Figure 5.1.6 : Kinetic and Internal energy Balance

To ensure a valid quasi-static solution the kinetic energy trend should also be monitored. A sudden increase or peaking in the kinetic energy indicates a invalid solution. If the solution has not already crashed then the results should be discounted. A typical ramping of the kinetic energy that indicated a solution failure is shown in figure 5.1.7.

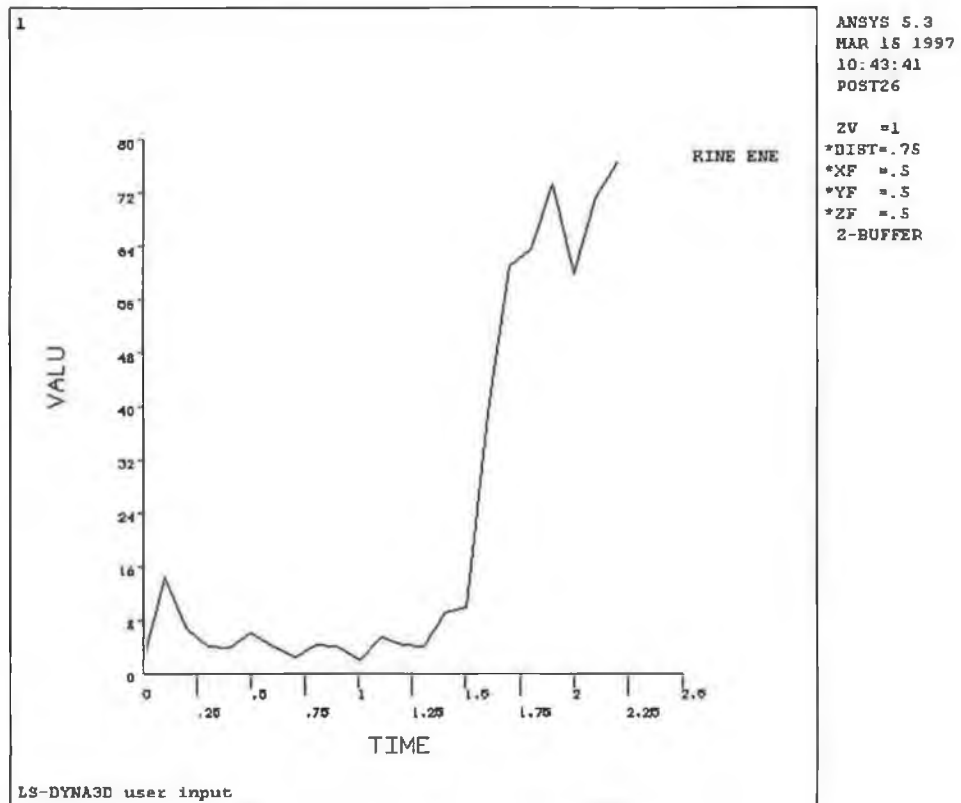


Figure 5.1.7 : Kenetic energy plot.

5.10 Solution Convergence Enhancement of Implicit code with Observations Draw from ANSYS 5.3 Implicit Code.

The convergence of FEA Models developed in this project was tested. Analysis runs were conducted with different solution enhancement tools. This is discussed in the following section with reference to solution convergence, and minimising the computational solution time.

The model developed in ANSYS implicit code presented many problems primarily due to the fact in that the contact algorithm used by contact 26 ground contact element in ANSYS 5.3 is in fact only a pseudo treatment of contact. Hence the method suffers from the following drawbacks, if the contact stiffness is too high the resulting large coefficients in the stiffness matrix causes convergence problems. These large coefficients within the stiffness matrix cause the solution scheme of gaussian elimination to develop rather small valued pivots leading to numerical instabilities manifesting in the form of stiffness matrix coefficients of near zero value. This problem can be overcome to some degree by the replacement of the gaussian elimination dependent frontal solver by the precondition conjugate gradient solver. But it must be stressed that it is the pseudo nature of the contact algorithm that is the major restriction to metal forming simulation solution. The application of a face pressure function for rigid to flexible contact element as provided by other codes would greatly enhance the rather limited use of contact 26 element present in ANSYS 5.3. The contact element would estimate a face pressure function based on the internal stress normal to the element edge or face. Reported improvements have been made to the contact algorithm of Ansys version 5.4 and 5.5, however the author is not in a position to comment on such. Contact surface convergence as shown in section 5.6, is highly dependent on the choice of contact stiffness.

Also the system may converge but due to a low contact stiffness the sheet blank surface may penetrate the tooling. This leads to an unacceptable solution due to non reflection of reality, bearing in mind that the actual stress path is strain history dependent this occurrence has to be prevented at all points in the analysis.

The F.E.A. model to analysis incipient flow and embossing of section 5.5 was conducted with a variety of ANSYS suggested solution convergent enhancement tools such as automatic time stepping (called bisection), is documented in the classical Newton Raphson method with bisection. Adaptive decent time step prediction method and line search method reefer to section 3.6 for an explanation of the above.

From extensive analysis runs it became apparent that the recommended solution scheme should encompass the line search method, coupled with the precondition conjugate gradient solver, for guaranteed solution convergence. Enabling for problems to converge within acceptable solution times.

The use of automatic time stepping algorithm which incorporates the Newton Raphson bisection method is strongly not suggested. This is due to the finding that as the force convergence norm calculated at equilibrium increases , it indicates a diverging solution. If the equilibrium solution continues to diverge the boundary loads are removed. The solution time step is set to a lower value, and the solution procedure is started all over again. This leads to an unacceptably long solution time. The use of adaptive decent leads to the actualisation of the secant matrix in solution leading to a further rift in the convergence norm experience of this ensures that solution convergence becomes less of a likelihood.

The strongly proposed method of line search, which enable solution via its continuous altering of the solution time step as the solution marches onward in time to ensure adequate capturing of local discontinuities due to non linearities such as contact and plasticity. The load step predictor algorithm helps to reduce the solution time by setting the next time step to a factor of the last successful time step. The line search method as explained in section 3.6.2 continuously augments the residual force work increment, leading to speedy capturing of the localised solution. By the minimisation of the potential energy of the system.

5.11 Solution Convergence Problems and Enhancement of Explicit Code with Observations drawn from LS DYNA Explicit Code

The solution time step is controlled by the critical time step which is dependent on the properties of disturbance propagation within the smallest element of the sheet blank. Solution time steps for LS DYNA are set from 51 to 100 typically. Non convergence of the system equations can result from the interaction of this critical time step and the contact time step which for the relevant contact algorithm employed in this work is given by equation 5.1.6. If the contact time step is below the critical time step by a factor of more than two the system equations will fail to converge. In the endeavour to reduce the solution time by mass scaling attention should be paid to its effects on solution convergence, the following discussion is hoped to give an insight to the pit falls. Mass scaling is used to increase the courant time step size by increasing the density of the finite elements. Care must be taken to insure that the integrity of the assumed Quasi static nature of the analysis is maintained. This can be done by observing the kinetic and internal energy over the solution time, to ensure that the kinetic energy doesn't exceed ten percent of the internal energy.

The analysis can be judged to be a failure if the solution does not effectively map the actual deformation imparted on the blank due in some cases to over penetration of the blank on the rigid tooling surface, this is averted by the correct formulation of the contact stiffness which is alluded to by the following. Use of contact algorithm options other than the default which is based on the minimum of master segment and slave node stiffness. For sheet metal forming, it was found that setting the penalty stiffness option to "weighted slave" which uses the area or mass weighting of the slave node element to set the contact stiffness. Alternatively the inverse proportion option which uses the slave node value inversely proportional to shell thickness was found to be useful in overcoming difficult contact problems. In general contact problems the manipulation of the scale factor for sliding interface penalties will help in combating contact convergence difficulties.

5.12 Considerations for Dynamic simulations

With Dynamic analysis the punch may upon contact with the blank shut into space due to a reaction to inertia loading. This leads to solution failure because the stiffness matrix now possess zeros upon the main diagonal resulting from unconstrained rigid body motion. To combat this springs can be employed that keep the punch in contact, with the blank, as shown in figure 5.1.8.

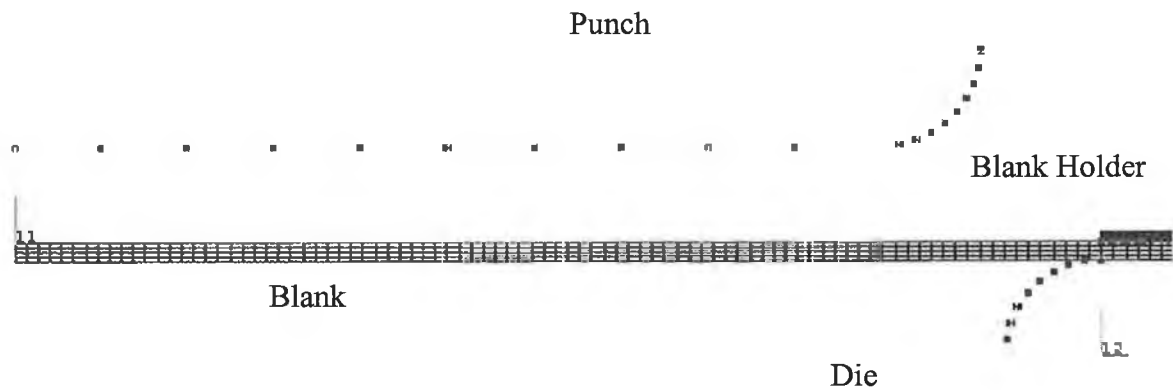


Figure 5.1.8 : Dynamic analysis solution aid

5.13 Conclusion

The convergence difficulties that this work has encountered for static and dynamic and quasi static explicit forms have been documented. Convergence enhancement methods that were applied are presented.

Chapter 6 : Finite Element Analysis Modelling

6.1 Introduction

This chapter introduces the analysis types that are used within Finite Element Analysis theory, namely static analysis; dynamic analysis; quasi static analysis. The stages of the drawing process with their respective finite element model is discussed. Finite Element Analysis (F.E.A) simulation of the sheet drawn process by 2D and 3D F.E.A simulation is developed. The process of mesh refinement is developed to ensure that the sheet blank discretisation error is removed from the F.E.A simulation to ensure accurate reflection of the Cup drawing process.

This chapter also documents the F.E.A. Models developed to simulate deep drawing. The models consist of static and transient models provided by the implicit code ANSYS. The quasi static analysis models provided by the explicit “Ls Dyna 3D code. Process modelling of a square box drawn product is presented. Factors effecting formability of sheet drawn products are presented. The Ohio State University (O.S.U) formability test is developed within an F.E.A. module enabling the development of material specific FLD forming limit diagrams.

6.2 Finite Element Analysis Types

The Finite Element Analysis of metal forming can utilise different systems of equations to model the theory. The major types of Finite Element Analysis applied in metal forming are static analysis, dynamic analysis under the implicit frame work, quasi static Analysis under the explicit frame work.

6.2.1 Static Analysis $\sum F = 0$ 6.1

The equation of equilibrium for static solutions is

$f = \{k\}\{u\}$. The Punch velocity is modelled by imposing displacement on the punch nodes. This is done for load steps over the solution time. The process time can be correlated to the sub step number for converged solutions.

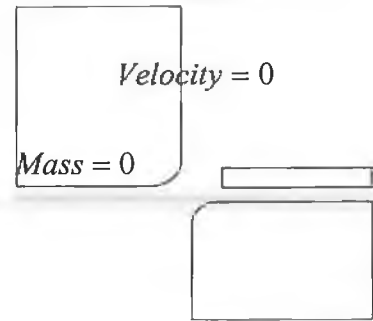


Figure 6 (a)

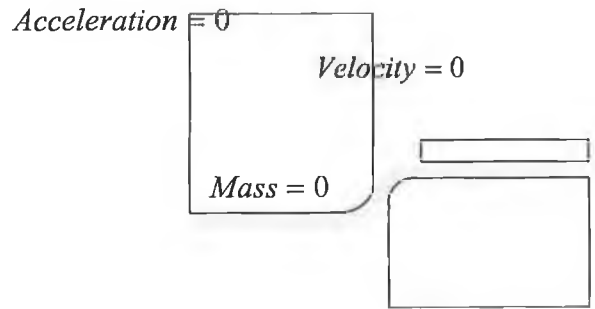


Figure 6 (b)

6.2.2 Dynamic Analysis $\sum F = M\ddot{a}$ 6.2

The equation of equilibrium for dynamic analysis is

$$\{F_{(t)}\} = [k]\{u\} + [C]\{\dot{u}\} + [M]\{\ddot{u}\} \quad 6.3$$

The solution is driven by the velocity of the punch

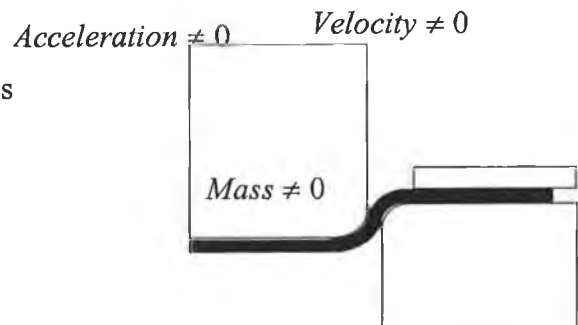


Figure 6 (c)

6.2.3 Quasi-static Analysis $\sum F \approx 0$ 6.4

The equation of equilibrium for Quasi-static analysis is

$$\{F_{(t)}\} = [k]\{u\} + [C]\{\dot{u}\} + [M]\{\ddot{u}\} \quad 6.5$$

$\approx 0 \qquad \approx 0$

Quasi-static analysis strives to reproduce the actual process by ensuring that the blank does not develop body forces $\{F\} = [M]\{\ddot{u}\} = 0$. 6.6

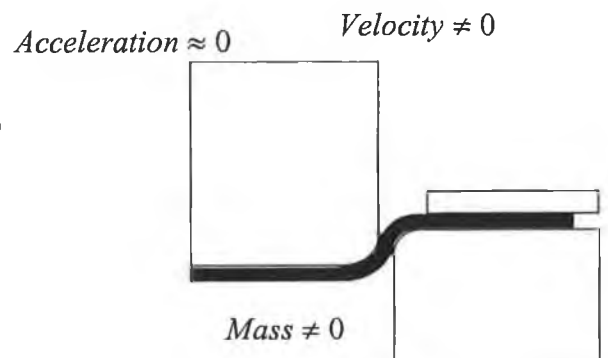


Figure 6 (d)

6.3 Finite Element Analysis simulation of the drawing process

The FEA Simulation of the drawing process is composed of local sub models of increasing complexity. As outlined below

6.3.1 Line Analysis

In line analysis one dimensional finite element models of local stripe of sheet metal near the boundary of the stamped component are made and their deformation behaviour under the action of the blank holder force and the punch motion, including draw beads is investigated the gained information can be used for a first assessment of the local blank cutting pattern, holding and punch force requirements and limiting blank holder pressure.

6.3.2 Zone Analysis

In stamped parts with complex geometry it is possible to identify local regions where stamping problems such as (tearing, wrinkling bulging are likely to occur. Isolated sub models of such regions with ad hoc boundary conditions can be made and used to assess the local strain patterns, need for and the number of steps in multi step processes, the danger of local under punch bulges and the introduction of local stamping artifices.

6.3.3 3D Analysis

Assessment of tool layout operational window of the blank holder pressure and the detection of large wrinkles and bulges. The assessment of type and distribution of local restraints draw beads step beads, draw bulges. A rough estimate of spring back requires a large number of shell element.

It is apparent from the following section that zone and 3D analysis is predominately applied.

6.4 Deep drawing simulation

For a comprehensive approach to the Cup drawing process simulation, the process has been divided into the following operations.

6.4.1 Binder wrap

The stages involved in deep drawing are divided into binder wrap, embossing, and cup drawing reference [6.1]. Binder wrap is the stage when the blank holder is presented to the blank and the blank holding force is developed, as shown in Figure 6.1. This process comprehensively strains the blank at the flange preventing the flange material from wrinkling as it is drawn into the die. This stage of deep drawing is simulated by the implicit static and implicit dynamic modules a description of which follows, by implementing the binder wrap stage within the first load step. Thus ensuring that the binder wrap stage has converged before the application of the other stages within the simulation.

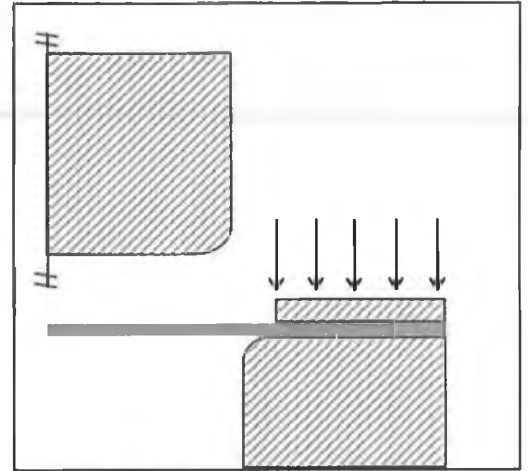


Figure 6.1 : Binder Wrap

6.4.2 Embossing

Embossing where the material is drawn over the tool profile radii. The punch force necessary to develop this deformation is typically 60 % of the total required punch force to form the cup [6.2]. This stage of deep drawing is simulated by the implicit static and implicit dynamic modules a description of which follows, by implementing the embossing stage within a load steps, subsequent to the first load step, as outlined for binder wrap. The height of the cup at the end of this analysis is typically twice the tool corner radius, which represents the limit of application of the implicit code ANSYS version 5.3. Due to the short coming of its pseudo contact algorithm.

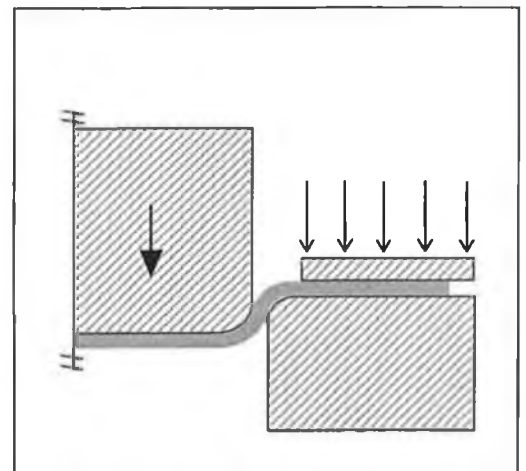


Figure 6.2 : Embossing

6.4.3 Cup Drawing

Cup Drawing is the completion of the process where the material is drawn to the full depth of the cup. This stage of deep drawing is simulated by the explicit code LS-DYNA 3D version 936.03. A description of the process of simulation follows in this chapter. The simulation utilises a 3D representation of the blank and the resulting high degree of 3D contact necessitates the use of the explicit solver which is more efficient than the implicit solver for this case.

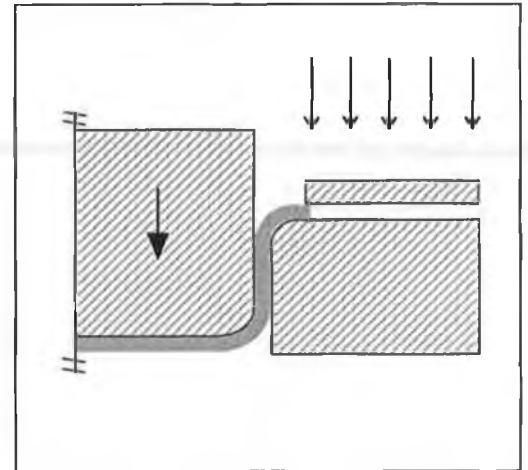


Figure 6.3 : Cup Drawing

6.5 Finite Element Analysis Types

The specific F.E.A. types introduced in section 6.2 are now developed in applied simulations of sheet drawing.

6.5.1 Implicit Finite Element Models

The implicit Finite Element models are sub divided into static and dynamic analysis modes. The static and dynamic modes have specific advantages when compared, in the area of convergence difficulty and speed of solution. The implicit static model takes advantage of the axis symmetry of the Cup, and models the cup wall by 4 noded bilinear axis symmetric quadrilateral elements (plane 42 in the ANSYS element library). The Tool is described by rigid ground 2D contact elements (contac 26 in the ANSYS element library), as show in Figure 4. The imposed punch motion and blank holder pressure is applied in separate load steps. Mesh refinement is developed in the deformation annulus which is acted on by the punch and die profile radius. Element size is set by the upper

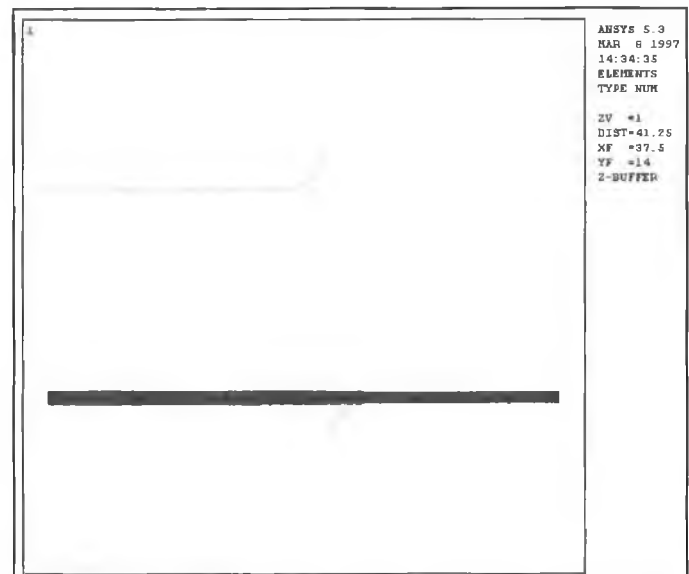


Figure 6.4 : Implicit finite element static model

limit of 30° bend allowance for an accurate solution ANSYS Theory Manual[6.3]. The plasticity model incorporates strain hardening and anisotropy (caused by the rolling process in the manufacture of the sheet) by allowing different stress strain behaviour in the elements co-ordinates system. The material model is based on von-Mises yield criterion and Hills plasticity formulation. Convergence enhancement tools for contact and plasticity are applied. These tools consists of; time step bisection, solution time step prediction, line search and adaptive decent. Blank Holder pressure is applied by imposed motion of the blank contact elements. The resulting pressure is calculated by the elastic constant of the material times the penetration distance of the target element surface within the contact nodes.

Convergence difficulties were encountered when the contact elements that represent the punch are presented to the blank. The intricacies of the contact convergence for element contac 26 lead to solution failure due to non convergence. To redress this problem it was found that if the punch contact element were spatially removed from the blank, then the simulation of binder wrap was successful| .

6.5.2 Implicit Dynamic Finite Element Models

The implicit dynamic model takes advantage of the axis symmetry of the Cup, and models the cup wall by 4 noded bilinear axis symmetric quadrilateral elements plane 42 in the ANSYS element library. The Tool is described by flexible 2D contact elements (contac 48 in the ANSYS element library). Tool geometry being created by 2D link elements. The link element is given a high value of young's modulus in order to stiffen it. The nodes are constrained in rotations, in order to ensure that the tool elements will be treated as a rigid element. This has to be done in ANSYS 5.3 as there are no rigid surfaces by which rigid tools can be developed.

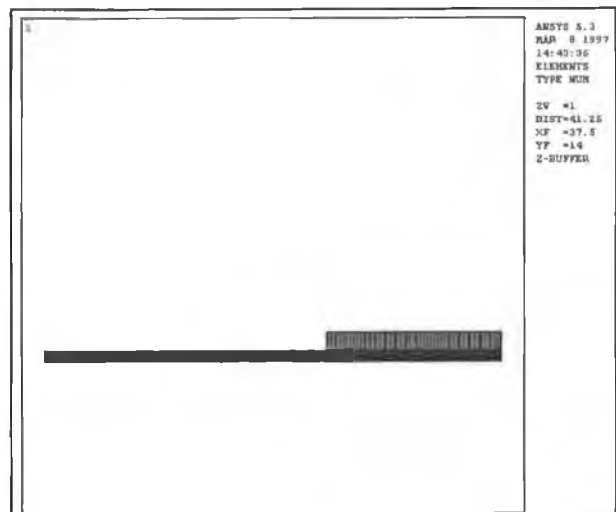


Figure 6.5 : Implicit finite element dynamic model

The automatic contact generation algorithm of ANSYS is used to create contact elements between the target elements on the blank and the contact element of the tooling 2D Link nodes.

Non symmetric contact was found more successful than the symmetric contact as the latter was found to be more computationally expensive with no improvement in contact convergence. The blank holder is represented by elements (plane 42 in the ANSYS element library). Blank holder pressure is applied by application of pressure to blank holder elements. Binder wrap is conducted in the first load step with the punch tool removed from the Blank. The FEA elements representing tooling and the blank are given a nominal density, to enable a transient, analysis to be conducted.

6.5.3 Explicit Finite Element Models

The explicit quadrilateral shell element (Belytschko/Tsay) [6.4] is employed with five through thickness integration points. Element size is set at approximately half the draw radius, indicated as the optimum by Mattiasson[6.4]. The tooling is represented as a discretised area with the elements constrained as rigid bodies as shown in Figure 6.6. Computational expense is reduced due to the fact that the rigid body mesh is treated within the DYNA contact algorithm as a VDA surface (the mesh is transformed to surface patches). The plasticity law is the anisotropy plasticity model developed by Barlat and Lian [6.5].

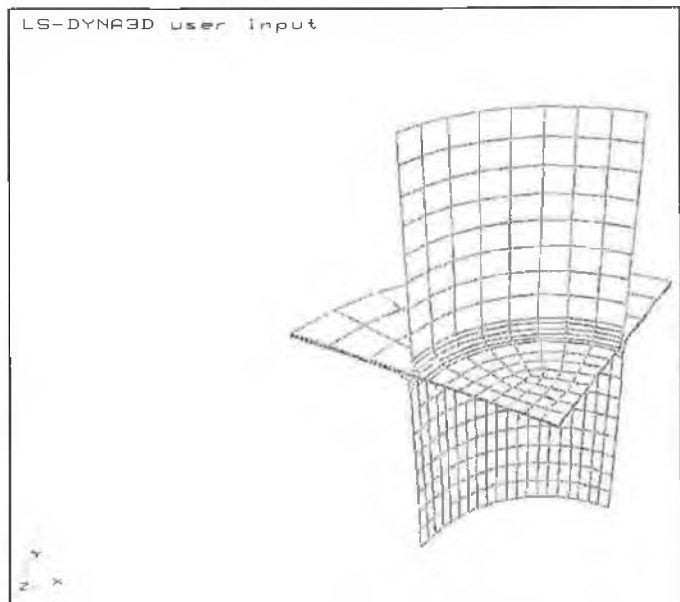


Figure 6.6 : Explicit finite element model

A sample example is included to explain the operation of the process simulation module. The Cup material is steel with the Barlat and Lian plasticity variables as out-lined.

Barlat exponent = 6 Lankford Parameter = 1.8 Strength Co-eff = 533 (MPa)

Hardening Co-eff = 0.22

The Cup and Tool geometry is as follows the original diameter of the blank D_0 is 120 mm. Final cup diameter D is 66 mm. Height of cup 32 mm. Punch and Die corner radii PCR and DCR is 5 mm, Clearance C is set at 1.25 mm and sheet thickness T is 1 mm.

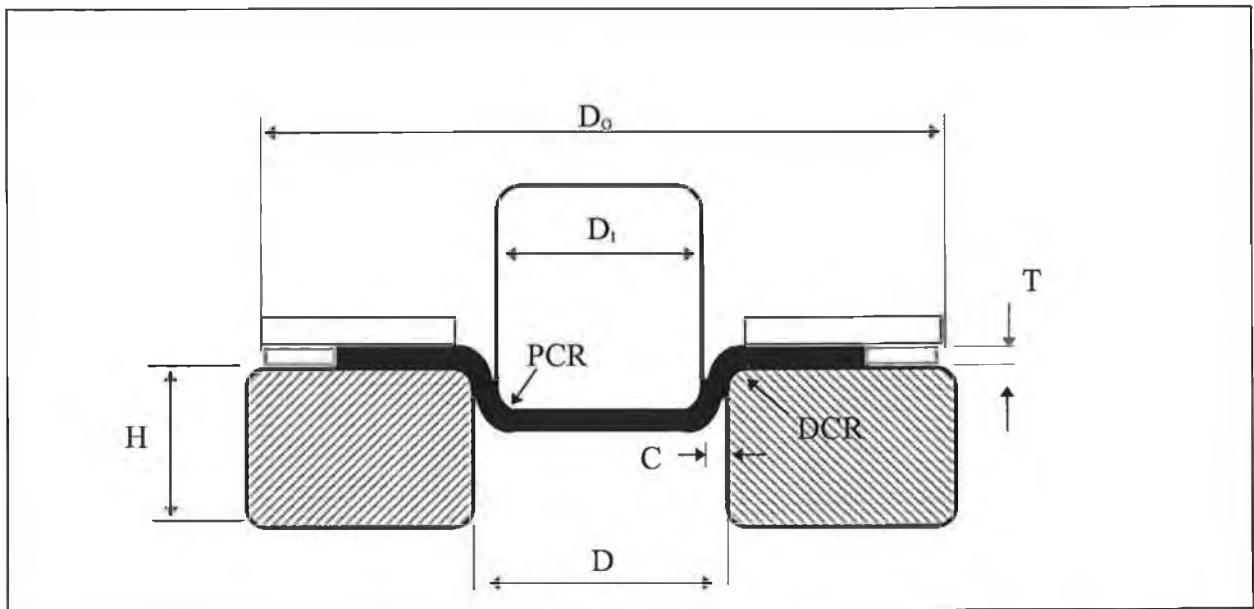


Figure 6.7 : Geometry of Drawn Cup

The material in the flange is subjected to compressive stress due to the pulling of the flange material toward the die orifice. While being squeezed the flange material increases in thickness towards the rim where the deformation becomes pure circumferential compression. Beyond this point the material in the wall which is subjected to radial tensile stress will experience thinning. Chung and Swift [6.6] show that after minimising blank holding and frictional effects, full cupping of 50% and 33% reductions respectively, resulted in 40% and 22% thickening at the blank rim.

Thinning of the cup wall results from the material experiencing stretching due to a bi-axial stress state which exceeds the yield strength of the material.

From analysis of the flanged cup wall thickness plot, in Figure 6, the finding of only 10% thickening at the rim from the analysis although seemingly contradicts Chung and Swift [6.6] can be rationalized by the fact that friction between the blank holder and blank was modelled.

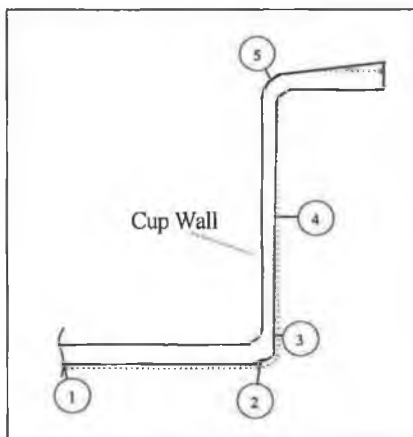
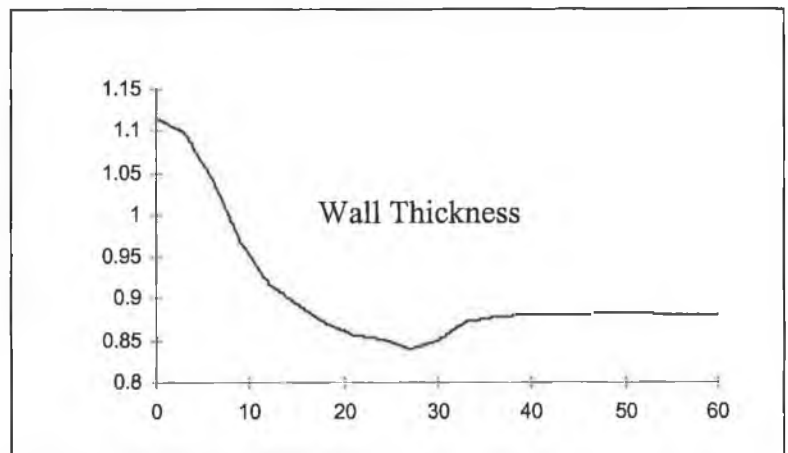


Figure 6.8 Cup Wall Thickness



Radial distance from cup centre

Figure 6.7: Wall thickness distribution

The resultant strains produce five distinct regions, each liable to develop particular kinds of defects. These regions are schematically described in Figure 6.8.

The regions most prone to thinning are the non work hardened regions. The blank material that is enclosed by the annulus of clearance. These regions do not work harden, because they are enclosed by the clearance annulus, and thus are not stretched and bent over the tool radii. This results in necking at these regions. This thinning is due to the lower yield strength of this area in relation to the remaining blank material which is work hardened.

Contour plots of equivalent plastic strain are a recognised analysis tool employed in sheet forming. The gradient of the equivalent plastic strain is an indication of how, process parameters are effecting formability. The regions of high equivalent plastic strain experience the most deformation and thus are an indication of the regions of the cup which have become work hardened. From Figure 6.1.1 it is clear that the material under the punch experiences little plastic strain therefore little work or strain hardening is

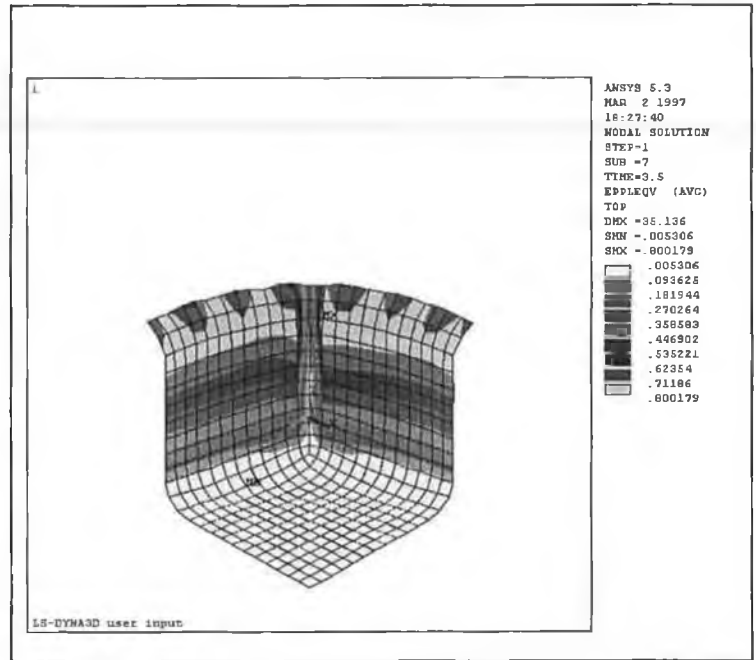


Figure 6.1.1 : Contour plot of equivalent plastic strain

experienced. Ideally the area around the two necking regions, should be subjected to work hardening as this would ensure that the likelihood of wall tearing at these most vulnerable sites would be removed, due to the increased yield strength resulting from work hardening.

6.6 The need for explicit and implicit modules

The solution times for implicit simulations increase exponentially with increase in numbers of elements contained in the F.E.A. model [3.1]. The ability to model the binder wrap and embossing process via 2D axis symmetric elements reduces the number of elements in the model.

Solution time for explicit simulation depend on the smallest element on the blank. Hence implicit F.E.A. simulations involving limited deformation solve faster than explicit simulations. So the binder wrap and embossing process are ideally solved via a implicit solver. The ability to examine the effects of tooling radii upon the through thickness stress and strain is delivered by the axis symmetric through thickness elements, which enables computation and depiction of these quantities. Implicit FEA modules enables the expert system to quickly ascertain the upper limit of the blank holder pressure under which the blank will slip between the blank holder and the die. This is termed the condition for incipient flow. They also enable the expert system to parametrically examine the consequences of changes in Tool radii upon the embossing stage,

and to arrive at an approximate of the required punch force. Implicit codes experience convergence difficulties when analysing problems involving 3D contact. For situations as this explicit codes are superior. From the above it is clear that there is specific circumstances when explicit or implicit codes are advantageous.

6.7 Discretisation of a Circular Blank

The importance of an optimum scheme of meshing for the sheet blank is reflected in the need to have a quad shaped element of uniform size through out the blank. For explicit elements the optimum shape is a square which ensure minimum distortion in calculating nodal stresses. This is important because in drawing as the element is bent by the die and punch radii the element size has a distinct effect on the mapping of the actual process deformation by the element. In that elements of different size would be subjected to differing amounts of bending stretching and compression , thus not correctly emulating the actual process. The area of the blank that is bent over the punch radii is referred to as the deformation zone and is described graphically by the series of sketches shown in figure 6.1.2.

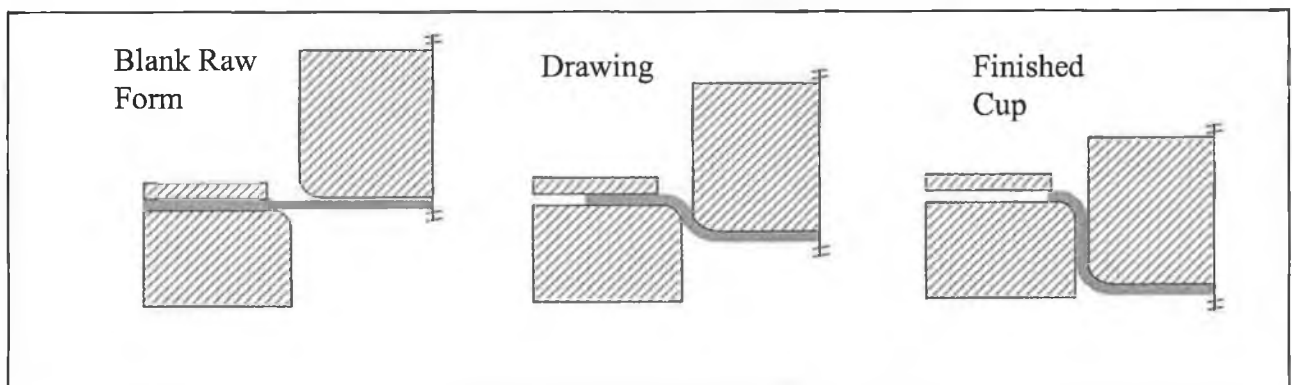


Figure 6.1.2 Deformation stages in Deep drawing

The deformation zone takes the form of the wall of the drawn cup. The element size has been set at 80% of the draw radius for maximum validity of the process for a reasonable cost in the required computer storage memory size and solution time. Many different scheme of subdividing the quarter representation of the blank into independent areas to be meshed, have been conducted. To ensure that the optimum scheme was adopted for subsequent work.

Four differing blank meshing schemes are presented in figure 6.1.3. The annulus on the graphic indicates the elements which make up the deformation zone. The optimum scheme has the uniformly sized quadrilateral shaped element within the deformation zone. Reference to quadrant two and four demonstrates that their meshing scheme have a non uniform element size, with larger element present, to the exterior of the deformation zone. Elements within the deformation zone of quadrant three are more uniform in size, but observation of the blank area under the punch shows that there are excessively small elements, the smallest of which leads to an exaggerated solution time. There is no benefit to having small element in the region of the blank area under the punch as these elements are only subjected to pure stretching and a larger element size is sufficient to model this simple deformation mode. The meshing scheme of quadrant one delivers a uniform element size with the smaller element contained within the deformation zone, consequently this meshing scheme is the optimum and will be used for subsequent work.

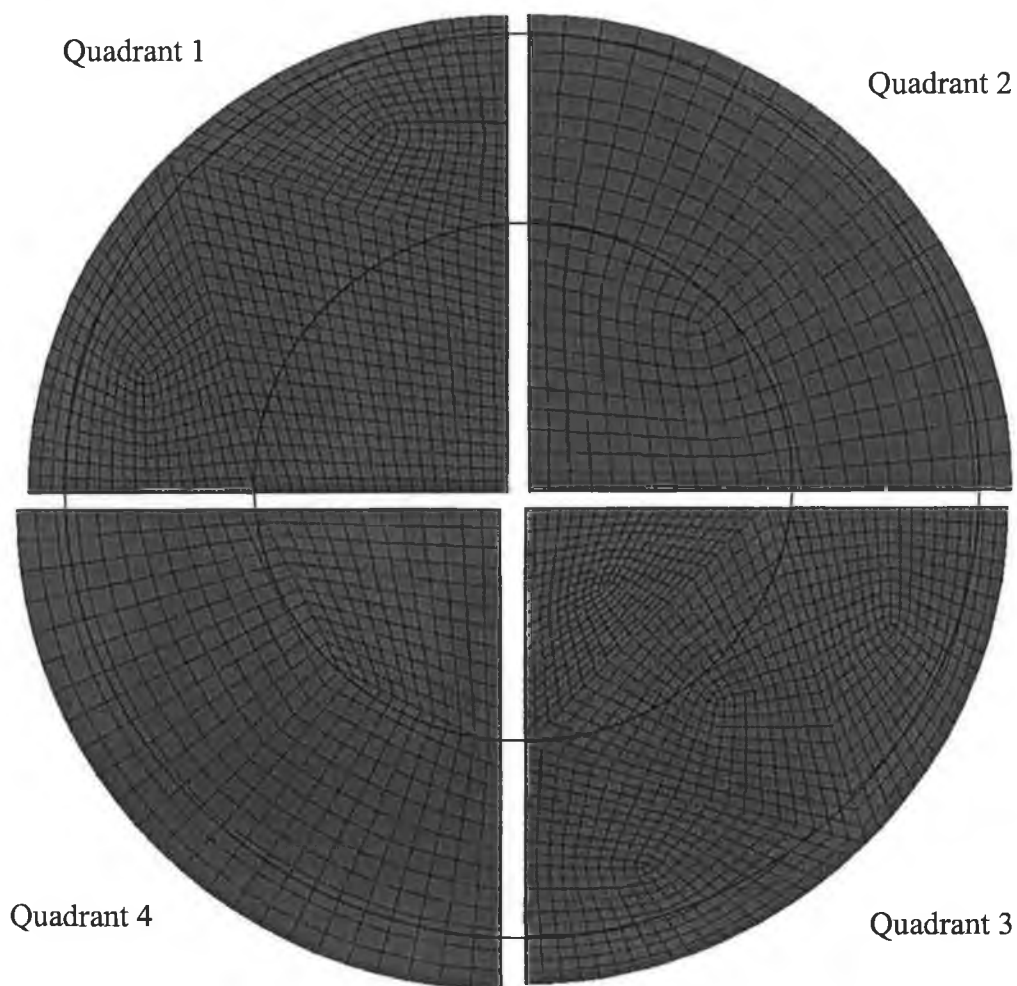


Figure 6.1.3 meshing schemes analysed for quadrant of blank sheet.

6.8 Mesh Sensitivity Study

In an endeavour to ensure the validity of the modelling process a measure of the accuracy of the solution has to be formulated. Simple error estimators have been formulated for linear elastic analysis Zienkiewicz [6.6] as follows. The Finite Element Method is an “Approximate Technique” which discretises a continuous medium into a discrete set of points and regions. Therefore there is always a “Discretisation Error” associated with a FE mesh, even if the problem is exactly specified in terms of geometry, material properties and boundary conditions. The error “ e ” depends on the accuracy of the mesh resolution, which varies with the mesh density. Hence element size “ h ” and the order of the polynomial used for the displacement function, “ p ”. Therefore $e = e(h,p)$. ANSYS does not provide for mid side noded elements within the contact algorithm, thus higher order elements cannot be used in metal forming analysis.

For a given element type the order of the polynomial “ p ” is generally fixed within the program. Therefore the error can be reduced by reducing the element size “ h ”. But as the element size is reduced the computation time increases along with the required computer storage. Thus we need to have an “Error Estimator” so that we can assess the accuracy of the solutions and where if necessary the mesh needs to be refined to improve the accuracy. In the displacement method the displacements are continuous between elements but the strains and hence stress are discontinuous because of the nature of the assumed displacement function. A typical distribution is shown below.

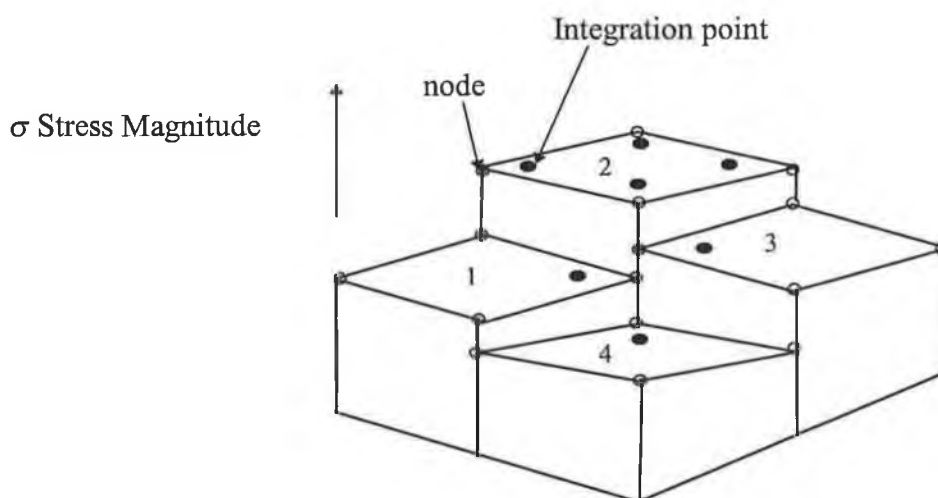


Figure 6.1.4 Un-smoothed stress distribution over Elements 1-2-3-4.

In the case of isoparametric elements it is known that the element integration points are the most accurate sampling points. The nodes which are the most useful output locations for stresses appear to be the worst sampling points. To counteract this difficulty many programmes use a technique known as “nodal averaging” take the average of the nodal stresses of all elements meeting at a common node. If the solution is accurate then the nodal average values will be close to the discrete element stress values. Therefore the difference between the nodal average derivatives i.e. (stresses) and the actual nodal values of an element give a tangible estimation for the discretisation error

The nature of the above procedure makes it unsuitable for non linear and transient problems. The author suggests from extensive research that the solution to this problem, can be supplied by a mesh enrichment algorithm Bonnet[6.7]. The mesh enrichment algorithms involves local and gradual modifications of the mesh in order to satisfy the error targets. In contrast the error estimators utilised in the mesh enrichment algorithm utilises strain differences rather than differences in stress. It is suggested that ANSYS and LS DYANA 3D incorporate such a mesh enrichment facility to ensure validity. Error estimation for this work involved a mesh sensitivity study, which was conducted as outlined in section 6.7.1. The mesh convergence was assessed for effective plastic strain as indicated below. The plot in figure 6.1.5 displays the values of the effective plastic strain for mesh sizes of varying density. It is evident that a mesh density of 30 elements along the blank edge, affords the most economic return in accuracy for solution time.

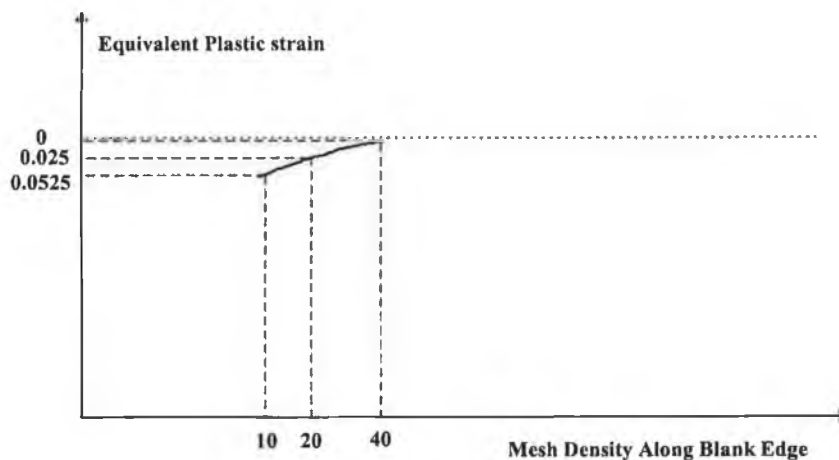


Figure 6.1.5 Mesh Sensitivity Study

It is therefore recommended that for cup drawing model development within the expert system a Tool profile radius to element size ratio of 0.7 will be applied.

6.9 Box Drawing

To assess the expert systems possible expansion into the realm of non axis symmetric shapes a study of the bench mark proposed in NUMI form [6.8] was conducted. Due to the geometry of the shape and anisotropy of the material, a one quarter model of the box will be analysed. The size of the original square blank is 150 (mm) x 150 (mm). A 30 X 30 mesh of 4 noded reduced integration shell elements was employed at first. The blank holder die punch were modelled as rigid surfaces. The friction coefficient between contacting bodies was 0.162. The punch speed in the simulation was set at 8 m/s. The blank holding force for one quarter model is 4.9 KN (19.6KN for the full cup). The tooling arrangement is as outlined in figure 6.1.6.

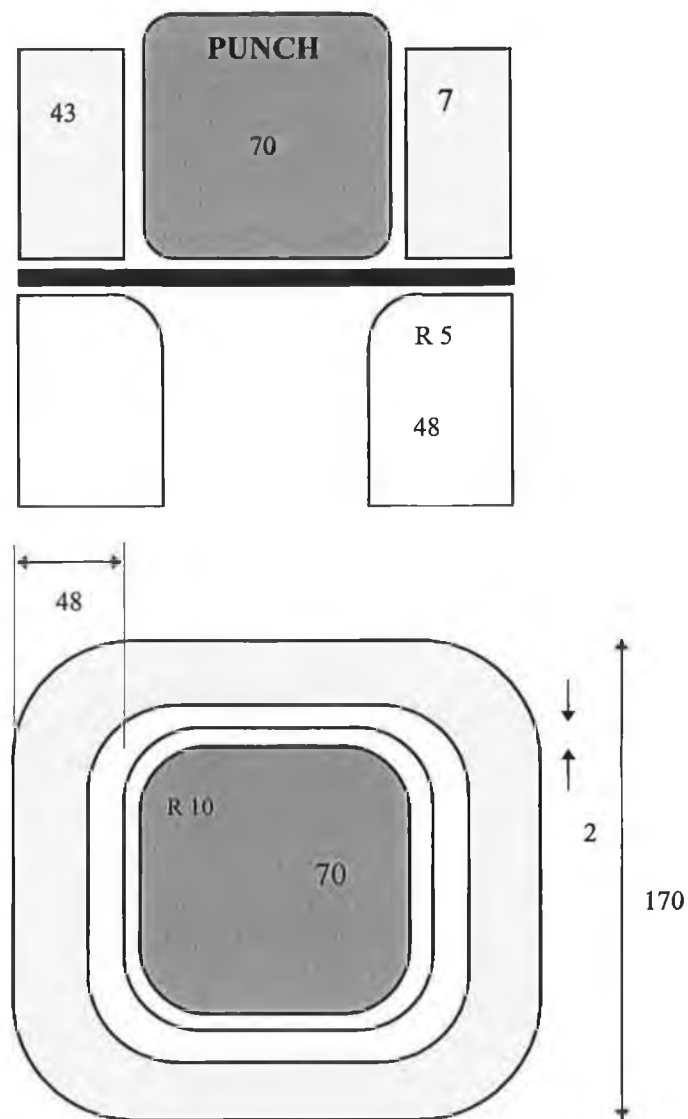
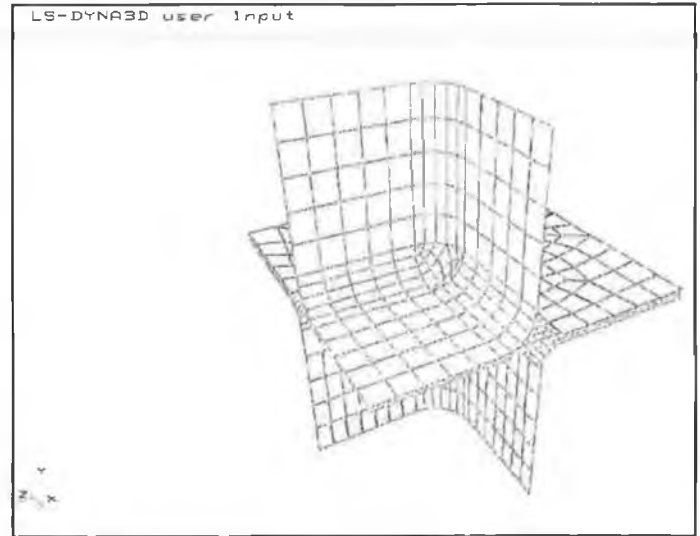


Figure 6.1.6 : Box drawing Tool geometry : Dimensions in mm.

The Finite Element model for box drawing is shown in figure 6.1.7. With the blank holder die and punch represented as rigid body VDA surfaces as for cupping in section 6.5.3.

Findings from this work indicate that box drawing is more sensitive to tool corner radius than cupping. In that the deformation process is more complex in box drawing. The mesh employed to discretise the blank should be dense enough to ensure that the complex deformation force is mapped. An adequate number of elements should be used to describe



the tool radii as a small number of elements lead to perturbations in the predicted punch force. This is due to elements of excessive size developing peaked contact loads as they slip over the tool radii. This is an inaccurate reflection of the actual state.

Thickness distribution

The comparison of actual experimental findings and the F.E.A resulting thickness distribution along line O - A is shown in figure 6.1.8. From which it is clear that the F.E.A results are valid.

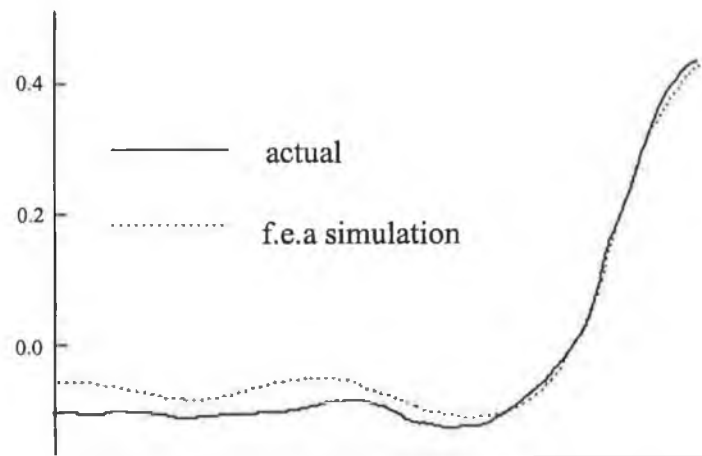


Figure 6.1.8 : Thickness distribution along profile o-a

The thickness distribution plot is shown in figure 6.1.9 from which it is evident that there is substantial thickening at the flange region of the drawn box, highly localised thinning at the box lower corner. It is clear from figure 6.1.9 that most metal flow when box drawing is from the sides. This is true for an isotropic case as shown in figure 6.1.9. The difference in the degree of metal flow from the sides and the corner of the blank is even more pronounced in the case of an anisotropic material. As indicated by figure 6.2.1.

From which it is clear that anisotropy of sheet material has a big influence in the draw ability of box shapes and thickness distribution.

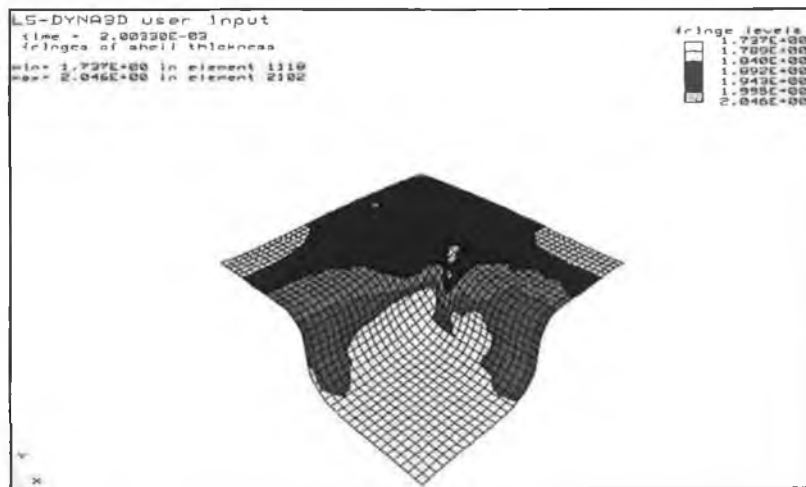


Figure 3 : Thickness distribution contour plot

Blank holder pressure sensitivity

Blank holder pressure as for cupping is critical to ensure a feasible draw. To test the sensitivity of the process the bhp was reduced by a fraction of 10%, the outcome being an unsuccessful draw with wrinkling accruing at a box height of 20 (mm). As indicated in figure 6.2.1. As the blank material within the flange is forced into the box by the application of punch force, it experiences compressive hoop stress. The resulting Poisson strains if not countered by the blank holder force will result in wrinkling as indicated in figure 6.2.1.

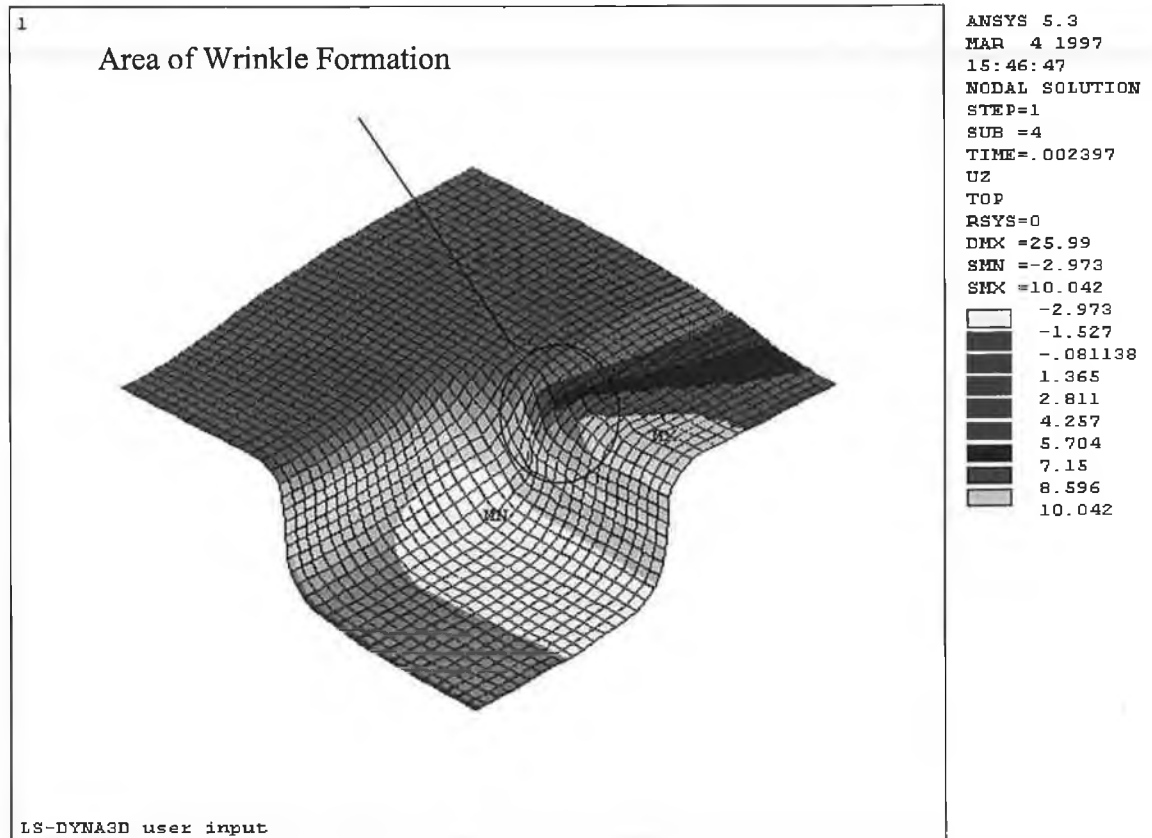


Figure 6.2.1 : Radial displacement contour plot

6.9.3 Hour glass control in box drawing.

For the box drawing analysis documented above, hour glass deformations were observed to occur. The use of hour glass control developed excessively large hour glass energy, which was over the recommended maximum of 10% of the internal energy. Therefore the only recourse was to use fully integrated elements which do not possess a hour glass deformation mode.

6.10 Formability in Sheet Drawing

The Following is a description of an industry standard Ohio State University (O.S.U.) formability test. Within the expert system the OSU test is developed in a virtual manner by a finite element analysis module. The approach for plotting the FLD (forming limit diagram), is presented.

Instability predictions are important in sheet metal forming processes, one such instability being splitting failures due to localised necking. The majority of such sheet metal industrial splitting failures occur near to the plane strain state . Therefore, sheet metal industries have been looking for an ideal formability test which allows them to evaluate sheets for their ability to resist splitting failures under near plane strain conditions. Such a test has been developed at the Ohio State University and hence it is referred to as the OSU formability test. Instabilities or defects limit useful shape changes during sheet metal forming. Puckering, wrinkling and tearing are some of the common instabilities that can develop during sheet metal forming. Sheet tearing is the most common and important instability that can be observed under stretching conditions and usually takes place in regions that have thinned locally (i.e. localised necks). Hill has predicted conditions for localised necking under conditions of negative minor strains under a bi axial state of stress [6.9] Hill,R. Mech,J.

Marciniak and Kuczynski [6.10] have introduced an approach (in which the sheet is assumed to contain an infinite length thickness defect) to predict localised necking under biaxial stretching conditions [6.10] Marciniak,Z and Kuczynski,K. .Wagoner's research group has used the Finite Element Method for the first time to predict limit strains under bi axial stretching conditions [6.11] Wagoner,R,H. Burford,D,

A significant practical departure from the traditional methods for assessing the press shop performance of metals occurred in 1965 when Keeler and Goodwin introduced the concepts of the forming limit diagram.

In the experimental approach the localised necking failures are measured and represented conveniently as a forming limit diagram (FLD), the latter being a representation of the critical combination of the two principal surface strains (major and minor) above which localised necking instability during stretching is quantified and measured in formability tests the latter allow the grading and ranking of sheet metals by evaluating their ability to resist necking instability which is observed. The ability of the sheet metal to resist necking instability during

stretching is quantified and measured in formability tests the latter allows the grading and ranking of sheet metal by evaluating their ability to resist necking instability.

Formability is the ability of the sheet metal to be stamped formed without developing any failure, thus formability is not easily quantified as it depends on several interacting factors. All of such factors (material flow properties, ductility, die geometry, die material, lubrication, press speed, contribute to failure or success of the stamping to varying degrees in an inter dependent manner. It should be noted that no single formability test can describe or quantify the formability for all types of the stamping applications.

The basic forming characteristics of sheet metals are obtained even from simple mechanical tests such as tensile, bulge and hardness tests. A high strain hardening exponent, n is related to the ability of the material to undergo large uniform strains before necking instability occurs.[6.12]. Hobbs,R,M. Duncan, J,l

Lower yield strength gives lower spring back and better fixing of shape in lightly formed parts. A high value of the strain rate sensitivity index, m also improves material formability by delaying the onset of localised necking, high magnitude of anisotropy index, r , gives better draw ability in material by resisting thinning due to the anisotropic properties of the sheet leading to less strain in the sheet thickness direction, while keeping the required peak loading to induce deformation to that of the isotropic case due to the fact that the deviatoric stress state for both the isotropic and anisotropic case are identical.

The important modes of deformation that exist in a industrial stamping are drawing and stretching. several formability tests have been developed that simulate this such formability tests are termed “ Simulative Tests”. Some of the popular simulative tests are The Swift cup test Chung ,S,Y and Swift ,H,W[6.13] The Erichsen [6.14]and the Olsen dome tests and the LDH test Hecker,S,S [6.15]

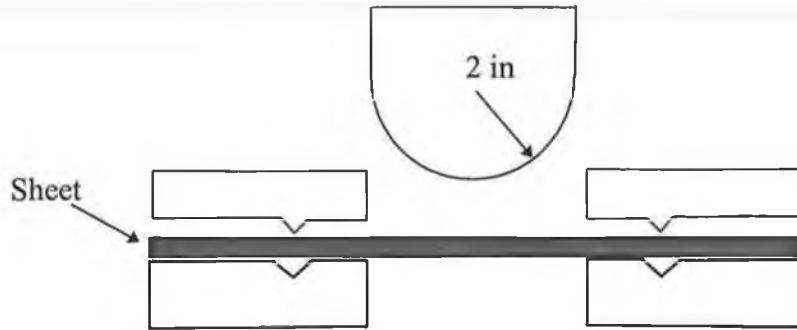


Figure 6.2.2: Geometry of the OSU Formability Test

As can be seen from Figure 6.2.2, the OSU formability test is similar to the LDH test geometry. This geometry is expected to produce more stable plane strain conditions because of the two dimensional nature of the punch. The test blanks are 178 (mm) in Length by 124 (mm) in Width.

6.10.1 Finite Element Module Forming Limit Diagram

The Finite Element Module Forming Limit Diagram is based on the OSU formability test, which is modelled within Ls Dyna the FEA model is shown in figure 6.2.3. The test geometry is modelled by a half symmetry FEA model, the clamping action is provided for by restraining nodes on the sheet to mimic the actual conditions. The OSU formability test lends itself very easily to FEA simulation in that the complexity of modelling the blank flange is removed.

LS-DYNA3D user input

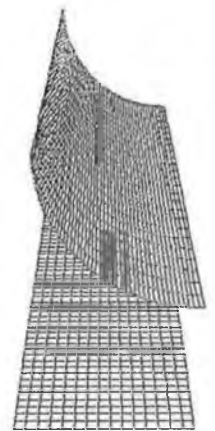


Figure 6.2.3 : OSU model

The thickness values are read by a macro program in ANSYS (APLD) which ascertains the thickness values for the elements in the test sheet. The thickness information is then interrogated to locate region of necking, the principle strains for these element are then outputted to a formatted file via ANSYS (APLD) commands. The resulting FLD is plotted with over laying process strain conditions for the simulation in progress, by LS DYNA 3D post processor or LS TAURUS.

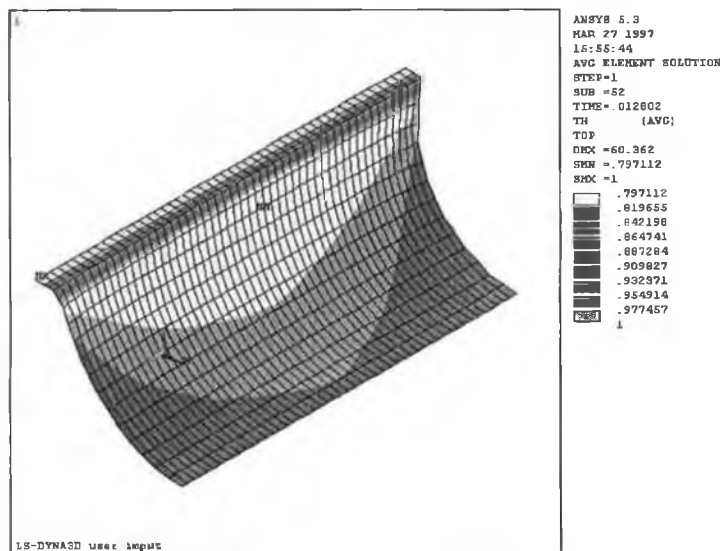


Figure 6.2.4 : Contour plot of thickness distribution for OSU test specimen

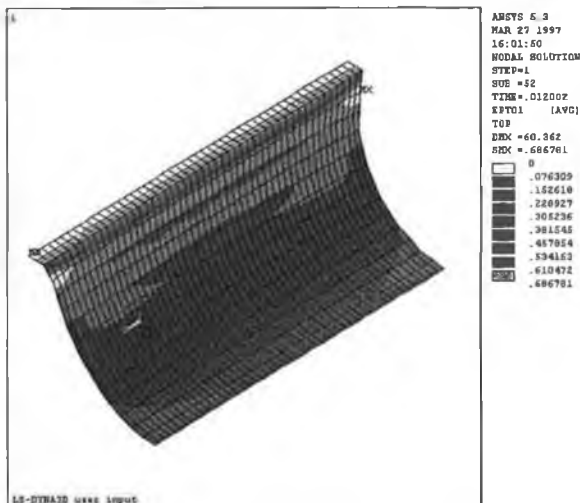


Figure 6.2.5 : Contour plot of 1st Principle

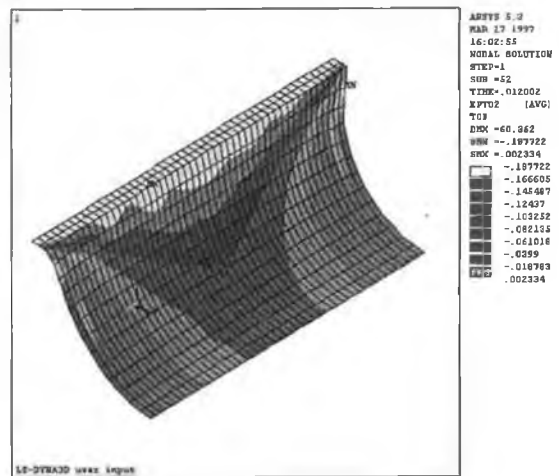


Figure 6.2.6 : Contour plot of 2nd Principle strain

From Figure 6.2.4 the Contour plot of thickness distribution for OSU test specimen it is visible that the test develops a high gradient in thickness changes, enabling the necking condition to be observed. The principle strains that drive this thinning are presented in figure 6.2.5 and figure 6.2.6.

6.10.2 Post processing

Post processing of the results of forming simulation must be user friendly, with interactive graphics and trade oriented vector plots. The essential features include easy plotting of deformed meshes, time histories, contours and distributions along selected sections of thickness, stress strains contact forces and distance to rupture.

Forming Limit Diagrams and detection of buckling via local zooming and amplifications. Global output variables comprise blank holder force and uplift, punch force, internal energy, contact friction energy, blank area tearing, buckling, thinning and wrinkling. Throughout this Thesis vector plot of thickness effective plastic strain and stress and sheet thickness line plots have been presented. Now the of a forming limit plot is presented. Post processing of analysis results by FLD is developed by superimposing elements principle strains on the forming limit curve, as illustrated by Figure 6.2.7.

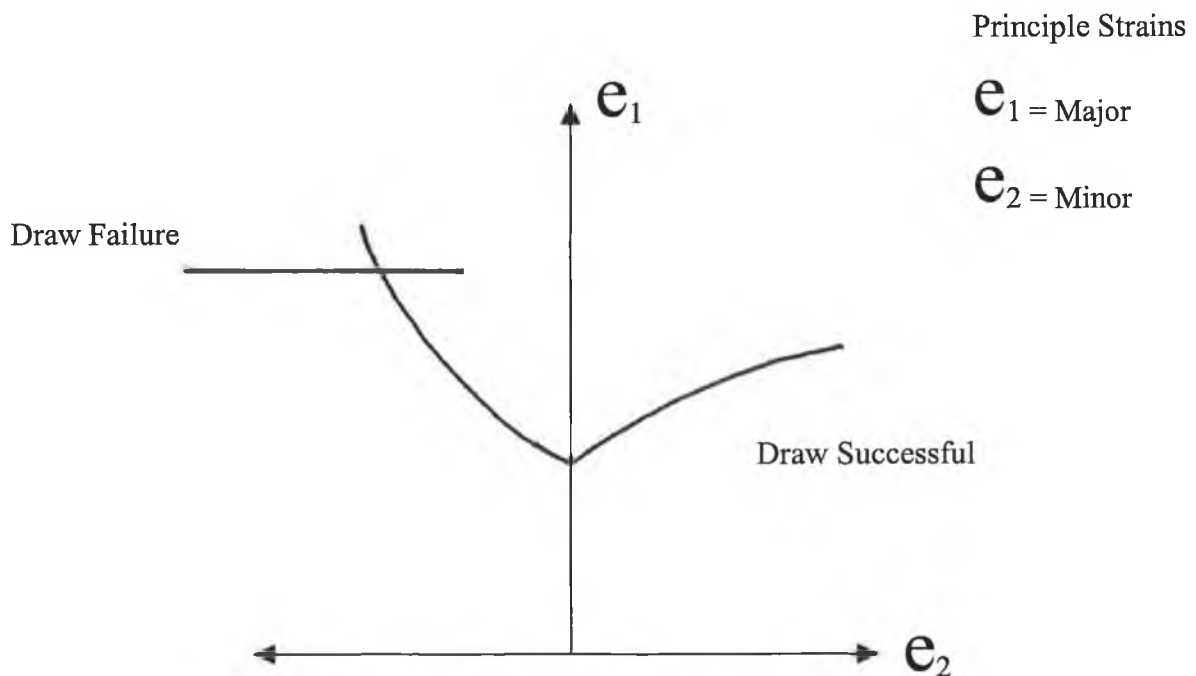


Figure 6.2.7 : Forming Limit Diagram

6.11 Conclusion

It is clearly apparent from this chapter that the implicit and explicit F.E.A. codes have specific areas of application, and for an effective expert system, implicit and explicit F.E.A. software provides a flexible simulation Tool. The 2D and 3D finite element modules which make up the knowledge base of the expert system were presented, their use and applicability being explained. The discretisation process to ensure that the F.E.A. simulation is accurate was discussed and formulated. The formability of sheet metal is discussed and an example run of the formability module is presented.

Chapter 7: Expert System Rule Development by Taguchi Experimental Design and results Analysis of Finite Element Analysis

7.1 Introduction

This chapter is dedicated to developing rules for the Expert system. The developed rules take the form of suggested process parameters to meet the required cup specifications. The Taguchi method of experiment design and results analysis is used to develop the F.E.A models and analysis the results of the simulation.

7.2 The Taguchi method of experiment design and analysis of results.

The Taguchi method of experiment design and results analysis will be applied to develop strategies for the design of the F.E.A. simulation. These experimental simulations are conducted to ensure that the most use is made of the F.E.A. analysis. This work also to indicate the process and F.E.A. solution variables that will enable the development of the best possible F.E.A. component to the expert system. This work leads to the development of accurate simulation of the metal forming process, reduction of computation times and the development of rules for specified stipulations on cup specifications.

The Taguchi method [7.1] calls for :

- The formulation of the problem in a clear statement of the objectives of the experiment.
- Determination of the response characteristic to be measured as the objective.
- Listing of the design variables which affects the process response and classification of these variables as controllable parameters (design variables) or noise variables.
- List pairs of control parameters whose interactions may potentially affect the characteristics of the process.
- Highlighting of the control parameter and noise that will effect the attainment of the objective.
- Decision on the tentative number of settings for each control parameter. Two levels per design variable results in smaller numbers of experiment, but three levels ensure that nonmonotonic response will be detected.

The arrays that Dr Taguchi uses are one form of fractional factorial design [7.1]. One important advantage is that they allow us to obtain almost the same amount of effective information as we could in a full factorial with significantly fewer experimental runs. Taguchi, however, uses orthogonal arrays for a very different purpose than most traditional approaches, to evaluate the effect of factors with respect to robustness. Dr Taguchi treats interactions between control factors as being equivalent to noise. It looks at interactions not as one factor affecting another, to be controlled, but as factors we cannot control. Our goal is to find the combination of control factors levels that is robust against noise. As will be demonstrated later, the underlying philosophy of parameters design is to separate control factors from noise factors and then to investigate interactions between control factors and selected noise factors using orthogonal arrays.

The signal to noise ratios are grouped in classes such as “smaller the better”, “nominal the best” and “larger the better”. For the work conducted in this section the “nominal the best” class is applied as the objectives as set out latter are a value present at approximately the mid point of a tolerance zone. The signal to noise ratios are computed on the response table as out lined below The Taguchi method progresses as out lined in the schematic of Figure 7.1. The response table signal to noise ratios and means are plotted and the Two Step Optimisation by Analysis of Variance is conducted as outlined below.

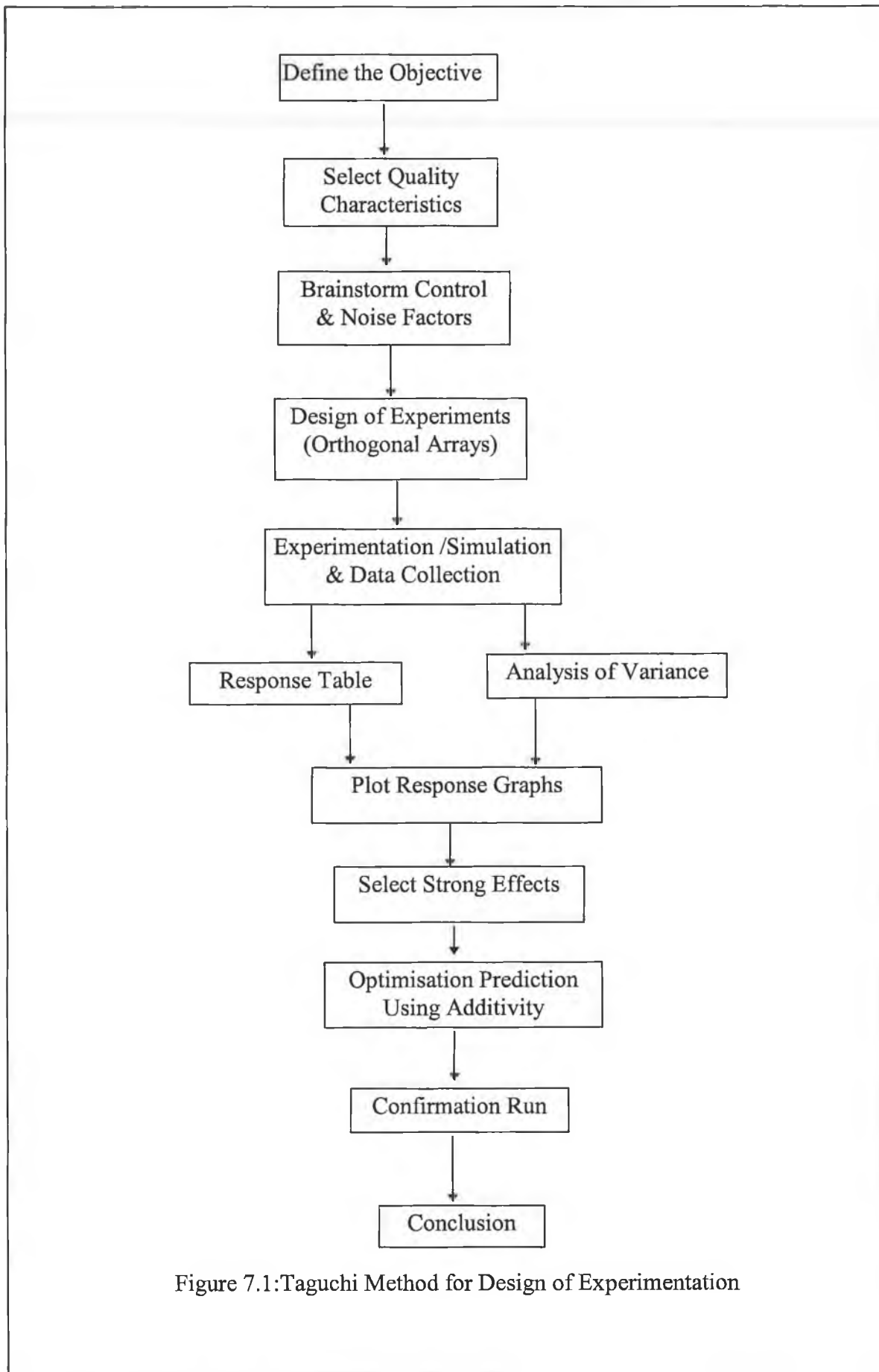


Figure 7.1: Taguchi Method for Design of Experimentation

The steps identified in figure 7.1 are developed in the following section.

Define the objective.

The objective of the Experiment is the quantity that is wished to be improved upon, for example cup wall thickness distribution.

Selects quality characteristics

The quality characteristic is the desired change in the objective. In this example to reduce punch force which leads to a quality characteristic of “nominal the best”.

Control and noise factors

The control factors are the process parameters that effect the objective. For the Punch force objective the control factors are die corner radius punch corner radius blank holder pressure.

Orthogonal array

The orthogonal array stipulates the form of the experiment That is the values that the control factors will take on for, the different runs. An example of such the L^4 is shown in figure 7.1. As depicted , the L^4 experiment consists of four rows and three columns where each row corresponds to a particular experiment and each column identifies settings of a control factor. In the first run for example, the three control factors are set at their low level (level 1), In the second run, the first parameter is set at level 1 and the remaining two variables are set to the high level (level 2), and so on

RUN	Control 1	Control 2	Control 3
No. 1	1	1	1
No. 2	1	2	2
No. 3	2	1	2
No. 4	2	2	1

Table 7.1 : L^4 Orthogonal array

Response Table

The response table contains the values of the objective output from the analysis runs.

Analysis of variance.

The Anova table contains the mean and the signal to noise ratio from the objective values contained in the “response table”.

Analysis of variance response plots

The Anova response plots contain plots of the mean and signal to noise ratio for the two levels of the control factors, as shown in figure 7.2 .

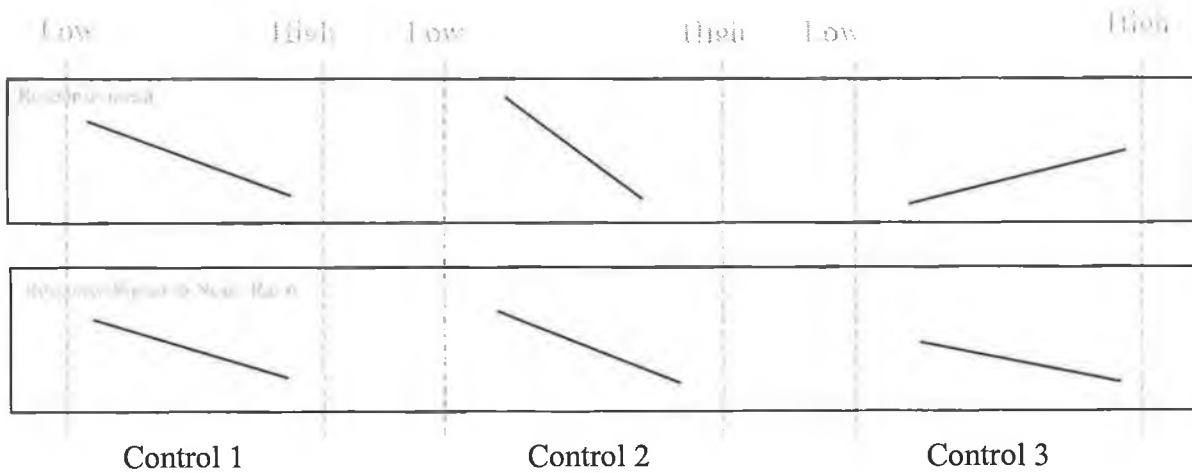


Figure 7.2 : ANOVA Mean and Signal to noise plots

A confirmation Run of the optimised setting is now conducted the S/N ratio for this confirmation run is compared with the S/N ratio predicted at the optimisation stage. If the predicted and confirmed S/N ratio compare favourably then the findings from the Taguchi analysis are adjudged to be valid.

7.3 Signal to noise ratio as a measure of variability [7.1]

The signal to noise ratios are developed by the following theory. Both the signal to noise ratio S/N (dB) and the variance (σ^2) measure variability. The signal to noise ratio S/N measures variability in relation to the mean in terms of \pm % of the mean σ^2 measure variability in terms of \pm absolute units. For characteristics on an absolute scale ($y \geq 0$), we can measure % variability in relation to the mean. As :

$$S/N = 10 \log \left[\frac{y^2}{\sigma_{n-1}^2} - \frac{1}{n} \right]$$

where : σ_{n-1}^2 is the sample variance (S^2) the standard deviation squared.

y is the mean of the sample response table values

This type of data is referred to as Nominal the best type I

For characteristics that can take on negative values, \pm % mean loses its meaning. Here we must use a measure that gives us variability in terms of \pm absolute units.

$$S/N = -10 \log \sigma_{n-1}^2$$

This type of data is referred to as Nominal the best type II

The reason for multiple forms of S/N ratio is that a lot of engineering knowledge is packed into the S/N ratios for different situations. The application of the appropriate one is necessary a valid application of the Taguchi method.

7.4 Two Step Optimisation by Analysis of Variance [7.1]

The operating window of the “type I” and “type II” nominal the best problems occur frequently in optimisation studies and is composed of the following two steps. Firstly 1 maximise S/N to minimise sensitivity to the effects of noise. To accomplish this, first identify the control factors that have significant slope in their S/N plots, and then select control factors that correspond to the maximum S/N values. Secondly adjust the mean response onto the target response. To accomplish this identify the control factor that has both the greatest slope from the mean plots and the smallest slope in the S/N plots. This control factor is used to adjust the mean.

The Anova plots Figure 7.2 are compared to identify the control factors that minimise variability. The key is that factors whose effect on the S/N ratio is relatively strong should be used to reduce variability. Factors whose effect on the mean is relatively strong should be used as scaling factors (type I NTB) or as tuning factors (type II NTB), or other S/N ratios.

By analysing the response plots for S/N and mean, the control factors can be classified into one of four types.

1. Those that affect both the mean and the S/N. The control factors that affect both metrics are typically used to minimise the effects of noise.
2. Those that affect the mean but not the S/N. A true scaling or tuning factor is one that has very little slope in the S/N plot, but a relatively large effect on the mean. A factor that has too much sensitivity to noise leads to difficulties when it is used to shift the mean, because it also increases variability.
3. Those that affect the S/N and not the mean. The control factors that affect only the S/N ratio should be set at the levels that give the highest S/N ratio values.
4. Those that affect neither the S/N or the mean. Typically those control factors that do not show significant effects on the S/N or the mean response are set at the most economical levels in order to keep costs low.

Once the strong effects have been selected by the analysis of variance as outlined above, the optimised levels of the control variables is found. A confirmation run is then conducted with the presented optimised values of control variables, if the predicted signal to noise run is close to the actual signal to noise ratio for the conformation run then the analysis and experimental findings are gauged to be correct. The process is then optimised by the control variables being set at the optimised settings.

7.5.1 Sensitivity study of punch and die Tooling radii to cup formability.

The work of Chung and Swift [7.2] showed that punch geometry i.e. punch corner radius is a major variable in deterring the limiting draw ratio of blank original diameter and cup diameter. Strain analysis in the neighbourhood of point 3 of figure 7.5 indicates susceptibility to tearing. Imperial finding from Hobbs [7.3]. Indicate that for a punch corner radius of less than or equal to twice the thickness the cup is highly prone to failure by tearing, whilst for a punch corner radius less than or equal to ten times the thickness stretching may be introduced. It was also found that within the range of $(4t \leq pcr \leq 10t)$ the exact radius does not significantly affect the limiting draw ratio. Thus punch corner radii in the order of these values will be used for the F.E.A. tooling simulations.

Variations in die corner radius have the following effects The larger the bend radius the greater the punch load profile over punch travel, also the greater the plastic work done in bending. Small die corner radii may cause local failures in the bending zones by increasing the tendency to work harden. The smaller the die corner radius the greater the peak punch load and the lower the limiting draw radius is. Increasing the punch load increases the load the cup wall and its weakest area (point 3 in Figure 7.4) has to withstand. An Analytical model of plastic bending of a sheet over a die radius was developed by Slater [7.10] the analysis assumed linear strain hardening, and assumed no thickness change. The model developed an expression for stress due to plastic bending as outlined in Equation 7.1.

$$\sigma_{bending} \approx \frac{\left\{ \sigma_y \left[1 + \left(\frac{\sigma_r}{\sigma_y} \right)^2 \right] \right\}}{\left\{ \sqrt{2.3} \left(r_{die} + \frac{t}{2} \right) \right\}} \quad 7.1$$

However in an effort to reduce the stress in bending with respect to Equation 7.1, by increasing the die corner radius too much leads to wrinkling at the die rim. The effects of die corner radius; dcr to sheet thickness ratio, original blank diameter Chung and Swift [7.2] is depicted by Figure 7.3.

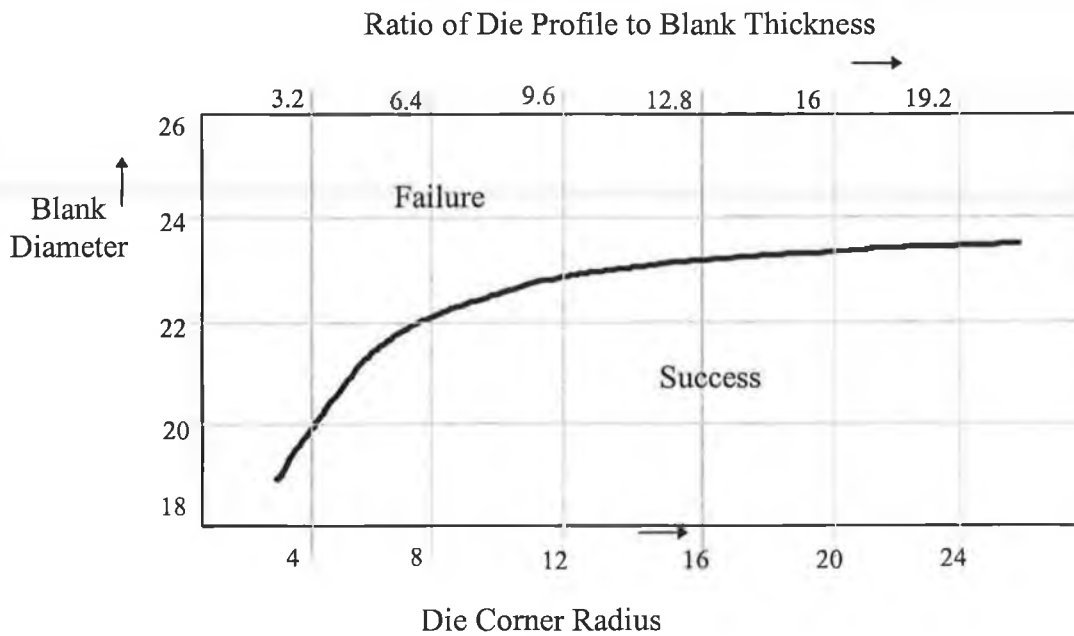


Figure 7.3: Effect of Die Profile on Formability [7.2]

The optimum die corner radius is set within the range of twice the sheet thickness to ten times the sheet thickness. The limiting draw ratio is affected by die radius on a nearly linear basis as indicated from Figure 7.3.

Work on the above is continued by a virtual treatment of Deep Drawing variables which are assessed via Finite Element Analysis. A brief introduction to the process variables of deep drawing is presented these variables are optimised for uniform thickness distribution by application of the Taguchi method of experiment formulation, and experimental results analysis. The finding of the F.E.A. simulation along with those already sourced from reference material will be used to construct rules, within the expert system. These rules present an optimisation, of the process variables encountered in the deep drawing operation.

The vertical cup drawing process variables which become control parameters as defined by taguchi, are punch corner radius (PCR), die corner radius (DCR) and blank holder pressure (BHP). The clearance of 25% as recommended by Johnson and Mellor [7.3] for a drawing ratio of approximately two has been used so as to remove any likely hood of ironing within the deep drawing process which is not being considered. For the F.E. analysis the element size is within that recommended by Mattiasson [7.4] 80% of the die draw radius.

7.5.2 Deep Drawing process variables.

Drawing is classified as shallow or deep drawing, when the drawn cup is less than one half the cup diameter, or more than one half the cup diameter respectively. Thinning of cup walls is more predominate in deep drawing, hence the process looked at is deep drawing. The geometry of the cup deep drawing process is outlined in Figure 7.4 and Table 7.2.

Punch Diameter	P
Die Diameter	D
Punch Corner Radius	PCR
Die Corner Radius	DCR
Clearance	C

Table 7.2 : Deep drawing variables

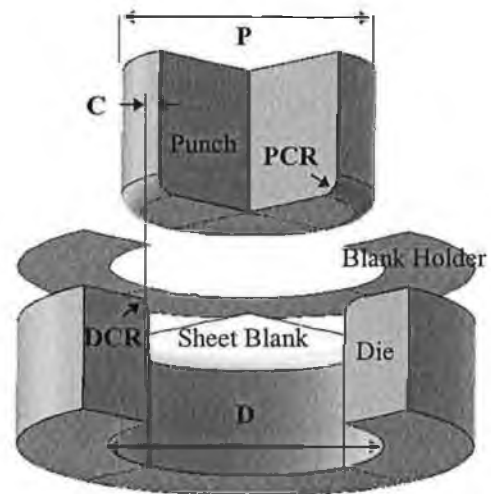


Figure 7.4 : Deep drawing geometry

The promotion of uniform wall thickness in cup drawing calls for; (1) an increasing blank holder pressure as the cup is drawn Kawai [7.11], and (2) an optimum (DCR) which is dependent on sheet thickness Hobbs [7.12]. Since varying Blank holder pressure and (DCR) over the process time is not feasible, a compromise between (BHP), (DCR) and (PCR) has to be arrived at to ensure uniform wall thickness. The objective of this study is to set these optimum levels.

7.5.3 The application of the Taguchi Method

Varying one factor (PCR) (DCR) (BHP) at a time does not account for noise factors within the process that have an effect on experimental results. This leads to non reproducibility of results, because the experiment as designed does not emulate production conditions. Full factorial experimentation where all possible combinations of control factors are investigated, leads to an impracticably high number of experiments. The Taguchi method [7.1] uses orthogonal arrays. Orthogonal experimental design is not interested in the results of one treatment combination, but

in the average change in the response over a number of experimental runs. Which increases reproducibility of results. The Taguchi method has been used in process improvement since the 1950's in Japan.

Noise factors are :

- Element size to Tool corner radii.
- Differences in plasticity development due to the varying strain paths of experimental runs.

These noise factors were eliminated by taking thickness readings at five points through the wall profile as shown in Figure 7.5. These points have been chosen as they are the points at which significant changes in the nominal sheet blank thickness will occur.

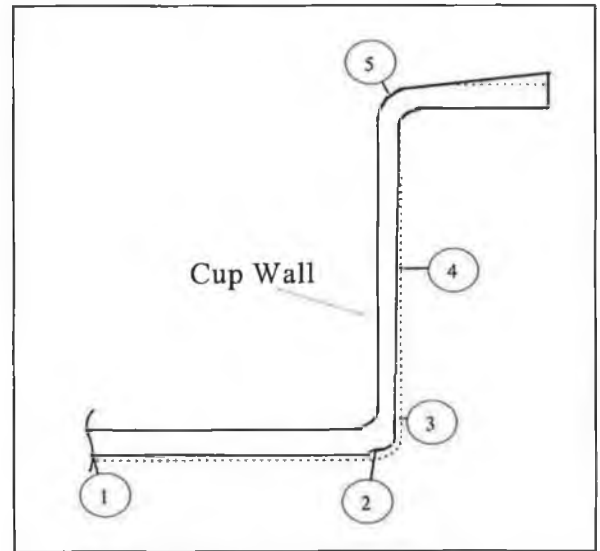


Figure 7.5 Cup Wall Thickness

Point 2 and 3 are located at the necking regions at which failure by tearing is expected

to occur. The signal to noise (S/N) ratio was evaluated for the performance stability of the output characteristic, namely reproducibility of the thickness profile.

7.5.4 Taguchi orthogonal array

The array chosen for the analysis was an L4 orthogonal array as shown in Table 7.3

The Finite Element Analysis was conducted with LS DYNA 3D code.

RUN	Control 1	Control 2	Control 3
No. 1	1	1	1
No. 2	1	2	2
No. 3	2	1	2
No. 4	2	2	1

Table 7.3 : L⁴ Orthogonal array

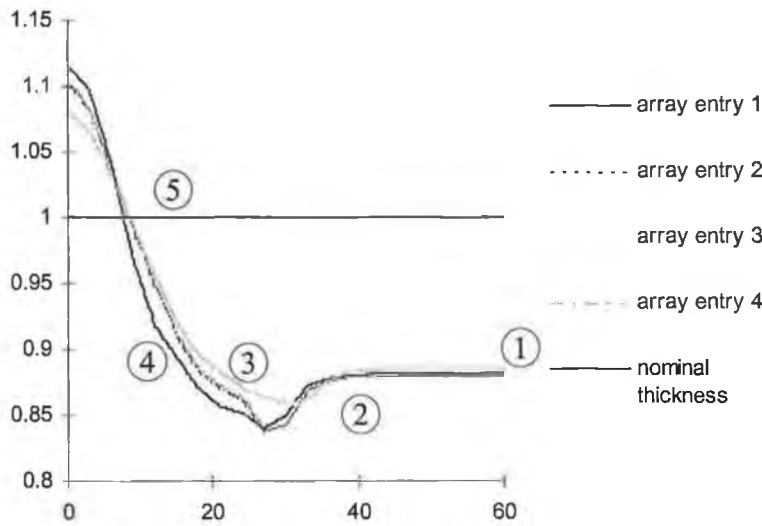
RUN	PCR	DCR	BHP
1	3	5	150
2	3	10	400
3	8	5	400
4	8	10	150

Table 7.4 : Analysis run variables

Dimensions in (mm) , Pressure in (PSI)

7.5.5 Finite Element Analysis results

The thickness distribution for the analysis run with variables set as in Table 7.4 is shown in Figure 7.5, shows a graph of the thickness distribution against the radial distance from the open end of the cup to the centre.



end of the cup to the centre. The trend of these plots shows that the base of the cup has thinning with substantial thinning (necking) occurring at points 2 and 3 as indicated from Figure 7.6. The vertical section of the cup shows a monotonically increasing thickness with distance from the centre of the cup.

Figure 7.6: F.E.A. resulting thickness distribution

7.5.6 Signal to Noise

The data for the Signal to noise ratio Table 7.6 was obtained from the thickness plots at point 1 to 5 indicated by Figure 7.5. and labelled on Figure 7.6 for clarity, is recorded in Table 7.5.

RUN	DEVIATION FROM NOMINAL THICKNESS AT POINT				
	1	2	3	4	5
1	0.11887	0.12725	0.14823	0.10611	0.0793
2	0.12006	0.13012	0.1381	0.09031	0.0655
3	0.12072	0.14247	0.1518	0.11734	0.0625
4	0.11407	0.13729	0.12936	0.0817	0.0537

Table 7.5 : Deviation from nominal thickness

7.5.7 Analysis of Variance (ANOVA).

RUN	PCR	DCR	BHP	RESPONSE AVE	RESPONSE S/N
1	3	5	150	0.12	13.13
2	3	10	400	0.11	11.12
3	8	5	400	0.12	10.69
4	8	10	150	0.1	9.41

Table 7.6 : Analysis of variance Response Table Results

The analysis of the ANOVA results in Table 7.6 consists of the following two steps.

- Step 1 Maximise S/N to minimise sensitivity to the effects of noise. To accomplish this, first identify the control factors that have significant slope in their S/N plots, and then select control factors that correspond to the maximum S/N values.
- Step 2 adjust the mean response onto the target response. To accomplish this identify the control factor that has both the greatest slope from the mean plots and the smallest slope in the S/N plots. This control factor is used to adjust the mean.

Optimisation of parameters involve the application of these two steps to figure 7.7.

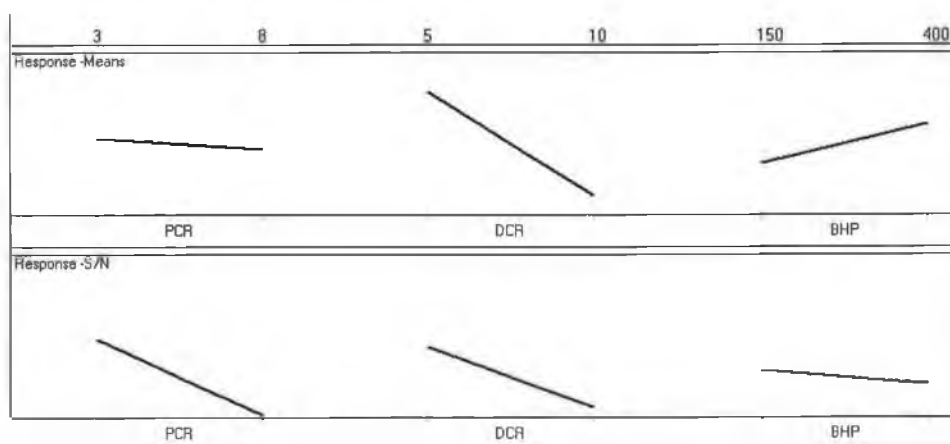


Figure 7.7 : ANOVA mean and signal to noise plots

From reference to Figure 7.7 the punch corner radius (PCR) and die corner radius (DCR) have the more significant slope on the signal to noise plot. Hence the maximum S/N values of the control pcr, dcr indicates the optimum levels as pcr = 3 mm (i.e. three times the sheet thickness) and DCR = 5 mm (i.e. five times the sheet thickness). Application of step 2 indicates (BHP) as the control factor to set the mean as it possesses the greatest slope from the mean plots and the smallest slope in the S/N plots. The Taguchi method optimisation of deep drawing sets the optimum condition for deep drawing variables to promote uniform wall thickness as follows. The (PCR) and (DCR) to be set to the lower value of the recommended range, and for the blank holder force to be the minimum possible while still preventing wrinkling.

7.5.8 Conclusion

A verification run with the above optimum settings was performed to validate findings. The predicted S/N ratio for the optimum was 13.1 dB, which compare very favourably with the actual S/N Ratio from the verification run of 12.2 dB, indicating valid findings from the application of the Taguchi method. The finding can be explained in a practical sense as follows. The highly localised bending due to the reduced tooling radius leads to a reduction in thinning due to bending stresses. The minimalist blank holding pressure ensures that thinning is reduced for the earlier stages of the draw by reducing the tensile stress in the cup wall.

7.6 Punch Force In Drawing

Experimental work conducted by Eary, D.F. and Reed [7.5] show that a punch load travel diagram has the characteristics as shown in figure 7.8. The load required to emboss, straighten and overcome static friction, to initiate static friction, accounts for 60 % of the full thrust [7.6]. After compression starts, the load increases due to work hardening to a peak. This maximum occurs typically within a region extending over one third to two thirds of the stroke, and depends upon the strain hardening characteristic of the blank. Drawing of flange less cups evolves the punch force to zero at completion of the cup upon when plastic deformation has ceased. Drawing of cups with a flange, results in the force attaining a minimum value above zero at the required cup height, due to cup wall spring back producing a resisting force upon the punch.

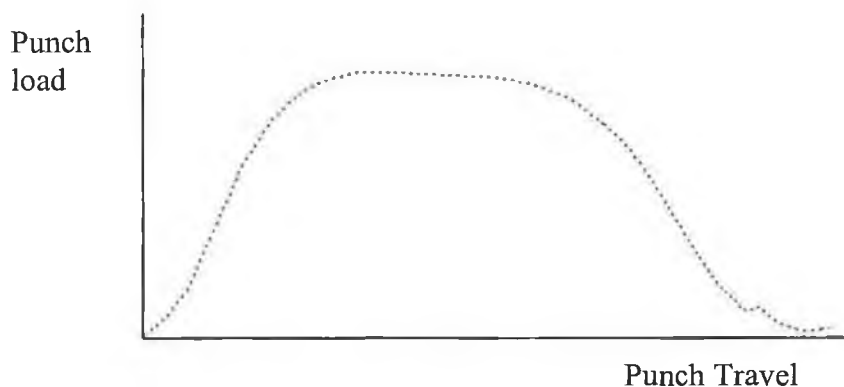


Figure 7.8 :Punch load versus Punch Travel

Although the contributing factors to the punch force have been developed for more than fifty years, an analytical treatment for materials under bi-axial stress is not possible due to the lack of adequate plasticity flow stress and work hardening models. This resulted in punch force being approximated by many empirical equations, such expressions are to be found in abundance in industrial presswork design hand books. From Duncan, J. and Johnson, W. [7.7] the most applicable empirical representation of the punch force is given by Equation 7.2.

$$P_{\max} = \frac{1}{4} \pi^2 d_{cup} t_o (\sigma_o + \sigma) \ln \left[\frac{D^2 + 1}{2} \right] / \sqrt{3} \quad 7.2$$

The empirical approximation of Equation 7.2 was found to comply favourably with the F.E.A. simulation punch force presented in Figure 7.9, hence equation 7.2 will be used as a predictive rule in the experts system rule base.

The most detailed analytical study of the deep drawing process is represented by work conducted by Avitzur [7.8] in which he develops an upper bound analysis to include flow along a die bend. This leads to a complicated and not directly applicable relationship for punch force. Assuming that uniform wall thickness is preserved, and applying a series of simplifying assumptions, the punch force is described as a function of DRR, TR, D, η , and blank holder force. Hence the need for an expert system driven by the results from a dependable source such as F.E.A. is plainly apparent.

7.6.1 Punch force sensitivity study

The object of this study is to build new rules and examine current suggested practice for cupping in a rigid manner by conducting Finite Element Analysis. The necessary Punch force to drive the deformation process is critical to deep drawing, in that the level of the punch force sets the tension in the wall of the drawn component. This develops a tensile stress in the wall, which can lead to thinning of the wall, resulting in draw failure due to necking. The punch force necessary to draw the component is set by the die corner radii and the blank holder force. The following analysis was conducted to assess the contribution of these two factors to punch force. This information will be used in developing rules for the expert system.

The process of cupping (drawing of vertical walled cylindrical cups) was analysed, three different analyses were conducted as outlined in table 7.6.

Analysis	DCR	BHP
A	Small	Low
B	Large	Low
C	Small	High

Table 7.7 : Analysis process combinations

The resulting plots for the analysis are shown in figure 7.8 , from which it becomes evident that increasing the pressure, as expected increases the required punch force. This increased punch force is a resultant of the friction in the flange between the blank and the tooling increasing due to the increased normal force of contact. Increasing the die corner radius reduces the required punch force as is evident from Figure 7.9. For an overall perspective the pressure contributes more to the required punch force, than reduced die corner radius. Observation of the initial slopes of punch force to punch travel indicates, that the material is subjected to less work hardening as the die corner radius is increased. The above conclusions and findings are to be incorporated into the rule base of knowledge for the expert system.

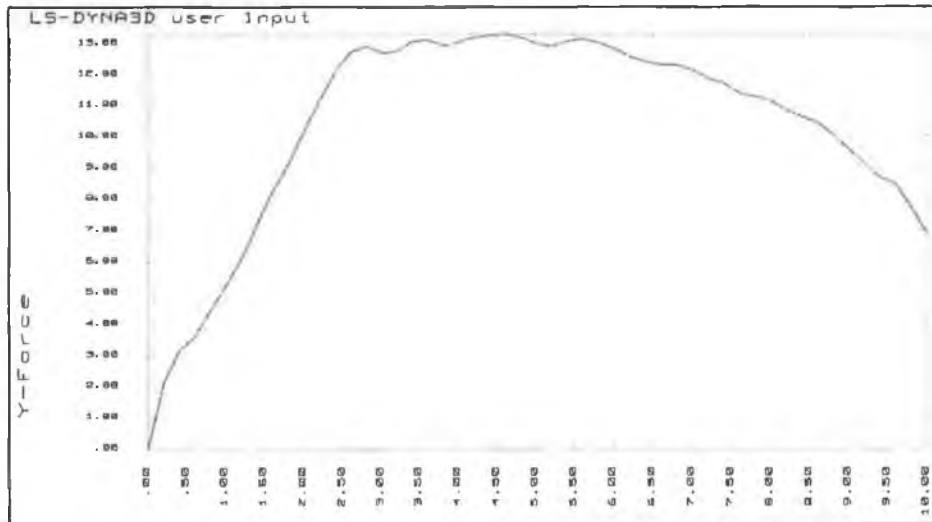


Figure 7.9 : Punch force verses Punch displacement for analysis A

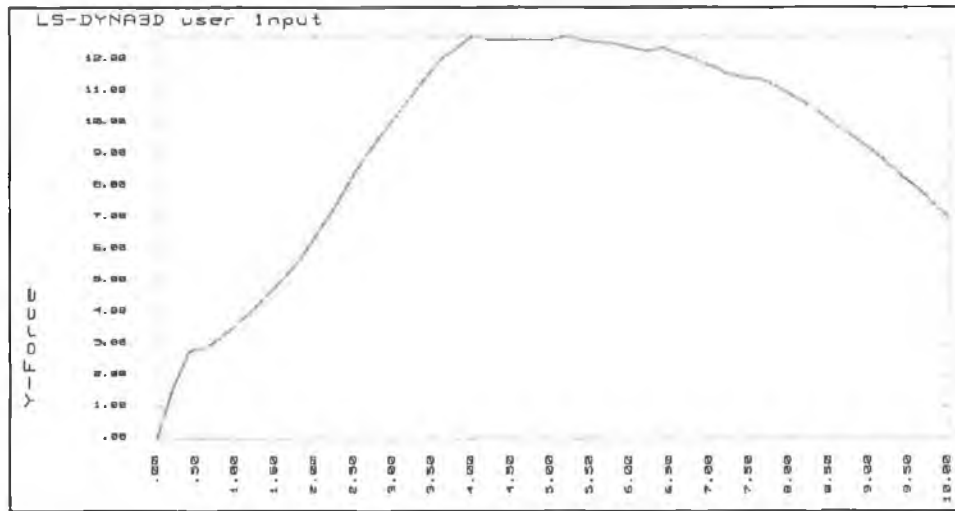


Figure 7.10 : Punch force verses Punch displacement for analysis B.

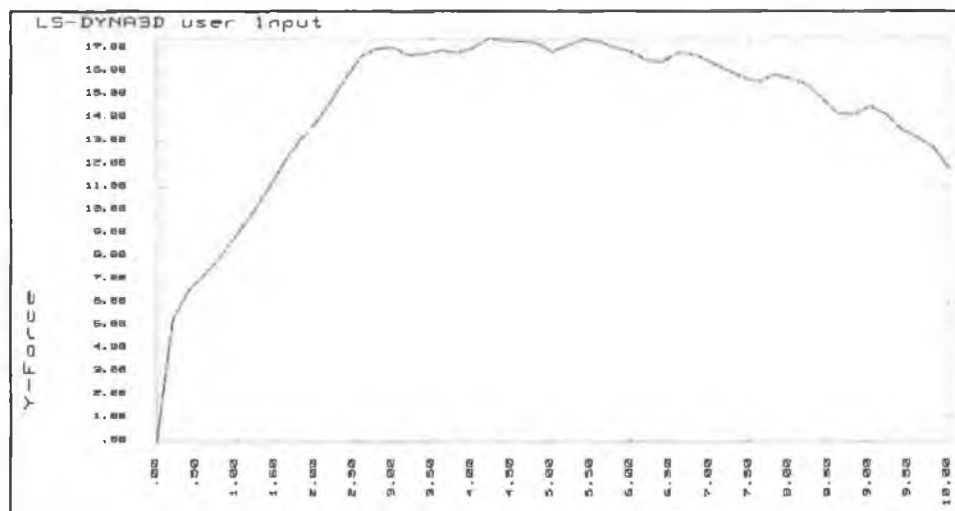


Figure 7.1.1 : Punch force verses Punch displacement for analysis C.

7.7.1 Paramaterisation of Explicit Finite Element Metal forming simulation variables by Taguchi methods

In the three dimensional code LS Dyna 3D there are many model variables within the solution phase which have an effect on the solution time. The purpose of this section is focus on virtual experimentation within Ls Dyna to reduce solution times by application of the Taguchi method. The plastic equivalent strain distribution across the wall of a vertically drawn cup is assessed as the “Objective” while the model variables are varied according to the control variable input array of Taguchi. The model variables that are varied are :

- Element size.
- Element integration scheme .
- Punch speed.

7.7.2 Element Size

The explicit integration procedure is conditionally stable, where the time step Δt is subjected to a limitation based on element size, according to the following equation.

$$\Delta t = 0.9 \frac{l}{c} \quad 97$$

Where :

$$c = \sqrt{\frac{E}{\rho(1-\nu^2)}} \quad 98$$

$$l = \frac{A}{\max(l_1, l_2, l_3, l_4)}$$

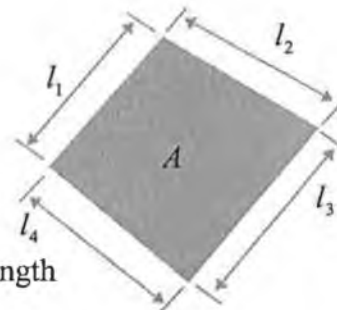


Figure 7.1.2 : element characteristic length

The integration of Explicit elements can be either reduced integration or full integration.

Reduced integration uses a single Gaussian integration point per element, full integration when you consider 2-D Elements, typically uses four gaussian integration points per element, this may effect the formulation of the element resultant stress which leads to inaccuracies.

7.7.3 Punch speed

Explicit codes simulating metal forming have to do so in a quasi-static scheme to ensure that the body forces of the sheet blank and punch blank holder have no effect on the solution. To this end a punch velocity of from 1(m/s) to 10 (m/s) is recommended. Since the punch has to travel a set finite distance the solution time is set by the critical solution time step and the punch velocity.

The punch velocity may have an effect on the correct performance of the contact algorithm. A punch moving too fast may lead to the nodes comprising the sheet blank escaping capture by the punch target surface. This results in over penetration of the punch and resulting erroneous solution.

7.7.4 Taguchi orthogonal array

The array chosen for the analysis was a L4 orthogonal array as shown in table 7.8

The finite element analysis was conducted with LS DYNA 3D code the thickness distribution for the analysis run with variables set as in table 7.8 is shown in

RUN	Control 1	Control 2	Control 3
No. 1	1	1	1
No. 2	1	2	2
No. 3	2	1	2
No. 4	2	2	1

RUN	Full Integration	Element Size	Punch Speed
1	Yes	Small	Slow
2	Yes	Large	Fast
3	No	Small	Fast
4	No	Large	Slow

Table 7.8 : L⁴ Orthogonal array

Table 7.9 : F.E.A. Analysis run settings

Dimensions in mm , Pressure in PSI

7.7.5 Signal to noise ratio table

The data for the outer results array table 7.1.1 was obtained from equivalent plastic strains nodal results in a radial direction from the centre of the cup. The location 1 to 5 are identified in Figure 7.5.

RUN	Plastic Equivalent Strain at location 1 -5 on the Cup				
	1	2	3	4	5
1	0.05945	0.09101	0.05250	0.03693	0.00503
2	0.07285	0.13976	0.04118	0.03521	0.03442
3	0.06274	0.09611	0.07029	0.05638	0.02707
4	0.06265	0.14269	0.025	0.01542	0.01205

Table 7.1.1 : outer results array

RUN	Full Integration	Element Size	Punch Speed	RESPON SE AVE	RESPON SE S/N
1	Yes	Small	Slow	0.49	3.84 dB
2	Yes	Large	Fast	0.65	3.22 dB
3	No	Small	Fast	0.63	7.99 dB
4	No	Large	Slow	-0.52	-0.52 dB

Table 7.1.2: ANOVA mean and signal to noise plots

7.7.6 Analysis of variance

The operating window and the type I and type II nominal the best problems occur frequently in optimisation studies and is composed of the following two steps.

- Step 1 Maximise S/N to minimise sensitivity to the effects of noise. To accomplish this, first identify the control factors that have significant slope in their S/N plots, and then select control factors that correspond to the maximum S/N values.
- Step 2 adjust the mean response onto the target response. To accomplish this identify the control factor that has both the greatest slope from the mean plots and the smallest slope in the S/N plots. This control factor is used to adjust the mean.

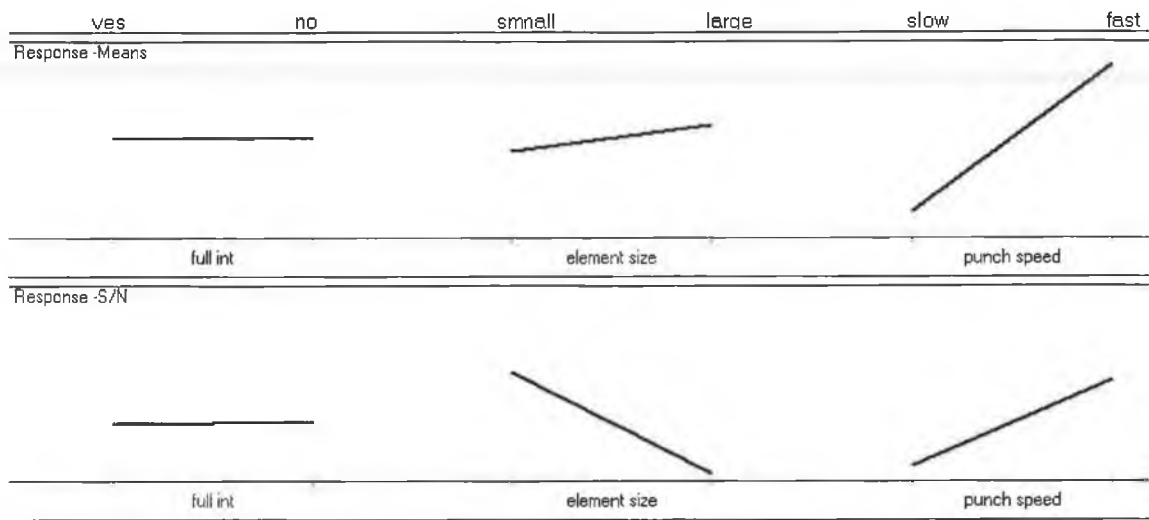


Figure 7.1.3 : ANOVA mean and signal plots

7.7.7 Conclusion

The optimised solution scheme found that the most critical aspect of the solution variables is element size. A smaller element size does more to reflect the actual deformation of the deep drawing process than the use of full integration, or a slower punch speed. Analysis of the S/N ratio plot shows that full integration has a very small slope. This indicates that at full integration has a low variance. This coupled to the fact that the mean plot for full integration has a zero slope, concludes that full integration does not contribute considerably to the mapping of the deformation process encountered in deep drawing. Bearing in mind the added computational cost of full integration in the case of some elements in the order of eight times that for reduced (single point) integration and it becomes evident that for cupping the exaggerated solution times encountered when full integration is applied, can be eliminated by the use of reduced integration.

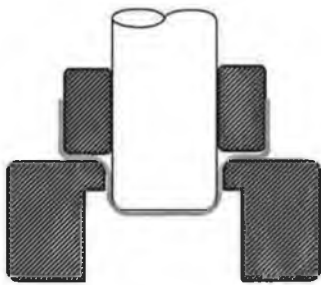
The punch speed S/N plot has a high slope indicating a high variance. The higher S/N ratio of a fast punch speed indicates that for this analysis a faster punch speed is optimum for solution time reduction. However care must be exercised in the selection of the simulation punch speed as observation of the high degree of slope on the punch speed mean plot indicates that true

mapping of the deformation process is highly dependent on the punch speed. This is an accepted fact in explicit finite element simulation of metal forming under quasi static conditions.

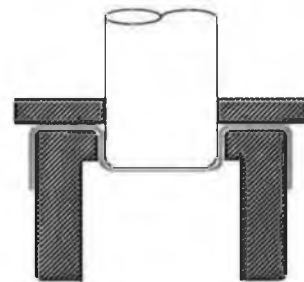
The resulting benefit of this analysis to the expert system, is that the expert system will use reduced integration elements, the mapping of the deformation process in deep drawing being afforded from sensitivities of element size.

7.8 Redraw process system appraisal conducted in F.E.A.

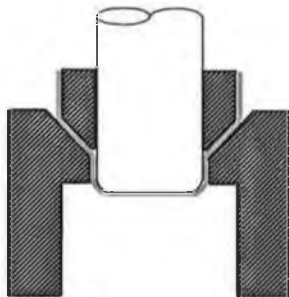
Redrawing facilitates the production of deeper and narrower cups and or stepped cups if the first drawing operation cannot produce a cup which is deep, tapered, or hemispherical enough, because of encountering a limiting draw, redrawing has to be employed. If the first redraw still can not produce the cup, a second redraw is employed, and so on. By utilising redrawing the compressive stresses are reduced due to the fact that the radial stress that generates them is smaller. Hence, the load that the wall has to transmit is lower leading to a more likely successful draw. Redrawing method used in press work fall into two categories direct and reverse. Within the direct redrawing the process can be straight cup tapered cup with blank holder or tapered cup free redrawing which is conducted without a blank holder. The principle tool alignment and displacements in each of the aforementioned methods are outlined in figure 7.1.4.



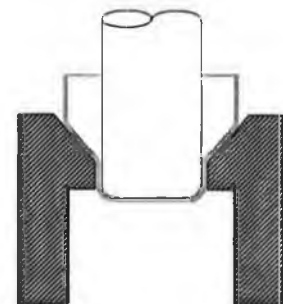
Direct Redrawing



Reverse Redrawing



Direct Redrawing /Tapered Cup/With
Blank Holder



Direct Redrawing /Tapered Cup/ No Blank
Holder

Figure 7.1.4 Redraw Tooling

Investigating the comparative redrawing capability of the above methods Chung and Swift [7.9] found that method (d) yields the most favourable results, it has a redrawing capacity higher by 8%. This stems from smaller energy dissipation during bending and unbending compared with methods a and b and reduced resisting frictional force compared with method c in which the supporting sleeve increase frictional resistance as a function of the blank holding force.

The redraw simulation was conducted with the following Cup and Tool geometry.

Initial cup diameter 85 (mm) : Redraw cup diameter 65 (mm) : Redraw punch corner radius 5 (mm) : Redraw die corner radius 5 (mm) : Redraw clearance 10%

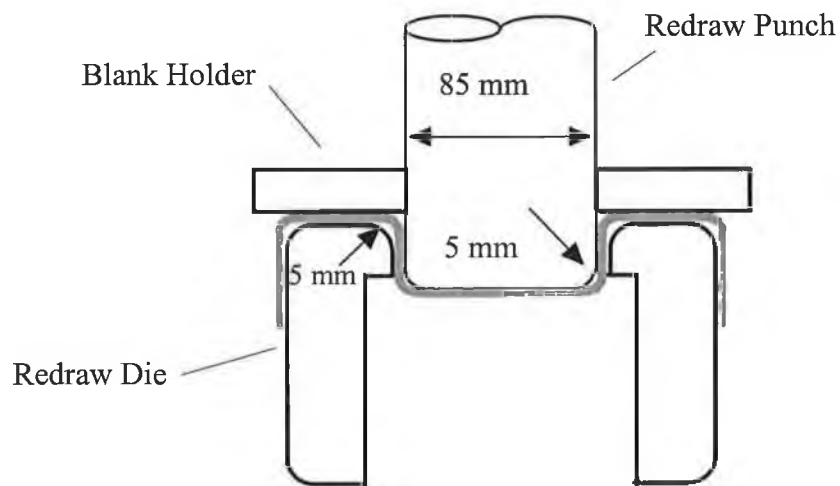


Figure 7.1.5 : Reverse Redrawing Tool Geometry

The following FEA analysis was conducted in Ls dyna 3D by re-actualising the stress strain history from a previously converged solution.

! Redraw analysis via a analysis restart.

Finish

resume

edstart,3,,,d3dumpo1

/prep7

edcdel,sts,1,2

edcdel,sts,1,3

edcdel,sts,1,4

asel,s,real,,2,4,1

aclear,all

K,##,##,##

Exits the previous analysis

Resume the solved data base

Read he previous stress strain history

Enter pre processor for Redraw Tool description

Delete first draw Tool Blank contact

Select elements which describe first operation Tooling

Delete elements which describe first operation Tooling

Develop Redraw Tooling by Keypoint Entry

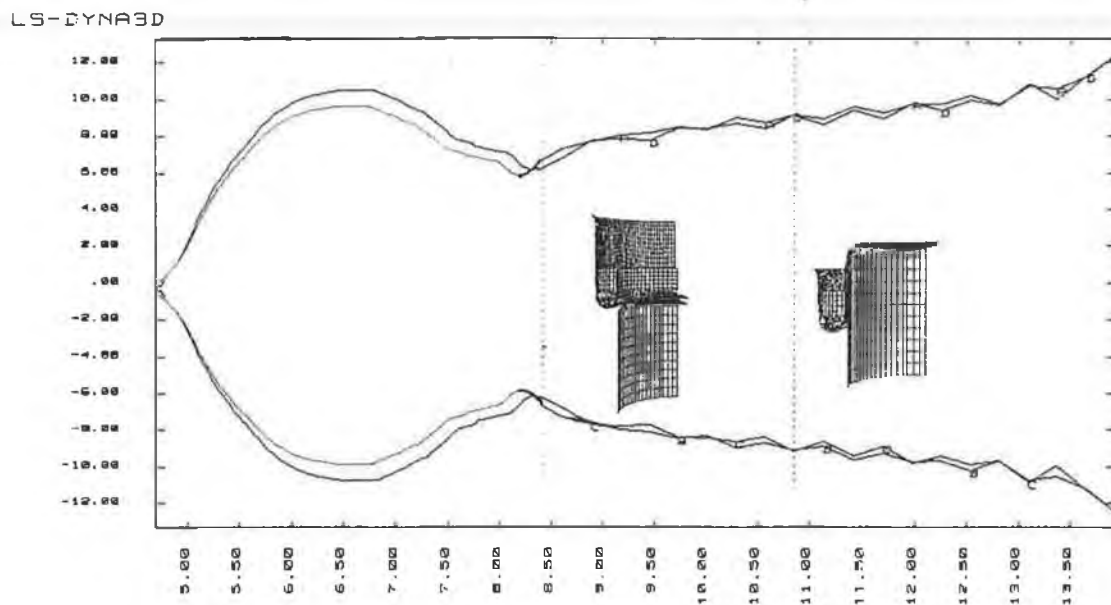


Figure 7.1.6: Redraw analysis Punch Force (kN) versus Punch stroke.

Reverse redrawing, eliminates two operations bending and unbending, thus requiring a smaller punch force, saving work and work hardening the cup to a smaller degree. This is apparent from the shallowness of the Punch force trace of diagram 7.1.6. These advantages point to reverse redrawing being a more efficient and capable process than direct redrawing. In the event of a necessitated redraw the expert system will suggest that the most feasible redraw process is that of reverse redrawing.

7.9 Chapter Conclusion

This chapter develops the use of the Taguchi method of experiment design and results analysis in developing the F.E.A. models and analysing the results of the simulation. A sensitivity study of punch and die radius effects on cup formability presented via F.E.A. analysis. Analysis of Punch force requirements in Cup drawing is presented for changes in tooling geometry. Simulation variables within the F.E.A. models have been analysed so as to effect an optimum solution. The Redrawing methods have been analysed and the optimum redrawing scheme has been suggested.

Chapter 8 : Expert System Architecture

8.1 Introduction

This chapter introduces the concept of an Expert System. A detailed description of knowledge based and rule based Expert Systems is described. Control and domain aspects are discussed with respect to the expert system for Cup drawing. Backward and forward chaining search algorithms are explained and implemented in the cup drawing expert system. This chapter documents the ways in which the expert system utilises the structure of logic to express problem solving knowledge in terms of rules. The structure of the expert system accounts for patterns of inference in addition to precise analytical models. The Expert System user interface is presented to explain its appearance and uses.

8.2 What is an expert system.

As an introduction to expert systems two established definitions of what an expert system is follow :

“Expert systems are interactive computer programs incorporating judgement, rules of thumb, intuition and other expertise to provide knowledgeable advice about a variety of tasks”

Gaschig [8.1]

A more extensive definition of an expert system is from Brachman [8.2].

“An expert system is one that has expert rules and avoids blind search, reasons by manipulating symbols, grasps fundamental domain principles, and has complete weaker reasoning methods to fall back on when expert rules fail and to be used in producing explanations. It deals with difficult problems in a complex domain, can take a problem description in lay terms and convert it to an internal representation appropriate for processing with its expert rules, and can reason about its own knowledge (or lack there of), especially to reconstruct inference paths rationally for explanation and self-justification.”

The basic architecture of an expert system is composed of the following aspects :

- Input/output facilities that allow the user to communicate with the system and to create and use a database of knowledge.
- A working memory that contains the specific problem data and is intermediate to final results produced by the system
- An inference engine that incorporates reasoning methods, which in turn acts upon the input data and the knowledge base to solve the stated problem and produce an explanation for the solution
- A knowledge base that contains the basic knowledge of the domain, including facts, beliefs and heuristics.
- A knowledge acquisition facility that allows the expert system to acquire further knowledge about the problem domain from experts, or automatically from libraries or data based of knowledge.

Reference to figure 8.1, shows the manner in which aspects of the expert system combine and interact.

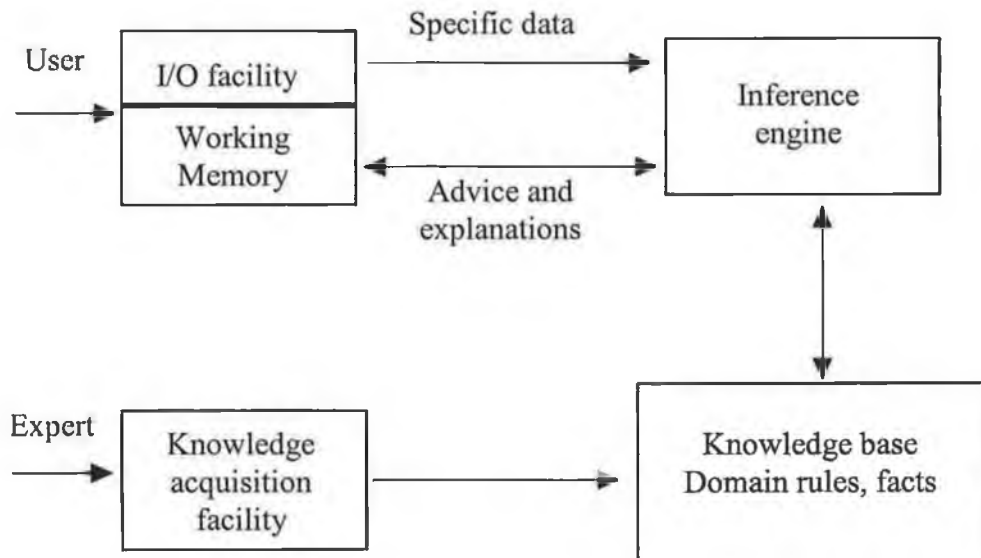


Figure : 8.1 The components of a basic expert system Dym, Feigenbaun [8.3]

8.3 How the Cup Draw Expert System Works

In attempting to solve a problem, an expert system performs a series of problem solving actions. Each action is triggered by data or a previously generated solution element, that applies some knowledge source from the problem domain, and generates or modifies a solution element. At each point in the problem solving process, several such actions may be possible. The control problem in relation to the expert system, is which of its potential actions should an expert system perform at each point in the problem solving process. This is implemented in the expert system via control file logic.

The control problem is fundamental to all cognitive processes and intelligent systems. In solving the control problem, a system decides, either implicitly or explicitly, what problems it will attempt to solve, what knowledge it will bring to bear, and what problem solving methods and strategies it will apply. It decides how it will evaluate alternative problem solutions, how it will know when specific problems are solved, and under what circumstances it will interrupt its attention, to selected problems or sub problems. Thus in solving the control problem a system determines its own cognitive behaviour. This is provided for within the expert system by nested IF THEN and ELSE statements which are employed to apply the relevant data.

Despite increasing sophistication in problem solving knowledge and heuristics. Most expert systems employ relatively simple control programs. In contrast people do not rely upon pre-determined control programs to guide all of their problem solving efforts. Instead, they draw upon a repertoire of control knowledge that includes proven control programs and heuristics for dynamically constructing, modifying, and executing control programs during efforts to solve particular domain problems. This adaptability in the control of ones own problem solving behaviour is the hallmark of human intelligence. Because of it, people do not simply solve a problem. They often know something about how they will solve the problem, how they have solved problems in the past, why they perform one problem solving action rather than another. Truly intelligent expert system must do no less. .Dym,.E.Levit [8.4]

Problem solving possesses the following behavioural goals :

1. Make explicit control decisions that solve the control problem.
2. Decide what actions to perform by reconciling independent decisions.

3. Adopt control heuristics that focus on whatever action attributes are useful in the current problem solving situation.
4. Adopt, retain, and discard individual control heuristics in response to the changing problem solving situation.
5. Reason about the relative priorities of domain and control actions.

8.4 Modelling within an expert system framework.

“The expert system uses models to represent the problem. The idea of modelling is inherent in the scientific method and is a central feature of engineering” Dym [8.5]

The form of models that are developed in expert systems can be grouped as follows :

- First principle : These are the basic physical laws of engineering. Such as the laws of solid mechanics.
- Phenomenological models : These are models typically expressed as ratios, differential equations, or non discrete mathematical forms often based on experimental results or on compiled high level extrapolations of the fundamental laws. An example of such a models is material stress strain relationships, inherent within the expert system FEA Model.
- Analytical models : These models are both exact and approximate, used to represent specific cases or subsets of the more general first principles and phenomenological models. These models employ continuous mathematics as their language for stating and manipulating the models. Examples are the analytical models used to predict Punch force, which are incorporated in the Cup drawing expert system.
- Numerical representations : These are the numerical versions of the analytical models just described. An example of which is the Finite Element Codes employed in the Cup drawing expert system. Where polynomials are used to approximate continuous and compatible displacement and strain fields.
- Heuristics or rules can be used to represent many different kinds of knowledge, this type of information transcends, in some sense, the entire hierarchy just listed. For example, rules may be used to express aspects of fundamental principles, compiled versions of both phenomenological and analytical models, preferences and assumptions about the use of numerical codes, experimental rule of thumb, and high level knowledge about how to use other kinds of Knowledge. The rules within the test algorithm of the expert system are heuristic rules.

8.5 Blackboard Architecture

A blackboard control architecture achieves the aforementioned goals. It has several pertinent features, some of which have been previously suggested by Lesser and Erman [8.6]. Such as the architecture explicitly represents domain and control problem knowledge. Blackboard architecture represents an approach to problem solving in which an assembly of knowledge sources are permitted to respond opportunistically as the solution develops. The knowledge sources actually represent a decomposition of the knowledge base according to some hierarchical or functional scheme so that each knowledge source represents one aspect (or level or perspective) of the problem being solved. Each source comes into play only when its level or perspective can provide some useful input to the solution as it is being developed. The Blackboard architecture implemented by the expert system bases the initial value of punch force based upon an imperial value stored in the rule base to define the solution search. Upon the solution of the 2D FEA punch force simulation analysis. The present value of the punch force stored in the blackboard is updated and the data base solution search reactivated. The notion of the blackboard comes into play because the solution is developed thereon and the sources are "reading" that blackboard to see if they have an opportunity to apply their specific knowledge. The architecture integrates domain and control problem solving in a single basic control loop. The architecture articulates, interprets, and modifies representations of its own knowledge and behaviour Clancey [8.7] this logic is developed within the control file. The architecture adapts its basic control loop to dynamic problem solving situations. Finally the architecture incorporates these features in a uniform blackboard architecture in which domain and control problem solving behaviours are characteristically incremental and opportunistic in Nature Mc Carthy [8.8].

8.5.1 Expert System Implementation of a Blackboard Architecture.

Blackboard architecture is a current hot topic in the area of artificial intelligence and expert systems. The application of blackboard architecture is simply that all the output from currently fired rules is stored in an area in computer memory referred to as the blackboard. As the process of solution and optimisation progresses the information that is stored on the blackboard may change as different rules are fired to further optimise the solution. The initial data stored on the blackboard is used to start the solution search of the data base for pertinent rules. Which are compiled and the output from these rules are stored on the blackboard to enable further

refinement of the solution process. The implementation of a Blackboard architecture within the expert system for metal forming is depicted in figure 8.2. The expert system prompts the user for relevant information on the geometry and specification of the desired Cup, material characteristics, the maximum Punch force and Blank Holder force that can be developed from the existing Plant. The knowledge data base is first checked against the inputted request data for a match. This involves a search that is made of the success data base which is a file that contains a listing of the current instances of a successful draws. The search is organised by comparison of the instances of semantic values with those inputted values of the geometry and specification of the desired Cup. The black board architecture is further built on by heuristic knowledge gained from problem specific F.E.A. Simulation as out-lined in Figure 8.2. The flexibility of the Expert System is provided by the black board architecture enabling the integration of F.E.A. simulation. This enables a dynamically changing control strategy and solution Domain Values.

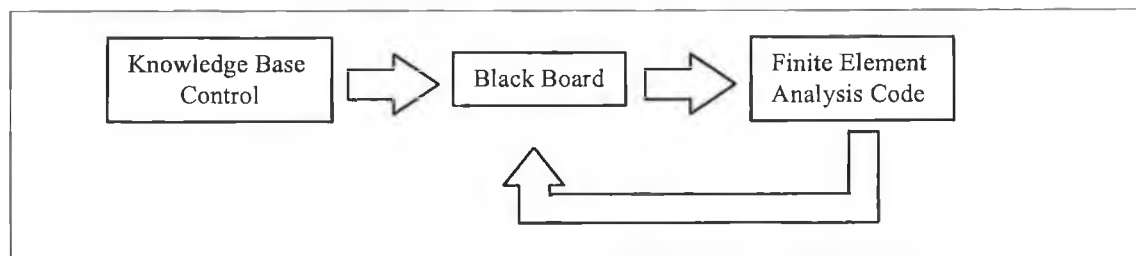


Figure 8.2 : Blackboard architecture

Within the realm of control behaviour the blackboard architecture philosophy is joined by the sophisticated scheduler and solution based focusing philosophies. Blackboard architecture provides the best marriage between the rule base and the numerical model representation of the F.E.A. module. Hence the control behaviour chosen for the expert system is that philosophy represented by a Blackboard Architecture.

8.6 Control Domain

“Although an intelligent system does not allow either the desirability or the feasibility of potential actions to dominate control problem solving, it drives the problem solving process in either direction under appropriate circumstances”. Hayes-Roth, B [8.9]

The control algorithm applies the following considerations when developing a control strategy.

- An intelligent system adopts control heuristics that focus on what ever attributes are useful in the current problem solving situation. For example, if a planning problem specifies tasks that vary widely in priority, the planning system adopts a heuristic favouring actions triggered by high priority tasks.
- Adopt heuristic to gain short term gains then abandon them. If knowledge based rules within the Cup drawing Expert System, leads to a Cup which is out of specification then the fired rule is abandoned.
- It is important to perform actions whose knowledge source are reliable, it is equally important to perform actions whose triggering information is accurate. The cup drawing expert system accounts for this as outlined in section [8.9.3]
- If problem solving time is important the control algorithm should identify the subset of potential actions that rate high on knowledge source speed and reliability.
- Dynamic planning also entails a readiness to interrupt, resume or re-plan performance of a strategic sequence of actions in response to dynamic problem solving situations. If the certainty factor for inferred knowledge within the Cup expert system goes below a predefined minimum then a new solution search is developed.

To summarise and apply the above the control software that supervises the use of domain knowledge within the expert system relies on a path methodology which incorporates a black board scheme. An intelligent system adopts, retains, and discards *control heuristics* in response to dynamic problem solving situations for example the planner might determine early in the problem solving process that the requested task targets are being met too widely. It immediately adopts a heuristic favouring actions triggered by high priority tasks for design efficiency.

It is important to perform actions whose triggering information is credible. If the expert system is feed with unfeasible inputs then it should detect this and correct it. The certainty factor within the cup drawn expert system provides for this.

Dynamic planning is implemented in the Cup Drawing expert system as follows. Until decision (a)'s criterion is met the planner uses all fired heuristics to decide which actions to perform. After (a)'s criterion is met, the planner abandons it and uses only the remaining heuristics as long as they don't affect the first heuristics attainment. e.g. Goal (A) develop Tooling to minimise Punch force. Goal (B) develop Tooling to provide for a specified minimum Cup wall thickness. The rules applicable are only fired if they don't affect the attainment of goal (A). These rules are referred to as the conflict set, which are a set of rules that are potentially applicable at any point in the solution process. Thus rule conflict is avoided by only letting the solution process effect those process geometry features such as increasing die corner radius to lower Punch load if it does not effect the attainment of the prescribed minimum Cup wall thickness. Typically the conflict set of rules selected is developed by a rule matching process. This matching algorithm sorts through the rule base and recognises those rules that are potentially applicable. The matching algorithm would be quite difficult if not impossible to write in FORTRAN code, therefore a suggested development on the current work would be the development of a rule matching algorithm in a shell representation language such as the C compilation facility within the (APDL) environment.

8.6.1 Control Domain Test Algorithm

The following Meta rules construct the control logic of the expert system. The Meta rules serve as pointers to specific knowledge that may be invoked in specific situation essentially Meta rules are rules about how to use rules.

The test algorithm is used to develop the control Domain. The logic that pertains to the Test Algorithm is outlined below in a series of IF THEN statements. The logical outputs form the Control Domain strategy.

if bend radii are to be specified and the element is one of the finished ones
then they should comply with the recess radii of the finished cup

if the sizes of the geometric features of the Cup (e.g. drr,drt,pr,rprt,tap) are the required finished ones and final sizing is to be employed
then it is necessary to design the intermediate shape so that each of the volumetric elements within the one to be sized, will undergo a minimal possible of plastic deformation

if the sizes of the geometrical features of the cup are not the required finished ones
then it is necessary to design the intermediate shape with optimal bend radii

if a flanged deformation zone is required
then one should employ the first draw to obtain the diameter of the finished flange

if bend radii of open elements are to be specified
then they should be designed such that their contribution to additional loads will be minimal

if bend radii are to be specified and the incipient load is satisfied
then bend radii should be designed so that they bring minimal susceptibility to defects

8.6.2 Control Knowledge

Control knowledge is stored within a control file, written in ANSYS (APDL). This file develops solution strategies, which are dependent on the users queries and inputted Cup specifications. This control file is concerned with control aspects of the expert system. The control file which forms the control domain is developed from logic outputs from the test algorithm

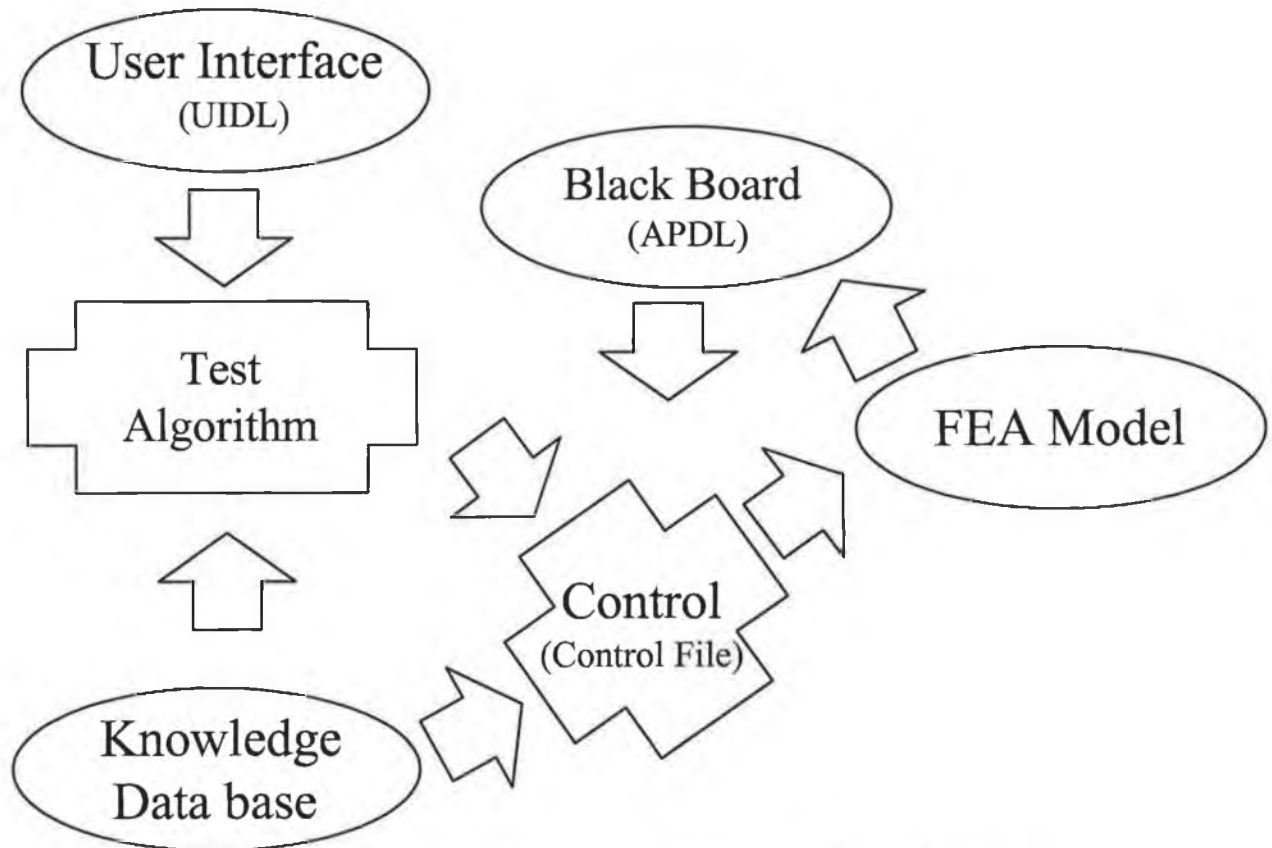


Figure 8.3. : Control Domain Architecture of Expert System.

8.7 Domain Knowledge

The domain aspects of the Expert System contains procedural knowledge. That is to say the rules of the expert system. Procedural knowledge is stored in user library files within the ANSYS APDL frame work. This is advantageous in that the code within the user file only becomes active when the user file is called. Thus ensuring smooth operation of the expert system protocol. The use of user files as procedural knowledge within the expert system is documented in Appendix D on domain knowledge of the expert system. Domain knowledge results from the application of specific knowledge inherent in the Rule Base.

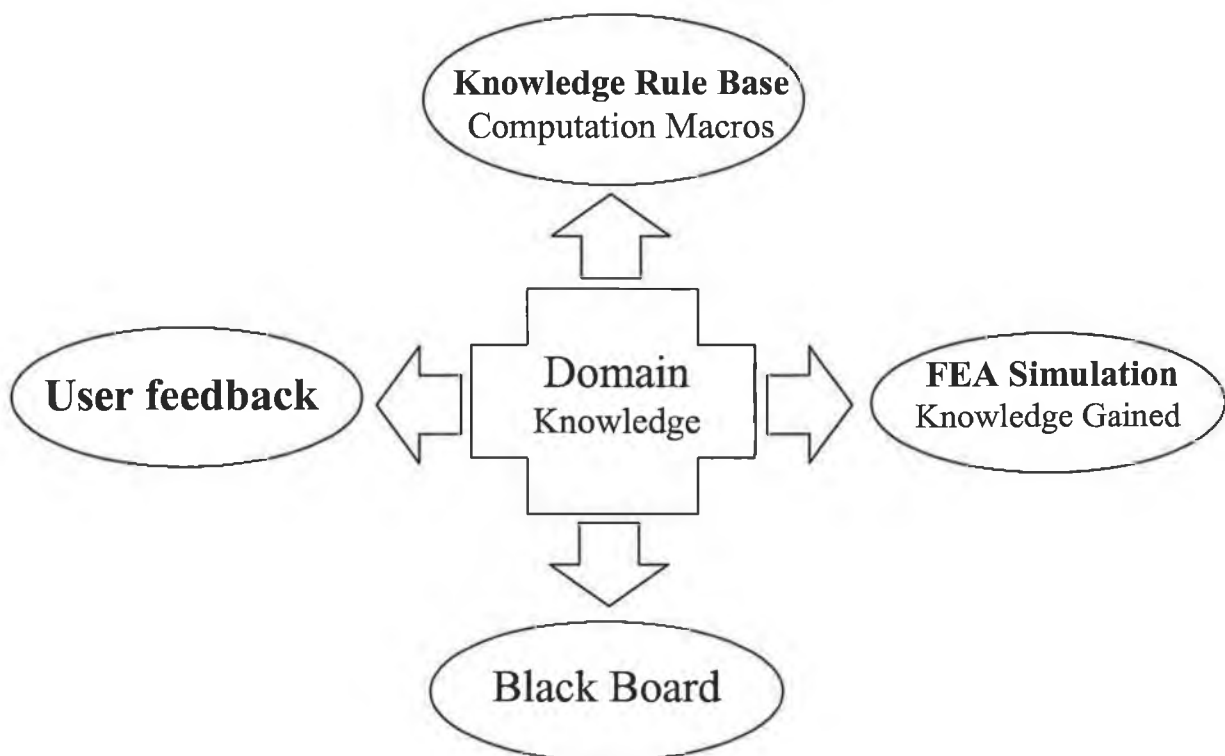


Figure 8.4 : Domain aspects of the Expert System.

8.8 Search strategies for expert systems

The spatial representation of an knowledge base expert system can be explained by a tree structure.

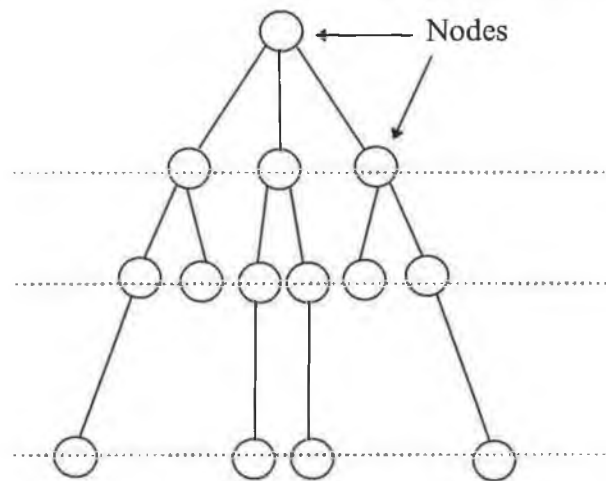


Figure 8.5 : Search tree topology

The nodes in Figure 8.5 represent predicate rule logic such as Cup diameter Sheet thickness. As the tree search progresses motion from one level of the tree to the next, occurs because of some condition or set of conditions that triggers an operator. These search operators are quite often defined in terms of rules in which the IF clause, the left-hand sides of the rules, define the situations (or predicate rule logic) that must be obtained before the rule can be applied or fired. The right-hand sides of the rules, the THEN statements, define a set of actions to be taken in a given situation, that is, if the data for the problem at hand match the situation data given in the left-hand side of the rule. The left-hand sides of rules are called the rule antecedents and the right-hand sides consequents.

There are two basic styles of using rules to define a direction of movement through the search space represented by the tree structure which are forward and backward chaining. The cup draw expert system directs the search through the search space represented the search tree structure in a forward and backward chaining manner. In forward chaining the problem data is matched against the antecedents of all the available rules a particular rule is selected from a set of applicable rules this rule is then fired. The action and knowledge is presented by the consequents of the fired rule. This kind of reasoning is data driven reasoning called forward chaining.

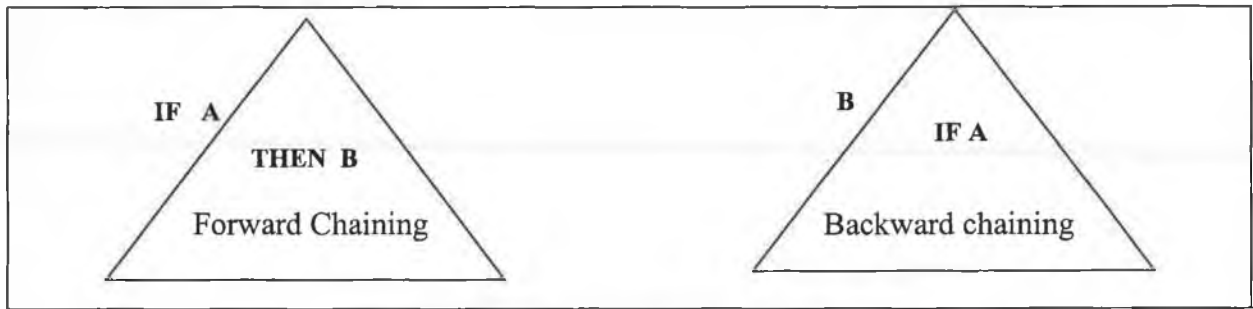


Figure 8.6: Solution chaining strategy

For those rules which have the desired outcomes B as in the above simple case for backward chaining, we examine the antecedent A to see what facts are required to enable these rules to be fired. If the relevant facts are not available to trigger these rules, the Expert System takes as subgoals the establishment of the relevant facts, and the search proceeds recursively in this fashion. This is goal driven reasoning or backward chaining. B is thus regarded as the goal to be verified or perhaps established as a subgoal in the search process.

The selection of rules from the rule base by the *USE (APDL) command within the Control file can be thought of as backward chaining. An example of which is :

```
B(*USE,BHLANKHOL)
  IF A (Blank Thickness X)
```

An example of forward chaining is the development of a rule within the rule base. An example of which is :

```
IF Blank Thickness is X
  Then K=2
IF Blank Thickness is Y
  Then K=1.5
```

Blank Holder force = $k \sigma_y$

8.8.1 Data Base Search Strategy.

In a more general treatment search strategies can be divided into exhaustive and directed searches. Exhaustive search algorithms that generate and examine every conceivable state, in a search space. Directed or guided search, where knowledge about the problem domain is used to guide the search and to make a more informed choice on the search path, during the search.

Breadth first search attacks the search tree layer by layer one layer at a time. That is, all the nodes at a given depth are examined to see if they are a solution before any of them are expanded.

In depth first search strategies the nodes are examined in a descending order with each node expanded, until the solution is achieved. A breadth first search strategy produces a solution at a cost of expanding more nodes than a depth first search procedure. Since the knowledge in the cup drawing expert system is directed i.e. can be aligned in a sequential manner a depth first search strategy is adopted.

8.9 Knowledge base expert systems (KBES) Versus Rule base expert systems (RBES)

A distinction has to be drawn between (KBES) and (RBES), (KBES) contains knowledge within its domain this knowledge is not restricted to the formulation of "rules" The knowledge can be presented in other forms such as heuristic for example high level knowledge. This type of strategic knowledge within a (KBES) calls for a specialised search engine to enable its use.

As opposed to the above strategies (RBES), use generate and test strategies.

The rules in (RBES), have their origins in a variety of sources. Some are heuristic that are based on experience on what is known to work from previous trials, such as the successful draw data of the Expert System. Other reflect "compiled knowledge" and are based on a compilation of or extraction from the first principles of a particular domain. Such as the analytical rules within the expert system for example the use or not of a blank Holder. Still other rules are causal in nature that is they describe very specific cause and effect relationships. Thus rules express or represent knowledge about a specific problem or domain. The analytical nature of the Deep drawing knowledge within the Expert System data base leads to the development of a Rule Base expert system being favoured. Hence a Rule Base is Employed in developing the Cup Drawn Expert System. Where the rule is first generated i.e. highlighted from the rule base and tested, to find a solution.

8.9.1 Rule Syntax

Rule Syntax is expressed as English like constructs are employed in established expert system such as SACON system Bennett [8.10] and its logical predecessors, the MYCIN and EMYCIN systems[Buchanan [8.11].

To make up the antecedents and consequents, clauses are combined with boolean operators, such as AND, OR, ELSE OR NOT, and with relational operators such as Equal to (=) less than (<), greater than(>) and so on Brownston [8.12].

SACON was designed to be a “front end” to the Marc finite element code, enabling the user to identify with efficiency and accuracy the portions of Marc that must be exercised in order to perform a numerical analysis of a particular structure.

8.9.2 Rule Based Search

A classic artificial intelligence paradigm was originally spelled out for rule based search NILSSON [8.13].

“ The facts and details of a problem represent the declarative knowledge of the domain. The algorithms that are concerned with the manipulation of the knowledge in the search process represent procedural knowledge, and finally we use the term control knowledge to describe the invocation of one or more strategies to solve a problem.”

The schematic of Figure 8.7 shows how the expert system applies the Nilsson paradigm

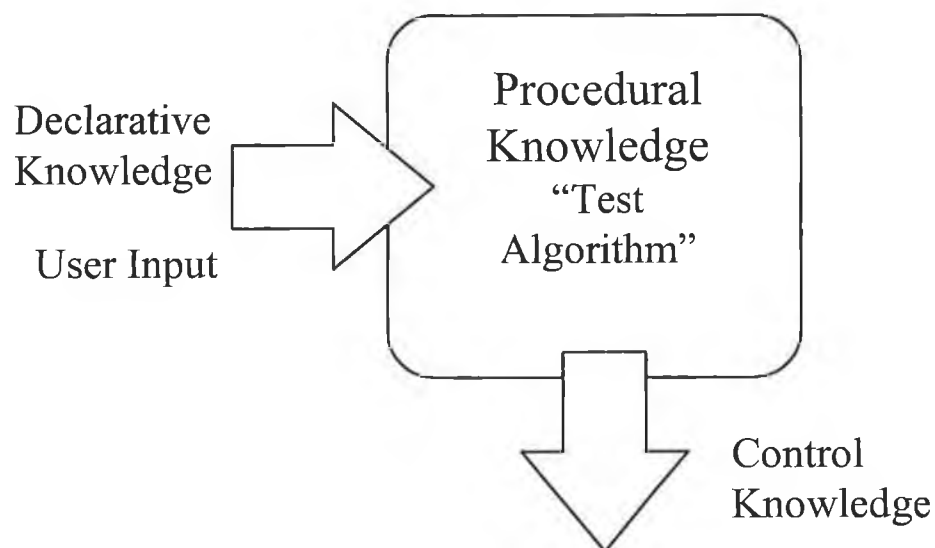


Figure 8.7 Control knowledge domain development

Considering the Cup drawing expert system the declarative knowledge is the desired Cup dimension, Cup geometry, material properties, machine process capabilities. The procedural knowledge (Rule on how to apply the declarative knowledge) is provided by the “test algorithm”.

The control knowledge is the application of the selection rules from the data base to effect a solution.

The search mechanism for the Cup Drawing Expert system follows a depth first search procedure in which the ordering of clauses in the body of successive rules governs the order of the deepening search. This initial hierarchical search path is complemented by a goal sub goal chaining process within rules. If the goals in a rule are ground facts, that is they contain no variables, then the solution process merely chains backwards through rules from a goal in the body of one rule to the matching head of another rule. This action is repeated until no further rules can be used to generate sub goals.

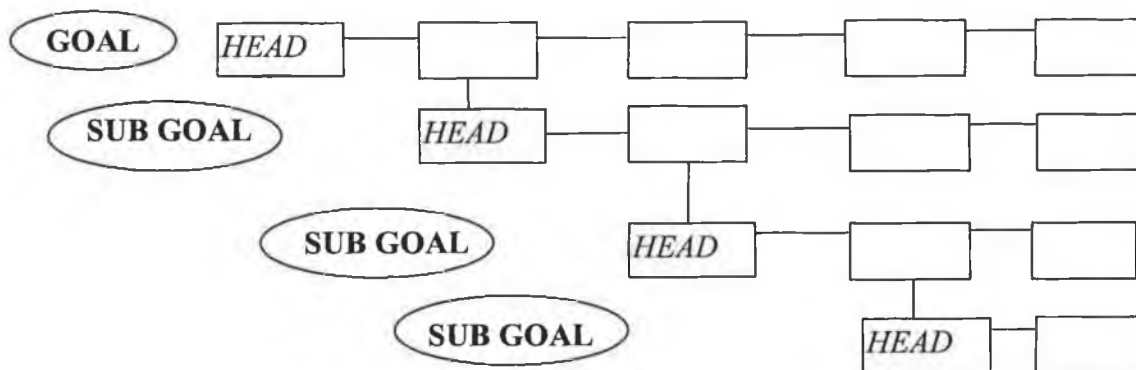


Figure 8.8: Dept first search strategy

For (RBES) a search strategy based on a depth first direction with a Generate And Test action is the optimum and will be employed in the expert system.

8.10 Uncertainty in Rule Base Knowledge Base.

We may think of the “likelihood ratio” as expressing the sufficiency of the rule $B \rightarrow A$ Parsaye [8.14]. That is, a high value of the ratio L implies that the evidence e is sufficient to confirm the hypothesis.

$$P(H/e) = \frac{P(H) \times P(e/H)}{P(e)}$$

$P(H/e)$ If the evidence e is present then the Hypothesis H is correct. Hypothesis H whose confirmation is sought on the basis of evidence e . Probability is utilised to reflect and process that knowledge we wish to capture in a Rule Based System. For example if the blank is a certain thickness the rule blank holder is necessary. Now application of the Bayesian rule can be cast in terms of the prior probability $P(A)$ and the likelihood ratio L . Thus :

$$L = \frac{P(B/A)}{P(B/\bar{A})} \quad L(\text{likelihood Ratio}) = \frac{\text{Probability of observing effects B in the presence of A}}{\text{Probability of observing effects B in the absence of A.}}$$

Where $P(B/\bar{A})$ is the conditional probability of observing the effects B in the absence of the effect A . $P(H)$ The faith that we have in this hypothesis eg. A rule expressed as a analytical model for punch force, as in how accurate is it. $P(e)$ The faith that we have in this evidence. If ground fact we have $P(e) = 1$. If resulting from some other calculation of probability then $P(e) \neq 1$. It enables the Meta Rules phase to select the rules to be fired based on the rules that have the highest likely hood ratio developed by the presented data. For multiple effects and where the evidence for these effects is itself uncertain the following is applied . $p(e/H)$ the applicability of this Hypothesis (H) to this evidence (e) maybe there is another Hypothesis (H) applicable to this evidence (e). Example rule applicability to thickness of blank, if thickness is small $p(e/H)$ is high, therefore rule is applicable, if thickness is large $p(e/H)$ is low, therefore rule is not applicable. The confirmation assessors $p(e/H)$, $p(H/e)$, L will be applied to the Cup Drawn Expert System as rules call yet more rules, and are presented to the user, to give an indication of the validity of the experts systems findings.

8.10.1 Certainty factor

In this approach we associate with every assertion A has a certainty measure $C(a)$ such that

- $C(a)=1$ if A is true.
- $C(a) = -1$. If $C(a)$ is false.
- $C(a) = 0$ if we have no information about the assertion, A .

A similar certainty factor is associated with every rule. This allows us to deal with the difficulty of obtaining meaning full prior estimates from judging the certainty of the knowledge base data.

Buchanan [8.11] states that certainty factors can be seen as heuristics that not only offers assessments of strength, they also may be indicative of the importance or usefulness of a particular assertion.

The rules within the RBES have specific certainty factors assigned to them. an example of which follows.

The following is an abstract from the Rule base the FPUNCH macro block, used to calculate a precursory value for puch force.

FPUNCH

!spunch punch force estimate

!predicate d,material-su,l,t

! punch force = k.su.l.t

!find k

**if,d,ge,2,then*
k=1

c(a)=0.9

**elseif,d,ge,1.75,then*
k=0.95

c(a)=0.9

**elseif,d,ge,1.5,then*
k=0.9

c(a)=0.9

**elseif,d,ge,1.4,then*
k=0.75

c(a)=0.85

**elseif,d,ge,1.3,then*
k=0.6

c(a)=0..85

**elseif,d,ge,1.2,then*
k=0.5

c(a)=0.8

**elseif,d,ge,1.1,then*
k=0.4

c(a)=0.8

**endif*

! pf = punch force
*pf = k*su*l*t*

/EOF

Rule specific $c(a)$ value are contained within the rule base and become active when their corresponding rules are fired

8.11 Fuzzy Set Theory

The Z(h) class is the class of all blanks of a certain thickness. To represent the fuzzy subset of the thin plates belonging to that class we define a membership function $BT(\text{blank thickness})$ that measures the strength of our belief that the blank belong to the class ZBT. Therefore blanks of thickness t_1, t_2, t_3 , are assessed as to whether they belong to the thin blank class ZBT(thin) by fuzzy set theory as follows : $ZBT(t_1)=1, ZBT(t_2)=0.8, ZBT(t_3)=0.5$. Blank t_1 is thin with 100% certainty. Blank t_2 is thin with 80% certainty. Blank t_3 is thin with 50% certainty.

8.12 Software Choice

Most existing expert systems are based on the list type Prolog language. List type languages are inherently suitable for the distributed knowledge within knowledge base expert systems, for the more structure knowledge within the rule base Expert System, the apparent advantage of a list type language is not applicable. Therefore since the Cup drawing expert system is predominately of the rule base nature the non list FORTRAN type code present in ANSYS APDL was used. More elaborate software based on C or FORTRAN can be developed subsequent to the testing of the development coding written in APDL. This can be so because the ANSYS shell supports a FORTRAN and C compiler. The present use of ANSYS APDL coding is justified by the fact that it is adequate for the proposed architecture, development time is quicker as the systems response can be more readily judged and the macro nature of APDL is highly portable to all platforms. The programming style is modular, with the application of APDL library macro file programming structure. The expert system can be made extensible by the use of modular programs, which are easily extended to incorporate new knowledge.

To organise the large set of rules within the rule base task decomposition or task relevancy can be used. This can be implemented by utilising a frame work to describe the drawn cup specification as a FORTRAN type “structure” class backward chaining can be used to develop the active rule base, by examining rule clause attributes for relevance to Cup specification.

8.13 Expert System User Interface

The user interface is written in the user interface dialogue language (UIDL) of ANSYS. This enables full compatibility with the Rule Base system developed in ANSYS advanced parametric design language (APDL), and housed within a macro file. Compatibility between the user interface and the parametric F.E.A Simulation Log file is also assured, enabling drawing geometry, inputted via the user interface to be passed to the parametric F.E.A simulation log files. Where F.E.A models are automatically built and the simulation variable set to ensure a successful converged F.E.A solution.

The open MOTIF architecture of ANSYS enables the development of customised menu and dialogue box applications. The coding for this which is quite involved and is listed in Appendix C.

Cup drawing expert system

The cup drawing expert system is accessed from the (Preprocessor) menu, which is a sub menu of the ANSYS Root (main menu). The CUP DRAWING menu hot spot is as shown in Figure 8.9. Upon selection of this CUP DRAWING menu item the CUP DRAWING EXPERT SYSTEM dialogue box appears on screen. The cup drawing expert system dialogue box prompts the user to reply “yes” or “no” to a series of questions. The user response to the question enables the expert system to develop Meta rules to, promote the test algorithm to ensure a prompt and accurate solution to the cup drawing problem by selecting pertinent rules within the rule base data base, and developing the F.E.A simulation with correct geometry and Tooling.

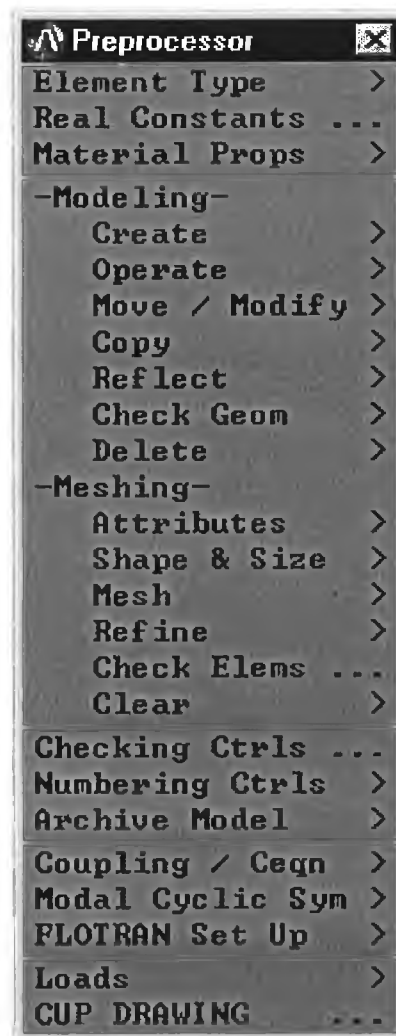


Figure 8.9 : Modified Preprocessor menu containing cup drawing expert system Feature.

: CUP DRAWING EXPERT SYSTEM

WILL THE FINISHED DRAWN CUP HAVE A FLANGE
"YES" OR "NO"

IS CUP BOTTOM FILLET RADIUS DESIGN SPECIFIED
"YES" OR "NO"

IS CUP TOP FILLET RADIUS DESIGN SPECIFICATION
"YES" OR "NO"

LET SYSTEM SET PRIMARY GEOMETRY
"YES" OR "NO"

Figure 8.10 : Cup Drawing Expert System Dialogue Box

Upon submission of the (Cup drawing expert system) dialogue box, the input primary geometry dialogue box is called to present on screen.

: INPUT PRIMARY GEOMETRY

INPUT BLANK DRAWING PRIMARY GEOMETRY

INPUT BLANK ORIGINAL DIAMETER <D0>

INPUT CUP INTERNAL DIAMETER <DI>

INPUT CUP HEIGHT <H>

INPUT CUP WALL THICKNESS <T>

CUP BOTTOM FILLET RADIUS <CBR>

INPUT CUP TOP FILLET RADIUS <CTR>

INPUT FLANGE WIDTH <FW>

: NOTE DIMENSIONS IN <MM>

Figure 8.11 : Input Primary Geometry Dialogue Box.

The input primary geometry dialogue box contains input prompts for primary geometry which is dependent on previous user input. The geometry is as outlined in figure 8.12.

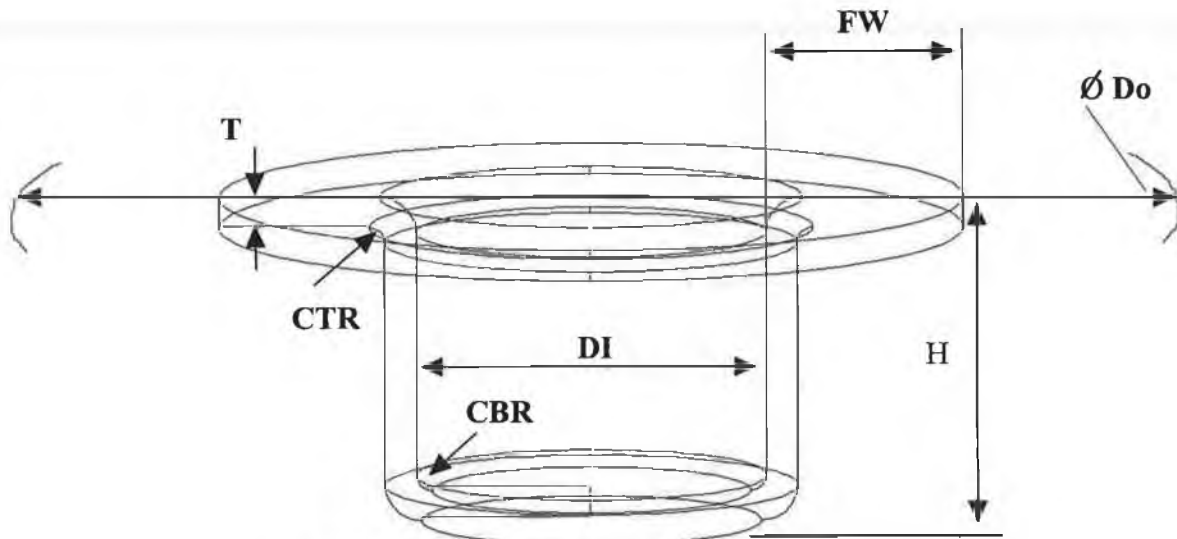


Figure 8.12 : Cup Primary Geometry

Upon submission of the input primary geometry dialogue box, the input drawing machine specification dialogue box is called.

The screenshot shows a dialog box with the following content:

- Window title: **: DRAWING MACHINE SPECIFICATION**
- Section: **INPUT MACHINE SPECIFICATION PARAMETERS**
- Field: **INPUT MAXIMUM AVAILABLE PUNCH FORCE** (text input)
- Field: **INPUT MAXIMUM AVAILABLE BLANKHOLDER FORCE** (text input)
- Field: **MACHINE IS CAPABLE OF DIRECT REDRAWING "YES" OR "NO"** (dropdown menu, selected: **YES**)
- Field: **MACHINE IS CAPABLE OF REVERSE REDRAWING "YES" OR "NO"** (dropdown menu, selected: **NO**)
- Note: **: NOTE UNITS OF FORCE (KN)**
- Buttons: **OK**, **Apply**, **Cancel**, **Help**

Figure : 8.13 Drawing Machine Specification Dialogue Box.

INPUT BLANK MATERIAL PROPERTIES

INPUT THE FOLLOWING PROPERTIES FOR THE BLANK MATERIAL

INPUT MATERIAL NUMBER FOR BLANK

YOUNGS MODULUS <EX>

BLANK MATERIAL DENSITY <DENS>

POISSON <MAJOR> RATIO <NUXY>

BLANK MATERIAL SHEAR MODULUS <G>

TENSILE YIELD STRENGTH OF BLANK

IS BLANK MATERIAL ANNEALED

: NOTE UNITS OF STRESS <MPa> : DENSITY <KG/M³>

OK Apply Cancel Help

Figure : 8.14 Input blank material properties Dialogue Box.

The input blank material properties box requests the user to input the specific material physical properties and characteristics that effect the drawability of the blank material, also enabling the material compliance matrix to be developed within the F.E.A simulation upon submission of this dialogue box . The user is automatically prompted to select a plasticity model which best describes the Blank stress strain behaviour.

SELECT PLASTICITY MODEL

[TB] Define/Active Data Table

Lab Type of data table

MAT Material ref. number

The following apply only to some data table

NTEMP No. of temperatures

NPTS No. of data points/temp

- Bilin kinem BKIN
- Multi kinem MKIN
- Multi isotr MISO
- Bilin isotr BISO
- Anisotrop ANISO

OK Cancel Help

Figure : 8.15 Select plasticity model dialogue box

The user is then prompted to provide information for the chosen plasticity model. Such as yield strength, plasticity tangent modulus, strength co-efficient, work hardening exponent, piece wise curve plasticity. Dependent on the chosen model.

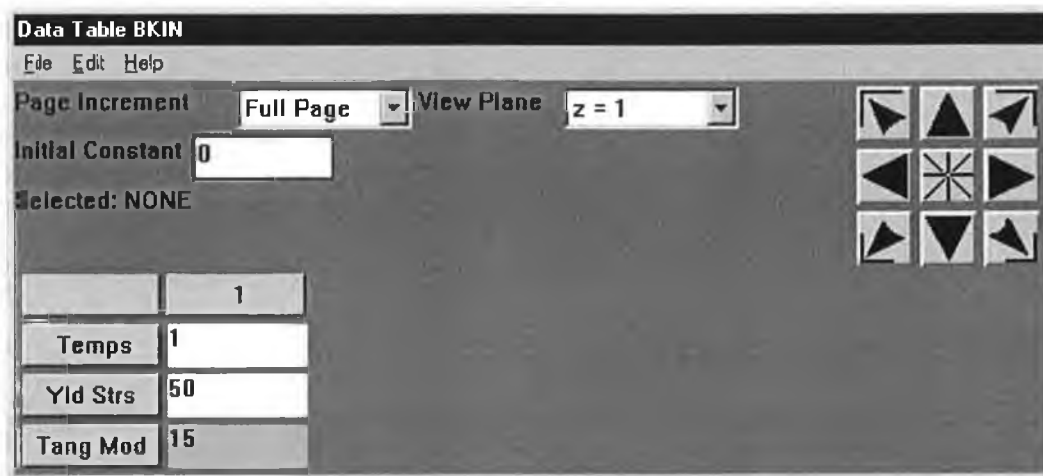


Figure : 8.16 Fill plasticity model dialogue box

The user is then prompted with the following query box Plot blank material stress strain curve. This is a useful feature as it allows the user to validate the plasticity model before the analysis has commenced thus assuring correct application of the plasticity model.

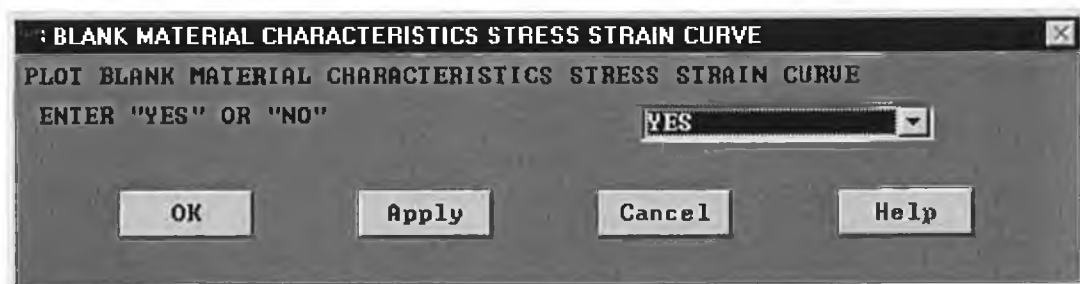


Figure 8.17 : Plot blank material stress strain curve.

If the user selects to plot the stress strain curve the expert system UIDL code automatically does so, as shown in Figure 8.18.

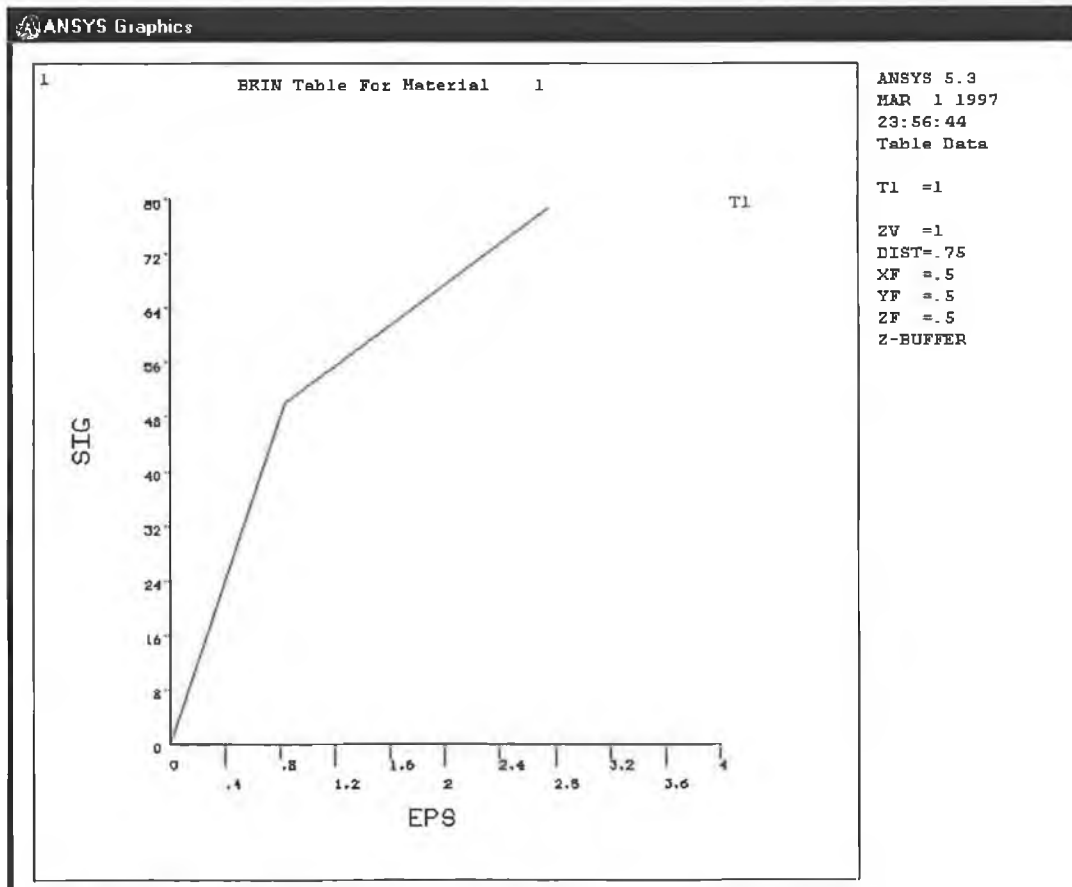


Figure 8.18 : A plot of a Bi-kinematic stress strain relationship

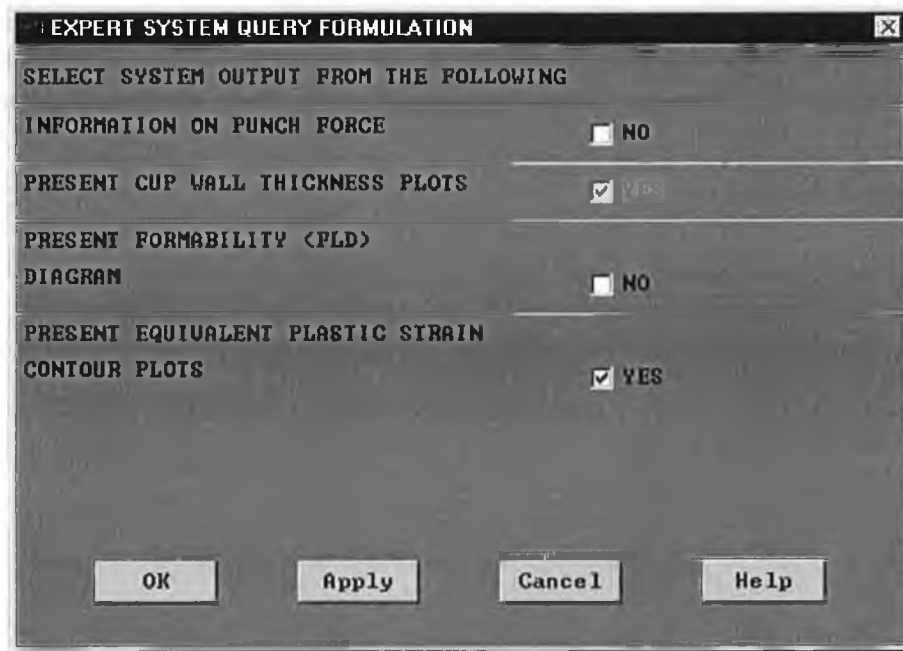


Figure 8.19 : Expert System Query Formulation Dialogue Box

The expert system query formulation data base enables the user to set the degree of the data base search. For example, for information solely on the required punch force the test algorithm would contain a search of the punch force rule base, and a two dimensional F.E.A simulation via the implicit F.E.A log file scripts. To predict cup wall thickness distribution a 3D F.E.A simulation via the explicit F.E.A log file script would be called upon.



Figure 8.20 : Overriding cup specification dialogue box

The overriding cup specification dialogue box sets the search bias to the desired drawn cup specification. The knowledge base search bias may be to minimise the punch force required to draw the cup by effecting tool and blank geometry, or to minimise the variability in the cup wall thickness, by again effecting the tool geometry.

8.14 Conclusion

The system architecture for the cup drawn expert system has been presented, with reference to domain and control knowledge. The black board architecture which encompasses the analytical rule data base of the geometrical modeller, the F.E.A. simulation models and successful draw records. The solution search method which is applied by the expert system is presented. A method of assessing the validity of Expert System solution is presented in the form of certainty factors. The choice and chosen software is explained. The Graphical user interface for the cup drawn expert system is presented outlining its form and application, its look and feel was developed for ease of use.

9 Thesis Summary.

The work conducted for this Thesis presents the theory applicable to Metal forming. The aims and objectives in developing the Cup drawing expert system have been fully met and outlined as follows. The Expert System for Cup drawing helps in conceptual design and process verification for new product. This is done by assessing the cup formability, by predicting the optimal material, process and geometry parameters, to ensure a successfully designed product and production process. As a failure analysis tool the expert system helps in detecting the causes for forming failure and suggests suitable modifications in the current process set-up to avoid such failures. The cup drawing Expert System uses heuristic knowledge to automatically invoke appropriate F.E.A codes, choose key design parameters and manage communication and interaction between the diverse technologies of F.E.A. codes and the geometric analytical modeller. The input to the expert system is composed off the geometry of the desired cup and constraints on processing parameters. The out put form the expert system sets the optimised Die geometry, material and process parameters for successful forming of the component. The generalised steps involved in the Cup drawing expert system are as outlined in Figure 9.

It is believed by the Author that this project holds the seeds for a useful tool for industrial interests in the area of Cup drawing. This research produced two academic papers that were presented at international conferences as follows. "*A USER FRIENDLY EXPERT SYSTEM FOR DEEP DRAWING OF CYLINDRICAL CANS* " **Proceeding of the Fifteenth Conference of the Irish Manufacturing Committee University of Ulster at Jordanstown 2nd to the 4th of September 1998.** "*OPTIMISATION OF CUP DRAWING GEOMETRY BY APPLICATION OF TAGUCHI METHODS ON FINITE ELEMENT ANALYSIS OF METAL FORMING SIMULATION.*" **International Postgraduate Research Student Conference DIT, Aungier st 20th & 21th of November 1998.** To conclude the research within this Thesis is adjudged a success from the delivery of the research papers and the attainment of the major research objectives.

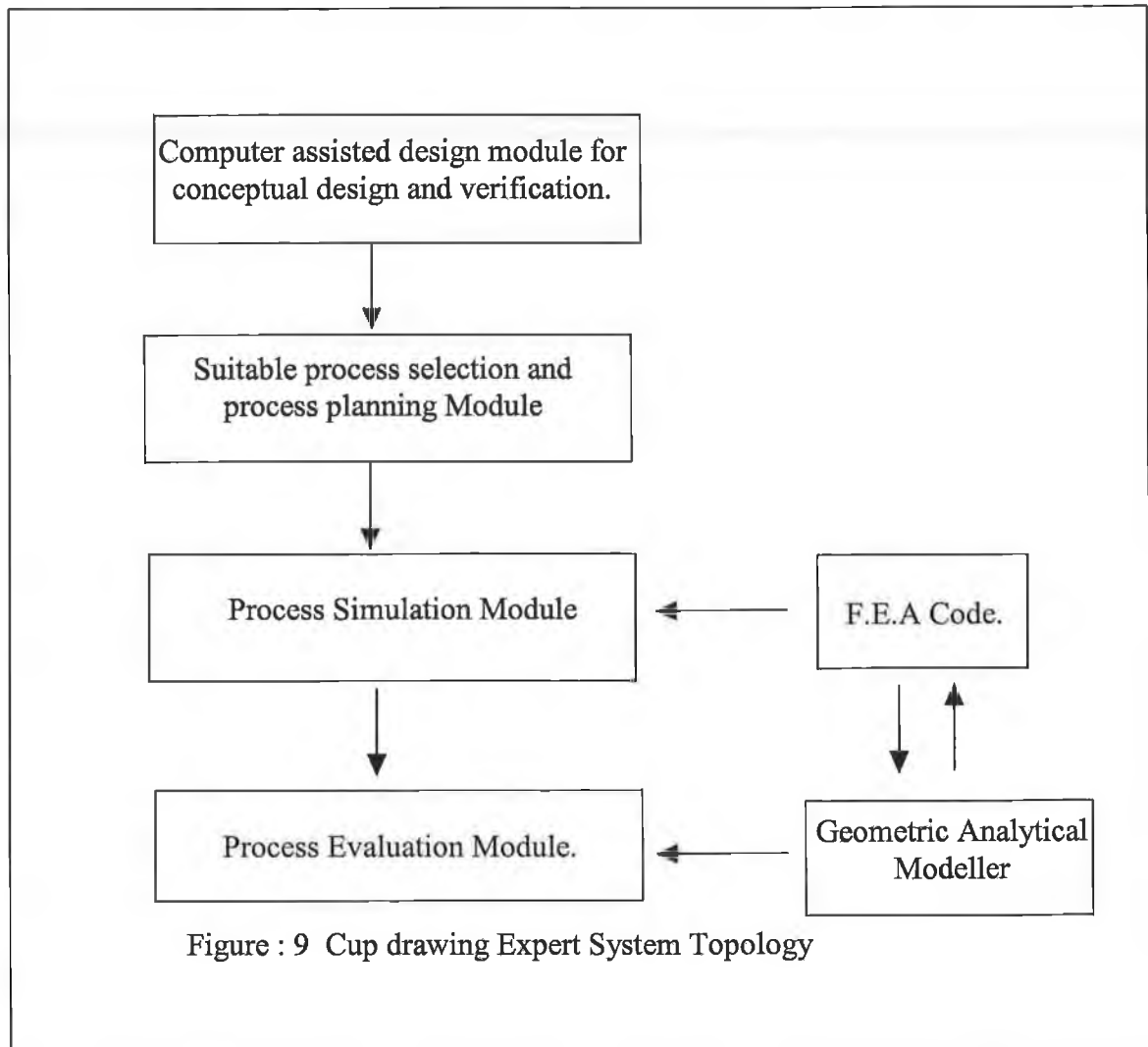


Figure : 9 Cup drawing Expert System Topology

REFERENCE

- 1.1 Eshel, G. Barash, M and Chang, T.C.
A Rule Based System for Automatic Generation of Deep Drawing Process Outlines.
Bound volume , Computer Aided Intelligent Process Planning, ASME Winter Annual Meeting Miami Beach FL Nov 1985
- 1.2 Hartery,p Pillinger,j sturgress,cen European development in simulation forming process using three dimensional finite element analysis Univ. of Birmingham, England p 12-14 1991 vol 43
- 1.3 Oh,s,I .Lahoti,g,d and Altan,t “ALPID A general purpose FEM program for metal forming” Proc NAMRC-IX, State Collge P,A, 1981
- 1.4 Wu,w,t. Lig,j .Tang,j,p and Tszeng,t,c “Automated mesh generation and re-generation for three dimensional metal forming simulations” Numiform 95
- 1.5 Martins p,a,f. Marmelo,j,m,cp Rodrigues,j,m,c and Barata,m,j,m “Plarmsh3 A three dimensional program for remeshing in metal forming” Computers and structures vol 53.No 5 pp 1153-1166 1994 .
- 1.6 Numerical methods in Industrial forming processes conference proceedings. Pub Balkema.
- 1.7 International conference on metal forming conference proceedings pub Elsevier.
- 2.1 Crandall.S.H; Dahl ,N.C; Lardner,T.J An introduction to the mechanics of solids. Pub Mc Graw Hill 1978.
- 2.2 Avitzur. Betzalel
Metal forming the application of limit analysis Pub : Dekker 1980.
- 2.3 Talbert S.H.; Avitzur.Betzalel
Elementary mechanics of Plastic Flow in Metal Forming. Pub : John Wiley & Sons.
- 3.1 Zienkiewicz.O.C,Taylor.R.L The Finite Element Method Publish Mc Graw Hill 1988.
- 4.1 Hill, R The Mathematical Theory of Plasticity oxford at the clarendon press 1950.
- 4.2 Yamada,Y.,Yoshimura,N.,and Sakurai,T. Plastic stress-strain matrix and its application for the solution of elastic plastic problems by the finite element method.Int.J.Mech. Sci 10, 343-54 (1968).
- 4.3 Dieter G Mechanical Metallurgy Pub McGraw Hill
- 4.4 Hill, R The Mathematical Theory of Plasticity oxford at the clarendon press 1950.
- 5.1 Lemaitre,j,Chaboche.J.L Mechanics of solid materials Pub Cambridge University Press.

- 5.2 Schweizerhof,Hallquist. LS-DYNA3D Theoretical manual LSTC 1993 PUB SAPIP INC.
- 6.1 Wick.C, Benedict.t.j, Veillveux.R.F “Tool and Manufacturing Engineers Hand book Vol 2. Forming , Society of manufacturing Engineers 1984.
- 6.2 Eary.D.F,Reed.E.A Techniques of pressworking sheet metal, Prentice Hall, Englewood Cliffs NJ 1958
- 6.3 ANSYS Theory manual volume IV 194 Pub Swanson Analysis Systems Inc
- 6.4 Mattiasson,K Bernspang,L Samuelsson,A Evaluation of a dynamic approach using explicit integration in 3 D sheet forming simulation. Numerical Methods in Industrial Forming Processes Chenot Wood & Zienkiewicz 1992 Balkema Rotterdam.
Hallquist.J.O, Stillman.D.W, Schweizerhof.k, Weimar.K “Improving standard shell elements, friction models and contact algorithms for the efficient solution of sheet metal forming problrms with LS-DYNA3D
- 6.5 Schweizerhof,Hallquist. LS-DYNA3D Theoretical manual LSTC 1993 PUB SAPIP INC.
- 6.6 Zienkiewicz.O.C and Zhu J.Z.[4] “A simple error estimator and adaptive procedure for practical engineering analysis”. Int Journal of Numerical Methods ENG 24 337-357 (1987).
Chung, S.Y. and Swift, H.W., “Cup Drawing From A Flat Blank, Part I. Experimental Investigation”, Proc. Instn. Mech Engrs., U.K., PP.199 - 211, 1951
- 6.7 Bonet Javier “Error estimations and enrichment proceedures for finite element analysisof thin sheet large deformation processes.” International journal for numerical methods in engineering. 1573-1591 vol 37 part 9 1994.
- 6.8 Mattiason,k.Evaluation of a dynamic approach using explicit integration in 3-D sheet forming simulation.Numerical methods in industrial forming processes. Chenot, Wood & Zienkiewicz editors 1992. Balkema, Rotterdam.
- 6.9 Hill,R. Mech,J .Phys.Solid,1 (1952) 19
- 6.10 Marciniak,Z and Kucynski,K. Int.J.Mech.Sci.9 (1967) 609
- 6.11 A Wagoner,R,H. Burford,D,A . Chan ,K,S and Keeler ,S,P. “Forming limit diagrams: Concepts metahods and applications, Tms Warrendale 7989 p. 167
- 6.12 Hobbs,R,M. Duncan , J,l a course on advanced sheet metal fromimng ,asm Metals Park, OH, 1979
- 6.13 Chung,S,Y and Swift,H,W, Proc Inst Mech Eng 165 (1951) 199
- 6.14 Erichsen A, German Patent No. 260180, 6 July 1912

- 6.15 Hecker,S,S Metals Eng Quarter .14 (1974).30
- 7.1 TAGUCHI METHODS Peace Glen Stuart Addison Wesley Publishing 1992
Engineering Methods for Robust Product Design William.Y.Fowlkes
Clyde.M.Creveling Addison Wesley publishing company 1995.
- 7.2 Chung, S.Y. and Swift, H.W., "Cup Drawing From A Flat Blank, Part I. Experimental Investigation", Proc. Instn. Mech Engrs, 1951 Vol 165 pp 143 - 223.
- 7.3 Johnson, W and Mellor, P.B, Engineering Plasticity, John Wiley and Sons, New York 1976.
Hobbs R.M AND Duncan J.L pres forming advanced Technology course NO. 4 American society for Metals 1979.
- 7.4 Mattiasson,k Bernspag,L Samuelsson,A Hamman,T Schedin,E Melander. A "Evaluation of a dynamic approach using explicit integration in 3-D sheet forming simulation" Numerical Methods in Industrial Forming Processes Numiform 92 (Pub Balkema) P 55, 67
- 7.5 Eary, D.F. and Reed, E.A , Techniques of press working sheet metal, Prentice - Hall, Englewood Cliffs nj, 1958.
- 7.6 Sachs, G "New Research on the drawing of cylindrical shells ", proc. Inst automobile eng, vol 29 p. 588, 1934-5
- 7.7 Duncan,j.l and jhomson, w Approximate Analysis of loads in Axis symmetric Deep Drawing, proc 9 th inter mach Tool Design and res conf p 303, pergamon press, oxford, 1969
- 7.8 Avitzur, B upper bound analysis of Deep Drawing on Eduktron publication 1977. Canada Proceeding of the 1982 north America metalworking research conference (NAMRC) Hamilton, may 1982.
- 7.9 Chung.S.Y ans Swift.H.W An experimental investigation of ReDrawing of Cylindrical Cups, Proc Instn mech Engrs, U.K,
- 7.10 Slater ,R.A.C., Engineering Plasticity, John Wiley & Sons, New York, 1997.
- 7.11 Kawai, N Critical conditions for wrinkling in deep drawing of sheet metals (3rd report, prediction, Prediction of Blank holding Pressure) Bull JSME 1961 VOL.4 NO. 13 pp. 182-192
- 7.12 Hobbs R.M AND Duncan J.L pres forming advanced Technology course NO. 4 American society for Metals 1979.

- 8.1 Gasching,J . Reboh,R and REITER,j ,Development of a Knowledge based system for Resources problems, Technical report No. 1619, SRI International, menlo park, ca 1981
- 8.2 Brackman, “ What are Expert Systems ? “ in Hayes-Roth F Waterman D,A Lanat D,B, Building Expert Systems Addison - Wesley, Reading, MA, 1983.
Dym C L. Salta S E “ Representation of stategic Choices in structural Modeling “ Proceedings of the 1989 ASCE Structures congress, San Franciso, 1989.
- 8.3 Feigenbaun E A Mc Corduck P, The fifth generation , Addison Wesley, reading, MA, 1983.
- 8.4 Dym.C.L,Levitt.R.E Knowledge Based Systems in Engineering Pub Mc Graw Hill
- 8.5 Dym C L Ivey E S Principles of Mathematical Modeling Academic Press, New York, 1980.
- 8.6 Lesser V R Fennell R Erman L D and Reddy D R “ Organisation of the HEARSAY-II Speech Understanding System,” IEEE Transactions on Acoustics, sppeech and Signal Processing ASSP-23(1),1975.
- 8.7 Clancey W J Acuring, representing and evaluating a competence model of diagnostic strategy. Tech. Rept. HPP-84-2, Stanford University, Stanford, C A 1984.
- 8.8 Mc Carthy J Programs with common sense in Proceedings Teddingon Conference on the Mechanisation of the thought process, 1960.
- 8.9 Hayes-Roth, B “ A blackboard Architecture for control” Artificial Intelligence 1985 pages 251-321.
- 8.10 Bennett.J.S, SACON A Knowledge Based consultant for structural analysis Proceedings of AAAI 1984.
- 8.11 Buchanan.B.G, Duda.R.O, “Principles of Rule Based Expert System” Advances in computers 22, Academic Press, New York 1983
- 8.12 Brownston.L,Farrel.R, Kant.E,Martin,N “Programming Expert Systems in OPS5, Addison Wesley, Reading,MA, 1985
- 8.13 Nilsson.J.L “Principles of Artificial Intelligence” Morgan Kaufmann, Los Altos CA 1980.
- 8.14 Parsaye.K, and Chignell.M, Expert Systems for Expeerts, John Wiley, Newyork, 1988.

APPENDICES

APPENDIX A

Lagrangian Multipliers

Lagrangian multipliers

Lagrangian multipliers, consider the problem of making a function Π stationary, subject to the unknown u obeying some set of additional differential relationships.

$$C(u)=0 \text{ in } \Omega \quad \text{A:1}$$

We can introduce this constraint by forming another functional.

$$\bar{\Pi} (u,\lambda) = \Pi(u) + \int_{\Omega} \lambda^T C(u) d\Omega \quad \text{A:2}$$

in which λ is some set of functions of the independent co-ordinates in domain Ω known as the lagrangian multipliers. The variation of the new functional is zero provided $C(u)=0$ and hence $\delta\Pi=0$.

It is of interest to investigate the form of equations resulting from the modified functional $\bar{\Pi}$ of the above equation, if the original functional Π gave as in the Euler equations a system, such as.

$$A(u)=0 \quad \text{A:3}$$

thus :

$$\delta\bar{\Pi} = \int_{\Omega} \delta u^T A(u) d\Omega + \int_{\Omega} \delta \lambda^T C(u) d\Omega + \int_{\Omega} \lambda^T \delta C d\Omega \quad \text{A:4}$$

Substituting the following trial functions. Provided that the constraints are a linear set of equations such that

$$C(u)=L_1 u + C_1 \quad \text{A:5}$$

yields :

$$\delta\bar{\Pi} = \delta a^T \int_{\Omega} N^T A(u) d\Omega + \delta b^T \int_{\Omega} \bar{N}^T (L_1 \hat{u} + C_1) \delta\Omega + \delta a^T \int_{\Omega} (L_1 N)^T \hat{\lambda} d\Omega = 0 \quad \text{A:6}$$

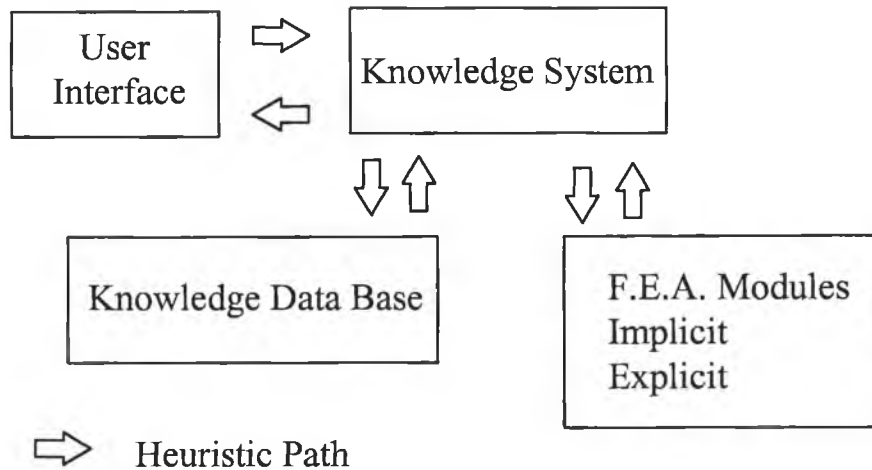
The solution of Equation A:6 yields the nodal displacements, which are subjected to the Lagrangian Multiplier constraint Equation.

APPENDIX B

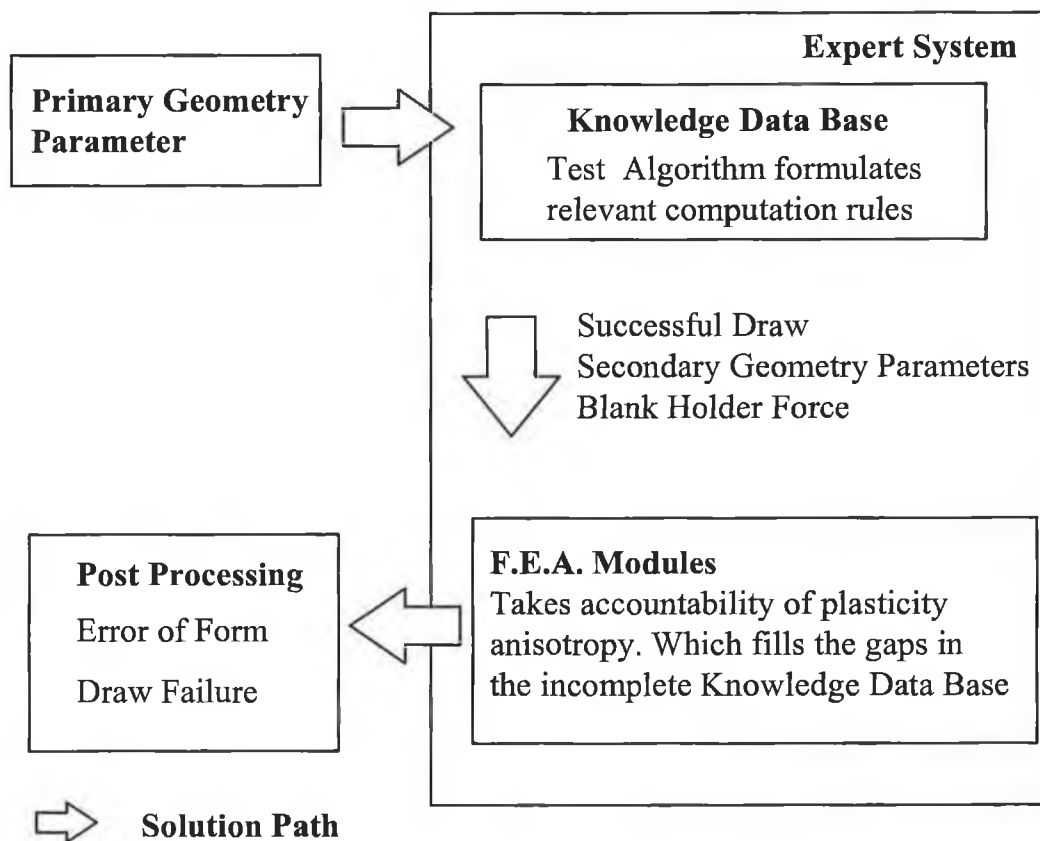
Expert System Software Code Architecture

The Expert System architecture is as outlined in the following Appendices. To ensure relevance to the Thesis text it's structure is now re-emphasised. The cup drawn expert system as explained in the text works as follows.

Expert System Topology

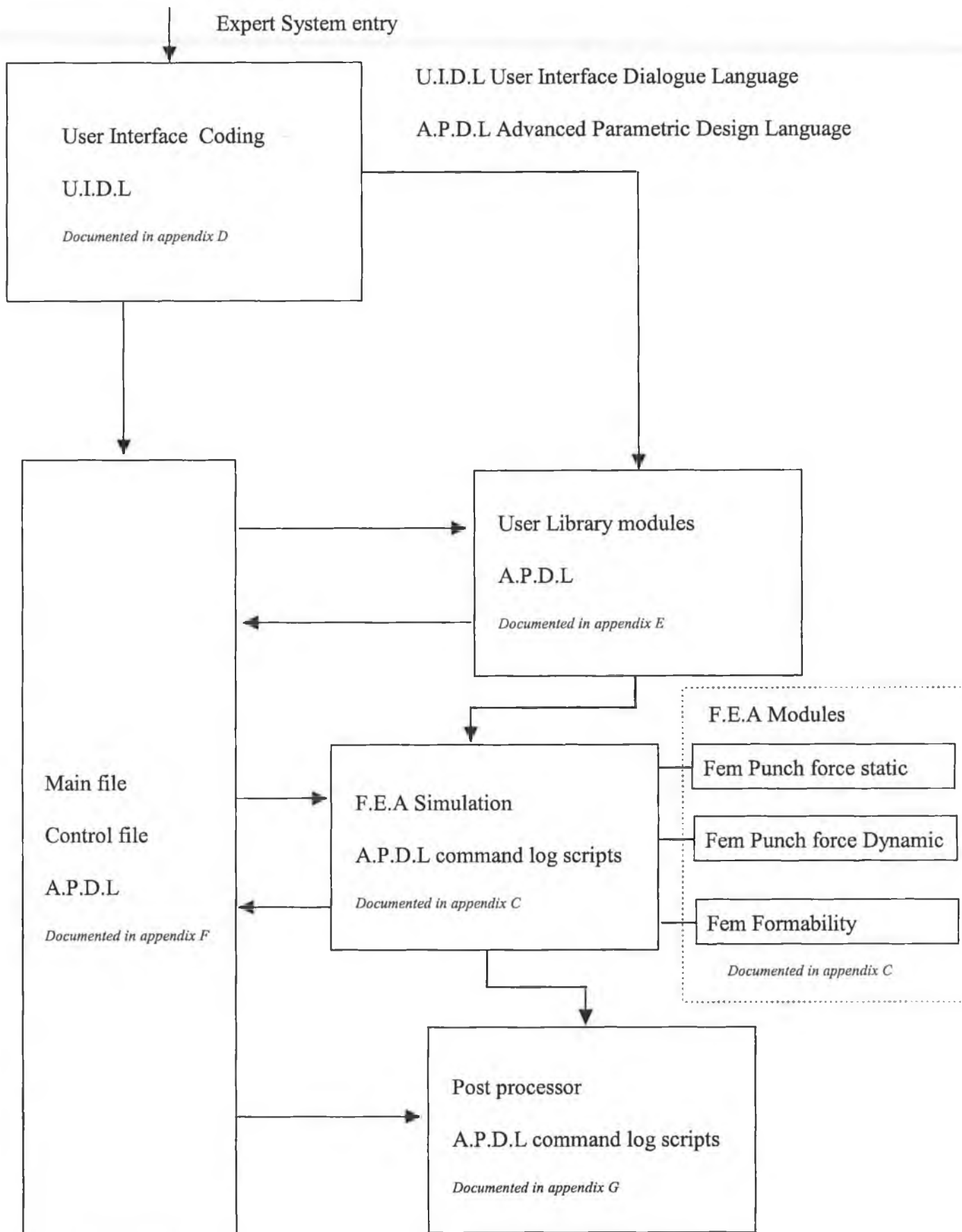


Axis Symmetric Cup Drawing Methodology



The ANSYS A.P.D.L coding that enable the above to be executed successfully are documented in the appropriate Appendices, that follow.

Over-All Code Architecture



APPENDIX C

*Finite Element Analysis ANSYS
Pre-processor Simulation Command
Code*

Fem Punch force static command log file listing

static analysis contact element 26 rigid Tooling

/pmacro

! macro file prompt

/FILE,DEV01

! file name

/prep7

*ASK,b,BLANK DIAMETER,200

! Input phase for deep drawing variables

*ASK,t,BLANK THICKNESS,.9

*ASK,p,PUNCH DIAMETER,100

*ASK,c,CLEARANCE,1.25

*ASK,pcr,PUNCH CORNOR RADIUS,5

*ASK,dcr,DIE CORNOR RADIUS,5

*ASK,s,STROKE,60

et,1,42,,,1,,1,3

! element type plane 42 ANSYS

n,1,,-.001

! Direct nodal generation punch and die representation

n,2,(p/2)-pcr,-.001

n,3,p/2,(pcr)-.001

n,4,p/2,(2*pcr)-.001

n,5,p/2+c,-(t+(2*dcr))

n,6,p/2+c,-(t+dcr)

n,7,p/2+dcr+c,-t

n,8,b/2,-t

n,11,,-t

bb= b/2

*do,i,0,320,1

! Direct nodal generation representation of blank

n,11+i,(bb/320)*(i),-t

*enddo

ngen,5,321,11,332,,,t/4,

e,11,12,333,332

! generation of element representation of blank

egen,320,1,1

egen,4,321,-320

alls

n,9,(p/2)+c+dcr

! Direct nodal generation blank holder definition

n,10,b/2

et,2,26,1,,,,,1,

!element type two contact node to ground

type,2

real,2

mat,2

real,6

e,1295,10,9
*repeat,320,1
d,9,ux,0,,10,,

! Blank Holder Contact definition

E,1295,2,1
*repeat,320,1
E,1295,4,3
*repeat,320,1,
real,3
E,1295,2,3
*repeat,320,1
alls

! Punch Contact definition

mat,3
real,4
e,11,7,8
*repeat,320,1
e,11,5,6
*repeat,320,1
real,5
e,11,7,6
*repeat,320,1
alls

! Die Contact definition

!et,10,39,,,,3
!r,10,1,10
!type,10
!real,10
!e,9,33
!e,10,51

! spring definition

d,5,ux,0,,8,1,uy
alls

! Die Constraints

esel,s,mat,,1
nsle
!nsel,s,loc,x,b/2
!d,all,ux,0
nsel,s,loc,x,0
nsel,u,node,,1
d,all,ux,0
alls

! Blank axisymmetric constraints

d,1,ux,0,,4,1

! Die constraints


```
MP,ex,1,207E3
MP,prxy,1,0.3
MP,MU,1,0.1
```

! material 1 sheet blank material properties

```
MP,ex,2,207E3
MP,prxy,2,0.3
MP,MU,2,0.1
```

! material 1 sheet blank material properties

```
tb,bkin,1
tbdat,1,2,230
tbdat,1,3,10e3
```

! material 1 sheet blank plasticity values

```
/solu
outres,all,all
! EQSLV,PCG,10E-5,2
ANTYPE,0
NLGEOM,ON
```

! ANSYS solution settings

! Preconditioned conjugate gradient solver

! Static analysis

!large deformation effects on

```
NSUBST,1,40,1,On
KBC,0
```

! sub step data

! sub step loads ramped

```
AUTOTS,OF
```

! automatic time stepping off

```
PRED,ON,,ON
```

! load step predictor on

```
LNSRCH,ON
```

! line search on

```
NROPT,1,,OFF
```

! full newton-raphson

```
NEQIT,75
```

! number of equilibrium iterations

! Load step file one definition

```
knbh = 1
```

! contact stiffness of blank holder and blank interface

```
kn = 5
```

! contact stiffness of punch and blank interface

```
r,2,kn,,,.01
r,3,kn,-pcr,0,.01
r,4,kn,,,.01
r,5,kn,-pcr,0,.01
r,6,knbh,,,.01
d,9,uy,-.01,,10,,
```

!contact element real constant

! blank holder target surface imposed movement to develop blank holding pressure

```
lswrite,1
lssolve,1,1,1
SAVE
FINISH
```

! load step one writing
! solution of load step one
! save model data base
! exit to ANSYS begin mode

! Solution restart to develop contact between punch and blank

```
/FILE,DEV
RESUME
/SOLU
ANTYPE,0,REST
```

!development of punch contact

```
/prep7
alls
!element type two
et,2,26,1,,,,,1,
```

!element type two contact node to ground

```
kn1=1
kn = 3
r,2,kn,,,01
r,3,kn,-pcr,0,.01
r,4,kn,,,01
r,5,kn,-pcr,0,.01
r,6,kn1,,,01
```

!contact element real constant

```
real,2
E,1295,2,1
*repeat,320,1
E,1295,4,3
*repeat,320,1,
real,3
E,1295,2,3
*repeat,320,1
alls
```

! Punch Contact definition

```
/solu
NEQIT,95
cnvtol,f,0.15
NSUBST,40,50,1,On
d,1,uy,-1,,4,1
solve
save /EOF
```

! number of equilibrium iterations
!force convergence tolerance setting
! sub step data
!punch imposed displacement
! solve restart
! save restart solution results

Fem Punch force Dynamic command log file listing

Dynamic analysis contact element 48 flexible Tooling

/pmacro	<i>! macro file prompt</i>
/FILE,DEV02	<i>! file name</i>
/prep7	<i>!ANSYA General Pre Processor</i>
*ASK,b,BLANK DIAMETER,200	<i>! Input phase for deep drawing variables</i>
*ASK,t,BLANK THICKNESS,.9	
*ASK,p,PUNCH DIAMETER,100	
*ASK,c,CLEARANCE,1.25	
*ASK,pcr,PUNCH CORNOR RADIUS,5	
*ASK,dcr,DIE CORNOR RADIUS,5	
*ASK,s,STROKE,60	
n,1,0,5	<i>! Direct nodal generation representation of Punch Tooling</i>
*do,i,1,10,1	
n,i+1,((p/2-pcr)/10)*i,5	
*enddo	
local,11,1,(p/2)-pcr,pcr+5,	<i>! local co-ordinate system 11 for creation of tooling radii</i>
csys,11	
j=11	
*do,i,10,90,10	<i>! development of punch tool radii nodes</i>
n,j,pcr,270+i,	
j=j+1	
*enddo	
csys,0	<i>! global Cartesian 11is active co ordinate system</i>
n,21,p/2,(pcr*3)+5	<i>! development of punch tool nodes</i>
nsel,all	
cm,punch,node	
cmsel,s,punch	
d,all,ux,0,,,,uy	
!die node development	

```
n,22,(p/2)+c,-(t+(dcr*3))
```

*! Direct nodal generation representation
of Punch Tooling*

```
n,23,(p/2)+c,-(t+(dcr))
```

```
local,12,1,p/2+c+dcr,-(t+dcr)
```

*! local co-ordinate system 11 for creation of
tooling radii*

```
j=23
```

```
csys,12
```

```
*do,i,10,90,10
```

```
n,j,dcr,180-i,
```

```
j=j+1
```

```
*enddo
```

```
csys,0
```

! development of die tool radii nodes

```
bf=(b/2-(p/2+dcr+c))
```

! computation of flange length bf

```
*do,i,1,10,1
```

```
n,31+i,(p/2+c+dcr)+((bf/10)*i),-t
```

```
*enddo
```

! development of blank holder nodes

```
nselect,all
```

```
nselect,u,,,punch
```

```
cm,die,node
```

```
alls
```

! creation of blank holder nodal component

```
et,1,42,,,1,,1,3
```

! element type plane 42 ANSYS

```
bb=b/2
```

```
*do,i,0,160,1
```

```
n,49+i,(bb/160)*(i),-t
```

```
*enddo
```

```
ngen,5,161,49,209,,,t/4,
```

*! Direct nodal generation representation
of sheet blank*

```
e,49,50,211,210
```

```
egen,160,1,1
```

```
egen,4,161,-160
```

*! generation of element representation of
blank sheet*

```
nselect,all
```

```
nselect,u,,,punch
```

```
nselect,u,,,die
```

```
cm,sheetnod,node
```

! creation of blank sheet nodal component

```
esel,s,mat,,1
```

```
cm,sheetelm,elem
```

*! creation of blank sheet elemental
component*

```

alls
bf=(b/2-(p/2+dcr+c))                                ! blank holder length definition

*do,i,0,100,1
n,1000+i,(p/2)+dcr+c+((bf/100)*i),                  ! blank holder nodes
*enddo
ngen,2,101,1000,1100,,bf/100
alls

nset,all
nset,u,,,punch
nset,u,,,die
nset,u,,,sheetnod

cm,blankhol,node                                     ! creation of blank sheet nodal component

et,2,42,,,1,1,3                                     ! element type 2 to nodal blank holder
type,2
mat,2
real,2

e,1000,1001,1102,1101                               ! generation of element representation of
egen,100,1,641                                     blank holder
esel,s,mat,,2

cm,blankpre,elem                                    ! creation of blank holder elemental
                                                    component

alls

cmsel,s,sheetnod
nset,r,loc,y,,
cm,top,node                                         !component of nodes on the top of the sheet
                                                    blank

alls

cmsel,s,sheetnod
nset,r,loc,y,-t,
cm,bottom,node                                     !component of nodes on the bottom of the
                                                    sheet blank

cmsel,s,blankhol
nset,r,loc,y,,
cm,blankcon,node                                   !component of nodes on the bottom of the
                                                    blank holder

alls

```

```
et,4,1
r,4,1
type,4
mat,4
real,4
```

! dummy element definition for punch

```
e,1,2
egen,18,1,741
e,22,23
egen,19,1,759
alls
```

! dummy element definition for die

```
et,3,48,0,1,1,,,,2,
type,3
!contact stiffness kn
kn=1
kt=.01
!contact punch sheet die
mat,3
real,3
r,3,kn,kt,
```

! 2D flexible contact element

```
gcgen,punch,top,,
!real,7
!r,7,kn,kt,
!gcgen,top,punch,,
real,5
r,5,kn,kt,
```

! automatic contact generation between punch and blank

```
gcgen,die,bottom,,5
!real,8
!r,8,kn,kt,
!gcgen,bottom,die,,5
!contact blank holder sheet
real,6
r,6,kn,kt,
```

! automatic contact generation between

```
gcgen,blankcon,top,,5
!real,9
!r,9,1,,0.001
!gcgen,top,blankcon,,5
alls
```

! automatic contact generation between blank and die

```
cmsel,s,die
D,ALL,UX,0,,,,UY
```

! die and blank holder constraint

```

cmsel,s,blankhol
D,ALL,UX,0,,,,
cmsel,s,sheetnod
nset,s,loc,x
D,ALL,UX,0

cmsel,s,punch
D,ALL,UX,0,,,,

cmsel,s,blankpre
sfe,all,3,press,,.5
alls

!esel,s,type,,4
!edel,all
!alls
! spring definition
et,10,39,,0,,3
r,10,1,10
type,10
real,10
e,1,693
e,9,750

*do,i,1,4,1
mp,ex,i,207e3
mp,prxy,i,0.3
mp,mu,i,.1
mp,dens,i,76.5
*enddo

/solu
outres,all,all
antype,4
nlgeom,on

timint,on,all
!eqslv,pcg,10e-5,2
time,0.5
trnopt,full

nsubst,5,200,5,off
kbc,0
autots,off
pred,on,,on
lnsrch,on

```

!blank sheet symmetry conditions

!punch constraint

!applied pressure of blank holder

! delete link element from data base

! material 1 sheet blank material properties

! ANSYS solution settings
! output results for all
! full transient analysis
!large deformation effects on

! Preconditioned conjugate gradient solver

! sub step data
! sub step loads ramped
! automatic time stepping off
! load step predictor on
! line search on

nropt,1,,off	<i>! full newton-raphson</i>
neqit,50	<i>! number of equilibrium iterations</i>
cnvtol,f,,0.05	<i>!force convergence tolerance setting</i>
!load step definition binder wrap	
alls	
lswrite,1	
!punch displacement	
nsubst,1,1,1,off	<i>! sub step data</i>
cmsel,s,punch	
D,ALL,UX,0	
D,ALL,UY,-5	
alls	
cnvtol,f,,0.05	<i>!force convergence tolerance setting</i>
time,2	
lswrite,2	
nsubst,80,,off	<i>! sub step data</i>
cmsel,s,punch	
D,ALL,UX,0	
D,ALL,UY,-10	
alls	
kn3=1500	
tl=.7	
r,3,kn3,kt,tl	<i>!contact stiffness setting</i>
r,4,kn3,kt,tl	
r,5,kn3,kt,tl	
r,6,kn3,kt,tl	
r,7,kn3,kt,tl	
r,8,kn3,kt,tl	
r,9,kn3,kt,tl	
time,4	<i>! time setting of transient load</i>
lswrite,3	<i>! write load step</i>
save	<i>! save database</i>
lssolve,1,3,1	<i>! solve load step 1 to 3</i>
save	<i>! save analysis results</i>
/EOF	

Fem formability command log file listing

Quasi Static Explicit Analysis

/pmacro	<i>! macro file prompt</i>
/FILE,DEV01	<i>! file name</i>
/PREP7	<i>!ANSYA General Pre Processor</i>
*ASK,D,BLANK DIAMETER,120	<i>! Input phase for deep drawing variables</i>
*ASK,T,BLANK THICKNESS,1	
*ASK,P,PUNCH DIAMETER,66	
*ASK,C,CLEARANCE,1.25	
*ASK,PCR,PUNCH CORNOR RADIUS,3	
*ASK,DCR,DIE CORNOR RADIUS,5	
*ASK,S,STROKE,35	
et,1,shell163	<i>! element type definition shell163 explicit lsdyna 3D element</i>
et,2,shell163	
et,3,shell163	
et,4,shell163	
K,1,0,-T/2	<i>! key point definition for tooling profile lines</i>
K,2,-D/2,-T/2	
K,3,0,0	
K,4,-P/2,0	
K,5,-P/2,S*1.1	
K,6,-D/2,-T	
K,7,-((P/2)+C),-T	
K,8,-((P/2)+C),-S*1.1	
K,9,0,-S	
L,1,2	<i>! line definition of tooling profile</i>
L,3,4	
L,5,4	
L,6,7	
L,7,8	
LFILLT,3,2,PCR	<i>! line filleting to create punch corner radius ! line filleting to create die corner radius</i>
LFILLT,4,5,DCR	
K,100,-(P/2+C),0	<i>! keypoint and subsequent line definition of blank holder geometry</i>
K,101,-D/2,0	
L,100,101	

! area of tool generation area 1-sheet blank 2 - punch 3 - die 4 - blank holder

```

AROTAT,1,,,,,1,9,90
AATT,1,1,1
AROTAT,3,6,2,,,,1,9,90,1
ASEL,U,MAT,,1
AATT,2,2,2
AROTAT,4,7,5,,,,1,9,90,1
ASEL,U,MAT,,1,2,1
AATT,3,3,3
AROTAT,8,,,,,1,9,90
ASEL,U,MAT,,1,3,1
AATT,4,4,4
allsel
    
```

! area generated by rotation of line about axis

! area attribute assignment

```

lesiz,3,,,8
lesiz,11,,,8
lesiz,14,,,8
lesiz,15,,,8
lesiz,16,,,8
lesiz,6,,,25
lesiz,12,,,25
lesiz,2,,,8
lesiz,13,,,8
    
```

! punch line sizing for meshed elements

```

lesiz,4,,,5
lesiz,17,,,3
lesiz,20,,,20
lesiz,21,,,20
lesiz,22,,,20
lesiz,23,,,20
lesiz,5,,,8
lesiz,19,,,8
lesiz,18,,,25
lesiz,7,,,25
lesiz,17,,,5
    
```

! die line sizing for meshed elements

```

lesiz,8,,,3
lesiz,26,,,8
lesiz,24,,,3
lesiz,25,,,8
    
```

! blank holder line sizing for meshed elements

!develop trim area of mesh to be cleared to simulate flange trimming

```

local,11,1,,,,,-90
    
```

! develop !local co-ordinate system 11 cylindrical

```

csys,11                                ! co-ordinate system 11 is active co
                                        ordinate system

k,200,75,80,-t/2                        ! keypoints of trimming line
k,201,75,190,-t/2
l,200,201                                ! trimming line
csys,0                                    ! global Cartesian 11 is active co
                                        ordinate system
asbl,1,27,,delete,keep,                ! area division by line

ASEL,U,MAT,,2,4,1
AATT,1,1,1                                ! area attribute assignment

lesiz,28,,20                             ! blank sheet trim area line sizing for
lesiz,9,,20                               meshed elements
lesiz,29,,20
lesiz,30,,20

lesiz,10,,20                             !blank sheet line sizing
lesiz,31,,3
lesiz,32,,3

shape,2                                  ! quadrilateral element mesh only
amesh,1,10,1                             ! mesh areas 1 to 8

enorm,#                                  ! ensure that all connected shell elements to
                                        # have surface normal as #
ensym,,,#                                ! Reverse direction of shell normal

mp,ex,1,207.                             ! material 1 sheet blank material properties
mp,dens,1,7.83e-5
mp,nuxy,1,.3
r,1,5/6,5,.9

*do,i,2,4
mp,ex,i,207
mp,dens,i,7.83e-6
mp,nuxy,i,.3
r,i,5/6,3,1,1,1,1
*enddo

tb,plaw,1,,3,                            ! material 1 sheet blank plasticity values
tbdatt,1,2
tbdatt,2,0.533
tbdatt,3,0.22
tbdatt,4,6

```

```
edmp,rigid,2,6,7 ! punch
edmp,rigid,3,7,7 ! die
edmp,rigid,4,6,7 ! blankholder
```

! rigid material definition punch die blank holder

```
esel,s,mat,,1
nsle
nset,r,loc,x
d,all,ux,,,,,roty,rotz ! yz symmetry
nsle
nset,r,loc,z
d,all,uz,,,,,roty,rotx ! xy symmetry
alls
```

!symmetry boundary condition (not for rigid bodies)

```
*dim,vtime,array,(2,1)
*dim,vload,array,(2,1)
vtime(1)=0.0,10
vload(1)=-3.5,-3.5,
```

! array containing punch velocity over time

```
edload,add,rbvy,,2,vtime,vload
*dim,ftime,array,2
*dim,fload,array,2
```

*! set punch velocity
! array containing blankholder force over time*

```
ftime(1)=0.0,12
fload(1)=0.001034218,0.001034218,
```

! set blank holder force

```
esel,s,mat,,4
cm,hold,elem
alls
```

! create blank holder element component

```
edload,add,press,,hold,ftime,fload
```

! explicit dynamic load setting

```
!edhist component
esel,s,mat,,1,4,1
nsle
cm,histcomp,node
alls
```

! explicit dynamic history component

```
edcontact,,1,1
edcontact,,2,,1,1,1,,10,2
```

! contact control

```
edcgen,sts,1,2,0.1,,,,10 ! sheet punch
edcgen,sts,1,3,0.1,,,,10 ! sheet blankholder
edcgen,sts,1,4,0.1,,,,10 ! sheet die
alls
```

! contact development

```
/solu
```

! ANSYS solution settings

```
edshell,,1  
edenergy,1,,1  
time,10  
edwrite,both,,,  
edopt,add,,both  
edrst,50  
edhtime,50  
edhist,hist
```

```
edout,gceout  
edout,glstat  
edout,matsum  
edout,spcforc  
edout,rbdout  
edout,rcforc  
edout,ncforc  
alls  
save  
solve  
save  
/EOF
```

! shell thickness change

! solution termination time

! write output to ANSYS and ascii

! frequency of out put

*! results outputted for the elements of hist
component*

! LSTAURUS ascii out put files

! select all

! save data base

! send jobname.k file to lsdyna 3D solver

! save results

Fem Punch force static command log file listing

static analysis contact 48 flexible Tooling

/pmacro

! macro file prompt

/FILE,DEV04

! file name

/prep7

!ANSYA General Pre Processor

*ASK,b,BLANK DIAMETER,200

! Input phase for deep drawing variables

*ASK,t,BLANK THICKNESS,.9

*ASK,p,PUNCH DIAMETER,100

*ASK,c,CLEARANCE,1.25

*ASK,pcr,PUNCH CORNOR RADIUS,5

*ASK,dcr,DIE CORNOR RADIUS,5

*ASK,s,STROKE,60

! Direct nodal generation representation

n,1,0,5

! Direct nodal generation representation

*do,i,1,10,1

of Punch Tooling

n,i+1,((p/2-pcr)/10)*i,5

*enddo

local,11,1,(p/2)-pcr,pcr+5,

! local co-ordinate system 11 for creation of tooling radii

csys,11

j=11

*do,i,10,90,10

! development of punch tool radii nodes

n,j,pcr,270+i,

j=j+1

*enddo

csys,0

! global cartesian 11 is active co ordinate system

n,21,p/2,(pcr*3)+5

! development of punch tool nodes

nset,all

cm,punch,node

cmsel,s,punch

d,all,ux,0,,uy

!die node development

n,22,(p/2)+c,-(t+(dcr*3))

! Direct nodal generation representation of Punch Tooling

n,23,(p/2)+c,-(t+(dcr))

```
local,12,1,p/2+c+dcr,-(t+dcr)
tooling radii
```

! local co-ordinate system 11 for creation of

```
j=23
csys,12
```

! development of die tool radii nodes

```
*do,i,10,90,10
n,j,dcr,180-i,
j=j+1
*enddo
csys,0
```

! computation of flange length bf

```
bf=(b/2-(p/2+dcr+c))
```

! development of blank holder nodes

```
*do,i,1,10,1
n,31+i,(p/2+c+dcr)+((bf/10)*i),-t
*enddo
```

! creation of blank holder nodal component

```
nselect,all
nselect,u,,,punch
cm,die,node
alls
```

! element type plane 42 ANSYS

```
et,1,42,,,1,,1,3
```

! Direct nodal generation representation of sheet blank

```
bb=b/2
*do,i,0,160,1
n,49+i,(bb/160)*(i),-t
*enddo
ngen,5,161,49,209,,,t/4,
```

! generation of element representation of blank sheet

```
e,49,50,211,210
egen,160,1,1
egen,4,161,-160
```

! creation of blank sheet nodal component

```
nselect,all
nselect,u,,,punch
nselect,u,,,die
cm,sheetnod,node
eset,s,mat,,1
cm,sheetelm,elem
```

! creation of blank sheet elemental component

```
alls
```

```
bf=(b/2-(p/2+dcr+c))
```

! blank holder length definition

```
*do,i,0,100,1
n,1000+i,(p/2)+dcr+c+((bf/100)*i),
*enddo
ngen,2,101,1000,1100,,,bf/100
```

! blank holder nodes

```
alls
nsel,all
nsel,u,,,punch
nsel,u,,,die
nsel,u,,,sheetnod
```

```
cm,blankhol,node
```

! creation of blank sheet nodal component

```
et,2,42,,,1,1,3
type,2
mat,2
real,2
```

! element type 2 to nodal blank holder

```
e,1000,1001,1102,1101
egen,100,1,641
esel,s,mat,,2
```

! generation of element representation of blank holder

```
cm,blankpre,elem
```

! creation of blank holder elemental component

```
alls
cmsel,s,sheetnod
nsel,r,loc,y,,
cm,top,node
```

!component of nodes on the top of the sheet blank

```
alls
```

```
cmsel,s,sheetnod
nsel,r,loc,y,-t,
cm,bottom,node
```

!component of nodes on the bottom of the sheet blank

```
cmsel,s,blankhol
nsel,r,loc,y,,
cm,blankcon,node
```

!component of nodes on the bottom of the blank holder

```
alls
```

```
et,4,1
```

! dummy element definition for punch


```
r,4,1
type,4
mat,4
real,4
```

```
e,1,2
egen,18,1,741
e,22,23
egen,19,1,759
alls
```

! dummy element definition for die

```
et,3,48,0,1,1,,,2,
type,3
!contact stiffness kn
kn=1
kt=.01
!contact punch sheet die
mat,3
real,3
r,3,kn,kt,
```

! 2D flexible contact element

```
gcgen,punch,top,,,
!real,7
!r,7,kn,kt,
!gcgen,top,punch,,,
real,5
r,5,kn,kt,
```

! automatic contact generation between punch and blank

```
gcgen,die,bottom,,5
!real,8
!r,8,kn,kt,
!gcgen,bottom,die,,5
```

! automatic contact generation between

```
!contact blank holder sheet
real,6
r,6,kn,kt,
```

```
gcgen,blankcon,top,,5
!real,9
!r,9,1,,0.001
!gcgen,top,blankcon,,5
alls
```

! automatic contact generation between

```
cmsel,s,die
D,ALL,UX,0,,,UY
cmsel,s,blankhol
D,ALL,UX,0,,,
```

! die and blank holder constraint

```

cmsel,s,sheetnod
nsel,s,loc,x
D,ALL,UX,0
    
```

!blank sheet symmetry conditions

```

cmsel,s,punch
D,ALL,UX,0,,,,
    
```

!punch constraint

```

cmsel,s,blankpre
sfe,all,3,press,,.5
alls
    
```

!applied pressure of blank holder

```

!esel,s,type,,4
!edel,all
!alls
! spring definition
et,10,39,,0,,3
r,10,1,10
type,10
real,10
e,1,693
e,9,750
    
```

! delete link element from data base

```

*do,i,1,4,1
mp,ex,i,207e3
mp,prxy,i,0.3
mp,mu,i,.1
mp,dens,i,76.5
*enddo
    
```

! material 1 sheet blank material properties

```

/solu
outres,all,all
antype,4
nlgeom,on
timint,on,all
!eqslv,pcg,10e-5,2
time,0.5
trnopt,full
    
```

! ANSYS solution settings

```

nsubst,5,200,5,off
kbc,0
autots,off
pred,on,,on
lnsrch,on
nropt,1,,off
neqit,50
cnvtol,f,,0.05
    
```

```
!load step definition binder wrap
```

```
alls
```

```
lswrite,1
```

```
!punch displacemant
```

```
nsubst,1,1,1,off
```

```
cmselect,s,punch
```

```
D,ALL,UX,0
```

```
D,ALL,UY,-5
```

```
alls
```

```
cnvtol,f,,0.05
```

```
time,2
```

```
lswrite,2
```

```
nsubst,80,,,off
```

```
cmselect,s,punch
```

```
D,ALL,UX,0
```

```
D,ALL,UY,-10
```

```
alls
```

```
kn3=1500
```

```
tl=.7
```

```
!contact stiffness setting
```

```
r,3,kn3,kt,tl
```

```
r,4,kn3,kt,tl
```

```
r,5,kn3,kt,tl
```

```
r,6,kn3,kt,tl
```

```
r,7,kn3,kt,tl
```

```
r,8,kn3,kt,tl
```

```
r,9,kn3,kt,tl
```

```
time,4
```

```
lswrite,3
```

```
save
```

```
lssolve,1,3,1
```

```
save
```

```
/EOF
```

APPENDIX D

User Interface Software Code

Cup Drawn Expert System User Interface Code written in the User Interface Dialogue Language (UIDL) of ANSYS.

:F ESINPT,GRN	<i>File Name of expert system UIDL protocol</i>
:I 0, 0, 0	<i>Indexing count</i>
:T Cmd	<i>Function block type command</i>
:!	
:N Men_Preproc	<i>Menu Block Pre-processor</i>
:S 0, 0, 0	<i>Menu Block Indexing</i>
:T Menu	<i>Type Menu</i>
:A Preprocessor	<i>Menu Label</i>
:C)/nopr	
:C)*get, _z1,active,,routin	<i>Ansys commands</i>
:C)*if, _z1,ne,17,then	
:C)_z2= '/PREP7'	
:C)*else	
:C)_z2='):'	
:C)*endif	
:C % _z2%	
:C)/go	
:D Preprocessor (PREP7)	
Men_ElemType	<i>Menu Block Calls</i>
Fnc_R	<i>Functionm Block Calls</i>
Men_Material	
Sep_	
-Modeling-	
Men_Create52	
Men_Create53	
Men_Operate52	
Men_Operate53	
Men_Move	
Men_Copy	
Men_Reflect	
Men_Check_geom	
Men_Delete	
-Meshing-	
Men_MeshAttrib	
Men_MeshSize	
Men_Mesh	
Men_Refine	
Fnc_CHECK_plt	
Men_Clear	
Sep_	
Fnc_Mesh_Check	
Men_NumCtrl	
Men_Archive	
Sep_	

Men_CoupCeqn	
Men_ModalCyclic	
Men_FLOTRAN	
K_LN(LSDYNA)	<i>Product Codes</i>
Sep_	
K_LN(LSDYNA)	
Men_DYNAPREP	
Sep_	
K_LN(ALPHA)	
Men_QA_Test	
Men_Loads	
Fnc_Cup_Draw	
:E END	<i>End Delimiter</i>
:!	
:N Fnc_Cup_Draw	<i>Function Block Name</i>
:S 0, 0, 0	
:T Command	
:C) *DEL,_Z1,	<i>Parameter Setting</i>
:C) *DIM,_Z1,,1	
:C) *DEL,_Z2,	
:C) *DIM,_Z2,,1	
:C) *DEL,_Z3,	
:C) *DIM,_Z3,,1	
:C) *DEL,_Z4,	
:C) *DIM,_Z4,,1	
:D CUP DRAWING EXPERT SYSTEM	<i>Function Block Label</i>
:A CUP DRAWING	
:!	
FLD_0	
TYP_LAB	
PRM_WILL THE FINISHED DRAWN	
CUP HAVE A FLANGE	
:!	
CMD_) *SET,_Z1	
FLD_2	
PRM_"YES" OR "NO"	<i>Yes No Scroll Box</i>
TYP_LIS_OPTIONB	
LIS_YES,1	
LIS_NO,2	
DEF_1	
:!	
FLD_0	
TYP_SEP	
:!	
FLD_0	
TYP_LAB	
PRM_IS CUP BOTTOM FILLET	

```
RADIUS DESIGN SPECIFIED
:|
CMD_) *SET, _Z2
FLD_2
PRM_ "YES" OR "NO"
TYP_LIS_OPTIONB
LIS_YES,1
LIS_NO,2
DEF_2
:|
FLD_0
TYP_SEP
:|
FLD_0
TYP_LAB
PRM_IS CUP TOP FILLET RADIUS
DESIGN SPECIFICATION
:|
CMD_) *SET, _Z3
FLD_2
PRM_ "YES" OR "NO"
TYP_LIS_OPTIONB
LIS_YES,1
LIS_NO,2
DEF_2
:|
FLD_0
TYP_SEP
:|
FLD_0
TYP_LAB
PRM_LET SYSTEM SET PRIMARY
GEOMETRY
:|
CMD_) *SET, _Z4
FLD_2
PRM_ "YES" OR "NO"
TYP_LIS_OPTIONB
LIS_YES,1
LIS_NO,2
DEF_2
CAL_Fnc_INP_PRGE3,2,EQ,1,1
CAL_Fnc_INP_PRGE2,2,EQ,1,4
:E END
:|
:|
```

Function Block Subjective Call

```
:N Fnc_INP_PRGE3
```

Function Block Input Primary Geometry

```
:S 0, 0, 0
```

```
:T Command
```

```
:D INPUT PRIMARY GEOMERTY
```

```
:A INPUT PRIMARY GEOMERTY
```

```
:C *DEL,_Z(1)
```

```
:C *DIM,_Z(1),,6
```

```
FLD_0
```

```
TYP_LAB
```

```
PRM_INPUT BLANK DRAWING
```

```
PRIMARY GEOMETRY
```

```
:!
```

```
FLD_0
```

```
TYP_SEP
```

```
:!
```

```
CMD_)*SET,_Z(1)
```

Real Parameter Array Filling

```
FLD_2
```

```
TYP_REAL
```

```
PRM_INPUT BLANK ORIGINAL
```

```
DIAMETER D0
```

```
DEF_BLANK
```

```
:!
```

```
FLD_3
```

```
TYP_REAL
```

```
PRM_INPUT CUP INTERNAL DIAMETER (DI)
```

```
DEF_BLANK
```

```
:!
```

```
FLD_3
```

```
TYP_REAL
```

```
PRM_INPUT CUP HEIGHT (H)
```

```
DEF_BLANK
```

```
:!
```

```
FLD_4
```

```
TYP_REAL
```

```
PRM_INPUT CUP WALL THICKNESS (T)
```

```
DEF_BLANK
```

```
:!
```

```
FLD_0
```

```
TYP_SEP
```

```
:!
```

```
FLD_5
```

```
TYP_REAL
```

```
PRM_CUP BOTTOM FILLET RADIUS (CBR)
```

```
DEF_BLANK
```

```
:!
```

```
FLD_6
```

```
TYP_REAL
```



```

PRM_INPUT CUP TOP FILLET RADIUS(CTR)
DEF_BLANK
:~
FLD_5
TYP_REAL
PRM_INPUT FLANGE WIDTH (FW)
DEF_BLANK
:~
FLD_0
TYP_SEP
:~
FLD_0
TYP_LAB
PRM_ : NOTE DIMENSIONS IN (MM)
:~
FLD_0
TYP_SEP
:~
CAL_Fnc_MAT_PROP
:~E END
:~
:~
:~N Fnc_INP_PRGE2
:~S 0, 0, 0
:~T Command
:~D INPUT PRIMARY GEOMERTY
:~A INPUT PRIMARY GEOMERTY
:~C *DEL,_Z(1)
:~C *DIM,_Z(1),,6
:~
FLD_0
TYP_LAB
PRM_INPUT BLANK DRAWING
PRIMARY GEOMETRY
:~
FLD_0
TYP_SEP
:~
CMD_)*SET,_Z(1)
FLD_2
TYP_REAL
PRM_INPUT BLANK ORIGINAL DIAMETER D0
DEF_BLANK
:~
FLD_3
TYP_REAL
PRM_INPUT CUP INTERNAL DIAMETER (DI)

```

Function Block Call

Function Block Input Primary Geometry

```

DEF_BLANK
:;!
FLD_3
TYP_REAL
PRM_INPUT CUP HEIGTH (H)
DEF_BLANK
:;!
FLD_4
TYP_REAL
PRM_INPUT CUP WALL THICKNESS (T)
DEF_BLANK
:;!
FLD_0
TYP_LAB
PRM_ : NOTE DIMENSIONS IN (MM)
:;!
FLD_0
TYP_SEP
:!!
FLD_0
TYP_SEP
:;!

:;!
CAL_Fnc_MAT_PROP
:E END
:N Fnc_INP_PRGE1
:S 0, 0, 0
:T Command
:D INPUT PRIMARY GEOMERTY
:A INPUT PRIMARY GEOMERTY
:C *DEL, _Z(1)
:C *DIM, _Z(1),6
:;!
FLD_0
TYP_LAB
PRM_INPUT BLANK DRAWING
PRIMARY GEOMETRY
:;!
FLD_0
TYP_SEP
:;!
CMD_)*SET, _Z(1)
FLD_2
TYP_REAL
PRM_INPUT BLANK ORIGINAL DIAMETER D0
DEF_BLANK

```

Function Block Input Primary Geometry

```
:!  
FLD_3  
TYP_REAL  
PRM_INPUT CUP INTERNAL DIAMETER (DI)  
DEF_BLANK  
:!  
FLD_3  
TYP_REAL  
PRM_INPUT CUP HEIGHT (H)  
DEF_BLANK  
:!  
FLD_4  
TYP_REAL  
PRM_INPUT CUP WALL THICKNESS (T)  
DEF_BLANK  
:!  
FLD_0  
TYP_SEP  
:!  
FLD_5  
TYP_REAL  
PRM_CUP BOTTOM FILLET RADIUS (CBR)  
DEF_BLANK  
:!  
FLD_6  
TYP_REAL  
PRM_INPUT CUP TOP FILLET RADIUS(CTR)  
DEF_BLANK  
:!  
FLD_0  
TYP_LAB  
PRM_: NOTE DIMENSIONS IN (MM)  
:!  
FLD_0  
TYP_SEP  
:!  
CAL_Fnc_MAT_PROP  
:E END  
:!  
:!  
:N Fnc_MAT_PROP  
:S 0, 0, 0  
:T Command  
:D INPUT BLANK MATRIAL PROPETIES  
:A INPUT BLANK MATRIAL PROPETIES  
:C) *DEL,_ZB,  
:C) *DIM,_ZB,,1
```

Function Block input blank material properties

```
:!  
FLD_0  
TYP_SEP  
:!  
FLD_0  
TYP_LAB  
PRM_INPUT THE FOLLOWING PROPERTIES  
FOR THE BLANK MATERIAL  
:!  
FLD_0  
TYP_SEP  
:!  
CMD_) *SET,ZB  
FLD_2  
PRM_INPUT MATERIAL NUMBER FOR BLANK  
TYP_INT  
DEF_1  
:!  
FLD_0  
TYP_SEP  
:!  
Cmd_UIMP  
FLD_2  
TYP_DEF_1  
:!  
FLD_3  
TYP_DEF_EX  
:!  
FLD_6  
TYP_REAL  
PRM_YOUNGS MODULUS (EX)  
DEF_BLANK  
:!  
Cmd_UIMP  
FLD_2  
TYP_DEF_1  
:!  
FLD_4  
TYP_DEF_DENS  
:!  
FLD_7  
TYP_REAL  
PRM_BLANK MATERIAL DENSITY (DENS)  
DEF_BLANK  
:!  
Cmd_UIMP  
FLD_2
```

```
TYP_DEF_1

FLD_5
TYP_DEF_NUXY
:!
FLD_8
TYP_REAL
PRM_POISSON (MAJOR) RATIO (NUXY)
DEF_BLANK
:!
Cmd_UIMP
FLD_2
TYP_DEF_1
:!
FLD_3
TYP_DEF_GXY
:!
FLD_6
TYP_REAL
PRM_BLANK MATERIAL SHEAR MODULUS (G)
DEF_BLANK
:!
FLD_0
TYP_SEP
:!
Cmd_) *SET,ZA
FLD_2
PRM_TENSILE YIELD STRENGTH OF
BLANK MATERIAL
TYP_REAL
DEF_BLANK
:!
Cmd_) *SET,ZJ
FLD_2
PRM_IS BLANK MATERIAL ANNEALED
TYP_LIS_OPTIONB
LIS_YES,1
LIS_NO,2
:!
FLD_0
TYP_SEP
:!
FLD_0
TYP_LAB
PRM : NOTE UNITS OF STRESS (MPa)
: DENSITY (KG/M^3)
:!
```

```

FLD_0
TYP_SEP
:!
CAL_Fnc_TBPLAS
:E END
:!
:!
:N Fnc_TBPLAS                                Function Block blank material plasticity characteristics
:S 0, 0, 0
:T Command
:A Define/Activate
:D Define/Activate Data Table
:K #(PREP7*SOLUTION)
:P (LINPLUS*ELECMAG)
:H Hlp_C_TB
Inp_NoApply
Cmd_TB
Fld_0
  Typ_Lab
  Prm_[TB] Define/Active Data Table
Fld_2
  Prm_Lab  Type of data table
  Typ_LIS_OptionB
  P_LN(FULL_ANS)
  LIS_Bilin kinem BKIN,BKIN
  P_LN(FULL_ANS)
  LIS_Multi kinem MKIN,MKIN
  P_LN(FULL_ANS)
  LIS_Multi isotr MISO,MISO
  P_LN(FULL_ANS)
  LIS_Bilin isotr BISO,BISO
  P_LN(FULL_ANS)
  LIS_Anisotrop ANISO,ANISO
  P_LN(FULL_ANS)
Fld_3
  Prm_MAT  Material ref. number
  Typ_INT
  Def_*PAR(ZB)
Fld_0
  Typ_Sep
Fld_0
  P_FL(LINPLUS)
  Typ_Lab
  Prm_The following apply only to some
  data table types
Fld_4
  P_FL(LINPLUS)

```

```

Prm_NTEMP No. of temperatures
Typ_INT
Def_Blank
Fld_5
P_FL(LINPLUS)
Prm_NPTS No. of data points/temp
Typ_INT
Def_Blank
:!  

CAL_Fnc_TB_plasedit  

:E END  

:!  

:!  

:N Fnc_TB_plasedit           Function Block input blank material plasticity characteristics  

:S 0, 0, 0  

:T Command  

:C)! Fnc_TB_edit  

:A Edit Active  

:D Edit Active Data Table  

:K #(PREP7*SOLUTION)  

:P (LINPLUS*ELECMAG)  

:H Hlp_C_TB  

Inp_P  

Cmd_)/NOPR  

Cmd_)TBLE  

Cmd_)STAT,, ,,, ,1  

Cmd_)/GO  

! Cust_Cmd_TBPT  

! Cust_Cmd_TBDATA  

! Cust_Cmd_TBMODIF  

CAL_Fnc_PLOT_QUERRY  

:E END  

:!  

:!  

:N Fnc_PLOT_QUERRY           Function Block plot blank stress strain characteristics  

:S 0, 0, 0  

:T Command  

:C) *DEL,_Zp,  

:C) *DIM,_Zp,,1  

:A Graph  

:D BLANK MATERIAL CHARACTERISTICS  

  STRESS STRAIN CURVE  

:!  

FLD_0  

TYP_LAB  

Prm_PLOT BLANK MATERIAL  

CHARACTERISTICS STRESS STRAIN CURVE

```

```

:!  

Cmd_) *set,_zp  

FLD_2  

Prm_ ENTER "YES" OR "NO"  

TYP_LIS_OPTIONB  

LIS_YES,1  

LIS_NO,2  

:!  

CAL_Fnc_TBPLLOT,2,EQ,1,1  

CAL_Fnc_ES_QUERY,2,EQ,2,1  

:E END  

:!  

:!  

:!  

:N Fnc_TBPLLOT Function Block plot stress strain curve  

:S 0, 0, 0  

:T Command  

:C)! Fnc_TBPLLOT  

:C)/NOPR  

:C)!  

:C)*DEL,_zc  

:C)*DIM,_zc,CHAR,24  

:C)_zc(1)='BKIN','MKIN','MISO','BISO',  

ANISO','DP','ANAND','HYPER'  

:C)_zc(9)='CREEP','SWELL','CONCR',  

'MELAS','EVISC','ANEL','BH','PIEZ'  

:C)_zc(17)='FAIL','WATER','PFLOW',  

USER','ALL','','NONE','MOONEY'  

:C)!  

:C)*get,_z8,common,,tblecm,,int,1 ! active table no.  

:C)*if,_z8,le,0,then  

:C)_z8=23  

:C)*elseif,_z8,gt,24,then  

:C)_z8=22  

:C)*endif  

:C)_z8=_zc(_z8)  

:C)!  

:C)/GO  

:H Hlp_C_TBPLLOT  

:A Graph  

:D Graph Data Tables  

:P (LINPLUS*ELECMAG)  

:K (lsdyna)  

Cmd_TBPLLOT  

Fld_0  

Typ_Lab  

Prm_[TBPLLOT] Graph Data Tables

```


(stress-strain and B-H curves only)

Fld_2

Prm_Lab Type of data table

Typ_LIS_OPTIONB

P_LN(FULL_ANS)

LIS_Bilin kinem BKIN,BKIN

P_LN(FULL_ANS)

LIS_Multi kinem MKIN,MKIN

P_LN(FULL_ANS)

LIS_Multi isotr MISO,MISO

P_LN(FULL_ANS)

LIS_Bilin isotr BISO,BISO

P_LN(FULL_ANS)

LIS_Multi elas MELAS,MELAS

P_LN(ELECMAG)

LIS_MagField data BH,BH

P_LN(FULL_ANS*ELECMAG)

LIS_NU vs. B**2 NB,NB

P_LN(FULL_ANS*ELECMAG)

LIS_MU vs. H MH,MH

P_LN(FULL_ANS*ELECMAG)

LIS_BH slope SBH,SBH

P_LN(FULL_ANS*ELECMAG)

LIS_NB slope SNB,SNB

P_LN(FULL_ANS*ELECMAG)

LIS_MH slope SMH,SMH

Def_*PAR(_z8)

Fld_3

Typ_INT

Prm_MAT Material number

Def_*GET(common,,tblecm,,int,2)

CAL_Fnc_ES_QUERY

:E End

:!

:!

:N Fnc_ES_QUERY

:S 0, 0, 0

:T Command

:C) *DEL,ZC,

:C) *DIM,ZC,,1

:C) *DEL,ZD,

:C) *DIM,ZD,,1

:C) *DEL,ZE,

:C) *DIM,ZE,,1

:C) *DEL,ZF,

:C) *DIM,ZF,,1

:D EXPERT SYSTEM QUERY FORMULATION

Function Block expert system query formulation

```
:A CUP DRAWING
:|
:|
FLD_0
TYP_SEP
:|
FLD_0
TYP_LAB
PRM_SELECT SYSTEM OUTPUT FROM
THE FOLLOWING
:|
FLD_0
TYP_SEP
:|
CMD_) *SET,ZC
FLD_2
PRM_INFORMATION ON PUNCH FORCE
  Typ_LOGI,NO ,YES
DEF_1
:|
FLD_0
TYP_SEP
:|
CMD_) *SET,ZD
  FLD_2
PRM_PRESENT CUP WALL THICKNESS
PLOTS
  Typ_LOGI,NO ,YES
DEF_1
:|
FLD_0
TYP_SEP
:|
FLD_0
TYP_LAB
PRM_PRESENT FORMABILITY (FLD)
CMD_) *SET,_ZE
  FLD_2
PRM_DIAGRAM
  Typ_LOGI,NO ,YES
DEF_1
:|
FLD_0
TYP_SEP
:|
FLD_0
TYP_LAB
```

```
PRM_PRESENT EQUIVALENT PLASTIC
STRAIN
:|
CMD_) *SET,ZF
  FLD_2
PRM_CONTOUR PLOTS
  Typ_LOGI,NO ,YES
DEF_1
:|
CAL_Fnc_CUP_SPEC
:E END
:|
:N Fnc_CUP_SPEC                                Function Block overriding cup specification
:S 0, 0, 0
:T Command
:C) *DEL,ZG,
:C) *DIM,ZG,,1
:C) *DEL,ZH,
:C) *DIM,ZH,,1
:D OVERRIDING CUP SPECIFICATION
:A CUP DRAWING
:|
:|
FLD_0
TYP_SEP
:|
FLD_0
TYP_LAB
PRM_SELECT THE CUP DRAWING PROCESS
SPECIFICATIONS TO BE ACHIEVED
:|
FLD_0
TYP_SEP
:|
CMD_) *SET, ZG
:|
FLD_2
PRM_MINIMISE PUNCH FORCE
  Typ_LOGI,NO ,YES
DEF_1
:|
FLD_0
TYP_SEP
:|
FLD_0
TYP_LAB
PRM_MINIMISE VARIABILITY IN CUP WALL
```

```
:!
CMD_) *SET, _ZH
  FLD_2
PRM_ THICKNES
  Typ_ LOGI,NO ,YES
DEF_1
:!
:E END
```

APPENDIX E

Expert System Rule Base

Abbreviation of variables applied within the Expert System Rule Base.

b, bo - Blank original diameter.

bc - Cup internal diameter.

P - Punch diameter.

t - Cup wall thickness

d - $\frac{bo}{bc}$ Draw ration $\frac{\text{diameter.of .blank}}{\text{diameter.of .final.cup}}$

pcr - Punch corner radius.

dcr - Die corner radius.

drr -Die rounding radius ratio $\frac{\text{diameter.of .die.throat}}{\text{radius.of .die.rounding}}$

drt -Die rounding to thickness ratio $\frac{\text{radius.of .die.rounding}}{\text{cup.wall.thickness}}$

bf - Blank flange area.

tr - Wall thickness ratio $\frac{\text{thickness.of .deformed.zone}}{\text{diameter.deformed.zone}}$

LD - Limiting value of d.

LDR - Limiting value of redraw ratio.

\$\$factor - The degree to which variable \$\$ impinges upon another variable.

MGEOMINT*Manual Geometry Initiative*

! user inputted pcr, dcr

!BLANK DIAMETER (b=Do)

b=z(2)

!BLANK THICKNESS (t=T)

t=z(4)

!CUP DIAMETER (p=Di)

p=z(3)

*ASK,c,CLEARANCE,1.25

!PUNCH CORNOR RADIUS (pcr= cbr)

pcr=z(5)

!DIE CORNOR RADIUS (dcr=ctr)

dcr=z(6)

/EOF

AGEOMINT*Automatic Geometry Initiative*

! optimum pcr,dcr

! user inputted pcr, dcr

!BLANK DIAMETER (b=Do)

b=z(2)

!BLANK THICKNESS (t=T)

t=z(4)

!CUP DIAMETER (p=Di)

p=z(3)

*ASK,c,CLEARANCE,1.25

pcr=4*t

dcr=10*t

!note if the above values are effecting
!error of form or draw failure with thickness
!set a macro to eliminate this can be called to
!re actualise pcr , dcr

/EOF

TESTPRED

Test Predicates

! test predicate macro

!predicates bo, bc, t, dcr, pc, r, c

bo = b

bc = p

! drawing ratio

d=bo/bc

! die rounding radius ratio

drr=(p+2+c)/dcr

! die rounding to thickness ratio

drt=dcr/t

!punch stem to punch profile radius ratio

prr=(p/2)/t

!flange deformation zone

bf=(b/2-(p/2+dcr+c))

!wall thickness ratio

tr=t/bf

! cup wall circumference

l=2*3.142*(bc+t)

/EOF

BLANKHOL

Blank Holder

! blankhol is blank holder necessary

! predicates tr

*if, tr, ge, 1/20, then

! no blank holder necessary


```
    bhreq=0
    *use,fempfif
    *msg,ui
    Blank holder not required for draw

*else
! blank holder necessary
    bhreq=1
    *use,fempfib
    *msg,ui
    Blank holder is required for draw
*endif
```

/EOF

PUNCHF

Punch Force

```
!fpunch punch force estimate
!predicate d,material,l,t
! punch force = k.su.l.t      ! pf = punch force
!find k

*if,d,ge,2,then
    k=1
    *elseif,d,ge,1.75,then
        k=0.95
    *elseif,d,ge,1.5,then
        k=0.9
    *elseif,d,ge,1.4,then
        k=0.75
    *elseif,d,ge,1.3,then
        k=0.6
    *elseif,d,ge,1.2,then
        k=0.5
    *elseif,d,ge,1.1,then
        k=0.4
    *endif
    pf = k*su*l*t
    *if,pf,lt,(maximum available punch force),then
    *msg,ui
        Punch force not sufficient to form specified cup.
*endif
```

/EOF

PBLANKAN*Blank Holder Pressure if Material is annealed*

!pblankhan blankholder pressure if blank material annealed

!pdicates y,su

```
*if,su,gt,0,then
p=(1/150)*(y+su)
*else
```

p=400 psi

/EOF

PBLANKH*Blank Holder Pressure if Material is not annealed*

!pblankh blankholder pressure if blank material is not annealed

!pdicates y,

```
*if,y,gt,0,then
ph=0.01*y
*else
ph=100 psi
*endif
```

/EOF

LD-LDR*Limiting draw - Limiting re-draw*

!ld-ldr working out ld lrd to see if cup can be formed

!predicates mat,prt,drt,tr,pf,ph

! rule ld =ldoptimal.tfactor.dr-factor.pr-factor

! rule lrd =lrdoptimal.tfactor.dr-factor.pr-factor

!area of flange af

! ldoptimal

```
*if,mat,eq,steel,then
ldop=2.25
*elseif,mat,eq,aluminium
ldop=2.2
*endif
```

$$af=(3.142*((bo*pvv*2)-((p+c+dcr)*pvv*2)))/4$$

```
! tfactor
! error trap for applicable optimal drt

    *if,drt,gt,2,then
        *if,drt,lt,10,then
            tfactor=1
        *endif
    *endif

!for when rules are expanded
    *if,tfactor,eq,1:tfactor

    *endif

:tfactor

    *if,tr,lt,0.015,then
        tfactor = 1
        *elseif,tr,le,0.025,then

            tfactor = 1+(tr/0.35)
        *endif

    *if,tr,gt,0.025
        tfactor=1.1
    *endif

! prfactor

    *if,prt,gt,1,then
        *if,prt,lt,5,then
            prfac = 1-(0.02*prt)
        *endif

    *if,prt,ge,5,then
        prfac=1
        *else
            *msg,note
            prt must be greater than 1
```

```
*endif

! drfactor

  *if,drt,gt,2,then
    *if,drt,lt,10,then
      drfac = 1-(0.01*drt)
    *endif
  *endif

  *if,drt,gt,10,then
    drfac=1
  *else
    *msg,ui
    drt should be greater than 10
  *endif

!Draw failuve or not
  *if,d,le,ld,then
    drawfail=-1 ! un-successful draw
  *msg,ui
  un-successful draw
*endif

/EOF
```

WRINKLIN*Wrinkling Prediction*

!wrinkling to check if wrinkling will occur with current geometry .

!predicates t,tr

```
*IF,T,LE,0.5,THEN
  *if,tr,lt,0.005,then
    *msg,ui
    wrinkling not a problem
  *else
    *msg,ui
    wrinkling is a problem
    ERFORM=-1
  *endif

*elseif,t,le,1,then
  *if,tr,le,0.015,then
    *if,tr,ge,0.005,then
```

```
        *msg,ui
        wrinkling not a problem
        *endif
*endif
        *else
ERFORM=-1
        *msg,ui
        wrinkling is a problem if thickness cannot be altered then the area &
        under the flange has to be increased by increasing (bo) with reference &
        to other rules&
        if cup is to be straight ie no flange then thickness has to be increased
*endif
```

/EOF

WRINKREC

Wrinkling Rectification

!To alter geometry so that wrinkling won't occur

!predicates t,d,

```
*ask,t-alter,can thickness be altered %/
Enter "YES" OR "NO"
```

```
*if,t-alter,eq,yes
    t=t*1.1
*endif
```

```
*if,t-alter,eq,no
    bo=bo*1.1
*endif
```

/EOF

PROCESREC

Process Redrawing Parameters

!redraw configuration

!table of reduction ratio

```
*msg,ui
To enable successful drawing of the proposed cup %/
a redraw process has to be involved
```

```
*ask,redraw,enter 1 for a conventional redraw %/ enter 2 for reverse redraw,1
!conventional redrawing data base
```

```
*if,redraw,eq,1,then  
    *if,t,lt,6,then  
        rr=0.4  
    *else  
        error=1  
    *msg,ui  
    epert system failure  
*endif
```

```
*endif
```

```
*if,redraw,eq,2,then  
    *if,t,lt,1.5,then  
        rr=0.4  
    *endif  
    *if,t,gt,1.5,then  
        *if,t,lt,3,then  
            rr=0.35  
        *endif  
    *else  
        error=1  
    *msg,ui  
    epert system failure  
*endif
```

```
*endif
```

!di is the diameter of the intermediate cup

```
di=dcup/(rr-1)
```

```
*msg,ui,di
```

The Expert System recommends a redrawing process with an &
intermediate Cup diameter of %G,

```
/EOF
```

APPENDIX F

*Main File Control File
A.P.D.L Coding*

Main File Control File A.P.D.L Coding

```
! #include type statements
```

```
*abbr,ES,*ulib,exsys,txt,/user/custom/ansys53/c:
```

```
ES !CALL TO OPEN EXPERT SYSTEM MACROS
```

```
*use,TESTPRED
```

```
!drt,prt,d, applicable error trap
```

```
    *if,drt,lt,2,then
```

```
    *if,drt,gt,10,then
```

```
        *msg,ui
```

```
        the drt ratio is out side the remit of the expert system &  
        drt should be with in the range ( 2 <= drt <= 10 )
```

```
    error=-1
```

```
    *endif
```

```
    *endif
```

```
    *if,prt,le,1,then
```

```
        *msg,ui
```

```
        prt should be greater than 1
```

```
        error=-1
```

```
    *ENDIF
```

```
    *if,d,lt,1.1,then
```

```
        *msg,ui
```

```
        The current draw ratio is unfeasible please &  
        reduce diameter of blank
```

```
    ERROR=-1
```

```
    *endif
```

```
*use,BLANKHOL
```

```
*use,PUNCHF
```

```
    *if,matann,eq,1,then
```

```
        *use,PBLANKAN
```

```
    *elseif,matann,ne,1,then
```

```
        !*use,PBLANK
```

```
    *endif
```



```
*use,LD-LDR
!call redraw or single draw /redraw
*if,drawfail,eq,-1,then
    *use,PROCEREC
*endif

*use,WRINKLING
!call rectification macros /wrinkrec
*if,erform,eq,-1,then
    *use,WRINKREC
*endif

    *if,bhreq,eq,1,then

        /input,dev01,log,c:\exsys\simulation,0,0

    *elseif,bhreq,eq,0,then

        /input,dev01,log,c:\exsys\simulation,0,0

    *endif
/EOF
```

APPENDIX G

*Post Processing A.P.D.L
Command Log Scripts*

Post Processing A.P.D.L Command Log Scripts***Cup Wall Thickness Results Collection***

```

! result post processing thickness plots
!local,11,1,,90,,90
/post1
esel,s,mat,,1
nsle
nsel,s,loc,x,0
*get,maxn,node,0,num,max
*get,minn,node,0,num,min
*get,mumn,node,0,count
count-1 = j
do I = 1, j
    do k = 0, j
nodei = minn + ((max-min/5)*k)
lpath,node1,node2,node3,node4,node5,node6,node7,node8,node9,node10
etab,th,nmisc,4
pdef,thp,etab,th
plpath,thp
/EOF

```

Forming Limit Diagram Results Collection

```

! result post processing forming limit diagram plots

```

```

local,11,1,,90,,90
!what should the results co ordinate system be
esel,s,mat,,1
nsle
*dim,a(i),array,###,1,1
*dim,b(i),array,###,1,1
*dim,c(i),array,###,1,1
*get,maxn,node,0,num,max
*get,minn,node,0,num,min
*get,mumn,node,0,num,count
*vget,a(i),node,i,etab,th
thickness = ###
*do,i,minn,maxn,1
    *if,a(i),lt,thickness,then
        i=aa(i)
    *endif
*enddo
*vget,b(i),node,aa(i),epto,1
*vget,c(i),node,aa(i),epto,1
*cfopen,flldata.dat,c:\
*vwrite,b(i),c(i)
(e10.3, e10.3)
/EOF

```

APPENDIX H

*A user friendly Expert System for Deep
Drawing of Cylindrical Cans*

A USER FRIENDLY EXPERT SYSTEM FOR DEEP DRAWING OF CYLINDRICAL CANS

J. Conerney¹ and G. O Donnell²

1 - Post Graduate Student, Galway GMIT

2- Lecturer, Galway GMIT

ABSTRACT

A USER FRIENDLY EXPERT SYSTEM FOR DEEP DRAWING OF CYLINDRICAL CANS IS PRESENTED IN THIS PAPER. THE EXPERT SYSTEM USES HEURISTIC KNOWLEDGE TO AUTOMATICALLY INVOKE APPROPRIATE FINITE ELEMENT ANALYSIS CODES, INCORPORATING A RULE BASE FOR AXIS SYMMETRIC DEEP DRAWING. THE EXPERT SYSTEM IS DRIVEN BY THE ANALYSIS RESULTS FROM THE EXPLICIT FINITE ELEMENT PACKAGE LS DYNA 3D VER 936.03 AND THE IMPLICIT FINITE ELEMENT PACKAGE IS ANSYS VER 5.3. THE SYSTEM IS MODELLED WITH A VIEW TO PROCESS OPTIMISATION ENABLING CURRENT OR NEW TOOLING TO ACHIVE A SUCCESSFUL DRAW WHILE ENSURING THE DESIRED CUP WALL THICKNESS DISTRIBUTION IS ACHIVED. THE RULE BASE WITHIN THE KNOWLEDGE DATA BASE IS COMPOSED OF RULES THAT ARE PRIMARILY BASED ON EMPIRICAL INVESTIGATION, BACKED UP WITH ANALYTICAL STUDIES.

1.1 INTRODUCTION

The Deep Drawing operation is a key process in can manufacturing. The particularity of canned durables is that their design is continuously changing in order to satisfy customer or marketing requirements. Cylindrical deep drawing is also used for the manufacture of specialised housings. This introduction details the analytical and imperical studies of deep drawing that have contributed to the knowledge system data base which has been developed as part of the expert system.

The first successful analytical solution to the radial drawing process was, made by Chung and Swift [1]. One of their primary assumptions was, that the numerical value of the equivalent strain is equal to that of the circumferential strain. This assumption was shown to be true for the plane drawing in the flange region by Hill [2], and later by Woo [3], who developed a method for analysing the axisymmetric forming process based on the general theories of rigid-plastic material modelling and equilibrium equations. This method was applied to the deep drawing processes by Woo [3,4]. Yamada [5] employed both total and incremental strain theories of plasticity in the analysis and predicted the punch force for the radial drawing of an isotropic material.

Information on deep drawing has been documented since the 1920's early workers Sachs, Crane, Swift, Eksbergian [6,7,8,9] measured changes in thickness undergone by a uniformly thin blank when drawn into a cup and tried to predict the drawing force. The need for an Expert System evolves from the tedious nature of simulating the various design options at the conceptual design stage, where the number of parameters affecting the final product are innumerable and systematic enumeration of all the possibilities by a human user is impossible. Currently lead exponents of metal forming with many years of experience, backed up with reference analysis solve the forming problems using a combination of thumb rules and procedures. The Expert System is to take the place of the Human Expert and build on the current incomplete data on axisymmetric deep drawing via problem specific FEM simulation.

2.1 EXPERT SYSTEM

The Expert System developed in this project looks at two design needs, namely machine feasibility and geometry feasibility, which determine if the proposed press has sufficient power to form the Cup from the selected material and blank dimensions. To this end a search of the knowledge base (machine-feasibility) data base is conducted. The finding from this empirically

recorded data base is cross checked for completeness by a Finite Element Method Analysis referred to as FEM module Punch Force

Once the Machine feasibility is satisfied, geometry feasibility is analysed. The geometry is outlined as in Figure 1.

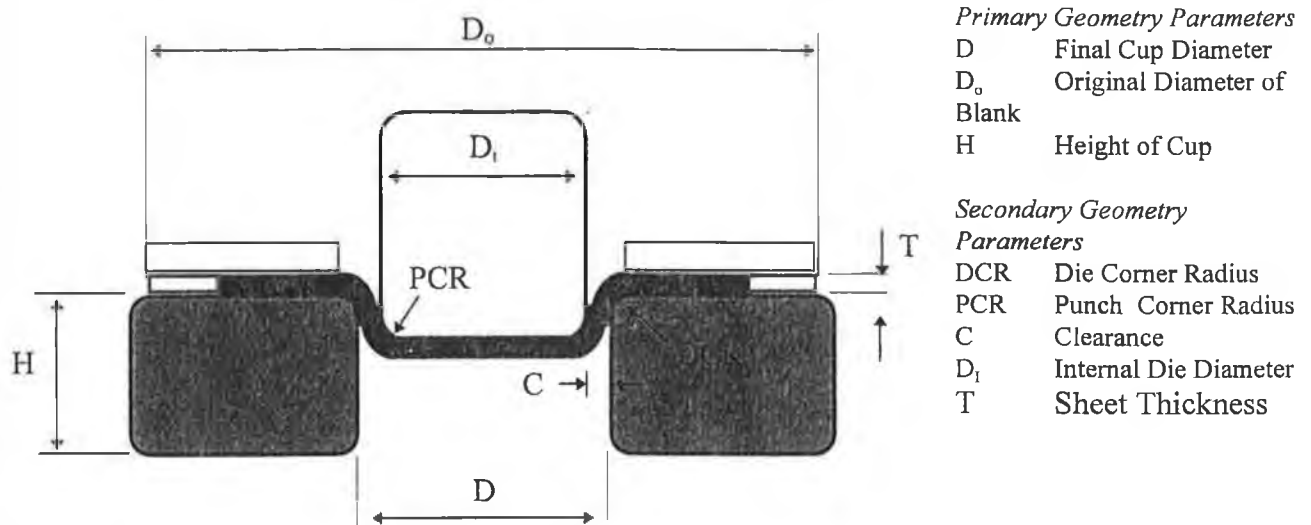


Figure 1 Geometry of Drawn Cup

The primary parameters are feed into the database and resulting optimum secondary geometry parameters are outputted with respect to the inputted blank dimensions and sheet material. The result will be a logic feasible or unfeasible draw. The user will be alerted to an unfeasible draw and a corrective change to secondary geometry parameters will be suggested as indicated in Table2.

These secondary geometry parameters may be design specified in which case they are fixed, or they may not be design specified in which case it is the manipulation of these parameters which has a distinct effect on the formability of the specified primary geometry parameters. For example an increase in Die Corner Radius (DCR) reduces the force necessary to form the part and consequently the tensile stress in the wall is reduced with a corresponding reduction in the likely hood of draw failure via wall tearing.

Increase DCR	Will lower required Punch force
Increase Blank Thickness	Reduces the likely hood of Wrinkling
Change Material	Improved Thickness Distribution

Table 2 : Process Change

Draw feasibility is assessed by computation-rules that predict “failure” or “error of form” . A “failure” classification for example is a tear in the cup wall i.e. the draw operation cannot be completed. An “error of form” classification includes wrinkling, wall thickness distribution, and earring of the flange, which effects the cup functionality.

The Finite Element analysis for draw feasibility with respect to “failure” utilises the FEM module Incipient flow to predict if metal flow can be initiated with the specified machine settings .For example excessive blank holder force may cause tearing at the outset of drawing.

The main FEM analysis tool for this section is FEM module Formability whereby “failure” and possible “error of form” are monitored through out the complete process. The knowledge system data base is incomplete due to its inability to map material non-linearities such as strain hardening and anisotropy. The FEM code acts to fill the gaps in knowledge inherent in the data base.

2.2 Expert System Proprietary System

The Expert System is controlled via Advanced Parametric Design Language (APDL) of ANSYS ver 5.3, the general purpose implicit Finite Element Analysis package. These (APDL) macros, interrogate macro files that contain the knowledge database. The interface is developed via menus and dialogue boxes programmed in the ANSYS User Interface Design Language (UIDL), these interfaces call specified macros depending on the test algorithm.

The test algorithm formulates the relevant computation-rules and tabulated data that will be extracted from the data base to validate the drawing process. The best design parameters extracted from the data base are feed to the FEA module analysis where the finite element model is automatically built with the use of command input macros. The analysis of these simulations is automated via the use of post processing macros. The conclusions of the analysis is communicated to the user in graphical and tabular form. Suggestions on corrective action in the event of a “draw failure” or unacceptable “errors of form” are presented to the user.

2.3 Expert System Rule Base

The following computational rules are examples of optimisation guides for deep drawing and give an indication as to the content of the draw feasibility rule base.

Computation rule 1

The Punch Corner Radius can be optimised by rules developed by Lyman [10] which decrease the likelihood of “draw failure”. The following decision tree is fired by the software.

If the material is stainless steel

then the (PCR) should be greater than or equal to four times the blank thickness.

If the material is mild steel

then the (PCR) should be greater than or equal to six times the blank thickness.

else

the (PCR) should be less than or equal to ten times the blank thickness.

Computation rule 2

To prevent wrinkling the thickness ratio is accessed and the possibility of “error of form” is decreased, due to the following rules developed by Early, Reed [11.]

The thickness ratio is equal to the sheet thickness divided by the diameter of the deformation zone.

For very thin sheets the thickness ratio should be greater than 0.005.

For thin sheets the thickness ratio should be greater than 0.015.

3.1 FINITE ELEMENT MODULES

The Finite Element Module automates the following steps: Creation of a geometric model consisting of the perform shape and Tooling; Imposition of the appropriate boundary conditions; processing of the raw output information into a meaningful form.

3.2 F.E.M module Punch Force Incipient Flow.

This FE numerical model takes advantage of the axis symmetry of the Cup, and models the cup wall by 4 noded bilinear axis symmetric quadrilateral elements. The Tool is described by rigid ground 2D contact elements as show in Figure 2. The imposed punch motion and blank holder pressure is applied in separate load steps. Mesh refinement is developed in the deformation annulus which is acted on by the punch and die profile radius. Element size is set by the upper limit of 30° bend allowance for an accurate solution. The plasticity model incorporates strain hardening and anisotropy (caused by the rolling process in the manufacture of the sheet) by allowing different stress- strain behaviour in the element co-ordinates system. The theory is based on von-Mises yield criterion and Hills plasticity formulation. Convergent enhancement tools for contact and plasticity such as time step bisection, solution time step prediction and adaptive decent is employed.

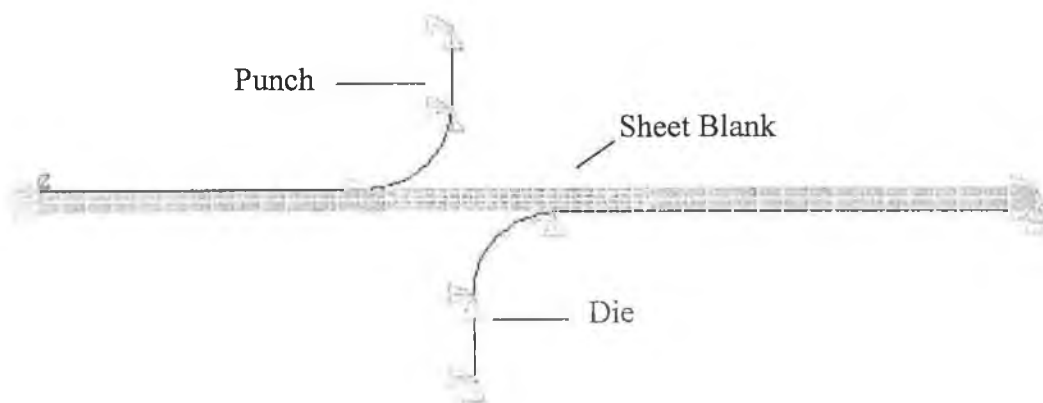


Figure 2 Model : F.E.M module Punch Force Incipient Flow

3.3 FEM module Formability

The explicit quadrilateral shell element (Belytschko/Tsay) is employed with five through thickness integration points. Element size is set at approximately half the draw radius, indicated as the optimum by Mattiasson[12]. The tooling is represented as a discretised area with the Elements constrained as rigid bodies as shown in Figure 3. Computational expense is reduced due to the fact that the rigid body mesh is treated within the DYNA contact algorithm as a VDA surface (the mesh is transformed to surface patches). The plasticity law is the anisotropy plasticity model developed by Barlat and Lian.

Post processing of analysis results utilises Forming Limit Diagrams (which are a recognised indication of formability) by superimposing element principle strains on the forming limit curve, see Figure 4. The radial thickness distribution is plotted, to ensure conformance with cup specification.

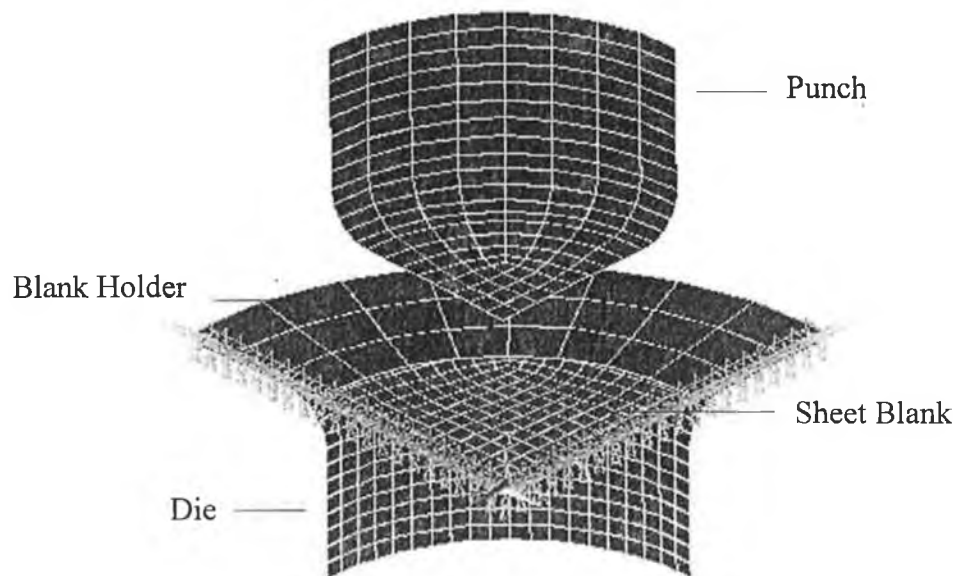


Figure 3 Model :FEM module Formability

If the outputted principal strains from FEM module Formability plotted on the material Forming Limit Diagram indicates a draw failure, then the draw has to be conducted in stages the analysis of this is handled by the FEM module Redraw.

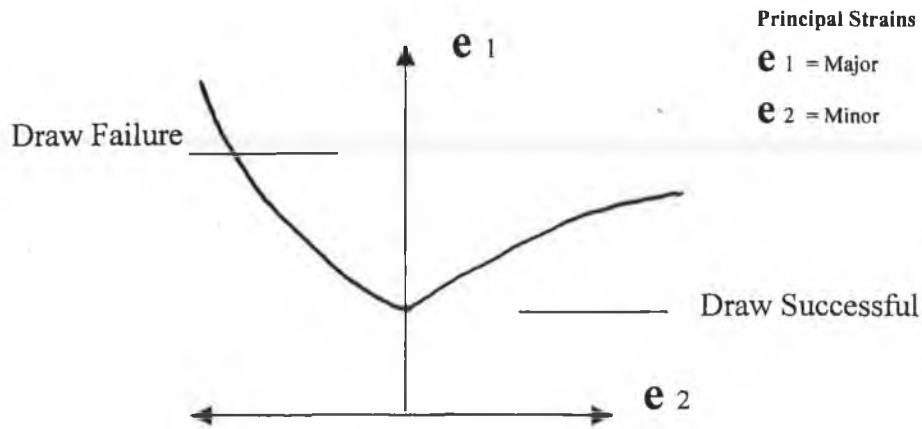


Figure 4 : Forming Limit Diagram

3.4 FEM module Redraw

The expert system data base is checked for information on redraw ratios and the FEA model for the tooling involved in the redrawing is developed as in Figure 5. FEM module Redraw takes the form of a reduced first reduction ratio (D_o / D_i) the FEM analysis of the preliminary draw is solved. The redraw re-actualises the strain history of the preliminary draw in the solution of the redraw. Post processing is similar to that mentioned in section 3.3 Redraw operations are conducted by deleting the contact between the first draw tooling and sheet within the model data base, and developing contact between the deformed sheet and the secondary tooling see Figure 5.

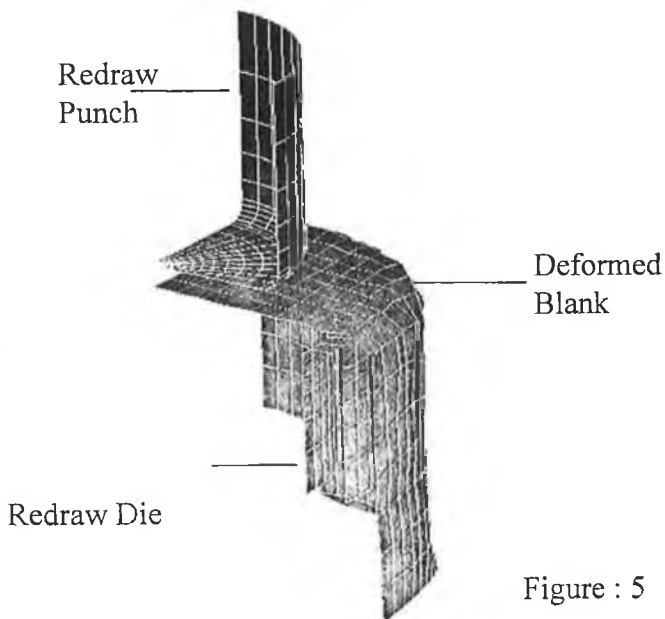


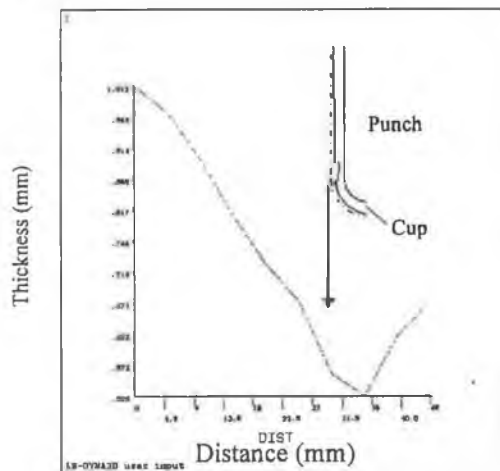
Figure : 5 FEM module Redraw (*Indirect Redrawing*)

4.1 POST PROCESSING

To demonstrate the post processing features of the Expert System a cup with the parameters outlined in Table 3 is analysed in FEM module Formability. The “error of form” cup wall thickness distribution for the draw is shown in Figure 6. The blank holder force is 55 (kN), the cup material is steel.

D	D _f	H	PCR	DCR	C	T
(mm)	(mm)	(mm)	(mm)	(mm)	(mm)	(mm)
200	100	60	5	5	1.25	0.9

Table 3.



Barlat Lain Plasticity

Barlat exponent = 6

Lankford Parameter = 1.8

Strength Co-eff = 533 (MPa)

Hardening Co-eff = 0.22

Figure 6 : Cup wall thickness distribution

The plot of wall thickness distribution shows that the area of the blank which under went the least plastic deformation and consequently less work hardening (i.e. the wall area above the Punch die corner radius) has experienced the most thinning. The user has to decide if this is an acceptable “error of form”.

5.1 CONCLUSION

The Expert System develops a process plan consisting of redrawn cups so that specified primary geometry are attained, while optimising available resources and delivering acceptable errors of form. Knowledge based systems with their heuristic reasoning capability, flexibility to handle uncertain data, user friendly interfaces and explanation capability have also been developed, for the many variables present in axisymmetrical deep drawing.

REFERENCE

- 1, Chung, S.Y. and Swift, H.W., "Cup Drawing From A Flat Blank, Part I. Experimental Investigation", Proc. Instn. Mech Engrs., U.K., PP.199 - 211, 1951
- 2, Hill, R., Mathematical Theory of Plasticity, Clarendon Press, Oxford, 1950
- 3, Woo, D.M., "On The Complete solution of the Deep-drawing Problem," Int.J.Mech. Sci., Vol. 10, 1968, pp83-94.
- 4, Woo, D.M., "Analysis of Cup drawing Process," J.Mech. Engng Sci., Vol. 6, 1964, pp.116-131
- 5, Yamada, Y., "Studies on Formability of Sheet Metals," Report of the Inst. Ind, Sci., Univ. of Tokyo, Vol. 11, No.5, 1961
- 6, Sachs, G., "New Research on the drawing of Cylindrical Shells", Proc. Inst Automobile Eng., Vol 29, p.588, 1934-5
- 7, Crane, E.V., Plastic Working of Metals, John Wiley AND SONS, New York 1931
- 8, Swift, H.w., "Two Stage drawing of cylindrical cups ", Transactions of the Institute of Engineering and Shipbuilding in Scotland, vol 86, p 195, 1942-3
- 9, Eksergian, G.L., "The Plastic Behavior of Metals in Drawing", ASME Transactions, vol, 48, p 609, 1926
- 10, Lyman, T Forming Metals Hand book, vol 4, 8th edition American Society for Metals, 1969.
- 11, Early, D.F. and Reed, E.A. Techniques of Pressworking Sheet Metal, Prentice Hall, Englewood cliffs NJ, 1958
- 12, Mattiasson, K Bernspag, L Samuelsson, A Hamman, T Schedin, E Melander. A "Evaluation of a dynamic approach using explicit integration in 3-D sheet forming simulation" Numerical Methods in Industrial Forming Processes Numiform 92 (Pub Balkema) P 55, 67

APPENDIX I

*A sample description of the Finite
Element Analysis result plates.*

A sample description of the Finite Element Analysis result plates

Figure I : Cup drawn product / Description of cup bottom tear.

Quarter symmetry for drawn cup, the excessive thinning at the base of the cup is indicated by the elongation of the elements at this area. The thickness of these elements is zero indicating a tear in the Cup wall.

The next three contour plots present the thickness distribution for changes in Tool geometry

Figure II : Thickness contours with pcr = 3 mm ; dcr = 10 mm ; bhp = 400 psi.

This is the thickness contour plot for a minimum punch corner radius and a maximum die corner radius with maximum blank holder force, it presents a uniform thickness distribution with highly localised thinning at the cup bottom.

Figure III : Thickness contours with pcr = 8 mm ; dcr = 5 mm ; bhp = 400 psi.

This is the thickness contour plot for a maximum punch corner radius and a minimum die corner radius with maximum blank holder force, it presents a non uniform thickness distribution with a large area of thinning at the cup bottom.

Figure IV : Thickness contours with pcr = 8 mm ; dcr = 10 mm ; bhp = 150 psi.

This is the thickness contour plot for a maximum punch corner radius and a maximum die corner radius with minimum blank holder force, it presents a semi uniform thickness distribution with a more even distribution of cup wall thickness bands.

Figure V : Tapered cup / Equivalent plastic strain contours.

The plastic equivalent strain contour plot is an indication of the amount of deformation that the blank regions have undergone. It is evident that the blank area under the punch and the undeformed annulus, which is visible just above the cup base has undergone the least amount of deformation. The resulting lack of strain hardening at these regions lead to excessive thinning and tearing, the thinning at the base is halted to some degree by the friction of the punch base to blank interface.

Figure VI : Tapered cup / Thickness contours.

The thickness contours for the tapered cup show highly localised thinning at the cup base, with thickening at the outer Cup flange.

Figure VII : Box drawn product Metal radial inflow

The varying degrees of metal inflow that the blank experiences, indicates that Anisotropic effects present early, in the box drawn process.

Figure VIII : Box drawn product / Von Mises Equivalent stress contours.

The maximum Von Mises Equivalent stress is located at the die rim, the high level of compressive stress in this area causes the blank to wrinkle, the formation of which is visible at the die rim.

The Ohio State University (O.S.U) formability test develops a state of plain strain in the test blank, as most failures encountered in sheet drawing are of plain strain induced tearing. This test is assessed in the following contour plates. in an effort to correlate the principle strains to the changes in blank thickness.

Figure IX : O.S.U formability test / 1st principle strain.

The first principle strain is on the whole uniform with high points at the test blank edge.

Figure X : O.S.U formability test / 2nd principle strain.

The second principle strain is highest at the test blank edge, it gradually increases in a symmetrical manner about the centre of the blank.

Figure XI : O.S.U formability test / Thickness contours.

The thickness of the blank increases about the centre of the blank with the minimum at the blank centre. It is clear that the reduction in thickness is dominated by the 2nd principle strain this correlates well with the existing state of plain strain.

Figure XII : Binder wrap / Stress in the radial direction, via axisymmetric analysis.

The stress plot in the radial direction indicates high stress locations at the blank top and bottom surfaces, due to bending induced by the application of the blank holder.

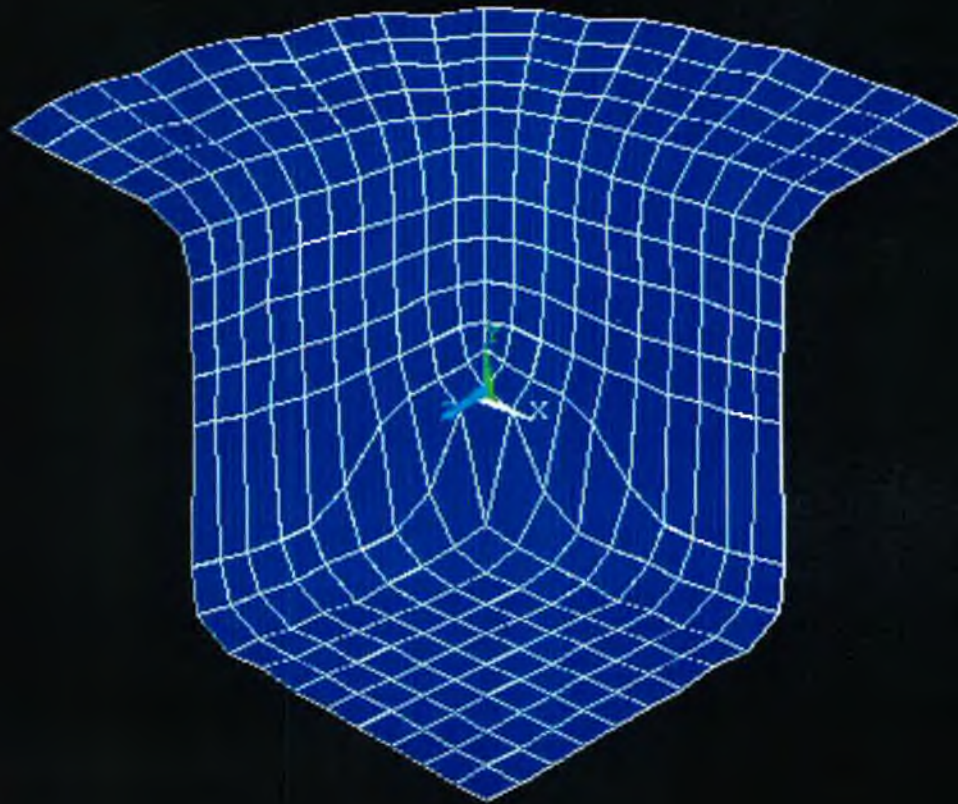
Figure XIII : Binder wrap / Strain in the radial direction, via axisymmetric analysis.

The strain contours indicate that the blank under the binder wrap phase, experiences localised strain at the die corner, due to the compressive force of the blank holder.

Figure XIII : Axisymmetric Dynamic Analysis.

The dynamic analysis utilises spring elements which are visible in this plot, to numerically stabilise the F.E.A equation formulation, by ensuring that the Punch remains in contact with the Blank, through out the solution convergence .

1

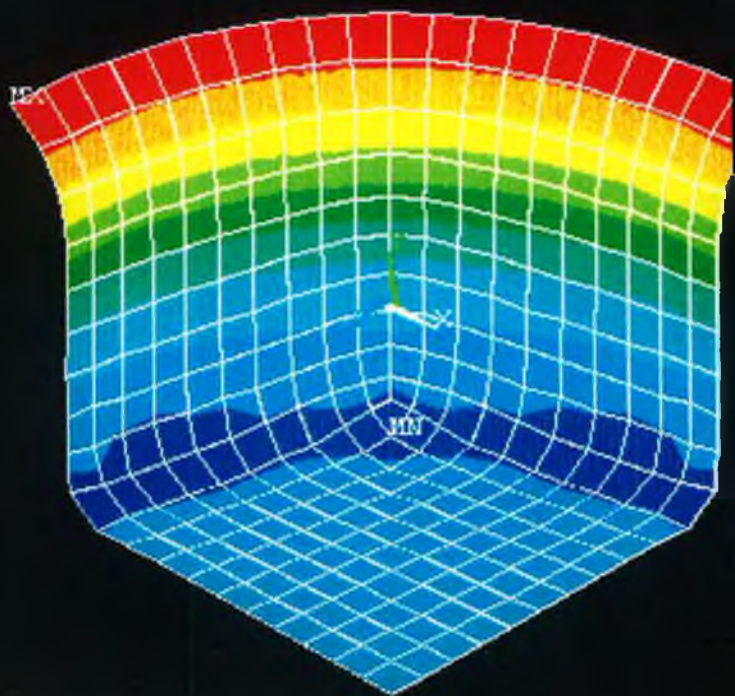


```
ANSYS 5.3  
MAR 3 1997  
15:54:29  
DISPLACEMENT  
STEP=1  
SUB =52  
TIME=4.001  
RSYS=0  
DIC: =61.081
```

```
*DSCA=1  
XW =1  
YV =1  
ZV =1  
DIST=77.782  
XF =-50  
YF =-29.996  
ZF =-50  
2-BUFFER
```

Figure 1: Cup drawn product / Depiction of cup bottom tear.

1



LS-DYNA3D user input

```
ANSYS 5.3  
MAP 5 1997  
14:57:00  
AVG ELEMENT SOLUTION  
STEP=1  
SUB =7  
TIME=10  
TH (AVG)  
TOP  
DICK =.85317  
SMW =.817968  
SICK =1.103
```

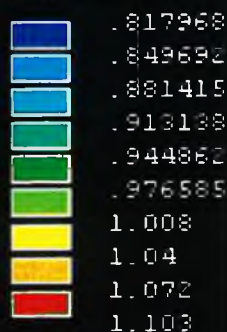
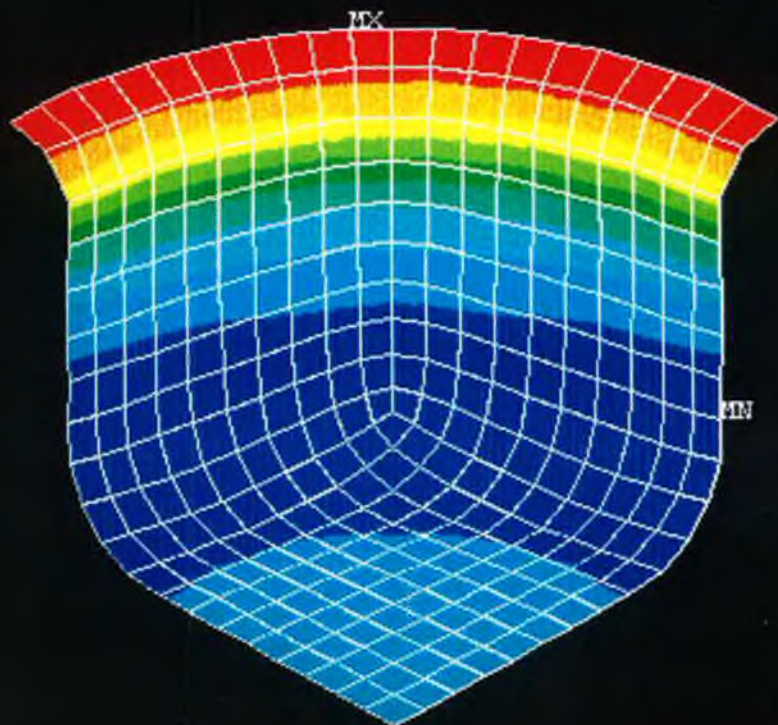


Figure II : Thickness Contours
with $p_{cr} = 3 \text{ mm}$, $d_{cr} = 10 \text{ mm}$,
 $bhp = 400 \text{ psi}$

1

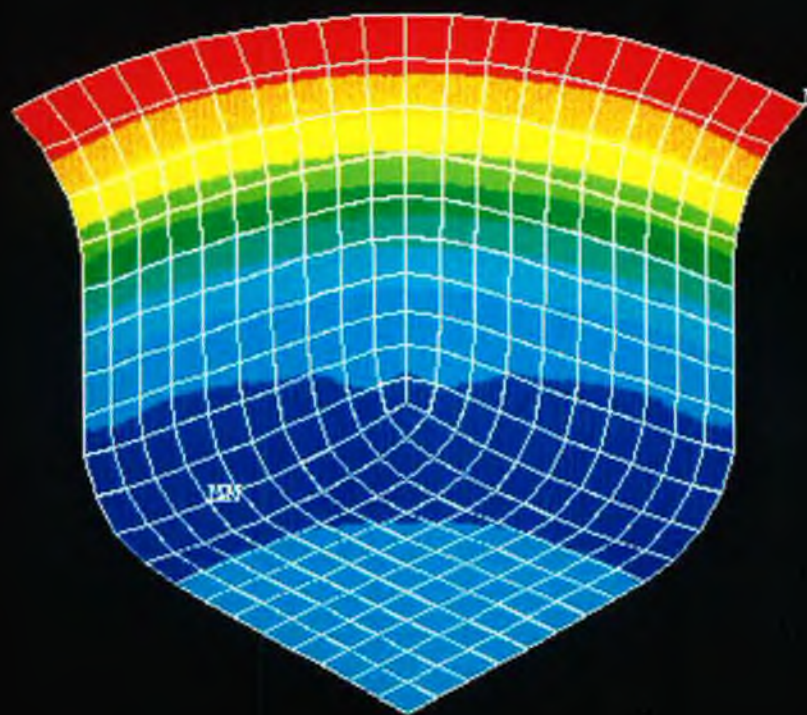


LS-DYNA3D user input

```
ANSYS 5.3
MAP 5 1997
15:03:12
AVG ELEMENT SOLUTION
STEP=1
SUB =7
TIME=10
TH (AVG)
TOP
DIE: =35.064
SMN =.844357
SMX =1.1
.844357
.872741
.901125
.92951
.957894
.986278
1.015
1.043
1.071
1.1
```

Figure III : Thickness contours
with $p_{cr} = 3 \text{ mm}$, $d_{cr} = 5 \text{ mm}$,
 $b_{hp} = 400 \text{ psi}$

1



LS-DYNA3D user input


```

ANSYS 5.3
MAP 5 1997
15:08:32
AVG ELEMENT SOLUTION
STEP=1
SUE =7
TIME=10
TH (AVG)
TOP
DIMX =35.064
SMN =.853143
SIX =1.081

```


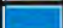
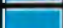







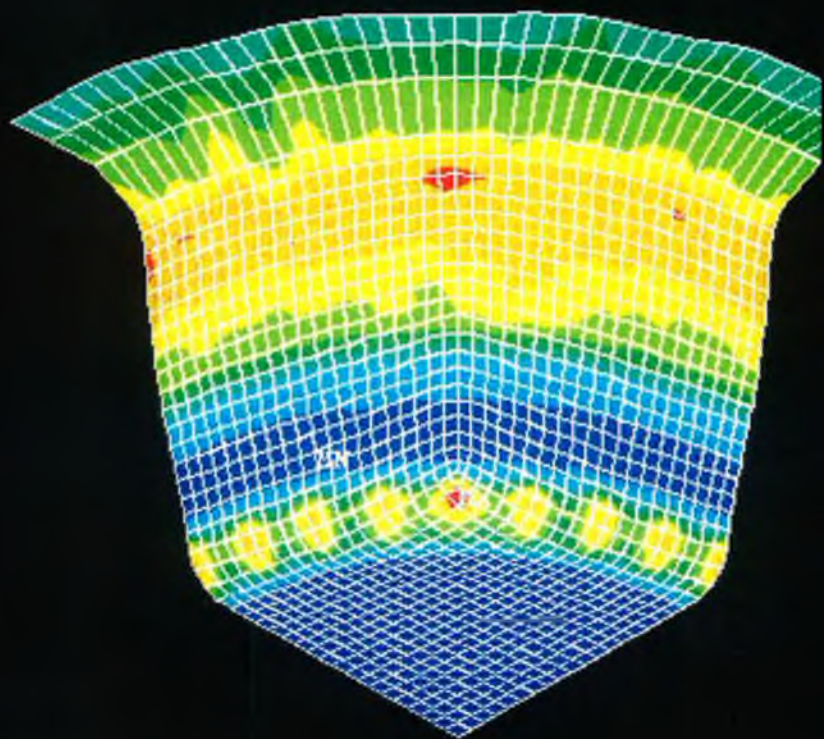
	.853143
	.878467
	.903783
	.929103
	.954422
	.979742
	1.005
	1.03
	1.056
	1.081

Figure IV: Thickness contours
with $pcr = 8 \text{ mm}$, $clr = 10 \text{ mm}$,
 $bhp = 150 \text{ psi}$

1



LS-DYNA3D user input

ANSYS 5.3
MAR 24 1997
22:44:29
AVG ELEMENT SOLUTION
STEP=1
SUB =52
TIME=10
EPS (AVG)
TOP
DMEK =30.069
SMN =.117219
SMEK =.518176

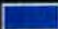
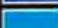




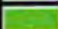



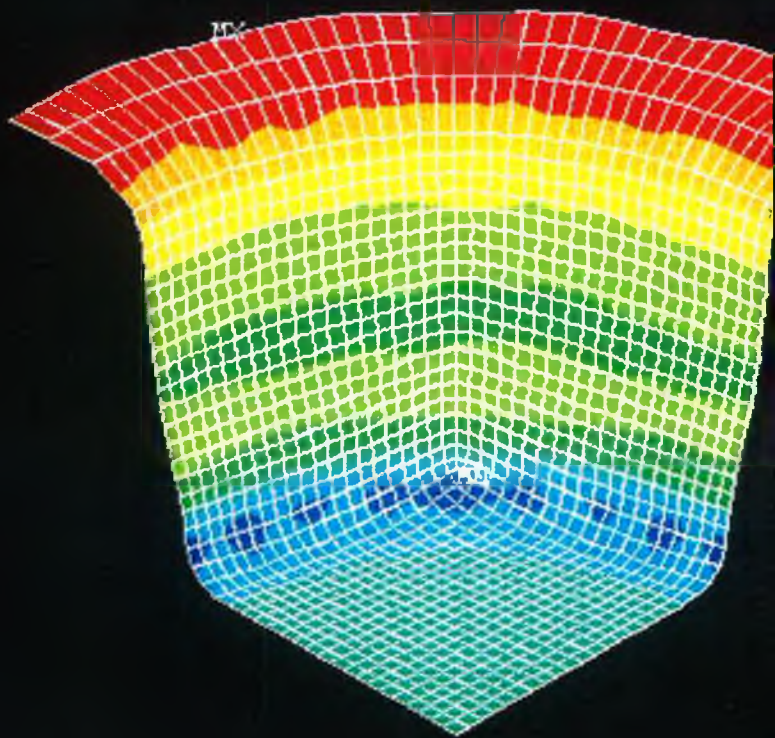
	.117219
	.16177
	.20632
	.250871
	.295422
	.339973
	.384523
	.429074
	.473625
	.518176

Figure V : Tapered cup / Equivalent plastic strain contours.

1



LS-DYNA3D user input

ANSYS 5.3
MAR 24 1997
22:45:49
AVG ELEMENT SOLUTION
STEP=1
SUB =52
TIME=10
TH (AVG)
TOP
DIK =30.089
SMN =.668531
SIX =1.023

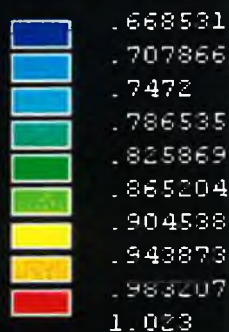
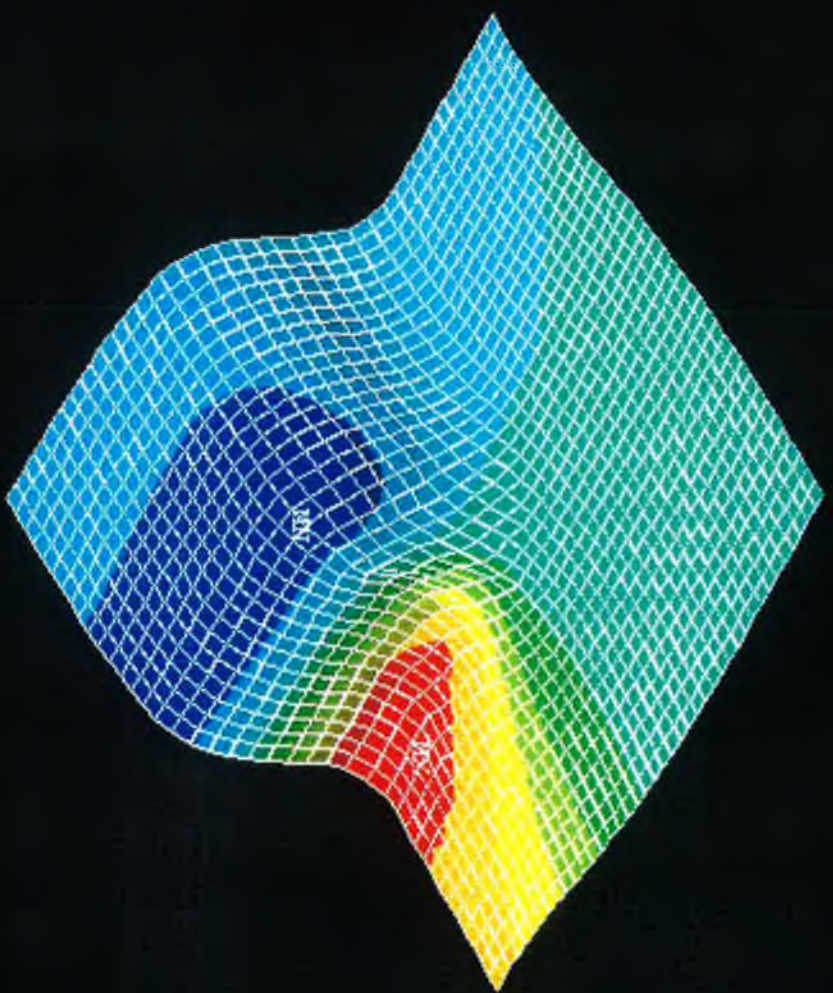


Figure VI : Tapered cup /
Thickness contours



AMSTS = 5.3
 MAPL 4 1997
 15:46:47
 MODAL SOLUTION
 STEP=1
 SUB = 4
 TIME = .002897
 UZ
 TOP
 PSYS=0
 DMC = 25.99
 SMDI = -2.973
 SMC = 10.042
 -2.973
 -1.527
 -.081138
 1.365
 2.811
 4.257
 5.704
 7.15
 8.595
 10.042

Figure VII : Box drawn product
Metal radial inflow

ANSYS 5.3
MAR 25 1997
14:15:38
ELEMENT SOLUTION

STEP=1
SUB =52
TIME=.002
SEQV (MEQVG)

TOP
DMX =20.429
SMN =.322599
SMX =57.387

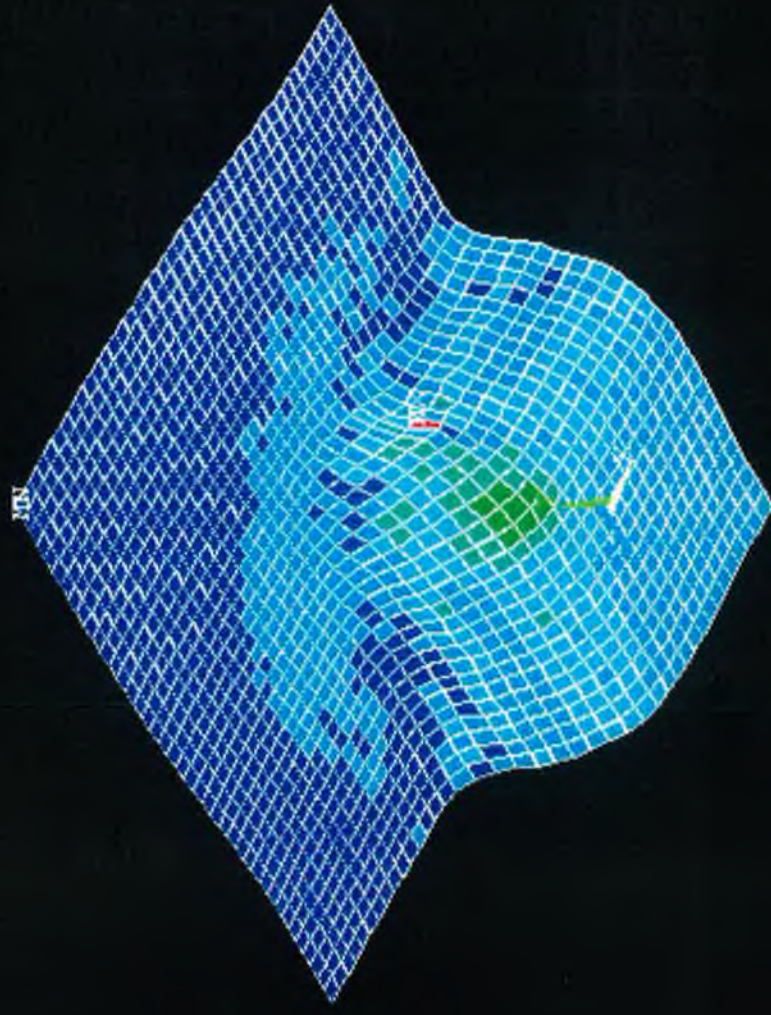
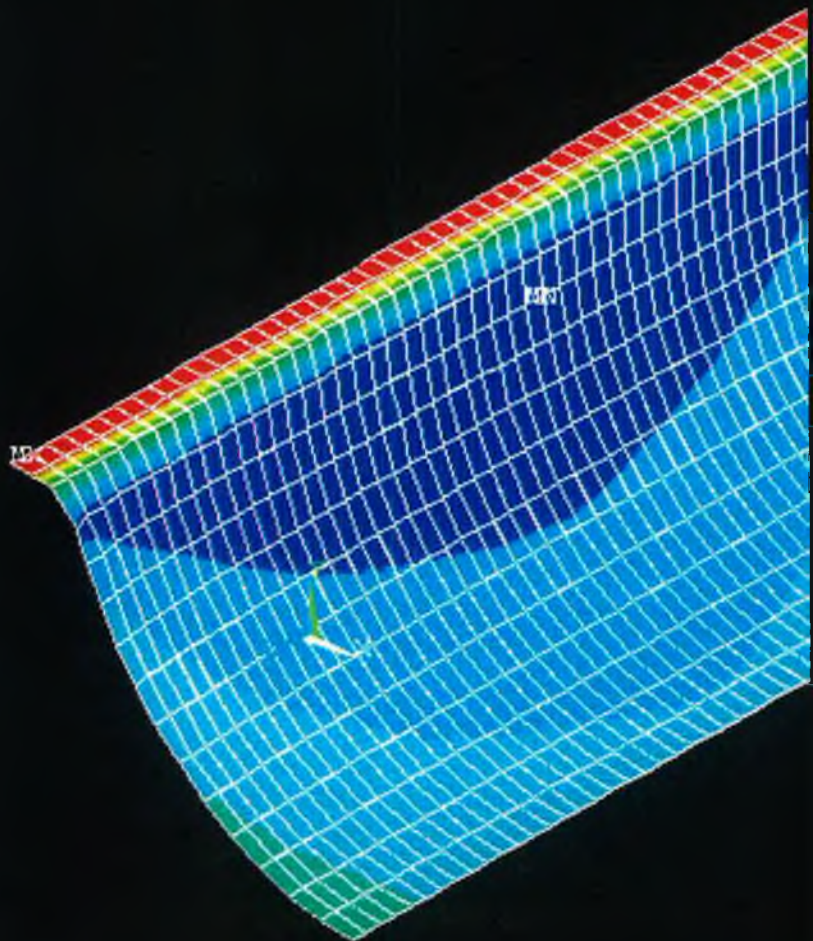
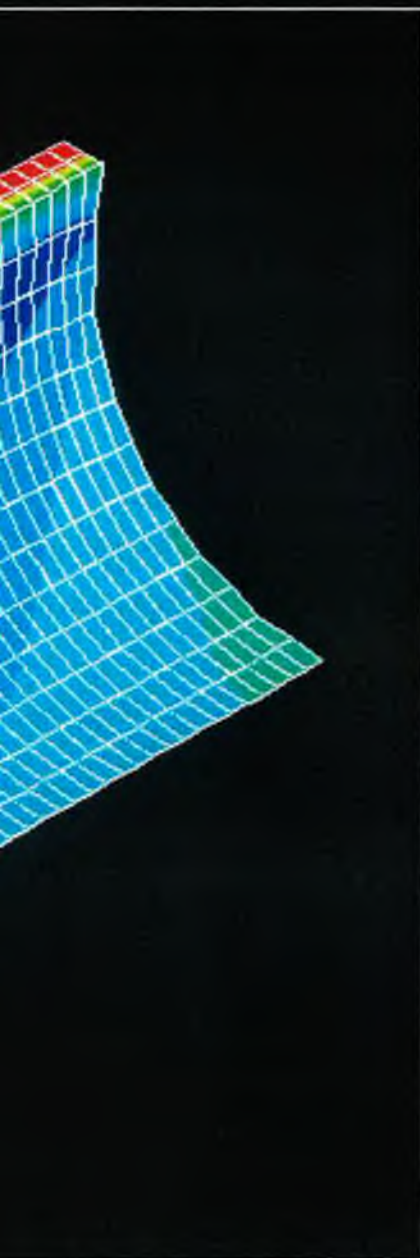


Figure VIII - Box drawn product /
Von Mises Equivalent stress
contours.

1



LS-DYNA3D user input



```

ANSYS 5.3
MAR 27 1997
15:55:44
AVG ELEMENT SOLUTION
STEP=1
SUB =52
TIME=.012002
TH      (AVG)
TOP
DMX =60.362
SMN =.797112
SMX =1

```

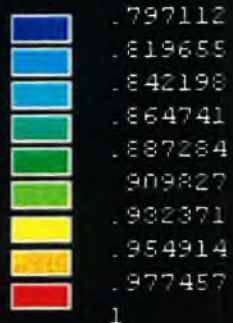
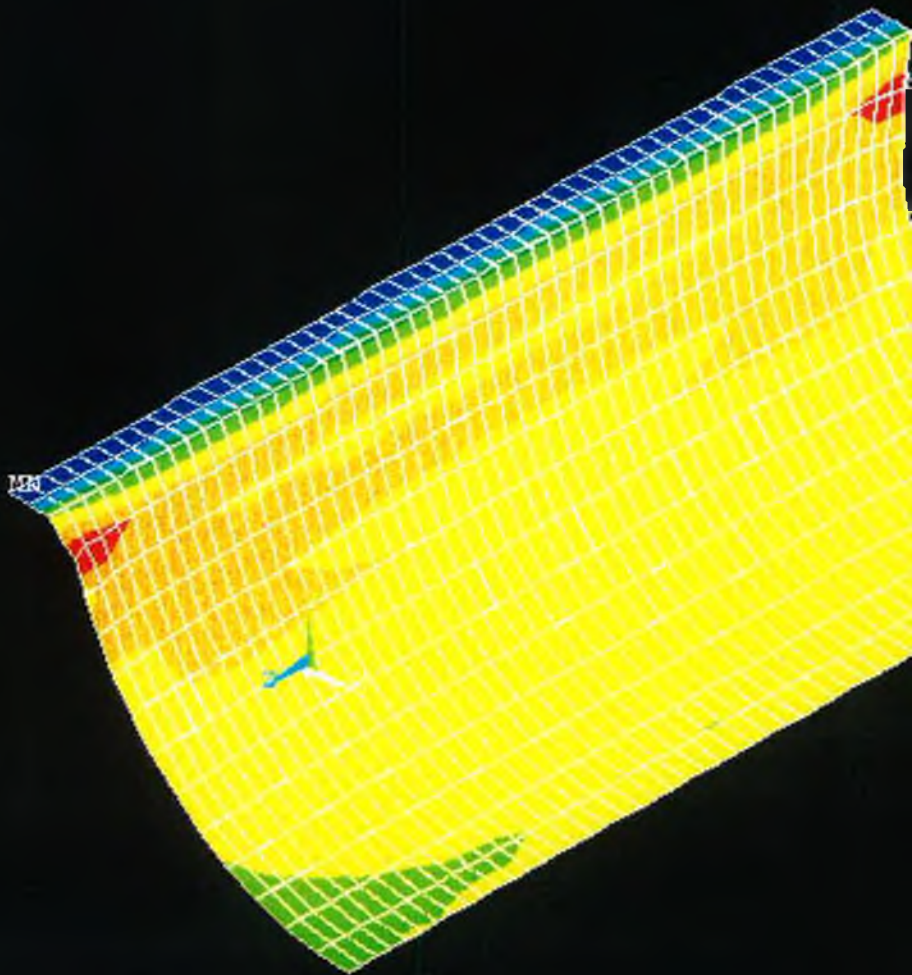


Figure XI : O.S.U formability test Thickness contours.

1



LS-DYNA3D user input

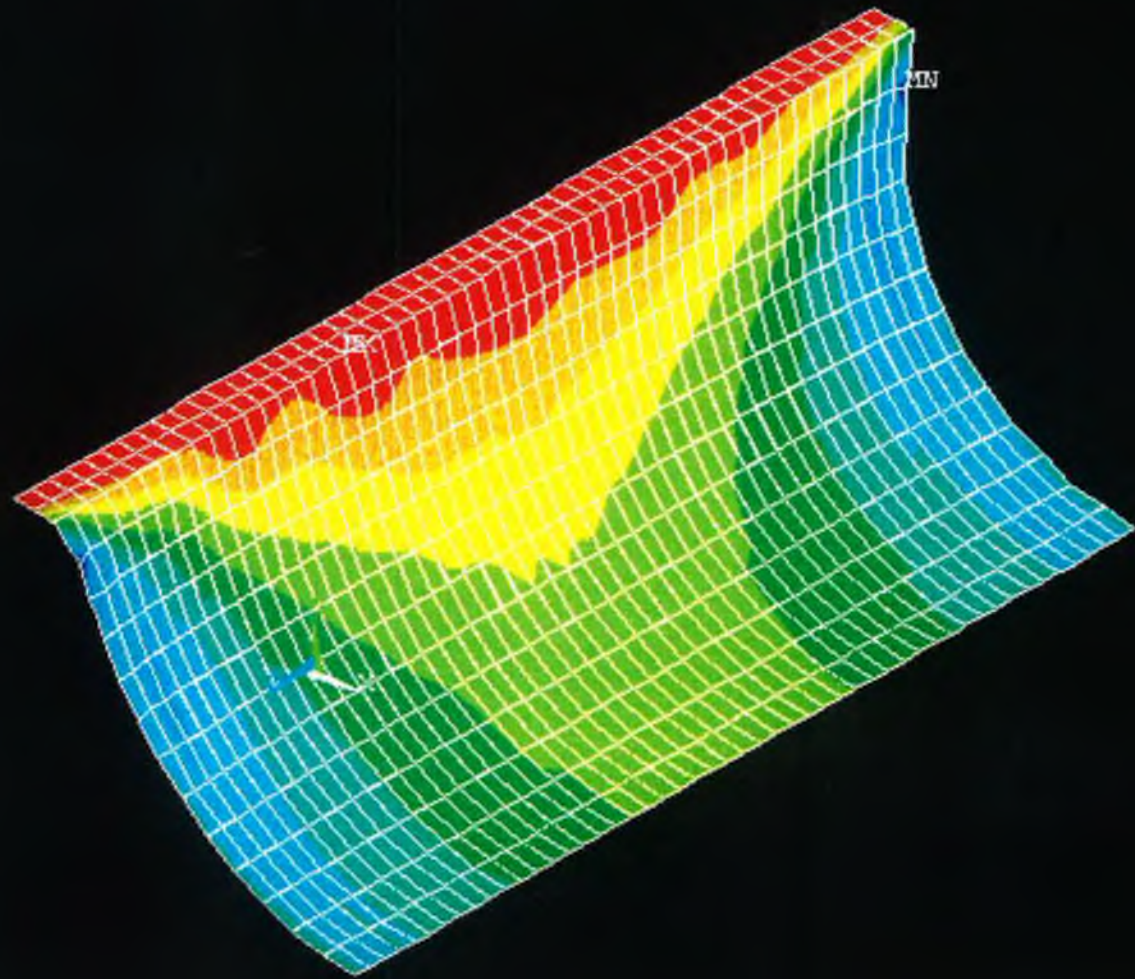
IX



```
ANSYS 5.3  
MAP 27 1997  
16:01:50  
NODAL SOLUTION  
STEP=1  
SUB =52  
TIME=.012002  
EPT01 (AVG)  
TOP  
DIX =60.362  
SIX =.686781  
0  
.076309  
.152618  
.228927  
.305236  
.381545  
.457854  
.534163  
.610472  
.686781
```

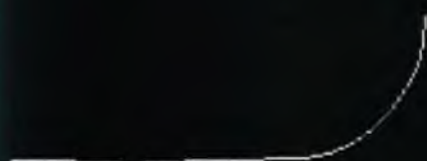
Figure IX O.S.U. formability test /
1st principle strain

1



ANSYS 5.3
MAR 27 1997
16:02:55
NODAL SOLUTION
STEP=1
SUB =52
TIME=.012002
EPT02 (AVG)
TOP
DICK =80.382
SMIN =-.187722
SICK =.002334
-.187722
-.186605
-.145487
-.12487
-.103252
-.082135
-.061018
-.0399
-.018783
.002334

Figure X: O.S.U. formability test /
2nd principle strain.



```

ANSYS 5.3
MAR 28 1997
19:57:24
MODAL SOLUTION
STEP=1
SUB =5
TIME=.5
SM          (AVG)
PSYS=0
DIE: =10
SMN =-.109182
SMD: =.013444

```


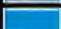






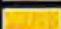

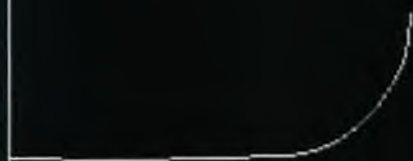
	-.109182
	-.095557
	-.081932
	-.068307
	-.054681
	-.041056
	-.027431
	-.013806
	-.181E-03
	.013444

Figure XII : Binder wrap / Stress in the x direction, via asymmetric analysis




```
ANSYS 5.3
MAP 28 1997
19:59:59
NODAL SOLUTION
STEP=1
SUB =5
TIME=.5
EPTOK:      (AVG)
RST5=0
DMLK =10
SMN  =-.580E-07
SIX  =.614E-07

-.580E-07
-.447E-07
-.314E-07
-.182E-07
-.492E-08
.834E-08
.216E-07
.349E-07
.481E-07
.614E-07
```

Figure XIII : Binder wrap / strain in the x direction, via axisymmetric analysis

1



ANSYS 5.3
MAP 28 1997
20:09:27
ELEMENTS
TYPE NUM

EV =1
*BIST=31.812
*XF =28.667
*YF =5.398
Z-BUFFER

Figure XIII : Axisymmetric dynamic analysis